UNIVERSITÀ
DEGLI STUDI
DI PADOVA

DEPARTMENT OF BIOMEDICAL SCIENCES

PhD Program in Experimental Biomedical Sciences

XXX cycle

Mesenchymal stem cells and their extracellular vesicles in the control of pathological angiogenesis

Coordinator: Prof. Paolo Bernardi

Supervisor: Prof. Antonella Viola

Co-Supervisor: Barbara Molon

Ph.D. Student: Roberta Angioni

A.A. 2016-2017

Bisogna pensare da saggi
e agire da folli

INDEX

RIASSUNTO I

RESEARCH SUMMARY IX

FIGURES XV

INTRODUCTION 1

1 PRINCIPLES OF THE INFLAMMATORY RESPONSE 1

1.1 Immune response activation by infectious agents 2

1.1.a Molecular mechanisms of immune cells transmigration 3

1.2 Antigen-presenting cells initiate adaptive immune responses 6

1.3 Resolution of the inflammatory response 7

2 INFLAMMATION AND ANGIOGENESIS: THE ENDOTHELIAL CELL ACTIVATION 9

2.1 The resting blood vasculature 9

2.2 Type I activation of endothelial cells 10

2.3 Type II activation of endothelial cells. 12

3 ANGIOGENESIS AND INFLAMMATION 14

3.1 Pro-angiogenic growth factors 14

3.2 Steps in angiogenesis 15

3.2.a Tip cell selection and migration 16

3.2.b Sprout extension 17

3.2.c Anastomosis, lumen formation and vessel maturation 18

3.3 ECM-driven signalling during angiogenesis 20

3.3.a Matrix metalloproteinases (MMPs) 21

3.3.b Invasiveness of Tip Cells 23

3.3.c MMPs modulate angiogenic factors 24

4 MESENCHYMAL STEM CELLS FOR IMMUNOSUPPRESSION 25

4.1 Definition of Mesenchymal Stem Cells (MSCs) 25

4.1.a Multipotency and self-renewal 25

4.1.b Markers of MSCs 26

4.2 In Vivo localization 27

4.3 Proposed physiological role of Mesenchymal Stem Cells *27*

4.3.a MSCs control the hematopoietic niche 27

4.3.b Perivascular MSCs in the tissue regeneration 29

4.3.c Immunomodulatory proprieties: the plasticity of MSCs 30

4.4 Clinical applications *33*

5 MSCs-DERIVED EXTRACELLULAR VESICLES 35

5.1 Exosomes *35*

5.2 Microvesicles *36*

5.3 Apoptotic bodies *36*

5.4 Toward a cell-free therapeutic approach *36*

AIM OF THE STUDY 39

MATERIALS AND METHODS 41

MICE 41

ISOLATION OF MSCs (MSCs) 41

COLLECTION OF CONDITIONED MEDIUM OF MSCs (MSC-CM) 42

EXTRACELLULAR VESICLES (EVs) ISOLATION 42

ENDOTHELIAL CELL LINES 43

IN VITRO ENDOTHELIAL CELL ACTIVATION 43

TUBE FORMATION ASSAY 44

CRYO-IMAGING 45

OPTICAL PROJECTION TOMOGRAPHY 45

3D IMMUNOFLUORESCENCE (3-DIF) 46

IMMUNOFLUORESCENCE 46

IMMUNIZATION WITH CFA/OVA 47

IN VIVO TIMP-1 IMMUNONEUTRALIZATION 47

TIMP-1 siRNA REVERSE TRANSFECTION 47

AAV-MEDIATED TIMP-1 OVEREXPRESSION 48

FLOW CYTOMETRY ANALYSES 48

Isolation and Differentiation of Mouse Bone Marrow–Derived Monocytes .. 49
Isolation and differentiation of Human Blood-Derived Monocyte 50
ELISA-Assay 50
LC-ESI MS/MS analysis 51
Scratch wound healing assay 52
Measurement of ROS by Fluorescence Microscopy 53
Mouse retina neovascularization model 53
Matrigel plug assay 54
EVs characterization 54
Statistical Analysis 55
RESULTS 57
MSCs transplantation affects endothelial activation in immune reactive lymph nodes 57
MSCs inhibit activation and elongation of HEVs and affect recruitment of T cells to dLNs 60
Endothelial Cells are a direct target of MSCs 63
MSCs inhibit in vitro angiogenesis through the release of TIMP-1 65
Proteomic based comparison between mouse and human MSC-CM 71
Functional evidence of human and mouse MSCs secretome similarities or differences 74
Macrophage colony-stimulating factor (M-CSF) 75
TIMP-1 77
Extracellular vesicles recapitulate the phenotype of MSC-CM from which they are isolated 81
The scratch wound healing assay reveals a second anti-angiogenic mechanism of EVs st- MSC-CM 83
CD39 and CD73 confer anti-angiogenic activity to EVs st-MSC-CM 85
EVs st-MSC-CM induce reactive oxygen species (ROS) in migrating endothelial cells 87

INHIBITION OF ANGIOGENESIS *IN VIVO* THROUGH THE TREATMENT WITH EVS DERIVED FROM ST- MSC-CM 90

DISCUSSION 93

BIBLIOGRAPHY 101

PUBLICATIONS 117

Riassunto

Le cellule staminali mesenchimali (MSCs) sono una popolazione eterogenea di cellule, aderenti alla plastica, con capacità di auto-rinnovamento. Esse hanno un'ampia distribuzione negli organismi adulti, infatti, possono essere isolate da diversi compartimenti tissutali tra cui il midollo osseo, il tessuto adiposo, il rene e il fegato (Crisan et al., 2008). In quanto cellule progenitrici multipotenti, le MSCs sono in grado di differenziarsi in vari tipi di cellule, in particolare quelle appartenenti alla linea mesodermica, rappresentando così un'importante opportunità per la medicina rigenerativa (Caplan, 1991). Oltre a questa proprietà, le MSCs sono in grado di controllare la sopravvivenza cellulare, la funzionalità dell'organo e l'infiammazione. Il terreno condizionato da MSCs, inoltre, può esercitare molti di questi effetti, suggerendo che il principale meccanismo d'azione delle MSCs è mediato da fattori solubili, piuttosto che dal contatto diretto con altre cellule (Madrigal et al., 2014, Zanotti et al. 2013).

Una caratteristica ben descritta di queste cellule è la loro capacità di inibire l'infiammazione, sia *in vitro* che *in vivo*. Diversi studi, infatti, hanno dimostrato che le MSCs controllano negativamente la risposta immunitaria associata a diverse patologie, come il diabete di tipo 1 (T1D), l'artrite reumatoide (RA) e la graft-versus-host disease (GVHD), ma anche il rigetto del trapianto e le malattie neurodegenerative, rappresentando cosi un interessante approccio terapeutico (Ram Sharma et al., 2014, Ying Wang et al., 2014, Klinker et al., 2015)

Per meglio caratterizzare il meccanismo paracrino responsabile delle proprietà immunomodulatorie delle MSCs, in collaborazione con la professoressa Gabriella Tedeschi dell'Università di Milano, abbiamo eseguito un'analisi proteomica del terreno condizionato da tali cellule. Dal momento che il fenotipo immunosoppressorio delle MSCs è indotto da un ambiente pro-infiammatorio (Bernardo ME et al., 2013, Groh ME et al., 2005), abbiamo stimolato le cellule con un insieme di citochine (IL1β, IL6 e TNFα). Tramite il confronto del secretoma delle MSCs stimolate (st MSC-CM), note per le loro proprietà immuno-modulanti, con quello delle MSCs non stimolate (unst MSC-CM), prive di effetti immunosoppressori, abbiamo identificato potenziali fattori responsabili dell'effetto terapeutico delle st- MSCs.

Innanzitutto, i dati ottenuti evidenziano che la stimolazione con citochine pro-infiammatorie (IL1β, IL6 e TNFα) induce un notevole cambiamento nell'intero secreto delle MSCs. In particolare, la maggior parte delle proteine rilasciate esclusivamente dalle MSCs attivate con citochine pro-infiammatorie risultano essere coinvolte nella regolazione dell'angiogenesi. Tra questi fattori abbiamo identificato l'inibitore tissutale delle metalloproteinasi 1 (TIMP-1), una specifica glicoproteina implicata nella soppressione endogena delle metalloproteinasi (Lambert et al., 2004). Abbiamo quindi dimostrato, sia *in vitro* che *in vivo*, che le MSCs attivate da citochine pro-infiammatorie influenzano l'infiammazione locale attraverso il rilascio di questa proteina. Mediante la secrezione di TIMP-1, infatti, le MSCs bloccano la formazione di nuovi vasi sanguigni nel linfonodo drenante, essenziali per il reclutamento di leucociti circolanti al tessuto infiammato. Questo evento è, di conseguenza, responsabile della soppressione locale della risposta immunitaria (Zanotti and Angioni et al., 2016).

Tutti questi dati sono stati, però, collezionati dallo studio di MSCs murine in un modello di infiammazione in topo. Con il fine ultimo di sviluppare un approccio clinico, abbiamo deciso di analizzare il secreto delle MSCs umane (hMSCs). Pertanto, in collaborazione con la professoressa Gabriella Tedeschi, mediante spettrometria di massa abbiamo esaminato come le citochine pro-infiammatorie modulano anche la composizione del secretoma umano. L'analisi comparativa del secretoma delle MSCs umane e murine, stimolate e non, ha confermato che l'esposizione a fattori pro-infiammatori determina, in entrambe le specie, un incremento nel rilascio di proteine legate all'immuno-modulazione e all'angiogenesi. In particolare, il 62% delle proteine nel secretoma umano, rilasciate in risposta a citochine pro-infiammatorie, è stato identificato nel suo corrispondente murino. Tale evidenza ha quindi dimostrato chiaramente l'esistenza di una somiglianza di tali specie cellulari nella risposta all'infiammazione. Tuttavia, nonostante l'analoga risposta alla stimolazione, i nostri dati indicano che i fattori solubili rilasciati da MSCs murine e umane possono indurre diverse risposte biologiche. Ad esempio, sebbene la secrezione del fattore di crescita M-CSF / CSF-1 sia indotta dopo stimolazione in entrambe le specie cellulari, solo nelle cellule umane questa induce efficacemente la differenziazione dei macrofagi; probabilmente per una diversa concentrazione di M-CSF secreto, maggiore nei surnatanti derivati dall'uomo. Per quanto riguarda l'angiogenesi, i nostri dati corroborano pienamente il ruolo anti-angiogenico delle MSCs, sia umane che murine, attivate da citochine pro-infiammatorie. Questo risultato identifica chiaramente, per la

prima volta, l'endotelio come target delle MSCs durante il processo di immunosoppressione. Inoltre, abbiamo confermato il ruolo chiave di TIMP-1, sia nel secretoma umano che murino, come mediatore di tale effetto anti-angiogenico, (Maffioli E et al., 2017). I dati completi di spettrometria di massa sono disponibili tramite ProteomeXchange con l'identificatore PXD005746.

Nonostante i trials clinici registrati che utilizzano le MSCs siano più di 600 in tutto il mondo (come riportato da www.clinicaltrials.gov), quest'approccio rimane ancora non completamente sviluppato e sicuro. Ad esempio, sono ancora mancanti sia un protocollo standardizzato per l'isolamento, il mantenimento in coltura e la via di somministrazione delle MSCs durante la terapia, che una standardizzazione dei parametri di qualità e sicurezza delle MSCs necessari per lo sviluppo di un efficiente terapia. Con lo scopo di superare queste problematiche, abbiamo volto la nostra attenzione su un approccio alternativo, potenzialmente più economico e sicuro, ovvero l'impego di derivati dalle MSCs, anziché direttamente le cellule stesse. Uno dei prodotti delle MSCs più studiati, e pertanto caratterizzati, sono le vescicole extracellulari (EVs) (Biancone L et al., 2012). Le EVs si originano dalla membrana plasmatica cellulare e vengono rilasciate dalle cellule come particelle lipidiche. Secondo le raccomandazioni della Società Internazionale per le vescicole extracellulari (ISEV), tali vescicole possono essere classificate in tre categorie principali sulle basi delle loro dimensioni, origini e metodi di isolamento,: (i) Microvesicole (dimensioni tra 50 e 1000 nm , originate dalla membrana plasmatica e arricchite in CD40); (ii) corpi apoptotici (dimensioni comprese tra 800 e 5000 nm, derivate da frammenti di cellule morenti e arricchite in istoni e DNA); e (iii) esosomi che sono piccole vescicole di origine endocitica (~ 30-120 nm) (arricchite da marcatori della membrana endosomale tardiva, compresi Tsg101, CD63, CD9 e CD81) (Yáñez-Mó, 2015). Diversi studi hanno riportato che le EVs provenienti da MSCs mostrano potenziali terapeutici simili a quelli delle loro cellule di origine (Merin-Gonzàles et al., 2016). Ad esempio, è stato dimostrato che le EVs di MSCs riducono la zona infartuata e migliorano la riparazione dei tessuti in malattie cardiovascolari (Lai et al., 2010). Più in generale, è stato riportato che le EVs derivanti da MSCs non stimolate possono ridurre la fibrosi e l'apoptosi, ma, contrariamente, sostenere la differenziazione delle cellule staminali, promuovendo così il processo di rigenerazione tissutale associato non solo a malattie cardiovascolari, ma anche lesioni renali, epatiche e polmonari (Sweta Rani et al., 2015).

Pertanto, con il fine ultimo di sviluppare un'efficace terapia immunomodulante, abbiamo analizzato l'effetto delle EVs rilasciate da MSCs sull'angiogenesi. Per questo, abbiamo innanzitutto isolato e concentrato le vescicole dal terreno condizionato da MSCs attivate con citochine pro-infiammatorie. In seguito, abbiamo valutato la capacità di tali vescicole di controllare il processo di formazione dei tubuli *in vitro* mediante l'utilizzo di cellule endoteliali (SVEC4-10). I nostri dati hanno confermato che solo le vescicole derivate da MSCs stimolate inibiscono il processo di tubulogenesi, ricapitolando l'effetto anti-angiogenico osservato con l'intero terreno condizionato da st- MSCs. Anche in queste condizioni, TIMP-1 svolge un ruolo cruciale. Infatti, l'utilizzo di un anticorpo bloccante per TIMP-1 è stato in grado di annullare questo effetto anti-angiogenico. A conferma di ciò, l'analisi con Western blot ha evidenziato l'espressione di questo enzima unicamente su vescicole derivanti da MSCs stimolate con citochine pro-infiammatorie.

Nel processo di tubulogenesi, la digestione del matrigel, sopra il quale vengono piastrare le cellule endoteliali e che mima la matrice extracellulare, rappresenta un processo essenziale per la formazione di una rete tubolare allungata e ben organizzata. TIMP-1, secreto da MSCs anche attraverso il rilascio di EVs, svolge un ruolo cruciale nell'inibizione di questo fenomeno, probabilmente bloccando l'attività delle metalloproteinasi necessaria per un'efficiente digestione del matrigel. Tuttavia, la migrazione delle cellule endoteliali rappresenta un altro passo fondamentale durante l'angiogenesi *in vivo*. Per studiare anche tale aspetto, abbiamo sfruttato un approccio sperimentale *in vitro* basato essenzialmente sulla capacità delle cellule di muoversi in uno spazio libero: il saggio di riparazione della ferita tissutale (Liang CC et al., 2007). L'esperimento consiste nel graffiare con un puntale un monostrato di cellule endoteliali (SVEC4-10) in modo da generare uno spazio vuoto nel quale esse possano liberamente migrare. Per valutare la capacità delle EVs di controllare la migrazione delle SVEC4-10, le cellule sono state trattate con vescicole provenienti dal surnatante di MSCs, stimolate e non con citochine pro-infiammatorie, e VEGF (un potente fattore pro-angiogenico), in presenza o in assenza dell'anticorpo bloccante per TIMP-1. Come previsto, il segnale pro-angiogenico (VEGF) aumenta la migrazione delle cellule endoteliali, mentre le EVs isolate dal terreno condizionato da MSCs stimolate, bloccano il processo. Tuttavia, in tale approccio sperimentale, l'inibizione di TIMP-1 non ha ripristinato la capacità migratoria delle cellule endoteliali, suggerendo, quindi, l'esistenza di un secondo meccanismo anti-angiogenico peculiare delle EVs provenienti da MSCs attivate.

La capacità migratoria delle cellule endoteliali dipende massivamente dalla rapida riorganizzazione della rete actinica. In questo processo, le specie reattive dell'ossigeno (ROS) hanno un ruolo cruciale di regolazione, essendo in grado sia di sostenere che di bloccare l'angiogenesi. Tuttavia, il loro meccanismo d'azione rimane ancora controverso e sembra dipendere principalmente dalla loro localizzazione e, soprattutto, dalla loro concentrazione (Marcelo L. Lamers et al., 2011, Carlos Wilson et al., 2015). Infatti, basse concentrazioni di ROS supportano la fosforilazione del recettore del fattore di crescita VEGF (VEGF-R), e, di conseguenza, controllano positivamente l'attivazione del segnale a valle (Lamalice et al., 2007). Contrariamente, elevati livelli ROS inducono una disfunzione endoteliale, causando alterazioni nella loro capacità migratoria, induzione dell'apoptosi e attivazione di senescenza (Lum et al., 2001, Rong Liu et al., 2014). Per verificare un'implicazione dei ROS nell'inibizione delle capacità migratorie delle cellule endoteliali indotta dal trattamento con EVs derivanti da MSCs stimolate, abbiamo analizzato la loro produzione in tali cellule, attraverso l'utilizzo di una sonda generica per le specie reattive dell'ossigeno (H2DCFDA). Mediante questo approccio sperimentale abbiamo dimostrato che le EVs originate da MSCs stimolate con citochine sono in grado di aumentare la produzione di ROS nelle cellule endoteliali durante la migrazione. Questa evidenza ha supportato l'ipotesi che uno squilibrio ossidativo possa partecipare all'effetto anti-angiogenico indotto da EVs provenienti da MSCs stimolate con citochine pro-infiammatorie.

Nox2 rappresenta il principale regolatore della produzione dei ROS nelle cellule endoteliali e l'adenosina è stata associata alla sua regolazione (Sapna Thakur et al., 2010). L'adenosina è generata tramite l'idrolisi dell'ATP (adenosina-5'-trifosfato) dagli enzimi CD39 (nucleoside trifosfato defosforilasi) e CD73 (ecto-5'-nucleotidasi). Inoltre, precedenti studi hanno dimostrato che le vescicole extracellulari possono esprimere questa coppia di enzimi (Clayton A et al., 2011, Schuler PJ et al., 2014, Amarnath S et al., 2015). Mediante Western Blot abbiamo, innanzitutto, verificato l'espressione di CD39 e CD73 in EVs provenienti da MSCs stimolate con citochine pro-infiammatorie. Inoltre, abbiamo dimostrato che l'utilizzo di entrambi gli inibitori ARL 67156 e AMP-CP, che bloccano rispettivamente CD39 e CD73, durante il saggio di riparazione della ferita tissutale, annulla l'effetto anti-angiogenico delle vescicole isolate da MSCs stimolate. Da tale risultato abbiamo, quindi, ipotizzato che le EVs derivate da MSCs attivate da citochine pro-infiammatorie, attraverso l'attività di CD39 e CD73, sono in grado di aumentare la

concentrazione di adenosina extracellulare che, legando specifici recettori sulla superficie delle cellule endoteliali, induce l'attivazione di Nox2 e, consecutivamente, la produzione di ROS. A supporto di ciò, l'inibizione dell'accumulo di ROS, ottenuta mediante l'utilizzo di un antiossidante generico (NAC), ripristina totalmente la migrazione endoteliale. Per corroborare ulteriormente la nostra ipotesi, stiamo programmando di eseguire esperimenti per identificare il recettore specifico dell'adenosina coinvolto in questo processo e il meccanismo attraverso cui esso controlla l'accumulo di specie reattive dell'ossigeno.

Al fine di sviluppare un approccio terapeutico da utilizzare a livello clinico, abbiamo convalidato i nostri risultati anche *in vivo*. Pertanto, abbiamo esaminato l'effetto anti-angiogenico delle EVs derivanti da MSCs stimolate da citochine pro-infiammatorie nel modello murino di vascolarizzazione della retina, un approccio sperimentale molto diffuso per lo studio del processo angiogenico *in vivo* (Andreas Stahl et al., 2010). Infatti, a differenza degli esseri umani, i topi presentano una rete vascolare retinica immatura alla nascita. La vascolarizzazione della retina, che si completa in alcune settimane, procede in modo strettamente regolato e organizzato, risultando così un modello efficiente per individuare eventuali difetti (Stahl et al., 2010). Così, topi C57BL / 6J sono stati iniettati intra-peritonealmente a un giorno di vita con EVs da MSCs, non stimolate o stimolate con citochine pro-infiammatorie, e sacrificati 5 giorni dopo per l'espianto delle retine. Mediante microscopia confocale, abbiamo osservato una diminuzione dell'arborizzazione vascolare della retina degli animali trattati con EVs provenienti da MSCs stimolate, ma nessun effetto con la controparte non stimolata. L'effetto anti-angiogenico di tali vescicole è stato ulteriormente corroborato mediante l'utilizzo di un altro modello murino: il saggio d'iniezione di un plug di matrigel. Quest'approccio consiste nella valutazione della vascolarizzazione del plug addizionato con EVs e impiantato nella parte dorsale posteriore di topi C57BL / 6-N. Anche tale modello ha confermato le proprietà anti-angiogeniche delle EVs derivanti da MSCs stimolate con citochine pro-infiammatorie. Collettivamente, tali evidenze suggeriscono la possibilità di sostituire le MSCs con i loro derivati, le EVs, per sviluppare un approccio terapeutico maggiormente standardizzabile e sicuro, senza l'impiego diretto di cellule.

Successivi esperimenti saranno eseguiti per misurare la concentrazione di ROS nell'endotelio delle retine trattate con EVs derivanti da MSCs stimolate con citochine pro-infiammatorie. Inoltre, per validare il duplice meccanismo d'azione, utilizzeremo *in*

vivo le EVs derivanti da MSC stimolate in cui è stato significativamente diminuita l'espressione di TIMP-1 (che abbiamo già ottenuto mediante siRNA) con o senza l'inibitore di CD39.

Per concludere, i nostri dati indicano che le cellule staminali mesenchimali agiscono specificamente sulle cellule endoteliali per controllare l'infiammazione, anche mediante il rilascio di vescicole extracellulari. In particolare, questo è determinato dalla secrezione di fattori solubili, tra cui le EVs, che bloccano il processo angiogenico. Questa inibizione è mediata da almeno due meccanismi cooperanti che agiscono su due processi differenti, ma ugualmente fondamentali, dell'angiogenesi. Infatti, da un lato TIMP-1, espresso sulle vescicole, inibisce le MMPs, e, di conseguenza, influenza negativamente le capacità delle cellule endoteliali di degradare la matrice extracellulare circostante. D'altra parte, la produzione locale di adenosina, data della presenza di entrambi gli enzimi CD39 / CD73 sulla superficie di queste vescicole, induce l'attivazione di Nox2 e la produzione di ROS nelle cellule endoteliali, compromettendo così la loro motilità e proliferazione.

Riteniamo che questi risultati siano di fondamentale importanza per comprendere pienamente il ruolo biologico delle MSCs e sfruttarle nella terapia. Infatti, i nostri dati confermano il concetto emergente di MSCs come sensori del microambiente, in grado di modulare gli eventi fisiologici e patologici. infatti, mentre in condizioni ipossiche le MSCs rilasciano vescicole che supportano il processo angiogenico (Consuelo Merino-González et al 2016, Gangadaran P. et al 2017, Jiejie Liuet al 2015, Suyan Bian et al., 2014), durante una risposta infiammatoria esse acquisiscono un fenotipo anti-infiammatorio, inibendo sia l'attività delle cellule immunitarie (Soraia C. Abreu et al., 2016, Claudia Lo Sicco ed altri 2017) sia l'angiogenesi ad essa associata (Angioni et al., manoscritto in preparazione, Maffioli et al.,2017, Zanotti and Angioni et al., 2016). Queste evidenze forniscono, pertanto, nuove prospettive per lo sviluppo d'importanti approcci terapeutici. Le EVs derivanti da MSCs stimolate da citochine pro-infiammatorie possono, infatti, rappresentare una terapia molto efficace per il trattamento dell'angiogenesi patologica per diverse ragioni: esse sembrano non soltanto agire selettivamente sull'endotelio, e inibire l'angiogenesi sfruttando meccanismi multipli, ma, in aggiunta, la terapia che ne potrebbe derivare avrebbe anche il grande vantaggio di essere più standardizzabile di quella basata sul trasferimento diretto di cellule.

Research Summary

Mesenchymal stem cells (MSCs) are a heterogeneous population of adherent cells with self-renewable capacity and with a wide distribution in adult organisms; they can be isolated from adult tissues including bone marrow, adipose tissue, kidney and liver (Crisan et al., 2008). As multipotent progenitor cells, MSCs are able to differentiate into various cell types, especially of the mesodermal lineage, thus representing an important opportunity for regenerative medicine (Caplan, 1991). Besides this application, MSCs are able to control cell survival, organ function and inflammation. Remarkably, conditioned medium collected from MSCs can exert many of these paracrine effects, suggesting that the major mechanism of action of MSCs relies on soluble factors rather than cell–cell contact (Madrigal et al. 2014, Zanotti et al. 2013).

A well-established feature of MSCs is their ability to inhibit inflammation and immunity, both in vitro and in vivo. Several studies have demonstrated that MSCs may be a useful therapeutic option for the treatment of immune-mediated disorders such as type 1 diabetes (T1D), rheumatoid arthritis (RA) and graft-versus-host disease (GVHD), but also transplantation rejection and neurodegenerative diseases (Ram Sharma et al. 2014, Ying Wang et al. 2014, Klinker et al. 2015)

In order to better characterize the paracrine mechanism responsible for MSCs immunomodulatory properties, we performed a shotgun proteomic analysis of the mouse MSCs-conditioned medium, in collaboration with Prof. Gabriella Tedeschi from the University of Milan. Since the MSCs anti-inflammatory phenotype is induced by a pro-inflammatory environment (Bernardo ME et al. 2013, Groh ME et a. 2005), we stimulated MSCs with a cocktail of cytokines (IL1beta, IL6 and TNFalpha) in order to compare the medium conditioned by activated MSCs (st MSC-CM), with that derived from unstimulated MSCs.

Interestingly, we found that the stimulation with pro-inflammatory cytokines (IL1beta, IL6 and TNFalpha) induces a remarkable change in the whole secretome; notably, most of proteins secreted by stimulated MSCs are involved in the regulation of angiogenesis. Among the factors up-regulated by conditioned MSCs, we identified the tissue inhibitor of metalloproteinases 1 (TIMP-1), a specific glycoprotein implicated in the endogenous inhibition of metalloproteinases (Lambert et al. 2004). We demonstrated that MSCs affect

local inflammation trough the release of TIMP-1, both in in vitro and in vivo experimental settings. Specifically, by the secretion of TIMP-1, MSCs block the formation of new vessels at the draining lymph node of immunized mice. This event results in a decreased recruitment of leukocytes from the blood flow into the inflamed tissue, leading to a local suppression of the immune response (Zanotti and Angioni, Leukemia 2016).

In order to design successful pre-clinical experiments as well as clinical trials, the analysis of human MSCs secretome was required. Thus, in collaboration with Prof. Gabriella Tedeschi, we performed a mass spectrometry based proteomic approach to analyse how pro-inflammatory cytokines modulate the composition of the human MSCs (hMSCs) secretome.

Comparative analysis of hMSC-CM and mMSC-CM confirmed that the exposure to pro-inflammatory cytokines results in increased secretion of a number of immunomodulatory and angiogenesis-related proteins by MSCs from both species. Notably, 62% of the proteins identified in st hMSC-CM were also identified in st mMSC-CM, clearly highlighting the existence of a common signature in the secretome of human and mouse MSCs. However, despite the similar proteomic signature in response to stimulation by pro-inflammatory cytokines of human and mouse MSCs, our data indicate that they may induce different biological responses. For example, although the growth factor M-CSF/CSF1 is up-regulated in both human and mouse MSC-CM upon stimulation, only hMSC-CM efficiently induce macrophage differentiation; this is probably due to the different concentration of secreted M-CSF, which is higher in human-derived supernatants. Concerning angiogenesis, our data fully corroborate the anti-angiogenic role of stimulated MSCs for both mouse and human samples. In particular, we confirmed the key role of TIMP-1 as anti-angiogenic factor, both in human and mouse cells (Maffioli E et. al 2017). Complete mass spectrometry data are available via ProteomeXchange with identifier PXD005746.

Although worldwide there are about 600 registered clinical trials evaluating the potential of MSCs-based cell therapy (see www.clinicaltrials.gov), this approach still remains far from a fully developed and safe clinical technology. Importantly, a standardized and unifying protocol addressing which source of MSCs should be used and which is the best route of administration is still missing. Moreover, even the parameters of quality and safety of MSCs are not universally established. To overcome all these issues, we focused

our attention on an alternative approach, exploiting products derived from MSCs rather than MSCs themselves, which may represent a cost-effective and safer approach.

One of the best-characterized MSCs product are MSCs-derived extracellular vesicles (EVs) (Biancone L et al., 2012). EVs arise from the plasma membrane and are released by cells as particles. In accordance with the recommendations of the International Society for Extracellular Vesicles (ISEV), EVs can be classified according on their size, origin, and isolation methods, into three main classes: (i) Microvesicles or shedding vesicles (size between 50 and 1000 nm, budding from the plasma membrane, and enriched in CD40); (ii) Apoptotic bodies (size between 800 and 5000 nm, derived from fragments of dying cells, and enriched in histones and DNA); and (iii) Exosomes, which are small (~30–120 nm) membrane vesicles of endocytic origin (enriched in late endosomal membrane markers, including Tsg101, CD63, CD9, and CD81) (Yáñez-Mó, 2015). Several studies have reported that MSCs-derived EVs display therapeutic potential in a similar fashion to their parent cells (Merin-Gonzàles et al. 2016). For example, it has been shown that MSCs-derived EVs reduce infarct size and enhance tissue repair in cardiovascular disease (Lai et al. 2010). More in general, it seems that EVs derived from unstimulated MSCs may reduce fibrosis and apoptosis, but sustain stem cell differentiation. Thus, MSCs-derived EVs are able to reinforce the regeneration process associated to not only cardiovascular disease but also liver, lung and acute kidney injury (Sweta Rani et al. 2015).

To investigate MSCs-derived EV effect on angiogenesis, we first isolated and concentrated vesicles from the conditioned medium of MSCs stimulated with pro-inflammatory cytokines. We analysed the effect of EVs in vitro by endothelial cell tube formation assay, using EVs released by unstimulated MSCs as control. Our data confirmed that vesicles derived from stimulated MSCs affect the tubulogenesis process, perfectly mimicking the anti-angiogenic effect of the whole conditioned medium. Remarkably, the neutralization of TIMP-1 by a blocking antibody was able to revert this effect. Accordingly, through western blot analysis, we found that TIMP-1 is present in EVs derived from stimulated MSCs only.

In the tubulogenesis assay, the degradation of the matrigel, with which plates are coated, is an essential step for the formation of an elongated and well-organized tube network. TIMP-1, secreted by st MSCs trough the release of EVs, plays a crucial role in the

inhibition of this process, likely by inhibiting the matrix metalloproteinase activity required for the efficient matrigel digestion. However, endothelial cell migration represents another fundamental step during angiogenesis. In order to investigate this aspect of the angiogenic process, we set up a different assay based on the ability of cells to move in a free space: the wound healing scratch assay (Liang CC et al. 2007). Wound was made by scratching a line across the bottom of the dish on a confluent endothelial monolayer. After that, cells were treated with EVs from MSC-CM plus VEGF, with or without TIMP-1 blocking antibody. As expected, the pro angiogenic signal VEGF increases the migration of endothelial cells and st- MSCs-derived EVs block this process. However, in this condition, the TIMP-1 blocking treatment didn't rescue the process. This suggests that st- MSCs-derived EVs are able to block angiogenesis through a second mechanism.

Endothelial cell motility depends on the rapid reorganization of the actin network that, in turn, modulates not only the cell shape but also cell migration. In this context, reactive oxygen species (ROS) have emerged as crucial regulators. However, their effect, supporting or inhibiting angiogenesis, remains still controversial, and seems to depend on their localization and, in particular, on their concentration (Marcelo L. Lamers et al. 2011, Carlos Wilson et al. 2015). Indeed, low oxidant concentration regulates VEGF receptor cross-phosphorylation and redox-dependent downstream signalling (Lamalice et al. 2007). In contrast, high levels of oxidative species cause endothelial cell dysfunction due to an alteration in migration, increased apoptosis and an induction of senescence (Lum et al. 2001, Rong Liu et al. 2014).

To investigate the role of ROS on the inhibition of endothelial cell migration induced by st MSCs-derived EVs, we analysed the production of oxidative species in migrating endothelial cells treated with unst- or st- MSCs-derived EVs. Interestingly, st MSCs-derived EVs were able to increase ROS production in the endothelial cells at the front of migration, thus suggesting that an oxidative unbalance could participate to the anti-angiogenic effect induced by st- MSCs-derived EVs.

Nox2 represents the main key regulator of ROS production in endothelial cells, and adenosine has been implicated in its control (Sapna Thakur et al. 2010). Adenosine is catabolized from ATP (adenosine-5'-triphosphate) by the enzymes CD39 (nucleoside triphosphate dephosphorylase) and CD73 (ecto-5'-nucleotidase). Previous studies have

demonstrated that exosomes may express this couple of adenosine-generating enzymes (Clayton A et al. 2011, Schuler PJ et al. 2014, Amarnath S et al. 2015). By western blot analysis, we demonstrated CD39 and CD73 expression in st- MSCs-derived EVs. Moreover, when performing the scratch assay in presence of an ecto-ATPase inhibitor ARL 67156 and AMP-CP, which inhibit respectively CD39 and CD73, we were able to rescue the migrating block caused by st MSC-derived EV treatment, and preliminary data suggest that the CD39 inhibition leads to a decrease in the ROS accumulation. This supports our hypothesis that st- MSCs-derived EVs, carrying CD39 and CD73, are able to increase the concentration of the extracellular adenosine, which binds adenosine receptors expressed on the surface of endothelial cells, leading to the activation of Nox2 and, in turn, to the production of ROS. Furthermore, the inhibition of ROS accumulation obtained using a generic antioxidant (NAC), fully rescued endothelial cell migration. We are planning to perform further experiments to identify the specific adenosine receptor involved in this process and its connection with Nox2.

To validate our results in vivo, we analysed the anti-angiogenic effect of st- MSCs-derived EVs in the retinal vascularization mouse model, a very useful tool in the study of physiologic vessel sprouting (Andreas Stahl et al. 2010). Indeed, in contrast to humans, mouse pups have an immature retinal vasculature at the birth; the development completes in some weeks. The retinal vascularization proceeds in a tightly regulated and organized manner, reliable for detection of any defect (Stahl et al. 2010). Thus, C57BL/6J pups were intra-peritoneally injected with unstimulated or stimulated MSCs-derived EVs, and sacrificed 5 days later to collect retinas. Samples were dissected and stained to measure the vasculature formation of developing retina by confocal microscopy. Remarkably, we observed a decrease in the retina vascular arborisation of pups treated with st- MSCs-derived EVs, but no effect with the unstimulated counterpart. We also took advantage of another mouse model, the matrigel plug assay, which consists in the analysis of the vascularization of a matrigel plug that was previously supplemented with EVs and then implanted in the dorsal back of C57BL/6-N mouse. Both models confirm that st MSC derived-EVs show anti-angiogenic proprieties.

Further experiments will be performed to measure the ROS concentration in retinas treated with st- MSCs derived-EVs. Moreover, we will use in vivo st- MSCs-derived EVs knock-down for TIMP-1 (that we already obtained by siRNA approach) with or without CD39 inhibitor to rescue the phenotype.

To conclude, our data indicate that MSCs specifically target endothelial cells to control angiogenesis through the release of extracellular vesicles. In particular, when exposed to pro-inflammatory cytokines, MSCs release EVs that strongly inhibit the angiogenic process. This inhibition is mediated by at least two co-operating mechanisms targeting two aspects of the angiogenic process. Thus, on the one hand, EVs-delivered TIMP-1, by inhibiting MMPs, affects the ability of endothelial cells to degrade the surrounding extracellular matrix. On the other, the local production of adenosine, due to the presence of CD39/CD73 enzymes on EVs released by st- MSCs, induces Nox2 activation and ROS production in endothelial cells, thus affecting endothelial cell motility and proliferation.

We believe that these findings are of utmost importance to understand the biological role of MSCs and to exploit them in therapy. Indeed, our data confirm the emerging concept of MScs as sensors of the microenvironment to control physiological and pathological events. Thus, while in hypoxic condition MSCs release vesicles enhancing the angiogenic process (Consuelo Merino-González et al. 2016, Gangadaran P. et al. 2017, Jiejie Liuet al. 2015,Suyan Bian et al. 2014), within the inflammatory milieu MScs acquire an anti-inflammatory phenotype by inhibiting both the immune cells' activity (Soraia C. Abreu et al. 2016, Claudia Lo Sicco et al. 2017) and the immune-associated angiogenesis (Angioni et al., manuscript in preparation; Maffioli E. et al.2017; Zanotti, Angioni et al. Leukemia 2016). This evidence provides new perspectives to exploit MSCs in therapy. EVs derived from st-MSCs may represent a very effective approach for the treatment of pathological angiogenesis for several reasons: they seem to target specifically the endothelium, inhibit the angiogenesis acting on multiple pathways, and are more standardisable than MSCs.

Figures

Figure I.A: The immune cells transmigration process _____ *5*

Figure I.B: Type I activation of endothelial cells _____ *11*

Figure I.C: Type II activation of endothelial cells _____ *13*

Figure I.D: Molecular signalling triggered by growth factors in endothelial cell _____ *15*

Figure I.E: Angiogenic sprouting _____ *16*

Figure I.F: Hypothesised mechanism for lumen formation _____ *19*

Figure I.G: Extracellular matrix underlying the vasculature _____ *22*

Figure I.H: Mesenchymal stem cells multypotency _____ *26*

Figure I.I: Mesenchymal stem cells in the haematopoietic niche _____ *29*

Figure 1 - MSCs affect size and cellularity of dLNs _____ *58*

Figure 2 - MSCs inhibit endothelial activation in dLNs _____ *59*

Figure 3 - MSCs inhibit HEV activation and proliferation in vivo _____ *60*

Figure 4 - MSCs suppress HEV lengthening and branching _____ *62*

Figure 5 - Endothelial Cells are a direct target of MSCs-secreted molecules _____ *64*

Table 1: common proteins up-regulated in stimulated vs unstimulated mouse and human MSCs secretome _____ *66*

Figure 6 - Distribution into biological processes of the proteins up regulated in MSC-CM _____ *67*

Figure 7 - TIMP-1 mediates the anti-angiogenic effect of MSC-CM in vitro and the anti-inflammatory effect of MSCs in vivo _____ *69*

Figure 7bis - TIMP-1 siRNA Reverse Transfection _____ *70*

Figure 8 - TIMP-1 over-expression in vivo mimics MSCs transplantation _____ *70*

Table 2: proteins overrepresented or present only in st- hMSC-CM _____ *72*

Figure 9 - Distribution into biological processes of the proteins overrepresented in stimulated hMSC-CM in human and mouse _____ *73*

Table 3: proteins overrepresented or present only in st- MSC-CM common to mouse and human _____ *74*

Figure 10 - Human and mouse MSCs conditioned media differentially stimulate monocytes differentiation _____ *76*

Figure 11 - Effect of human or mouse MSCs conditioned medium on tube formation assay _____ *78*

Figure 12 - Timp-1 blocking reverts the anti-angiogenic effect of mouse and human MSCs conditioned media _____ *79*

Figure 13 - Mouse and human MSCs-derived TIMP-1 quantification _____ *80*

Figure 14 - EVs from MSC-CM fully mimic the whole conditioned medium _____ *82*

Figure 15 - EVs from st- MSC-CM inhibit the migration of endothelial cells stimulated with VEGF _____ *84*

Figure 16 – Adenosine mediates the second anti-angiogenic effect of the EVs derived from st- MSC-CM _ *86*

Figure 17 – Adenosine affects migrating endothelial cells, with a mechanism dependent on ROS accumulation _____ *89*

Figure 18 – In vivo therapeutic potential of EVs derived from MSCs for the control of angiogenesis _____ *91*

Introduction

1 Principles of the Inflammatory Response

Inflammation is the organism's response to damaging endogenous or exogenous stimuli, including physical, chemical, or biologic agents. It serves to completely eradicate harmful mediators by killing and or removing them[1]. If the response is successful, the process is resolved and followed by reconstitution of the tissue architecture. In contrast, if the damaging agent persists, the inflammation evolves into a chronic response that may lead to major alterations of tissue architecture and functions.

Inducers of inflammation can be endogenous or exogenous. Exogenous stimuli can have a non-microbial or a microbial origin. Non-microbial exogenous inducers include allergens, irritants, foreign bodies and toxic compounds. Instead, microbial agents can be divided in virulence factors and pathogen-associated molecular patterns (PAMPs). They are recognized by host cellular receptors such as Toll-like receptors (TLRs), nucleotide oligomerization domain (NOD)-like receptors (NLRs), retinoic acid-inducible gene-I (RIG-I)-like receptors (RLRs), C-type lectin receptors or a set of specific pattern-recognition receptors (PRRs)[2], principally exposed on the surface of phagocytic cells and antigen presenting cells (APCs)[3]. Moreover, local inflammation can induce host cell death and or release of host cellular components that act as danger signals. All these endogenous mediators are recognized as damage-associated molecular pattern (DAMPs)[2] and they can trigger an inflammatory response by the interaction with specific PRRs. DAMPs can be classified depending on their origin and chemical nature in several different classes that range from the small uric acid, ATP and proteins to even part of organelles.

Notably, there is a high number of PPRs binding with PAMPs that are responsible even for the identification of DAMPs, thus further boosting the inflammatory response to eradicate the pathogen. Indeed, once PAMPs and/or DAMPs bind to their specific PRRs, they activate the immune response mainly by inducing gene expression and synthesis of a broad range of molecules, such as cytokines, chemokines and cell adhesion molecules, that all play a crucial role in the activation of the immune response. Final

functions induced by PAMP/DAMP-stimulated PRRs include the activation of the complement and coagulation cascade, opsonisation, phagocytosis, induction of pro-inflammatory signalling pathways and apopstosis[3].

1.1 Immune response activation by infectious agents

Once inflammation is induced, phagocytic cell-derived cytokines trigger another crucial step for the development of the inflammatory response: the endothelial cell activation (further details at point 2). Indeed, over a period of hours, resting endothelial cells, stimulated by immune cell-derived pro-inflammatory cytokines, acquired new proprieties supporting the leukocytes recruitment. This process underlies the four cardinal signs of inflammation *rubor et tumor cum calore et dolore* (redness and swelling with heat and pain)[1]. These symptoms are due to vascular changes - vasodilatation and plasma leakage – orchestrated to allow leukocyte migration from the blood flow into the injured tissue, thus supporting the inflammatory response.

The concomitant activation of both immune cells and endothelial cells provides the perfect combination to sustain the inflammatory response. Indeed, inflammatory cells, but also endothelial cells, can synthetize chemokines (like CXCL12, CCL21, CXCL1, CCL2 and CCL25) and others chemoattractants (such as C5s, leukotrienes and kallikreins). These molecules, accumulating by transcytosis or deposition on the endothelial luminal surface, augment endothelial adhesiveness. Thus, circulating immune cells easily stick to vessel wall and extravasate toward the site of the infection, where they are attracted by chemokine gradients[4].

According to that, once the inflammation begins, neutrophils are rapidly recruited in the damaged tissue, where they identify and destroy pathological agents. After that, immune response continues, firstly by recruiting monocyte-derived macrophages, and then by activating lymphocytes. These latter are essential players in the antigen-specific immune response, universally recognized as adaptive immunity (see section 1.2). Notably, initial phase of immunity gives a crucial contribution to adaptive immunity by presenting antigens required for lymphocyte activation.

1.1.a Molecular mechanisms of immune cells transmigration

The leukocyte recruitment from the blood flow into the inflamed tissue is a complex process, involving *tethering and rolling, adhesion, crawling* and *transmigration* of immune cells. This event implicates that immune cells cross not only layers of endothelial cells and pericytes, but also the basement membrane (BM), that is the specialized connective tissue rich in type IV collagen and laminin that underlies endothelial cell layers[5].

During the initial step of this process, endothelial selectins, such as E-selectin and P-selectin, mediate the leukocyte capture from the blood flow. Their expression in the resting vasculature is promoted by several pro-inflammatory signalling pathways. P-selectin, for example, also known as CD62P or GMP-140 or PADGEM, is usually stored in specific endothelial granules, called Weibel-Palade bodies (WPBs). In response to a variety of inflammatory signals such as thrombin, histamine, complement factors, oxygen species and cytokines, P-selectin is rapidly moved to the membrane surface, where, generally, it has a short half-life (about minutes). During this short-exposition on the luminal surface of the vessel, P-Selectin could interact with leukocytes mainly through P-selectin glycoprotein ligand-1 (PSGL-1), triggering their extravasation[6]. Contrary to P-selectin, E-selectin is not stored in specific vesicles, but its synthesis is transcriptionally regulated by cytokines. E-Selectin is largely spread within the vessels at sites of inflammation, where it drives the adhesion of neutrophils, monocytes and some memory T-cells, carrying many ligands of E-selectin like ESL-1 ligand (E-selectin ligand-1) and PSGL-1 (P-selectin glycoprotein ligand-1) [6].

Importantly, both P- and E- selectin are able to bind another crucial selectin constitutively express on leukocytes, L-selectin. L-selectin, or CD26L, LECAM-1, LAM-1, gp90MEL-14 has a prominent role in the leukocyte binding to activated endothelium at inflamed tissues, and to high endothelial venules (HEVs) in draining lymph node during the inflammatory response.

The selectin-based weak interaction of immune and endothelial cells induces leukocyte to start touching the vessel wall[7]. In case of inflammation, increased chemokines and chemoattractants, accumulated on the apical endothelial cell surface, determine more frequent contacts between immune and endothelial cells, thus resulting in the leukocyte rolling[5]. This transient interaction accomplishes the formation of membrane tethers at the

rear of leukocytes, that allows the deceleration of the rolling movement[5]. Consequently, the slow-movement of leukocytes give them the chance to adhere to endothelial cells trough another group of cell-adhesion molecules, called integrins. Integrins are a family of αβ-heterodimers, with 18 α-subunits and 8 β-subunits in vertebrates, that can assemble into 24 different known receptors[5]. Lymphocyte function-associated antigen 1 (LFA1 or αLβ2 integrin) is the most important integrin involved in the extravasation process during an inflammatory response.

Integrins bind a panel of immunoglobulin-like cell adhesion molecules (CAMs), such as VCAM and ICAM, expressed by endothelial cells exclusively after their exposure to a pro-inflammatory microenvironment[8]. Notably, integrins acquire a high-affinity ligand-binding site to CAMs afterwards a combination of events, encountering the integrin conformational changes induced from the cytoplasmic side together with the presence of a co-stimulus, like the binding of P- or E- selectin to PSGL1[5].

Integrins-CAMs interaction leads leukocytes and endothelial cells to be firmly connected, thus resulting in leukocytes adhesion and spreading on the luminal surface of the endothelium[5]. Finally, leukocytes start to crawl perpendicularly to the flow direction, following a chemotactic gradient, until they squeeze and transmigrate through the endothelial barrier. Notably, transmigration can occur via transcellular route, where leukocytes penetrate the endothelial cell, or, more often, via paracellular route, where they pass in tight narrow spaces among endothelial cells, generated as endothelial cell junctions transiently opened. Importantly, it has been reported that several endothelial cell adhesion molecules and receptors regulate the transmigration process, including platelet endothelial cell adhesion molecule 1 (PECAM1)[9], junctional adhesion molecules (JAMs)[10], endothelial cell-selective adhesion molecule (ESAM)[11] and CD99[12] (see sections 2 for more details).

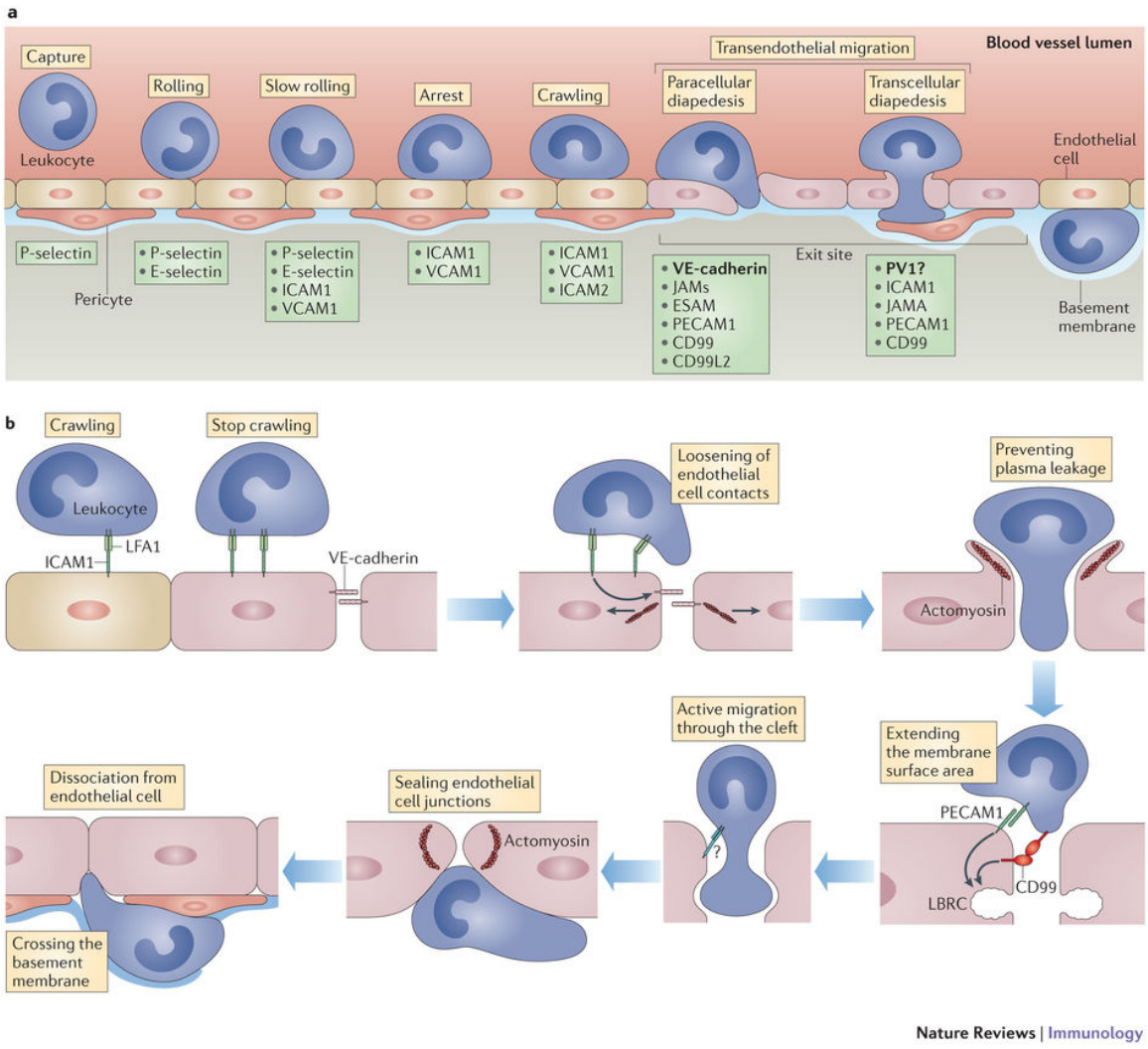

Figure I.A: The immune cells transmigration process

The bottom of the panel (a) provides a schematic representation of the diapedesis process. It encounters firstly capture, rolling, arrest and crawling of leukocytes on the luminal endothelial cell surface. Then, in a process that required few minutes to complete, immune cells cross the endothelial barrier. Several adhesion receptors of endothelial cells, partially listed here, are involved in this movement. B) Details of the final transmigration of immune cells into the injured tissue. Leukocytes take 15-20 minutes to pass the basement membrane underlying the vessels, and to accumulate into the damaged site. For the paracellular route, Vascular endothelial cadherin (VE-cadherin) has a prominent role, whereas plasmalemma vesicle protein 1 (PV1, component of fenestral and stomatal diaphragms) is the exclusive candidate involved in the transcellular diapedesis. CD99L2, CD99 antigen-like protein 2; ESAM, endothelial cell-selective adhesion molecule; ICAM, intercellular adhesion molecule; JAM, junctional adhesion molecule; LFA1, lymphocyte function-associated antigen 1; PECAM1, platelet endothelial cell adhesion molecule 1; VCAM1, vascular cell adhesion molecule 1. Picture from Nature Reviews Immunology 15, 692–704 (2015), doi:10.1038/nri3908.

Moreover, additional barriers have to be passed during leukocytes transmigration, such as the basement membrane and the extracellular matrix. To do that, leukocytes release different proteases such as metalloproteases (MMPs) and serine proteases that, through enzymatic digestion, degrade surrounding barriers and allow immune cells to follow chemotactic gradients, thus reaching the injured tissue.

1.2 Antigen-presenting cells initiate adaptive immune responses

Most tissues are inhabited by resident antigen-presenting cells (APCs) derived from bone marrow precursors, such as the immature dendritic cell (DC). In these sites, APCs activation allows the initiation of the adaptive immune response, mainly by supporting the activation of infiltrated leukocytes.

Principal sites of APC - T cell encountering are the secondary lymphoid organs (SLOs), such as spleen, lymph nodes, tonsils and Peyer's patches. Here, factors required for the activation of an adaptive immune response, such as antigen and its cognate T or B cells, are brought in close contact, thus increasing the possibility of their activation[13]. Antigens are presented to leukocytes by follicular dendritic cells (FDCs) and potentially also by macrophages derived from the subcapsular sinus. These latter are essentially involved in the clearance of both blood- and lymph- derived molecules and in the transfer of unprocessed antigens to DCs. Nevertheless, their implication in the antigen presentation to leukocytes remains to be determined. Thus, DCs predominantly guide the leukocyte response[13]. In all the tissues, including SLOs, immature DCs scrutinise the microenvironment looking forward pathogens or their derivate. Once the DC detects a pathogen or DAMPs, it gets activated. Thus, it undergoes maturation, that comprises changes resulting in the acquisition of a highly effective antigen-presenting cell (APC) phenotype. Accordingly, activated DCs digest the recognized pathogen, finally exposing its antigens on the membrane surface, in complex with the class I or class II mayor histocompatibility complex (MHC class I or II). Generally, endogenous peptides derived from cytosolic proteins are packed with MHC class I molecules and are exposed to CD8+ T cells. Differently, MHC class II molecules are loaded with exogenous antigens to be recognized by the TCR of CD4+ T cells[13]. Importantly, the T cell receptor (TCR) has evolved predominantly to distinguish antigens presented by APCs. Once bound to its peptide, TCR-mediated pathway induces T cells differentiation toward different cellular subsets. The TCR consists of two chains (α and β) and it is usually associated with a complex, known as CD3, composed of γ-, δ-, ε-, and ζ-subunits. Following the TCR ligation to its antigen, the CD3-cytosolic region initiates to propagate the intracellular signal responsible for leukocyte activation. Furthermore, CD4 or CD8 co-receptors are associated with the TCR to support and to stabilise the T cell-APC binding. Indeed, multiple additional signals are required for a complete and functional T cells activation.

They comprise even co-stimulatory molecules and stimulatory cytokines, belonging to the CD28 and tumour necrosis factor (TNF) families, which are expressed by mature DCs in response to inflammation. These signals prompt the leukocytes response, by promoting their survival and their differentiation in long-lived memory T cells[14].

To notice, despite these are the canonical functions of CD4 and CD8 T cells, antigen-stimulated leukocytes can be genetically programmed into a variety of different subsets depending on the cytokine environment. Thus, for example, helper CD4 T cells can generate Th1, Th2, Th17, Th9, Tfh, and Tregs[14]. Every subset has a specialized effective function, and a specific signature cytokine. Among them Th1 cells secrete IFN-γ, Th2 cells produce IL-2 and TNF-α as well, even if they are mostly specialized in the release of IL-4, IL-5, and IL-13. Furthermore, Th17 cells are characterized by IL-17A, IL-17F, and IL-22[14].

1.3 Resolution of the inflammatory response

The resolution of the inflammation is an active event aimed to the clearance of immune cells and the re-establishment of the functional homeostasis.

Starting when pathogens are removed, it consists in the activation of pathways blocking the synthesis and the release of pro-inflammatory factors, with the concomitant elimination of any mediator remaining in the extracellular space. This, in turn, decreases the number of leukocytes recruited in the injured tissue, further limiting the oedema formation. Additionally, infiltrated leukocytes return in the blood flow, instead eosinophils and neutrophils undertake dying process, such as apoptosis.

Another mechanism involved in the resolution process is the release, by both immune cells and resident cells, of soluble factors that actively inhibit the inflammatory response. Among them, there are glucocorticoids, catecholamines, prostaglandins of the E-series, nitric oxide (NO), and the cytokines interleukin IL1 receptor antagonist, IL-4, IL-13, IL-10, transforming growth factor (TGF)-β, and the soluble receptors for IL-1RII, TNF-RI/II, or the Duffy receptor for IL-8. To note, it has been reported that these soluble factors allow apoptosis and necrosis in the same cells[15].

Macrophages represent one of the most important source of anti-inflammatory and reparative mediators. In particular, these functions have been ascribed to alternatively activated macrophages (M2), able to release IL1 receptor antagonist, IL10, TGF-β and VEGF, in order to regulate cell proliferation and extracellular matrix (ECM) remodelling, thus supporting the resolution phase[16]. For example, macrophage-derived TGF-β induces myofibroblast differentiation and the activation of tissue inhibitors of metalloproteinases (TIMPs), involved in ECM regulation and collagen deposition. Furthermore, VEGF, a potent angiogenic factor, initiates the angiogenesis process during the resolution phase with the consequent restoration of oxygen supply (described in the section 2.4)[16].

Importantly, many other cells are involved in the repair of the injured tissue. In particular, T regulatory cells (Treg) are recruited in the inflamed site. They are a subset of CD4+CD25+ T lymphocytes, identified by the expression of the transcription factor Foxp3. Treg cells are responsible for the release of immunosuppressive and pro-resolving cytokines, such as IL10 and TGF-β, in order to both suppress an activated immune response, that is no more required, and to repair tissue architecture. In the case of insolvency process, the inflammation is preserved and it determines the development of autoimmune and chronic disease.

2 Inflammation and angiogenesis: the endothelial cell activation

As described above, a fundamental step during the inflammatory response is the rapid recruitment of immune cells. In this contest, vascular endothelial cells (ECs) have a major role by initiating the "endothelial cell activation", which entails a series of processes to modify resting EC phenotype in order to support various phases of the inflammatory response. Endothelial activation can occur rapidly, in a manner independent of new gene expression (type I activation), and, subsequently, slower depending on the gene expression regulation (type II activation) [17].

2.1 The resting blood vasculature

Arteries, veins and interconnecting capillaries, compose the blood vasculature. It represents the system through which nutrients, metabolites and cells circulate through the whole body. The most important site where exchange occurs is the microvasculature, constituted by arterioles, capillaries and venules. All mature vessels are surrounded by a basement membrane (BM), composed mainly of collagen IV and laminin, and pericytes, which sustain the vessel stability. In addition, endothelial cells (EC) assemble the vessel inner layer[18].

Despite the crucial structural role of endothelial cells, the endothelium is also specialized in regulating blood fluidity, vessel wall permeability and leukocytes recruitment both in resting and in inflammatory conditions[19].

In non-inflamed tissue, the blood fluidity, for example, is actively maintained by EC through the suppression of the coagulation event by tissue factor pathway inhibitors (TFPIs). Both heparan sulphate proteoglycans, binding to anti-thrombin, and thrombomodulin inhibit thrombin activity, thus blocking the cleavage of fibrinogen, a key step in the blood clot formation[17]. Moreover, the release of nitric oxide (NO) and prostaglandin I_2 (PGI_2) by resting endothelial cells eliminates the platelet activator signals[17]. This anti-coagulation effect is further supported by sequestering the von Willebrand factor (vWF), crucial for platelet adhesion, in specific endothelial granules called Weibel-Palade bodies (WPB)[20].

Another fundamental function of the resting endothelium is to maintain the quiescence in circulating leukocytes. Indeed, since venules represent the principal sites where leukocytes extravasate from the blood flow into the tissue during an inflammatory response, activation of EC is required for efficient leukocyte transmigration. Basically, resting endothelial cells block this process by minimally synthetizing or by hiding adhesion molecules, such us P- selectin or VCAM, necessary for the attachment and the recruitment of immune cells[21]. Additionally, the endothelium directly acts on leukocytes by secreting NO, able to prevent the switch of immune cell phenotype from the naïve one to the motile form[17].

Therefore, endothelial cell activation is essential for a correct inflammatory response, as following described.

2.2 Type I activation of endothelial cells

Hemodynamic changes, encountering vasodilatation and increased permeability, are the first observable events in the inflammation. At the injured site, branches start an extensively vasodilatation that increases the blood flow. As a consequence, augmented leukocytes recruitment is induced and the inflammation supported.

Relaxation of vascular smooth muscle cell tone has prominent role in this process. It is primarily induced by vasodilators, as nitrates, that directly relax muscle cells, or by factors, such as prostacyclin (PGI_2), that act indirectly on endothelial muscle tone by stimulating the release of relaxing mediators, such as thrombin, histamine and leukotriene[17].

The binding of these specific vasodilatation inducers, to the extra-cellular domain of endothelial heterotrimeric G-protein-coupled receptor (GPCR) typically triggers the type I activation in the endothelium[17]. This interaction induces the appropriate GPCR structural changes on its cytoplasmic loops and tail, which catalyse the exchange of GDP with GTP on the α subunit of the G protein. Consequentially, the G-protein αq subunit dissociates from the G-protein $\beta\gamma$ dimer and it activates β isoforms of phospholipase C ($PlC\beta$). This latter, in turn, catalyses the release of inositol-1,4,5-trisphosphate ($InsP_3$) from the membrane lipid phosphatidylinositol-4,5-bisphosphate ($PtdIns_{(4,5)}P_2$). Free $InsP_3$

induces the release of $Ca^{2+}$from the endoplasmic reticulum stores causing transient intracellular elevations in the cytosolic free Ca^{2+}. The increased cytosolic free Ca^{2+}has a triple effect on the vascular branch: indeed, it supports vasodilatation, but also permeability, diapedesis and, concomitantly, the vessel activation.

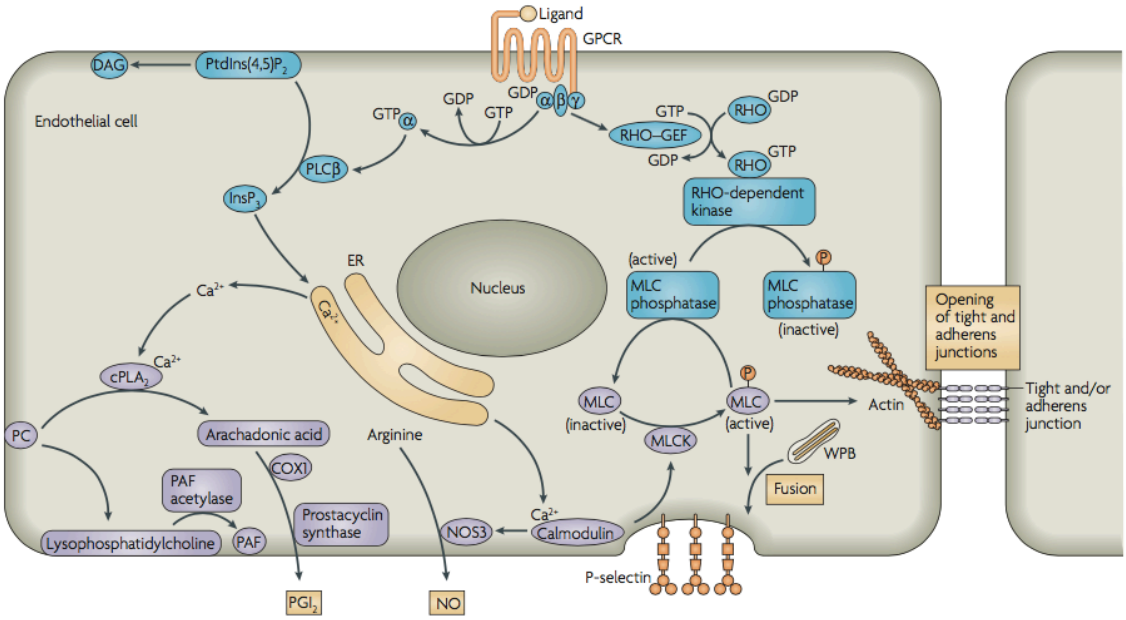

Figure I.B: Type I activation of endothelial cells

Here, the molecular mechanisms induced by the binding of vasodilatation-inducers to GPCRs on the endothelial cell surface, are described. The process leads to the accumulation of cytosolic free Ca^{2+}, with the consequent vasodilatation, augmented permeability and diapedesis that all support the leukocytes recruitment into the damaged tissue. In particular, cytosolic free Ca^{2+} is involved 1) in the prostacyclin synthase into prostaglandin I2 (PGI2 or prostacyclin), 2) in the activation of nitric-oxide synthase 3 (NOS3) and, thus, in the production of nitric oxide (NO), 3) in the phosphorylation of myosin light chain (MLC). Picture from Nature Reviews Immunology 7, 803-815 (October 2007), doi:10.1038/nri2171

Vessel dilatation allows the recruitment of cells in the injured tissue. The free Ca^{2+} mediates this process, by activating the cellular phospholipase A2 (cPLA2) that cleaves membrane phosphatidylcholine into arachidonic acid and lysophosphatidylcholine. Free arachidonic acid is sequentially converted first to prostaglandin H2 (by COX1) and then to PGI2 (by prostacyclin synthase). PGI2 acts on the smooth muscle of arterioles, with the final vascular tone relaxation[17]. This effect is synergized also by Nitic Oxide (NO), another product downstream the Ca^{2+} signalling. Indeed, free Ca^{2+} binds the adaptor protein calmodulin, leading to the activation of nitric-oxide synthase 3 (NOS_3) that starts to produce NO, a potent vasodilator. In addition to this effect, the Ca^{2+}-calmodulin

complex positively influences the vascular permeability by activating myosin-light-chain kinase (mlCK). These kinases mediate the myosin-light-chain phosphorylation, that is required to induce the filament contraction[22] and thus the opening of gaps between adjacent endothelial cells.

Besides an augmented vasodilatation and permeability, Ca^{2+}- signalling in EC is also able to support immune cell recruitment. Indeed, actin filament contraction determines also the release of storage granules, known as Weibel–Palade bodies (WPB), bringing P-selectin to the luminal surface of EC[17]. As described before, this is a crucial step for the immune cell tethering, rolling, adhesion, crawling and transmigration during the diapedesis[23]

2.3 Type II activation of endothelial cells.

The type II activation can follow the first phase of endothelial cell activation. It requires a more persistent inflammatory response and implicates gene expression regulation.

Important mediators of this process are two proteins secreted mostly by activated leukocytes: tumour-necrosis factor (TNF; also known as TNFα) and interleukin-1 (Il-1). Both signals initiate different cascades converging to specific transcription factors, nuclear factor-κB (NF-κB) and activator protein 1 (AP1), able to mediate new genes transcription [24]. In particular, type-II-activated endothelial cells display enhanced PGI_2 synthesis, due to the genetic induction of COX2, and also increased synthesis of chemokines and adhesion molecules such as CXCL8, E-Selectin, VCAM1 and ICAM1[17]. Thus, the furtherly induced vasodilatation and the high expression of attractive and adhesive proteins boost the recruitment of immune cells and their activation.

To switch off this process, it results strictly necessary to remove the activator signals, by for example the elimination of the infection, in synergy with the induction of a variety of negative feedback loops that shut off inflammatory gene expression, for example by terminating NF-κB activation[25].

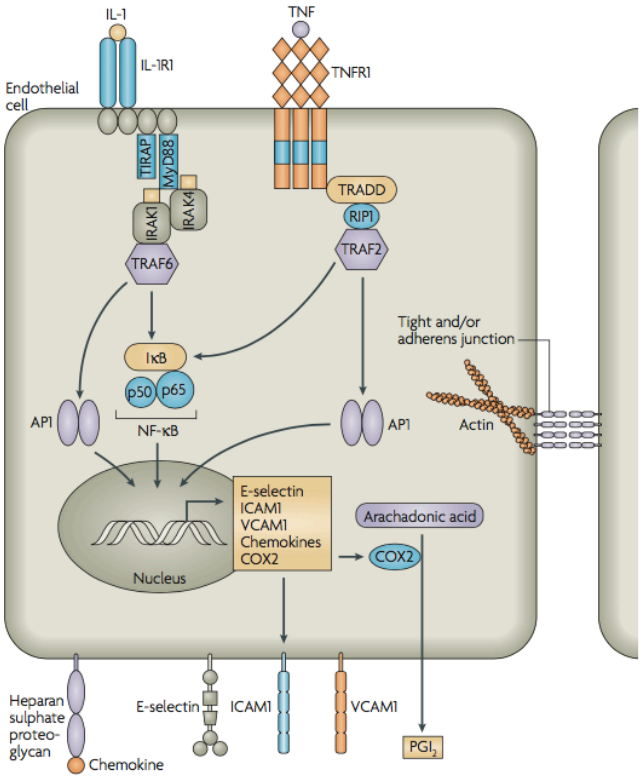

Figure I.C: Type II activation of endothelial cells

Once pro-inflammatory cytokines, like interleukin-1 (IL-1) or tumour-necrosis factor (TNF), bind their receptors on endothelial cell surface, type 1 IL-1 receptor (IL-1R1) and TNF receptor 1 (TNFR1) respectively, signalling complexes are activated. Thus, in response to these stimuli, mitogen-activated kinase kinase kinases (MAPKKKs) are activated and, in turn, transcription factors translocate into the nucleus. In particular, the activation of transcription factor nuclear factor-κB (NF-κB) and activating protein 1 (AP1) initiate the expression of pro-inflammatory mediators, such as E-selectin, intercellular adhesion molecule 1 (ICAM1) and vascular cell- adhesion molecule 1 (VCAM1); chemokines; enzymes, such as cyclooxygenase-2 (COX2); and unknown effector proteins that reorganize actin filaments. Finally, the synthesis of PGI_2 is supported, actin filament reorganization is induced to open exit sites and leukocytes recruitment is further enhanced. Picture from Nature Reviews Immunology 7, 803-815 (October 2007), doi:10.1038/nri2171

3 Angiogenesis and inflammation

The failure of the immune system to resolve inflammation and the consequent requirement of further leukocytes leads to an important additional change, the initiation of the vascular remodelling.

Angiogenesis is a finely tuned process, that involves endothelial cell proliferation and migration, rearrangement of the basal membrane, and that, finally results in a new capillaries network[26]. Beside the precise inducer of this process remains unclear, activated T cells and mononuclear phagocytes had been suggested to be the principal source of pro-angiogenic factors during the adaptive immune response[27].

Accordingly, the vascular remodelling and the generation of new blood vessels support the inflammatory response, sustaining the leukocyte recruitment within the inflamed tissue. For that reason, disease states associated with a chronic inflammation, such as diabetes, rheumatoid arthritis, asthma and infection are often connected with a dysfunctional vasculature[26].

3.1 Pro-angiogenic growth factors

Typically, in hypoxia or inflammatory conditions, growth factors trigger angiogenesis. Among them, the best described pro-angiogenic factors are cytokines such as vascular endothelial growth factors A, B, C and D (VEGF-A, VEGF-B, VEGF-C and VEGF-D), fibroblast growth factor 2 (FGF2) and angiopoietin-1 and -2 (Ang1 and Ang2), which signal respectively through VEGFR2 and VEGFR3, FGF receptor 1 (FGFR1), and tyrosine kinase receptor2 (TIE2).

Growth factor receptors are mostly receptor tyrosine kinases (RTKs). Thus, after binding their ligands, RTK dimerization occurs with the phosphorylation of the homodimer partners, in a process known as cross-phosphorylation. Upon this, three different pathways are usually triggered; the RAS − extracellular − signal − regulated kinase 1 (ERK1)/ERK2 pathway, the phosphoinositide 3 − kinase (PI3K)-AKT pathway and the Ca^{2+} - PLCγ pathway[28]. All these cascades support the angiogenic response by promoting endothelial cell growth, survival and migration.

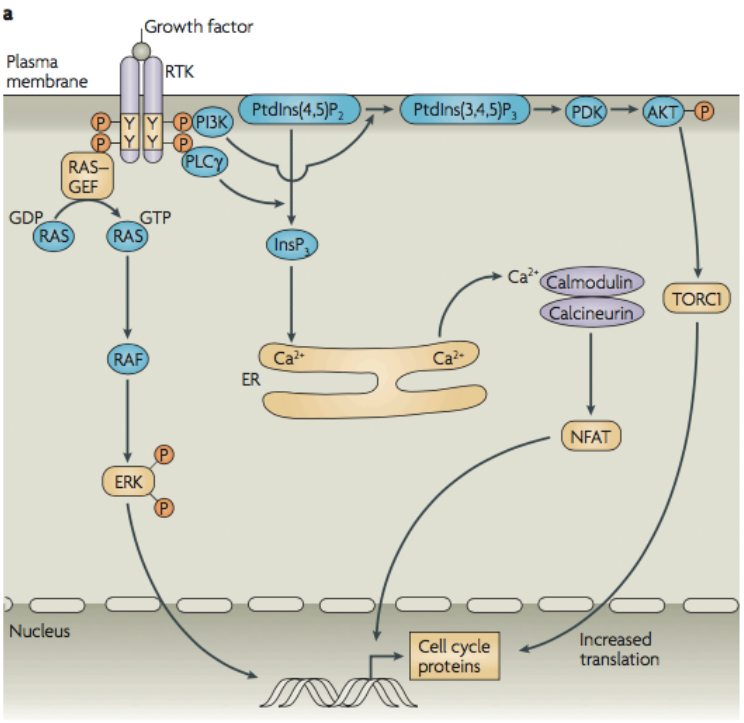

Figure I.D: Molecular signalling triggered by growth factors in endothelial cell

In response to growth factors, angiogenesis initiates. The involved signalling cascade encounters the activation of receptor tyrosine kinases (RTKs). They, in turn, 1) recruit constituents of the RAS–GEF (guanine nucleotide exchange factor) complex, required for the activation of ERK, 2) phosphorylate and activate phospholipase Cγ (PLCγ), that γ initiates the accumulation of cytosolic free $Ca^{2+}$and 3) bind regulatory subunits of phosphoinositide 3-kinase (PI3K). Finally, several transcription factors are translocated into the nucleus and specific genetic targets are modified. Picture from Nature Reviews Immunology 7, 803-815 (October 2007), doi:10.1038/nri2171

3.2 Steps in angiogenesis

Angiogenic sprouting is one of the most extensively characterized mechanism of blood vessel formation in the adult organism[29]. It consists first in the activation phase, that triggers a switch in quiescent endothelial cells to a sprouting, migrating and proliferating phenotype; then, a resolution phase occurs, leading to the maturation and stabilization of the new branches[30]. It is now well accepted and described in literature that several types of specialized endothelial cells are required to form a functional branch. Among them, tip cells, which lead the way, stalk cells, that proliferating elongate the sprout, and phalanx cells, that consolidate the new vessel, play the most important roles[31]

During capillary sprouting and development, four different and crucial steps can be described, each influenced by the function of specific endothelial cells[32]:

- Selection of sprouting Tip cells;
- Elongation of the new branch by proliferating Stalk Cells;
- Sprout fusion and lumen formation
- Vessel stabilization and maturation with the pericyte recruitment.

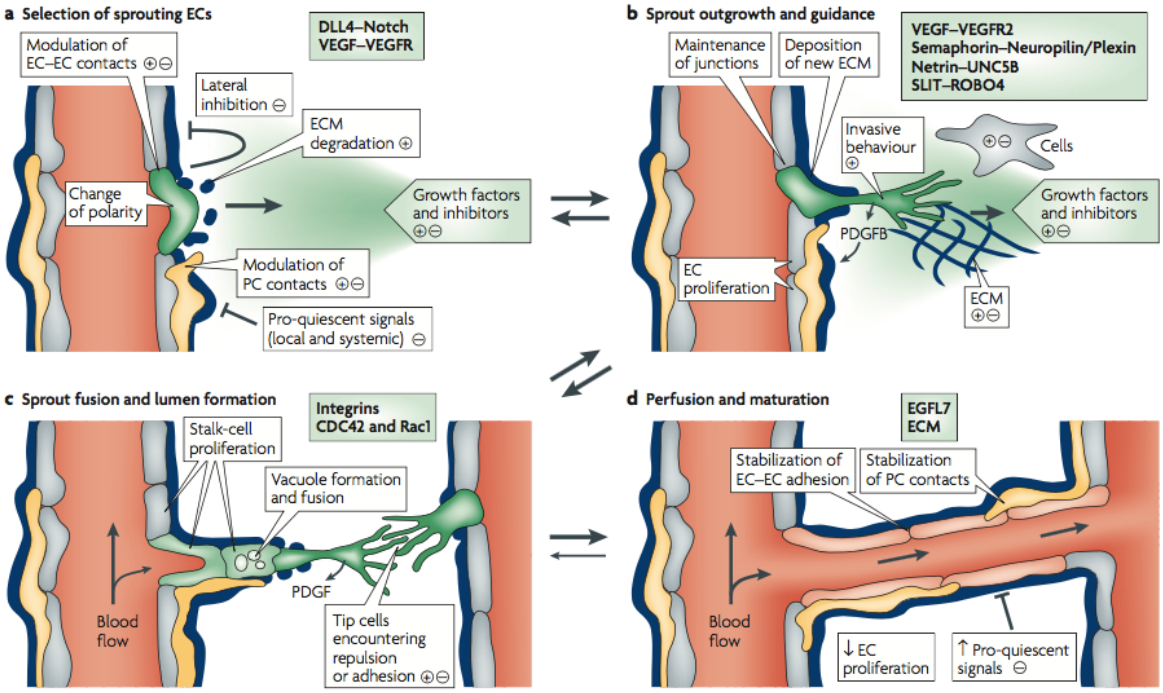

Figure I.E: Angiogenic sprouting

Angiogenic sprouting is a finely regulated process, regulated by the balance between pro-angiogenic signals (+), and quiescence inducers (-). A) In some conditions, such as during an inflammatory response, pro-angiogenic factors can be accumulated, and a pro-angiogenic gradient is generated. In this context, A) some endothelial cells (green-tip cells) are selected to sprout, despite others fail to respond (grey-stalk cells). B) Tip cells undergo phenotypical changes to acquire a motile state, thus, leading the elongation of a new branch protrusion. C) Once adjacent new vessel protrusions encounter each other, anastomosis drives their fusion and, consequently, the lumen is formed. Lumen formation involves mostly stalk cells, although the precise mechanism is not yet described. The maturation of the new vessels D) is accomplished with the stabilization of cell junctions, the recruitment of pericytes and the deposition of the basement membrane. DLL4, delta-like-4 ligand; EGFL7, epidermal growth factor ligand-7; ROBO4, roundabout homologue-4; VEGFR2, VEGF receptor-2. Nature Reviews Molecular Cell Biology 8, 464-478 (June 2007) | doi:10.1038/nrm2183

3.2.a Tip cell selection and migration

In the presence of a growth factor gradient, for example induced by activated immune cells, vessel-surrounding pericytes detach from the basement membrane by proteolytic degradation and, at the same time, endothelial cells modify their cell-cell junctions. This results in vessel dilatation and consequently in plasma protein extravasation, finally leading to the deposition of a provisional extracellular matrix (ECM) scaffold.

The pro-angiogenic gradient drives endothelial cells into this ECM scaffold, by inducing in them an invasive phenotype. Thus, one specific endothelial cell flips its apical basal polarity, modulates intercellular connections and acquires motile activity, becoming the cell directing the vascular sprout, known as tip cell. In this process, tip cells to avoid the diffusion of the motile phenotype in the neighbouring cells activate negative feedbacks. In this way, contemporary movement of all cells is prevented and the sprouting of tubular

structures can correctly occur. Indeed, the endothelial cells exposed to high levels of growth factors, the potential tip cells, increase the expression of Dll4 and JAGGED1. Dll4 and JAGGED1 are specific ligands of Notch receptors (Notch 1, 3, 4) that are expressed on the endothelial cell membrane. After the Dll4 or JAGGED1 binding to their receptors on the membrane of the neighbouring endothelial cells (future stalk cells), Notch is cleaved. Consequently, the Notch intracellular domain (NICD) acts as transcriptional factor, regulating EC specification by suppressing the tip cell phenotype and positively controlling the stalk cell phenotype. In this way, only tip cells gain and retain the leading position, allowing the correct tubular sprouting of the migration front[33].

Therefore, the principal role of tip cells is to migrate. The EC migration is a dynamic process involving the adhesion of the cellular front and the detachment of the rear in response to pro-angiogenic factors. The attractive signal, is sensed by these plasma membrane protrusions, inducing actin polymerization with the consequent elongation of filopodia and lamellipodia, through wich ECs probe the surrounding space. Lamellipodia are characterised by a veil-structure with a highly branched actin network. In contrast, filopodia, that usually sprout from lamellipodia, are long membrane protrusions containing tight parallel bundles of filamentous actin (F-actin)[31].

Profilin, Ena/Vasp, and Formin families play a crucial role in this process, supporting the polymerization of G-actin into long F-actin strings, components of filopodia and lamellipodia. Once extended, these membrane protrusions attach to the extracellular membrane (ECM) by the binding of their superficial integrins with several extracellular matrix components such as laminin, fibronectin, and collagen. These interactions induce the formation of focal adhesion points, regulated by focal adhesion kinase (FAK), and the following attachment of the cellular front to the ECM. Finally, the contraction of actin filaments pulls the cell toward these directions, inducing forward movement [34] and the initiation of tubular structure formation. However, to fully complete tube formation, the elongation of the new branch, thanks to the prominent role of stalk cells, is required.

3.2.b Sprout extension

Stalk cells play a crucial role in the formation of tubes and mature branches. In comparison to tip cells, stalk cells have less filopodia and lamellipodia, but they are characterised by a higher proliferative potential. This stalk cell proliferation is strongly

required for the sprouting of the new vessel branch. Indeed, decreased stalk proliferation correlates with branch regression[35]. A further crucial step for the correct outgrowth of the nascent vessel is the direction of the stalk cells division. This movement is usually perpendicular to the long axis of the vessel, toward the growth factor gradient. Interestingly, pro-angiogenic gradients orientate the stalk proliferation, and consequently the vessel sprouting, only in the absence of the blood flow[35]. Indeed, in perfused vessels, the shear stress induced by blood flow, that is sensed by the transmembrane proteins PECAM1, VE-cadherin and VEGFR2 and transduced by CDC42-dependent signalling, dictate the EC polarity. Thus, it has been suggested that only vessels with a blind-ended, and consequently non-perfused, are able to elongate in response of the growth factor gradients and not to the shear stress.

Once the new branch is formed, stalk cells also create junctions with neighbouring cells and accumulate basement membrane to stabilise the new spout.

Notably, Notch activation, typical of stalk cells, leads to the down-regulation of tip cell-related genes, which include VEGFR2, platelet-derived growth factor B (PDGFB), the netrin receptor unc-5 homolog B (UNC5B), the notch ligand DLL4, EC-specific molecule 1 (ESM1), the CXCR4 and the membrane-inserted matrix metalloprotease 14 (MMP14) [36,37,38]. Contrarily, stalk cells up-regulate VEGF decoy receptors VEGFR1 and soluble VEGFR1, thus reducing the VEGFR2 signalling, responsible for the induction of the tip cell differentiation.

Thus, proliferating stalk cells elongate the branch protrusion in the tip cell direction[35].

3.2.c Anastomosis, lumen formation and vessel maturation

To form a blood vessel, elongated sprouts have to connect each other and to organize into a mature branch. Vascular anastomosis is the process that drives the sprout fusion. It can involve two sprouting tip cells ('head-to-head' anastomosis), or one spouting tip cell and a mature blood vessel ('head-to-side' anastomosis). In both conditions, the fundamental step is the development of a stable contact between two endothelial cells. To do that, in the initial phase of the anastomosis, sprouting tip cells weakly contact surrounding cells by moving toward and backward membrane protrusions several times, until one single connection is settled and stabilized. This occurs trough the accumulation of junction

proteins, such as occludins and cadherins, responsible for the formation of intercellular adherent connections.

Besides that, another essential step for the complete branch development is the formation of a vascular lumen. Lumen formation is a critical step during angiogenesis and several mechanisms have been proposed to explain it, including[35]:

a. **Intracellular vacuole coalescence**, in which intracellular and intercellular vacuoles can connect each other to form a lumen;
b. **Intercellular vacuole exocytosis**, which consists in the release of vacuoles that accumulating in the extracellular space can induce the formation of the lumen;
c. **Luminal repulsion** determines by the repulsion of the negatively charged apical membrane (luminal) of stalk cells.

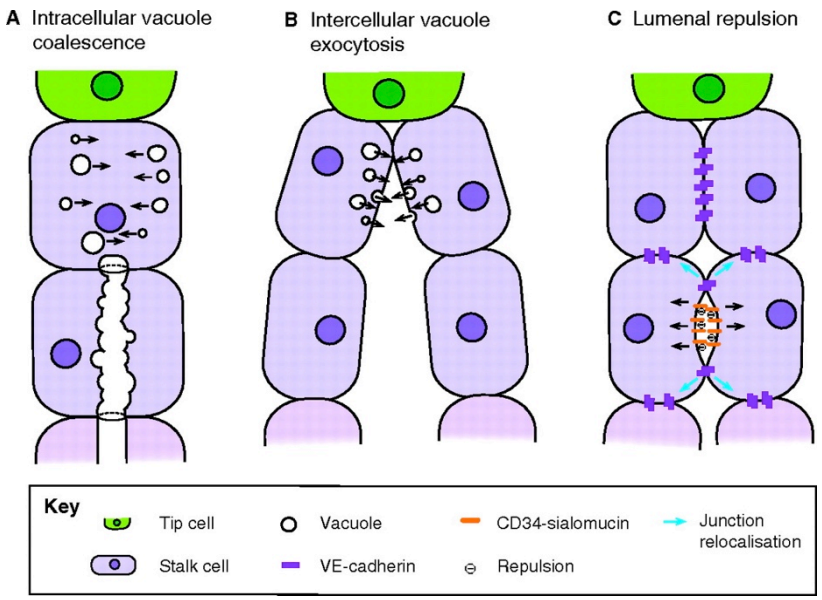

Figure I.F: Hypothesised mechanism for lumen formation

Schematic representation of A) intracellular vacuole coalescence. The lumen is formed by the fusion of intracellular vesicles of neighbouring cells. B) Intercellular vacuole exocytosis. Endothelial cells release vacuoles by exocytosis. Accumulation of vacuoles into the intercellular space initiates the lumen formation. C) Luminal repulsion. The last model proposed encounters the repulsion of the apical luminal membrane of endothelial cells in the new branch. This is due to the high concentration of negatively charged CD34-sialomucin (orange) at the cell-cell contact sites. Thus, the electrostatic repulsion determines the separation, thereby establishes the lumen formation. Development 2011 138: 4569-4583; doi: 10.1242/dev.062323

Once a vessel branch is formed, ECs become quiescent; for that, only 0.01% of endothelial cells are dividing in an adult organism[31]. The most quiescent ECs are the "Phalanx cells"; they form a smooth monolayer, lining the new vessel, and thus

resembling ancient Greek soldiers in a phalanx formation[39]. Indeed, phalanx cells migrate poorly in response to pro-angiogenic factors, extending only few filopodia. In contrast, they are able to modify the surrounding ECM and the intercellular connections, by depositing a basement membrane and establishing junctions. Most importantly, differently from stalk cells, phalanx cells are characterized by increased quiescence and reduced mitogenic response to VEGF[31].

As described, tip cells selection, sprout extension, anastomosis and lumen formation drives the formation of a new tubular structure. However, a new vessel remains immature until basement membrane is deposited and mural cells are recruited.

Depending on their density, morphology, location and markers expression, mural cells can be classified in vascular smooth muscle cells (vSMCs) and pericytes. vSMCs represent the contraction force of arteries and veins, where they form multiple concentric layers. In contrast, pericytes reside at the interface between the endothelium and the surrounding tissue, embedded within the basement membrane of capillaries[40]. During an angiogenic process, pericytes recruitment to a new vessel is driven by PDGFB, expressed mainly by the sprouting endothelium. However, the precise function of these cells is not fully elucidated. Several functions, all relevant for a correct angiogenesis, have been proposed; among them, pericytes can sense pro-angiogenic stimuli and hemodynamic forces, modify the ECM by degrading or deposing it, control endothelial proliferation and differentiation and, covering all the tube length, they can integrate signals from distant ECs. Accordingly, their recruitment is recognized as a hallmark for ending the angiogenesis process.

3.3 ECM-driven signalling during angiogenesis

Vascular sprouting, as already described, is the prevalent mode for the vascular expansion. It involves the invasion of avascular areas by proliferating and migrating endothelial cells, thus requiring proteolytic degradation of the extracellular matrix (ECM). The major proteinases involved in ECM modification are the matrix metalloproteinases (MMPs) and the ADAMT (a disintegrins and metalloproteinases with thrombospondin domains) metalloproteinase[41]. These enzymes play a crucial role not only in the matrix

invasion of tip cells, but also in the formation of biologically active molecules that sustain the accumulation of pro-angiogenic signals, also known as matrikines.

3.3.a Matrix metalloproteinases (MMPs)

The initial stage of new vessel formation, in terms of both the induction of pro-angiogenic signals and the tip cell migration *per se*, requires the fragmentation of the basement membrane and of the interstitial matrix.

The basement membrane is the layer underlying the blood vessel endothelium. It is composed mainly of fibrillar type I collagen and, depending on the tissue type, different amounts of type III and type V collagens, non-collagenous glycoproteins (such as tenascins, fibronectin, vitronectin) and proteoglycans carrying glycosaminoglycan chains (such as chondroitin-, dermatan- and keratan-sulphate proteoglycans)[42]. Underneath the basement membrane, there is the interstitial matrix of the tissue stroma. This is a tightly crosslinked network (50–100 nm in thickness) constituted mainly of 1–2 laminin isoforms, nidogen 1 and/or nidogen 2, the heparan sulphate proteoglycan perlecan and several glycoproteins. The collagen-degrading enzymes, involved in the continuous basement membrane rearrangement, are members of matrix metalloproteinases (MMP) family[43]. MMPs, which comprise 25 different members in mice and 24 different members in humans, are endopeptidases with several conserved protein domains, among them a Zn^{2+} binding motif in the catalytic domain[44]. Factors including pro-inflammatory cytokines, growth factors and hormones control their gene expression. Once expressed, they are secreted as zymogens or pro-enzymes, that acquire a catalytic activity only after the removal of their amino-terminal pro-domain[44]. This cleavage can be mediated by other MMPs or proteases. Each MMP has a specific molecular mass (between 20-100 kDa) and specific substrates. For example, fibroblast type collagenase (MMP-1), neutrophil type collagenase (MMP-8), and membrane type 1 matrix metalloproteinase (MT1- MMP or MMP-14) cleave types I, II and III collagens. Type I and type IV collagens are targets of gelatinase A/type IV collagenase (MMP-2). However, type IV can be also digested by gelatinase B/type IV collagenase (MMP-9)[44].

Importantly, the MMP activities are endogenously regulated by TIMPs (tissue inhibitors of metalloproteinases). The TIMP family includes four members, TIMP-1, TIMP-2, TIMP-3 and TIMP-4, with a tissue specific, constitutively expressed or induced by cytokines and growth factors[45]. They are multifunctional proteins, that, with certain degree of preference, regulate MMP activity by forming tight-binding inhibitory complexes[43] (Figure I.H, Table 1). All TIMP proteins are soluble, with the exception of TIMP-3 that is linked to the ECM; however their structural organization is well conserved; indeed, all mammalian TIMPs maintain two distinct domains, the N-terminal domain (about 125 amino acid residues) and the C-terminal domain (about 65 residues), each stabilized by disulphide bonds[41].

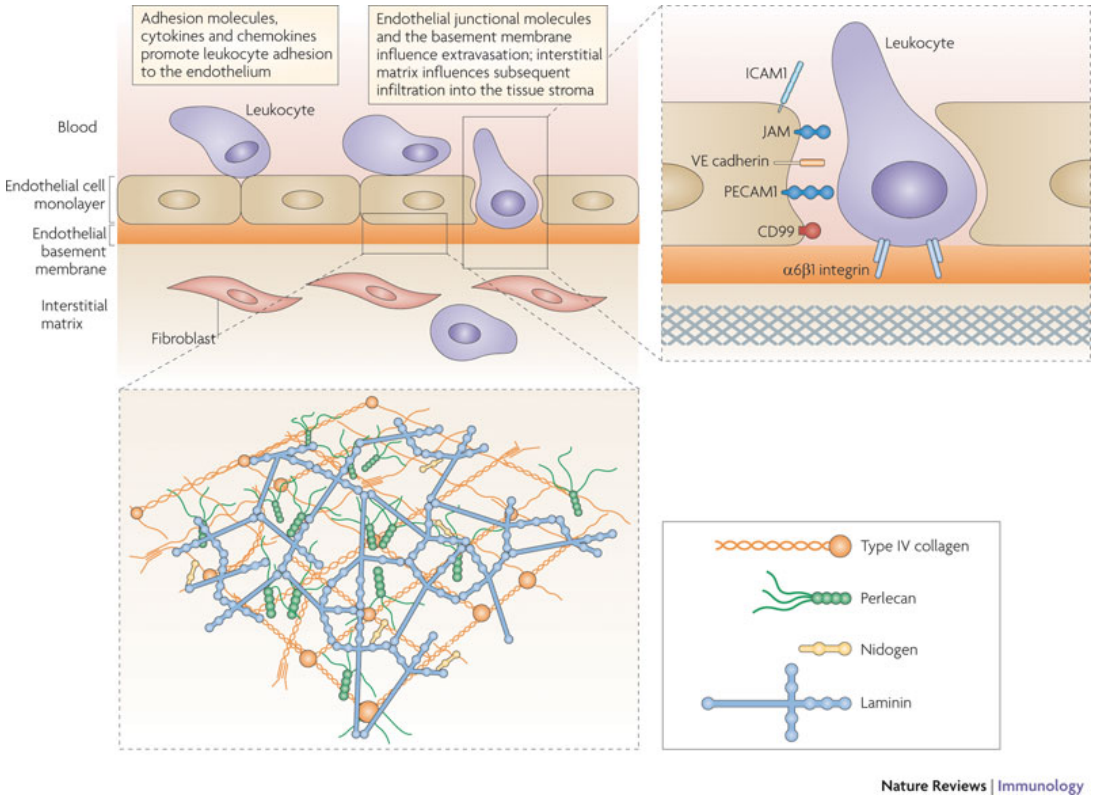

Figure I.G: Extracellular matrix underlying the vasculature

Vessels are underlined by the basement membrane and the interstitial matrix. They are distinct structures of the extracellular matrix (ECM). In particular, the interstitial matrix is mainly characterized by fibrillar type I collagen, type III and type V collagens (depending on the tissue type), non-collagenous glycoproteins (such as tenascins, fibronectin, vitronectin) and proteoglycans carrying glycosaminoglycan chains (such as chondroitin-, dermatan- and keratan-sulphate proteoglycans). In contrast, the basement membrane is usually composed by a singular type IV collagen isoform, nidogen 1 and/or nidogen 2, the heparan sulphate proteoglycan perlecan and several minor glycoproteins. ICAM1, intercellular adhesion molecule 1; VE cadherin, vascular endothelial cadherin. Nature Reviews Immunology 10, 712-723 (October 2010) doi:10.1038/nri2852

Property	TIMP-1	TIMP-2	TIMP-3	TIMP-4
Glycosylation	Yes	No	Partial	No
p*I*	8.47	6.48	9.14	7.21
No. of residues[a]	184	194	188	194
M_r[b]	20,709	21,755	21,690	22,329
MMP inhibition	Weak for MMP-14 -16, -19, and -24	All	All	Most
Other MMP inhibition	ADAM10	ADAM12	ADAM10, 12, 17, 28 and 33; ADAMTS-1, -4, and -5, ADAMTS-2 (weak)	ADAM17[d] and 28, ADAM33 (weak)
Pro-MMP interactions	Pro-MMP-9	Pro-MMP-2	Pro-MMP-9 and pro-MMP-2	Pro-MMP-2
Other partners	CD63 and LRP-1 (MMP-9 complex)	$\alpha 3\beta_1$ integrin LRP-1	EFEMP1, VEGFR2 and Angiotensin II receptor	
Apoptotic effects	Negative	Positive Negative	Positive	
Angiogenesis	Negative	Negative	Negative	Negative
Chromosomal location: human	X11p11.23–11.4	17q23–25	22q12.1–q13.2	3p25
Mouse	X A1.3	11 E2	10C1–D1	6 E3
Synapsin gene[c]	I	None	III	II
Genetic disorder			Sorsby fundus dystrophy	

[a]Mature protein.
[b]Excluding any glycans.
[c]Nested in intron V of the listed synapsin.
[d]Inhibited by N-terminal domain of TIMP-4.

Additionally, TIMPs are important determinants of cell function, since they exert their role not only by inhibiting MMPs activity, but also control apoptosis and cell cycle by a MMP-independent mechanism[45]. For example, it has been reported that TIMP1 has anti-apoptotic effects on some cell types (like Burkitt lymphoma cells and breast cancer cells) and, together with TIMP2, promotes cell proliferation. Indeed, it has been reported that TIMP1 is involved in the survival signalling network mediated by the tetraspanin CD63 and by focal adhesion kinase, phosphoinositide 3-kinase and ERK[45]. Furthermore, TIMP2, once linked to α3β1 integrin, induces G1 phase arrest.

This anti-apoptotic effect is further exerted by TIMP3, on several tumor cell lines, endothelial cell and smooth muscle cells, even if with a mechanism dependent on metalloproteinase activities. Notably, TIMP3 can either promote or inhibit apoptosis depending on the model system[45].

Therefore, the finely regulated balance between MMPs and TIMPs is extremely important to control angiogenesis, for its implication in the invasiveness of tip cells and the release of angiogenic factors as described below.

3.3.b Invasiveness of Tip Cells

Degradation of ECM is crucial in the early step of capillary formation. Basement membrane represents the first barrier that sprouting tip cell encounter. Accordingly with their demand of matrix remodelling, tip cells express high levels of MMPs[46]. In particular, it has been reported that the tip cell leading front is rich in MMP-14, while stalk cells are characterized by its lower expression[31]. Additionally, VEGF and bFGF, pro-angiogenic

factors that trigger angiogenesis, elicit in ECs rapid activation of MMP-2,-9 and surface expression of MMP-14, thus further supporting the tip cells invasiveness[47,48]. The acquisition of this migratory phenotype is also supported by the VE-cadherin cleavage mediated by MMPs, responsible for the intercellular adhesions disruption[49]. Therefore, once matrix has been invaded and tube-like structures are formed, incorporation of pericytes in the nascent vessel is required for capillary stabilization. Further, through the secretion of PDGF-B, endothelial cells attract PDGF receptor-β expressing pericytes, causing a cascade of reactions regulated by MMP[50], able to regulate both pericytes migration and proliferation[51].

Besides this, MMPs contribute to angiogenesis by also mediating the releasing ECM-bound pro-angiogenic factors, as described below.

3.3.c MMPs modulate angiogenic factors

In addition to degrading ECM components and activating other MMPs, MMP activity is required for the release of pro-angiogenic factors.

Almost two decades ago, Davis et al.[52] coined the term matricryptic site to indicate the biologically active site of ECM molecules, that can be exposed only after protein modification, thanks to proteolysis but also to mechanical forces, novel interactions, multimerization, and conformational changes. These changes occur in the injured site and are usually resulting from the interaction between cells and ECM through a series of receptors, including integrins, cell surface proteoglycans, and a type of cell-surface-expressed tyrosine kinase receptors with high affinity for ECM components[52].

Once ECM molecules-derived fragments had been generated, they are called matrikines, and are functional active. A variety of matrikines have been identified during the last years and, in conjunction with MMPs and other pro- or anti-angiogenic factors, they orchestrate any step of angiogenesis. Their mechanism of action has to be better elucidated, however it is becoming clear that they compete with intact ECM proteins for the binding of integrins, thus altering the endothelial migration behaviour[53]. Proteolysis-derived ECM fragments also affect the inflammatory response, by generating chemotactic gradients and by modifying gene expression in immune cells[54]. Importantly, VEGF function is affected by MMPs. Indeed, MMP-3, MMP-7, MMP-9 and MMP-19 cleave VEGF at 113 aa, thus sustaining the sprouting angiogenesis[55].

4 Mesenchymal Stem Cells for immunosuppression

Mesenchymal stem cells (MSCs) are a heterogeneous population of cells with multi-potency and self-renewal capacity that can be isolated from several adult tissues. MSCs were first described by Friedenstein and colleagues, when it was reported that heterotopic transplanted bone marrow (BM) stroma generate bone, fat cells, cartilage and reticular cells *in vivo*[56]. This suggested the existence in BM stroma of non-hematopoietic stem cells, with skeletal and adipose potential. After further characterizations, these cells were identified as fibroblast-like cells, colony-forming unit fibroblasts (CFU-Fs), cells adherent to plastic surfaces and able to be expanded *in vitro*[57]. Thus, they were categorized by Caplan and colleagues[58] as stem cells, and the name **mesenchymal stem cell** was coined.

4.1 Definition of Mesenchymal Stem Cells (MSCs)

4.1.a Multipotency and self-renewal

MSCs are considered stem cells, principally for showing two fundamental staminal proprieties: self-renewal and multipotency.

The first criteria for defining a stem cell is the self-renewal, that is the capacity to undergo numerous cell divisions while maintaining a stem cell phenotype. MSCs can be cultured *in vitro* for many passages without losing their multipotency property. Additionally, multipotency indicate the ability of a stem cell to differentiate into several types of functionally mature cells[59]. Indeed, MSCs can differentiate into multiple cell varieties, mainly belonging to the mesodermal lineage. In particular, it has been demonstrated that MSCs can differentiate in osteoblast, adipocytes and chondrocytes *in vitro*[60] and they give rise to bone and cartilage after ectopic transplantation *in vivo*[61,62]. Subsequent studies reported MSCs differentiation in cell types with both mesodermal and non-mesodermal origin, including endothelial cells, cardiomyocytes, hepatocytes and neural cells[59]. However, this multipotential property of MSCs remains debated. This is mainly due to the lack of globally standardized methods for their isolation, expansion and identification[59].

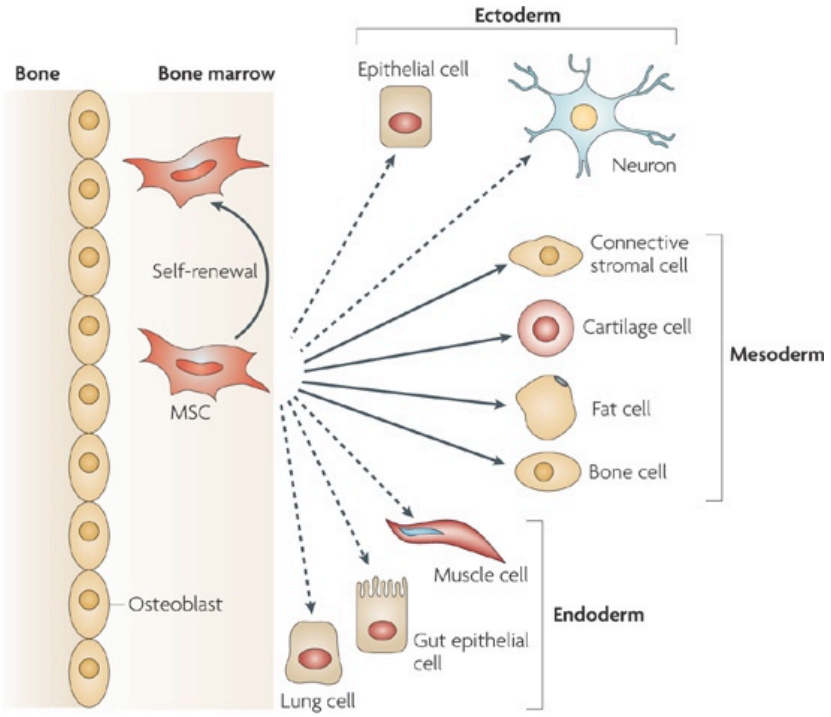

Figure I.H: Mesenchymal stem cells multypotency

The figure shows a schematic representation of the ability of mesenchymal stem cells (MSCs) to self-renew (curved arrow) and to differentiate (straight arrows) towards the mesodermal lineage. It is also reported (dashed arrows) the MSCs ability to transdifferentiate into cells of other lineages (ectoderm and endoderm). Nature Reviews Immunology 8, 726-736 (September 2008) doi:10.1038/nri2395

4.1.b Markers of MSCs

A deep characterization of MSCs is still far to be completed, especially for their extremely low frequency in tissues and the lack of unique markers[59]. However, there is a general consensus that MSCs lack endothelial and haematopoietic cells markers CD45, CD34 and CD31 or the co-stimulatory molecules CD80, CD86 and CD40. In contrast, they express CD105 (also known as endoglin), CD73 (ecto-5′ nucleotidase), CD44, CD90 (THY1), CD71 (transferrin receptor), the ganglioside GD2 and CD271 (low-affinity nerve growth factor receptor)[57]. Nevertheless, the expression of all these markers is not homogeneous throughout MSCs of different sources, isolated with different protocols and cultured for different numbers of passages. For this reason, a unique set of markers for MSCs detection *in vivo* is still missing. Recently, it has been identified a population of $CD146^+$ perivascular cells with self-renew ability and with a osteoprogenitor-like phenotype[63]. Moreover, surface cell antigen 1 (SCA1) and platelet- derived growth factor receptor-α (PDGFRα) were used to identify a subset of non-haematopoietic cells, in close contact with arteries, that gives rise to osteoblasts, reticular cells and adipocytes *in vivo*[64]. Finally, it was reported that nestin, a neuronal cell marker, specifies BM-resident MSCs[59]. Thus, a lot of specific proteins, or a combination of them, were proposed for MSCs *in vivo*

identification. Conversely, none of them is still recognized, universally, as mesenchymal stem cell marker.

4.2 In Vivo localization

As mentioned, MSCs can be isolated from different adult tissues, including bone marrow, adipose tissue, periosteum, tendon, periodontal ligament, muscle, synovial membrane, skin and lungs[65]. This ample variety of MSCs sources can be explained by three possibilities.

Firstly, stem cells, acting as reservoir of fully differentiated cells in different tissues, once isolated and cultured, behave all as MSCs. Thus, we are categorizing different stem cells with the same name. Secondly, it is possible that there is only one specific organ for MSCs location *in vivo*, from which MSCs could exit to reach several sites, where they give rise to fully mature cells by differentiating themselves. The third, and most accepted, idea is that MSCs are constant component of an anatomical structure common to the majority of tissues, such as the vasculature, thus explaining their presence in almost all organs. Supporting this idea, several recent studies have suggested a perivascular confinement of MSCs[66], on the basis of the immunohistochemical analysis of a perivascular localization of $CD45^-/CD31^-/Sca\text{-}1^+/Thy\text{-}1^+$ cells, potentially MSCs[66,67]. Additionally, the same perivascular localization was found by using others MSCs markers; indeed, $Stro\text{-}1^+/CD146^+$ MSCs were found to line blood vessels in human bone marrow and dental pulp[66], furtherly supporting the notion that MSCs are integral part of many different tissues.

4.3 Proposed physiological role of Mesenchymal Stem Cells

4.3.a MSCs control the hematopoietic niche

Despite MSCs spread throughout the entire adult organism, they were firstly identified as a component of the bone marrow. Since their discovery, the investigation of MSCs physiological roles in this tissue has represented the principal aim of several studies. Nowadays, they are thought to critically control the homeostasis of the haematopoietic compartment[59].

In particular, it has been proposed, and partially demonstrated, that MSCs provide structural and modulatory signals to the niche where haematopoietic stem cells (HSCs) are confined. This effect on haematopoietic niche organization is mediated either through their direct interaction with specific niche components, such as extracellular matrix proteins and surrounding cells or, through their ability to organize vascular networks[59]. However, they have not only a prominent structural role, but also an effective function. Indeed, it has been reported that the control of the HSC proliferation and differentiation can be ascribed to BM-MSCs, that act by maintaining HSCs in the G0 phase of the cell cycle[57].

Supporting the hypothesis of the specific bone marrow-function of MSCs, it has been recently demonstrated that HSCs localize near a subset of fibroblastic reticular cells. These CXCL12-abundant reticular cells (CARC cells) highly express CXC chemokine ligand 12 (CXCL12 or SDF1) and have osteogenic and adipogenic potential[68], suggesting that they might correspond to MSCs. Additionally, MSCs positive for nestin, that, as already described, is a proposed marker for MSCs, have been found in the central areas of the bone marrow, and they also show high level expression of CARCs genes including CXCL12[69]. This, again, strikingly adds evidence of the MSCs localization and function in the bone marrow.

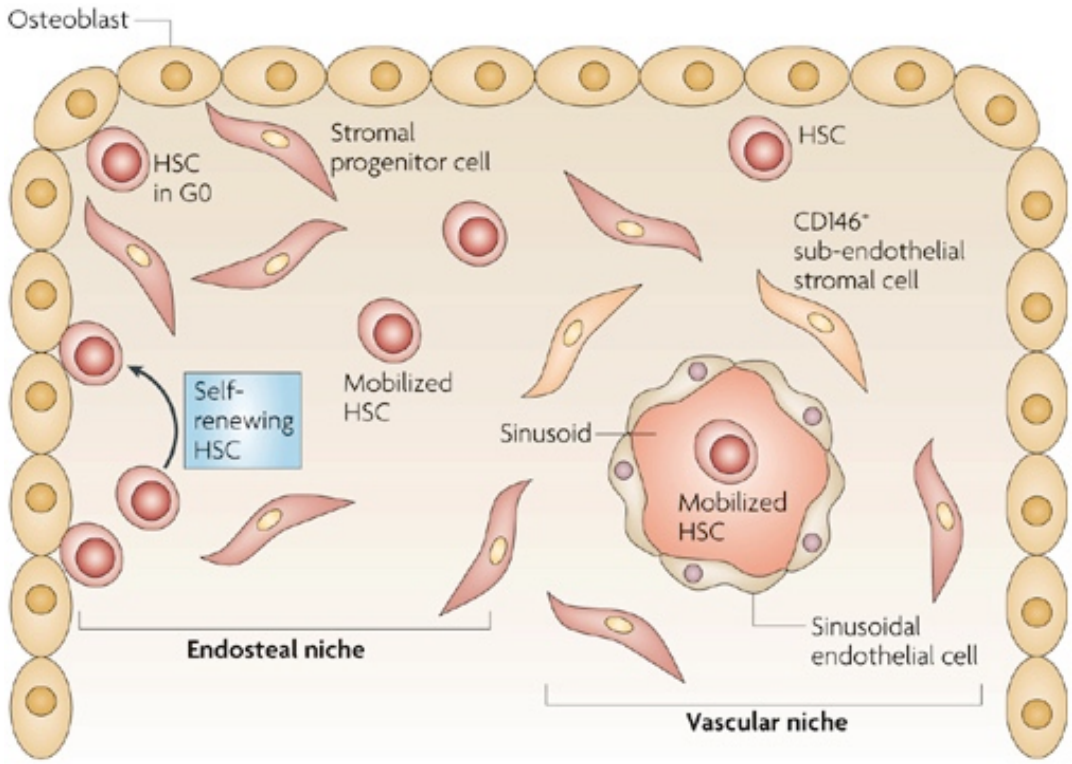

Figure I.I: Mesenchymal stem cells in the haematopoietic niche

Mesenchymal stem cells contribute to the structure and function of the haematopoietic stem cell (HSC) niche. In particular, in the endosteal niche, MSCs, together with osteoblasts, maintain HSCs in the G0 phase of the cell cycle, supporting their quiescent state. This control is further regulated, in the vascular niche, by sub-endothelial and perivascular MSCs through the orchestration of HSCs proliferation, differentiation and recruitment from the endosteal niche. Nature Reviews Immunology 8, 726-736 (September 2008) doi:10.1038/nri2395

4.3.b Perivascular MSCs in the tissue regeneration

The MSCs perivascular restriction is becoming rapidly an accepted concept. Besides that, to understand whether there is and what is MSCs physiological role in this compartment is far to be elucidated. It has been suggested that MSCs in the perivascular niche act as *reservoir* of progenitors required for postnatal vasculogenesis, particularly during the tissue rigeneration[70]. In line with this idea, it has been recently shown that, MSCs, confined in the adventitia of blood vessels, exit from their niche in response to the attractive signals released by tumor cells. Thus, they support the tumor vascular remodelling by differentiating into pericytes, and, consequently, sustaining the maturation of newly formed branches[71]. Additionally, once reached the tumor site or the damaged tissue, MSCs mediate cell replacement and cell empowerment[72,73,74,75]. Notably, preclinical and clinical studies suggested that MSCs transplantation could enhance tissue regeneration[72]. However, the number of MSCs really embedded in the damaged site is poor and their

survival after engraftment is not long enough to justify a prominent role for their differentiation in the regenerative process[76].

In conclusion, although the perivascular localization of MSCs is well documented, the physiological role of these cells has still to be clarified. Moreover, it is becoming clear that the MSCs mechanism of action is principally mediated by soluble factors, by which they can control tissue homeostasis, but also inflammation, as described in the following section.

4.3.c Immunomodulatory proprieties: the plasticity of MSCs

Almost two decades ago, for the first time it was reported the immunosuppressive effect of bone marrow-derived MSCs, since they have been demonstrated to inhibit lymphocyte proliferation and activation[77,78]. Since this discovery, the scientific committee moved the attention from the regenerative to the immunosuppressive function of MSCs. Thus, a lot of evidence has been collected showing that MSCs interfere with the activation and the function of immune cells belonging to both innate and adaptive response. The key results can be summarised as follows:

- **MSCs inhibit maturation of dendritic cells (DCs)**: the maturation of both monocyte and $CD34^+$ haematopoietic progenitor cells into DCs is affected by MSCs with a IL-6-dependent mechanism. Additionally, mature DCs express lower levels of MHC class II molecules, CD11c, CD83 and co-stimulatory molecules, when cultured with MSCs. Furthermore, interleukin-12 (Il-12) and TNF production by DCs is decreased in the presence of MSCs, but IL-10 release is increased in plasmacytoid DCs (pDCs). MSCs-derived PGE_2 seems to be involved in all of these effects[57].
- **MSCs affect natural killer cell (NKs) activity**: NKs have a prominent role in the immune response for their cytolytic activity and their ability to secrete pro-inflammatory cytokines. These functions are both affected by MSCs. Indeed, they downregulate the expression of NK receptors, that have a prominent role in the activation of resting NKs, including NKp30 and natural-killer group 2-member D (NKG2D). Furthermore, NK proliferation and IFNγ production are dampened when NK cells are incubated with MSCs[57]. Cell-to-cell contact and the secretion

of soluble factors by MSCs, like transforming growth factor beta 1 and PGE_2, seems to mainly exert these effects.

- **MSCs inhibit neutrophil killing capacity**: it has been reported that MSCs reduce the neutrophil respiratory burst rapidly triggered by their activation. This involves an IL-6-dependent mechanism, which signalled by activating STAT-3 transcription factor. Furthermore, MSCs are responsible for the delay in the spontaneous apoptosis of activated neutrophils, by reducing reactive oxygen species again with a IL-6-dependent mechanism[57].
- **MSCs alter macrophage polarization**: MSCs alter the macrophage switching from the proinflammatory phenotype (M1), to the anti-inflammatory one (M2)[79,80]. MSCs activated by pro-inflammatory cytokines are, indeed, able to secrete high levels of PGE_2. This latter, in turn, reprogram monocytes and macrophages to secrete strong amounts of the anti-inflammatory IL-10. Additionally, IL-10 prevents cytotoxic T cell-activation and neutrophil recruitment into the injured tissue, thus further limiting the inflammatory response[57]. It has been also reported that the secretion of Il-1 receptor antagonist (Il-1RA) by activated MSCs, inhibits not only the effect of Il-1α-producing T cells but also the activity of TNF- producing macrophages[57].
- **MSCs inhibit T cell response**: most studies focused their attention on the interplay between MSCs and T cells. In particular, it has been highlighted that MSCs dampen the differentiation of Th1 and Th17 subsets, that promote the inflammatory response, and, conversely, they support the generation of regulatory T cells (Treg cells) suppressing the inflammation. These effects seem to be principally due to an induction of T cell arrest in the G0/G1 phase of the cell cycle, thus resulting in the lower secretion of pro-inflammatory factors such as IFNγ. Indeed, the T cells-inhibitory process mediated by activated MSCs, is associated with decreased IFNγ production, and contrarily an increased in Il-4 production by T helper 2 (Th2) cells. It indicates a shift in T cells phenotype, from a pro-inflammatory state (IFNγ-producing T cells), to an anti-inflammatory activity (proper of Il-4-producing cells, or Th2).

  Additionally, MSCs interfere with $CD8^+$ T lymphocytes (CTLs), reducing their cytotoxic activity. To support the immunosuppressive effect, MSCs can also

indirectly promote Treg cells, prompting DC secretion of IL-10, which, in turn, support Treg differentiation[72].

- **MSCs inhibit B cell functions**: the effect of MSCs on B cells has not been completely understood. Indeed, different results have been collected in all these years, probably for not universally adopted experimental conditions. Of note, MSCs can inhibit B cells proliferation, differentiation and their expression of chemokine receptors. *In vitro* studies have also suggested an implication of both MSCs soluble factors and a cell-cell contact to induce these effects[57].

Importantly, several secreted factors, including TGF-β, nitric oxide (NO), indoleamine 2,3-dioxygenase (IDO), TSG6, prostaglandin E2 (PGE_2), IL-1 receptor antagonist, IL-10 and antagonistic variants of CCL2, have been reported to partially mediate these MSCs immunosuppressive functions[72]. The release of these molecules can be constitutive or, as it happens for IDO, induced by the interaction with target cells[57].

Notably, by secreting IDO, which removes from the extracellular space tryptophan, essential for T cells proliferation, MSCs can block immune-mediated Th1 cells proliferative expansion. This inhibitory process is further enhanced by MSCs induced nitric-oxide synthase (iNOS), that results in the large production of toxic NO in T cells[57]. NO is a rapidly diffusing gaseous that can interact with many enzymes, ion channels, and receptors. It has been shown that NO inhibits cytokine production, suppress STAT5 phosphorylation and, finally, inhibit the TCR-induced T cell proliferation. However, the mechanism controlling iNOS in MSCs has not been fully elucidated[57].

IDO and NO are thus identified as key immunosuppressive MSCs soluble factors, even though murine MSCs exert their effect mainly by NO, and human MSCs by IDO[81]. Other soluble factors have been reported to mediate the anti-inflammatory properties of MSCs, such as PGE_2, secreted by both human and mouse MSCs, that, prompts macrophage shift toward the more anti-inflammatory phenotype M2, characterized by the release of IL-10, that in turn, moves the balance of T cells to the Th2 type[81].

Therefore, it is even more clear that a complex plethora of soluble mediators is responsible for the immunosuppressive effects of MSCs[57]. In addition, almost all these evidence have been collected from *in vitro co-colture* studies, and the mechanisms responsible for the MSCs anti-inflammatory function also *in vivo need to be clarified*.

Ultimately, it has been suggested that MSCs do not specifically act on target cells but they rather regulate the immune response by modifying the microenvironment of injured tissue[57].

Of note, the surrounding space that MSCs encounter when *in vivo* administrated seems to significantly modulate the outcome of MSCs treatment. Indeed, for example, it is well described that the immunosuppressive phenotype of MSCs requires a specific activation of these cells to be established. Accordingly, MSCs cannot suppress the inflammatory response unless they are licensed by a combinations of inflammatory cytokines, including IFN-γ, IL-1, IL-6 and TNF-α[72]. Supporting this concept, it has been reported that graft-versus-host disease (GVHD) can be successfully treated by MSCs transplantation only when they are administered during the acute phase of the pathology. Indeed, only in this phase of GVHD the microenvironment is characterized by the proper combination of inflammatory factors able to license MSCs toward an immunosuppressive phenotype[82,83].

4.4 Clinical applications

Bartholomew and colleagues were the first to test *in vivo* the immunosuppressive effect of transplanted MSCs[78]. They showed that allogeneic MSCs administered in primates increased the skin-graft survival[78]. In the recent years a lot of pre-clinical trials were performed to investigate to beneficial role of MSCs in a wide panel of experimental diseases[57]. Among them, MSCs were observed to ameliorate the endogenous restoration of pancreatic islets and renal glomeruli in a mouse model of diabetes[84]. Other studies indicated that MSCs rescue the renal function by blocking the accumulation of proinflammatory cytokines, such as IL-1 ,TNF-α and IFN-γ, and the apoptosis of target cells[85]. In a similar way, in a model of lung fibrosis, MSCs-secreted IL-1RA suppresses the effects of IL-1 -producing T cells and TNF- producing macrophages[86].

Importantly, the low frequency of MSCs engraftment and differentiation in the damaged tissues provide the evidence that the multipotence of these cells is not essential for their clinical effect and that their positive effect is mainly related to their immunosuppressive functions. Therefore, once the MSCs immunosuppression was validated in pre-clinical studies, several clinical trials were started. Notwithstanding, MSCs mechanism of action is still unknown. Notably, the first MSCs clinical administration was performed by Le Blanc

et colleagues[87] by injecting two times haplo-identical MSCs into a 9-year-old child with GVHD at grade VI, who was resistant to the treatment. In this case, MSCs rescued all the symptoms and increased the survival beyond 1 year. On the contrary, 24 patients without MSCs administration died in 2 months after bone marrow transplantation. The strong success of this therapy leads the way for the first large-scale clinical trial supported by Osiris Therapeutics. Thus, allo-MSCs were tested in patients with GVHD and acute myocardial infarction[88]. Nowadays, there are at least 300 clinical trials examining the safety and the efficacy of MSCs preparation in different diseases. Both allogeneic and autologous cells have been exploited for the therapy of a wide spectrum of diseases, mostly with autoimmune origin, but also related to solid organ transplantation, neurological disorders and even autism[89].

However, several critical points are associated with MSCs therapy. First of all, the exact number of MSCs to be injected to obtain a specific therapeutic result is unknown. Indeed, it has been reported that while high number of MSCs display an anti-inflammatory function, lower numbers support immune cellular response[90]. Furtherly, to obtain the huge number of stem cells capable to exert the immunosuppressive effect, multiple donor sources are required, thus increasing variability in the final out-come. The extreme heterogeneity associated to MSCs therapy is also due to the phenotypical changes induced in MSCs following long-term *in vitro* culturing[90]. Others considerations for the commercial expansion of MSCs therapy, are cellular time and storage. Unfortunately, at the moment, there are no optimized and standardized protocols that ensure an effective long-term preservation.

5 MSCs-derived extracellular vesicles

Although many clinical trials provide persuasive and substantial evidence about the efficacy of MSCs transplantation, their mechanism of action is not fully elucidated. In addition, the low number of follow-up studies does not offer a clear idea about MSCs therapy-side effects. Moreover, currently, no tests are universally exploited to evaluate MSCs safety and quality before the *in vivo* administration.

To the purpose of reducing heterogeneity of MSCs cell therapy, since it has been recognized that the MSCs immunosuppression is mediated prominently by soluble factors, several works focused their attention on the characterization of MSCs secretome.

Importantly, despite the huge amount of soluble proteins and lipids released in extracellular medium, it was also reported that MSCs secrete Extracellular Vesicles (EVs)[91].

EVs are cell-derived particles, which size ranges from 50 and 5000 nm, that can be released by different cell types. They can be classified in exosomes, microvesicles and apoptotic bodies depending on their biophysical properties (size, cellular origin, molecular cargo, and biogenesis)[92]. Through a specific process, including endocytosis, fusion and phagocytosis, EVs interact with a target cell, mediating intercellular communication and thus regulating physiological and pathological conditions[92].

Therefore, MSCs-derived EVs, if administered to patients, might potentially recapitulate the immunosuppressive effect of MSCs overcoming the issues associated with MSCs cell transplantation.

5.1 Exosomes

Exosomes are a homogeneous population of particles, whose dimension is about 40 and 150 nm, with an endosomal origin[97]. They are released thanks to the fusion of multivesicular bodies with the plasma membrane. Thus, tetraspanins (examples CD63, CD81, CD9), gangliosides, sphingomyelin, and disaturated lipids characterize their highly rigid membrane surface, that confers them resistance to degradation and strong stability.

5.2 Microvesicles

Microvesicles are generally more heterogeneous populations of particles. Their size ranges from 50 to 2000nm. Contrary to exosomes, microvesicles sprout directly from the plasma membrane, inducing an accumulation of plasma membrane proteins on their surface, as well as cytosolic proteins, nucleic acids, and other metabolites[91]. Indeed, the composition of microvesicles membrane is predominantly conditioned by the original cell. However, they are generally enriched in integrins, glycoprotein Ib (GPIb), and P-selectin[92].

5.3 Apoptotic bodies

Apoptotic cells undergo fragmentation, thus releasing bodies (apoptotic bodies) with a diameter that range between 50 and 5000 nm. They carry plasma and organelle membranes, but mostly DNA binding histones. Contrary to exosomes and microvesicles, they are depleted in glycoproteins[92,91].

5.4 Toward a cell-free therapeutic approach

Beside all the MSCs-related disputes, in terms of their multi-potency, self-renewal and ability to trans-differentiate into lineages of other germ layers, MSCs have an evident and unequivocal beneficial effect in the control of inflammatory disorders. Experimental evidence demonstrated that the MSCs-inhibitory effect prominently depends on the paracrine activity of MSCs and not on their engraftment. Thus, this intriguing data suggest novel cell-free therapeutic perspectives based on the exploiting of MSCs-derived extracellular vesicles. Interestingly, it has been reported that EVs isolated from the medium conditioned by MSCs are able to mediate an immunosuppressive effect. Specifically, MSCs-derived EVs alter the proliferation of B cells, reducing also their antibody secretion, in a dose dependent manner. Moreover, EVs affect the T cell proliferation, but support the accumulation of anti-inflammatory cytokines (IL-10) and the induction of T regulatory cells[90]. So far, several studies have been focused on the investigation of the EVs-based therapy as alternative approach to MSCs transplantation. In support to this hypothesis, some promising data have been collected. Indeed, human MSCs-derived EVs have been shown to suppress kidney inflammation, but also to prevent

chronic tubular inflammation and damage to renal function in a model of acute kidney injury[90]. The beneficial effect of EVs administration was also described in an osteochondral defect model, where it was reported that EVs from human MSCs completely repair cartilage and subchondral bone[90]. Additionally, also clinic studies confirmed the immunosuppressive potential of MSCs-derived EVs. Indeed, the EVs treatment of a patient with treatment-refractory graft-versus-host disease (GVHD) firstly provided evidence of no apparent side effects associated with this approach. Most importantly, it was reported a significantly improvement in clinical symptoms, even 4 months after the treatment[94].

Since promising results have been collected so far by using MSCs-derived EVs, the replacement of a MSCs administration with a cell-free therapeutic approach is becoming a concrete alternative. Several advantages can be encountered describing a EVs-based therapy. Firstly, EVs are only a cellular product, and not living biological entities; therefore, they are not regulated by FDA procedures. In addition to that, this results in a limited risk of carcinogenesis and no possibility of aneuploidy or other chromosomal abnormality. Moreover, due to their high stability, they can be stocked by freezing and thus easily preserved for a long time. Also their distribution in the organism can be enrolled among the benefits of this approach. Indeed, in contrast to MSCs, they pass the blood-brain barrier, which could represent a crucial expedient in the treatment of patients with the contribution of central nervous system. In the perspective to replace a cell therapy, it is to note that the immortalization process of MSCs displays only negligible effect on the EVs and RNA/protein content packaged. Finally, all these advantages further support the fascinating opportunity of an industrialized EVs-based therapy[90].

Aim of the study

Currently, MSC transplantation represents a promising therapeutic option for the treatment of several immune-related diseases, such as GVHD, diabetes, lung fibrosis and heart failure[57]. Nonetheless, despite the encouraging results observed in pre-clinical models, MSC-based approaches for the therapy of inflammatory disorders still need a deeper comprehension of their mechanism of action to be successfully translated to patients. In line with this, the numerous clinical trials exploiting MSCs provided unsatisfactory and still debated results. A reasonable explanation for this failure could be mainly ascribed to the lack of a consensus protocol to isolate, culture, store and administer these cells, and the paucity of knowledge regarding their physiological functions *in vivo*[95].

Indeed, although it has been demonstrated that MSCs interfere with the activation and the function innate and adaptive responses *in vitro*, their mechanism of action *in vivo* in models of inflammation is not yet fully elucidated. Our group had demonstrated that sub-cutaneous transplantation of MSCs encapsulated in alginate micro-spheres, and thus unable to migrate within the body and home into specific target organs, strikingly prolongs the survival of mice with GVHD[96]. Our data unequivocally provided evidence that: i) MSCs do not require homing to specific organs to control inflammation; ii) MSC immunosuppressive effects do not depend on mechanisms requiring cell-to-cell contacts; iii) the immunomodulatory MSC-based therapy is mediated by soluble factors released during the inflammatory response.

In order to improve the development of more efficient MSC-based therapies, **the aim of this study was to deeper investigate the mechanisms of action of MSCs *in vivo* focusing on the factors - secreted proteins and extracellular vesicles - released by these cells during an inflammatory response.** In particular, considering that MSCs were found to line blood vessels within the human bone marrow and the dental pulp[66] and that leukocyte recruitment to inflamed tissues is accompanied by endothelial activation and vascular expansion, we speculated that endothelial cells may represent a specific MSC target during inflammation. Additionally, our study by

analysing the cross-talk between MSCs and endothelial cells enlarge the current knowledge on MSC physiological role, that could be exploited for the definition of novel therapeutic approaches.

Materials and Methods

Mice

C57BL/6J mice were purchased from Charles River Laboratories (Italy). All mice used as primary cell donors or recipients were between 8 and 12 week of age. Procedures involving animals and their care conformed to institutional guidelines in compliance with national (4D.L. N.116, G.U., suppl. 40, 18-2-1992) and international (EEC Council Directive 2010/63/UE; National Institutes of Health Guide for the Care and Use of Laboratory Animals) law and policies. The protocol was approved by the Italian Ministry of Health on June 18th, 2007 and modified by Protocol 162/2011-B. All efforts were made to minimize the number of animals used and their suffering. In all the experiment the mice were sex and age matched, no further randomization was applied.

Isolation of MSCs (MSCs)

MSCs were isolated by flushing the femurs and tibias from 8 week-old, C57Bl/6 female mice and cultured in 25 cm^2 tissue culture flasks at a concentration of $2x10^6$ cells/cm^2 using complete Dulbecco modified Eagle medium low glucose (DMEM, Lonza, Braine-L'Alleud, Belgium) supplemented with 20% heat inactivated fetal bovine serum (Biosera, Ringmer, United Kingdom), 2mM glutamine (Lonza), 100 U/ml penicillin/streptomycin (Lonza). Cells were incubated at 37°C in 5% CO_2. After 48 hours, the non-adherent cells were removed. After reaching 70–80% confluence, the adherent cells were trypsinized (0.05% trypsin at 37°C for 3 minutes), harvested and expanded in larger flasks. MSCs at passage 10 were screened by flow cytometry for the expression of CD106, CD45, CD117, CD73, CD105, MHC-I, SCA-1 and CD11b and used to perform experiments (BD Pharmingen, Oxford, UK).

Human MSCs were prepared were provided by Orbsen Therapeutics Ltd (Galway, Ireland). Ethical approvals are granted from the NUIG Research Ethics Committee and the Galway University Hospitals Clinical Research Ethics Committee (CREC). Briefly, bone marrow was harvested from volunteers, and the cell culture was maintained in

MEM Alpha with Glutamax supplemented with 2% FBS, 2mM glutamine, 100 U/ml penicillin/streptomycin and 1ng/ml human FGF[97].

All samples were obtained with informed consent. Procurement of the sample conformed to European Parliament and Council directives (2001/20/EC; 2004/23/EC).

Collection of conditioned medium of MSCs (MSC-CM)

MSCs were plated and let grow until confluence in ventilated cap flask. Growth medium was substituted with DMEM low glucose supplemented with 10% FBS, 2mM glutamine, 100 U/ml penicillin/streptomycin, with or without 25ng/ml mIL1b, 20ng/ml mIL6, 25-ng/ml mTNFa for 24 hours. Then this medium was changed with DMEM low glucose supplemented with 2mM glutamine, 100 U/ml penicillin/streptomycin for the following 18 hours. Conditioned medium was harvested and centrifuged at 4000 rpm for 10 min. Thus, we obtained unstimulated MSCs-conditioned medium (unst MSC-CM) or stimulated MSCs-conditioned medium (st MSC-CM).

Human MSCs were plated and let grow until confluence in ventilated cap flask. Growth medium was substituted with MEM Alpha with Glutamax supplemented with 2% FBS, 2mM glutamine, 100 U/ml penicillin/streptomycin, with or without 25ng/ml hIL1b, 20ng/ml hIL6, 25 ng/ml hTNFa for 24 hours. Then this medium was changed with MEM Alpha with Glutamax supplemented with 2mM glutamine, 100 U/ml penicillin/streptomycin for the following 18 hours. Conditioned medium was harvested and centrifuged at 4000 rpm for 10 min. Thus, we obtained unstimulated MSCs-conditioned medium (unst hMSC-CM) or stimulated MSCs-conditioned medium (st hMSC-CM).

Extracellular vesicles (EVs) isolation

Extracellular Vesicles (EV) were isolated from unst or st MSC-CM by ultrafiltration using Amicon® Ultra 15 mL Filters (Merck Millipore) following manufacturer's instructions. Briefly, each tube was first sterilised with 70% ethanol and then washed two times by centrifuging it at 4000g for 10 minutes. Subsequently, 12 ml of unst or st MSC-CM were

loaded into the tube and centrifuged at 2800g per 20 minutes at RT. This last step was repeated by adding 10 ml of PBS at RT at the obtained EVs. Finally, EVs were collected, concentrated in about 150µl of PBS, and directly stored at -80°C.

Endothelial Cell lines

SVEC4-10 (ATCC #CRL-2181 Manassas, VA), an endothelial cell line from murine axillary lymph nodes, were cultured in a humidified incubator with 5% CO_2 and 37°C, in DMEM (ATCC 30-2002 Manassas, VA) supplemented with 10% heat-inactivated FBS, 1% penicillin and streptomycin. The murine lymphatic endothelial cell line MELC[98] and murine microvascular endothelial cell line 1G11[99] were kindly provided by M. Sironi and A. Vecchi (Humanitas Clinical and research centre, Milan, Italy). MELC were cultured in Dulbecco's modified Eagle's medium (DMEM) supplemented with 1 mM L-glutamine, 1% non-essential amino acids, 1 mM Na pyruvate, penicillin-streptomycin, 10% heat-inactivated fetal calf serum (HyClone Laboratories, Logan, Utah), 100 µg/ml ECGS (Sigma, St. Louis, Mo.), 100 µg/ml heparin (Sigma), and 10% supernatant from sarcoma 180 cells (only for MELC). All the plastics used for lymphatic endothelial cells culture were pre-coated with 1% gelatin in PBS (37°C for at least 2 hours). Cells were subcultured using 0.05% trypsin, 0.02% EDTA solution. Cells were routinely tested for Mycoplasma.

Human Umbilical Vein Endothelial Cells (HUVEC, Lonza C2519A) were cultured in a humidified incubator with 5% CO_2 and 37°C with EBM-2 Basal Medium supplemented by EGM-2 BulletKit (CC-3156 & CC-4176). All the plastics used for HUVEC culture were pre-coated with 0.2% gelatin in H_2O (37°C for at least 2 hours). Cells were subcultured using 0.05% trypsin, 0.02% EDTA solution.

In vitro endothelial cell activation

MELC and 1G11 were plated in 48 well and incubated 5% CO_2 and 37°C in growing conditions until confluence. The medium was substituted with DMEM low glucose (Lonza, Braine-L'Alleud, Belgium) supplemented with 10% heat inactivated fetal bovine serum (Biosera, Ringmer, United Kingdom), 2mM glutamine (Lonza), 100 U/ml

penicillin/streptomycin (Lonza) or with MSC-CM added with 10% FBS, w/wo 20 ng/ml mTNFα. The cells were incubated for 24 hours, harvested with Accutase and stained for FACS analysis.

For NF-kB staining, MELC and 1G11 cells were seeded on fibronectin coated slides (overnight) and stimulated for 6 hours with MSC-CM added with 10% FBS, w/wo 20 ng/ml mTNFα. Fixed and permeabilized cells were incubated with anti-NF-kB p65 (Santa Cruz Biotechnology) and Texas Red conjugated-phalloidin. After washing, the appropriate Alexa-conjugated secondary antibodies were used (Molecular Probes). The nuclei were counterstained with Hoechst 33342 (0.1 µg/mL, Molecular Probes) and mounted with ProLong (Invitrogen). Negative controls included slides incubated with the secondary antibodies alone. Quantification of translocation from cytoplasm to nucleus is expressed as percentage of the total in both cell lines (40x, 20 fields for each condition), using ImageJ software.

Tube formation assay

Matrigel Matrix (354234 Corning) was thawed overnight at 4°C. Tips and 96-well plates flat bottom were pre-chilled overnight before performing the experiment. The day of the assay, 80 µl of Matrigel were seeded in the 96-well plate and left to polymerize at 37°C, 5% CO_2 for at least 30 minutes. $1.5x10^4$ SVEC4-10 or $2x10^4$ HUVEC were first suspended in 100µl of MSC-CM, supplemented with 10% FBS, alone or with anti-TIMP-1 (respectively AF980 or AF970 R&D) antibodies at the final concentration of 5 ug/mL, and then seeded on the solidified matrix. The formation of the tube networks develops in 4 hours at 37°C 10% CO_2. DMEM low glucose for SVEC4-10 or MEMalpha for HUVEC supplemented with 10% heat-inactivated FBS were used as positive controls. At the end of the incubation, tubes were imaged with a phase contrast inverted microscope at 4× objective magnifications and analysis was performed with ImageJ Angiogenesis Analyzer.

Cryo-imaging

MSC labelled with qTracker 655 (Life Technologies) were subcutaneously injected into a control mouse or a mouse previously immunized with CFA/OVA. Mice were euthanized 4 days later, frozen and cryo-imaged using the CryoViz™ cryo-imaging system (BioInVision, Inc., Cleveland, Ohio, USA) as described in[100],[101]. Cryo-images were acquired using the ProSCI™ software as described in[101].

The imaging protocol was modified to incorporate a smart tissue imaging technique that selectively captures images of tissue-rich regions from the block face, significantly improving throughput and optimizing data storage space. Processing throughput was further aided by concurrent pre-processing afforded by the CryoViz™Preprocessor software that stitches in real-time, and in 3D, to incrementally build a mouse volume in parallel with the imaging session. Following pre-processing, the images were introduced in the CryoViz™ 3D Visualizer software that automatically segments out embedding medium, selectively highlights various anatomical details and generates bright-field and fluorescence volumes of the mouse[102]. From these image volumes, standard animation frames were generated to build the 3D movies.

Optical Projection Tomography

5µg of Alexa-594 MECA-79 antibody (conjugated according to manufacturer's instructions using the Alexa-594 conjugation kit (Invitrogen, Carls- bad, CA, USA) were injected intravenously 15 min before organ harvest. Brachial LNs were excised, cleaned of surrounding fat and then incubated with AlexaFluor 488–conjugated anti-B220 (0.67 µg/mL) as previously described (21). OPT scanning was performed according to the manufacturer's instructions (Bioptonics) with the following filter sets: exciter 425/40, emitter LP475 for auto-fluorescent signal; exciter 480/20, emitter LP515 for green fluorescent signal; and exciter 545/30, emitter 617/75 for red fluorescent signal. 3D voxel dataset was obtained by raw data using NRecon software from Bioptonics. Reconstructed virtual xyz data sets as .TIFF or .bmp files were analysed with IMARIS (Bitplane) for iso-surface calculation of total LN volume and other parameters as described[103]. IMARIS reconstructions were carefully adjusted to fit original NRecon reconstructions. Lymph

node volume data are representative of 14 LNs /group analysed from 2 independent experiments. B follicles volume data are representative of a total of 8 LNs /group from 2 independent experiments. HEV data are representative of a total of 7 LN for CFA/OVA group and 9 for +MSCs group from 2 independent experiments.

3D immunofluorescence (3-DIF)

Mice were immunized and transplanted as described above. On day 3 after immunization single cell suspensions were obtained from LNs of C57/Bl6 mice. $CD4^+$ T cells were isolated using the mouse $CD4^+$ T cell isolation kit (Stem Cell technologies), according to the manufacturer's protocol. The lymphocytes were fluorescently labelled, injected intravenously into CFA/OVA immunized recipient mice and allowed to home for 20 minutes before blocking further homing with anti–L-selectin mAb. After 20 minutes, dLNs were isolated, treated and analysed as previously described (22). Data are representative of 8 (CFA/OVA) and 9 (+MSCs) mice from 3 independent experiments.

Immunofluorescence

The draining lymph nodes were fixed in formalin 4%, transferred in PBS-sucrose 30% and frozen in OCT. 8 μm sections were cut, rehydrated, permeabilized and incubated with the following primary antibodies: anti-VCAM-1 (Becton Dickinson), anti-ICAM-1 (Cedairlane), anti-CD31 (R&D Systems), anti-Lyve-1 (R&D Systems). After washing, the appropriate Alexa-conjugated secondary antibodies were used (Molecular Probes). The nuclei were counterstained with Hoechst 33342 (0.1 μg/mL, Molecular Probes) and mounted with ProLong (Invitrogen). Negative controls included slides incubated with the secondary antibodies alone. Images were acquired by a confocal microscope Fluoview FV1000 (Olympus), with an oil-immersion objective (40× or 60×/1.4 NA Plan-Apochromat; Olympus), using laser excitation at 405, 488, 594, or 633 nm. Images were processed using Adobe Photoshop 9.0.2. To perform colocalization analysis, the images were obtained with a 60×1.4 NA objective with a resolution of 800×800 and a laser excitation at 405, 488, 543 and 633 nm. Differential interference contrast (Nomarski

technique) was also used. The images of double stained sections (VCAM-1:CD31, ICAM-1:CD31, VCAM-1:LYVE-1, ICAM-1:LYVE-1) were analysed with imaging software ('Co-localization' module of Imaris 5.0.1, 64-bit version; Bitplane AG, Saint Paul, MN). The quantification of co-localization was expressed as Manders' coefficient, that in this experimental setting indicates the fraction of VCAM-1 or ICAM-1 positivity that colocalizes with the corresponding endothelial marker.

Data are representative of 5 mice/group from 1 representative experiment out of 3 independent experiments.

Immunization with CFA/OVA

1 mg/ml OVA (Sigma-Aldrich) was emulsified in Complete Freund Adjuvant (CFA) (Sigma-Aldrich), and 100 µl of emulsion were injected subcutaneously in three sites in the back. After 24 hours 1 x 10^6 MSCs were injected subcutaneously in the lumbar region. Immunized mice were sacrificed 4 days later and the brachial draining LNs (dLNs) were collected and frozen in OCT for immunofluorescence or digested for FACS analysis.

In vivo TIMP-1 Immunoneutralization

Goat polyclonal anti-TIMP-1 IgG[104] (catalog no. AF980; R&D Systems) was intravenously administered (0.5 mg/kg) in immunized mice 18 hours after MSCs transplantation. As a control, additional mice were given equivalent doses of an isotype-matched goat IgG (catalog no. AB- 108-C, R&D Systems). Immunized mice were sacrificed 2 days later and the brachial draining LNs (dLNs) were collected and digested for endothelial cell analysis by FACS. Data are representative of 36 LNs /group analysed from 4 independent experiments.

TIMP-1 siRNA Reverse Transfection

Timp-1 Silencer® Select Pre-designed siRNAs (Ambion) were exploited for mMSCs transfection, and Silencer® Select Negative Control No. 1 siRNA (Ambion) was adopted

as scramble. siRNAs were diluted in Opti-MEM I reduced Serum Medium (Gibco) at the final concentration of 50 nM. Diluted siRNAs were placed 100 ul/well in a 24-well tissue culture plate in presence of 1 ul of Lipofectamine2000 (Invitrogen), according to manufacturer's instructions. Murine MSCs were seeded at a density of $6x10^4$cells/well and cultured in antibiotic-free medium. Medium was replaced 24 hours post transfection with fresh DMEM low Glucose, 2mM L-glutamine and 10% FCS Biosera. mMSCs TIMP-1 secretion was analysed at 24, 48 and 72 hours after transfection by ELISA (R&D). In vivo data with siRNA MSCs are representative of 20 dLNs from 2 independent experiments.

AAV-mediated TIMP-1 overexpression

All the AAV vectors used in this study were generated by the AAV Vector Unit (AVU) at ICGEB Trieste (http://www.icgeb.org/avu-core-facility.html) as previously described[105]. Briefly, AAV vectors of serotype 9 were produced in HEK293T cells, using a triple plasmid co-transfection method. Viral stocks were collected after $CsCl_2$ gradient centrifugation. The total number of viral genome was determined by real-time PCR; the viral preparations had titers between 1×10^{13} and 3×10^{13} viral genome (vg) particles per ml. AAV9-TIMP1 was intraperitoneally injected at dose of 2×10^{11} vg in 100 µl PBS-/-. Equal amount of AAV9-LacZ was used as control. One day after AAV9 administration, mice were immunized with CFA/OVA as discussed above (6 mice/group). Brachial draining LNs (dLNs) were collected 4 days after immunization and digested for FACS analysis. Data are representative of 1 experiment out of 2.

Flow Cytometry analyses

For endothelial cell analysis, we generated single cell suspensions from dLNs by enzymatic digestion, as already described[106]. Endothelial cells were quantified by staining with rat anti–mouse CD45 (30-F11; BD Biosciences) and rat anti–mouse CD31 (MEC13.3; BD Biosciences), rat anti-gp 38 (clone 8.1.1.; Biolegend) and rat anti-PNAd (MECA-79; RnD System) followed by goat anti–rat IgM (Alexa) as a secondary antibody. Data are

representative of 28 LN/group from 3 independent experiments. To determine *in vivo* endothelial cell proliferation, mice received intraperitoneal injections of 2 mg BrdU (Sigma-Aldrich) 24h and 1h before the analysis and were fed with water containing 0.8 mg/ml BrdU in between[106]. Cells were stained according to the protocol for the APC BrdU Flow Kit (BD Biosciences). Data are representative of 16 LN/group mice from 3 independent experiments. Absolute counts of leukocytes were performed using TruCount tubes (BD Bioscience) according to the manufacturer's instructions. Cells were analysed using a FACS CANTO II or LSR Fortessa (BD Biosciences) and post-analysis of flow cytometry data was performed using FlowJo software (Tree Star Inc.).

Isolation and Differentiation of Mouse Bone Marrow–Derived Monocytes

Bone marrow cell suspensions were obtained by flushing femurs and tibias of 8- to 12-week-old C57Bl/6N mice (Charles River; Sulzfeld, Germany) with complete DMEM low Glucose supplemented with 10% FCS, 1% Pen/Strep and 1% L-Glutamine. Possible cellular aggregates were removed by pipetting and red cells were eliminated through ACK lysis buffer (10-548E, Lonza). Cells were washed twice with medium, seeded on 24-well plates (Corning Costar; Schiphol-Rijk, the Netherlands) at the concentration of 10^6 cells/mL and maintained in a humidified incubator with 5% CO2 and 37°C. Cells were supplemented with 20 ng/mL mM-CSF as positive control, or cultured in mMSC-CM supplemented with 10% FBS. MSC-CM and mM-CSF were replaced three days later. Cells were harvested five days later by gentle pipetting and repeated washing with phosphate buffered saline (PBS), and 2 mM EDTA. Monocytes differentiation was analysed by flow cytometry.

The expression of macrophage surface markers was evaluated by Flow Cytometry analysis. Briefly, cells were washed and stained in PBS supplemented with 2% fetal calf serum. After 20 minutes of incubation at 4°C with Purified Rat Anti-Mouse CD16/CD32 (Mouse BD Fc BlockTM 553142), fluorescent antibodies were diluted in PBS supplemented with 2% fetal calf serum, to identify mouse macrophages (CD11b:PeCy7 BD 552850 and F4/80:Alexa Fluor® 488 BioRad MCA497F). Cell viability was assessed

with the Live/Dead Fixable Aqua Dead Cell Stain Kit (Invitrogen), following the manufacturer's instructions. After the final wash, cells were fixed in 1% paraformaldehyde and acquired with the BD FACS Canto™ II system. Post-analysis of flow cytometry data was performed using FlowJo™ software (Tree Star Inc.).

Isolation and differentiation of Human Blood-Derived Monocyte

Peripheral Blood Monocyte Cells (PBMCs) from healthy donors were isolated by centrifugation on Ficoll-Paque solution and placed on Percoll 46% vol/vol solution (Amersham Biosciences) in RPMI 1640–10% FCS and 4 mM. Monocytes were harvested, suspended in medium 2% FCS, and let to adhere to plastic (1 hour at 37°C) in order to eliminate contaminating lymphocytes. For macrophage differentiation, 3×105 monocytes were seeded in 24-well plates with MEMalpha supplemented with 20% FBS in the presence of 100 ng/mL h-M-CSF as positive control, or they were cultured in hMSC-CM plus 20% FBS. After five days of differentiation, monocyte-derived macrophages were analysed by flow cytometry using CD14 staining.

The expression of macrophage surface markers was evaluated by Flow Cytometry analysis. Briefly, cells were washed and stained in PBS supplemented with 2% fetal calf serum. After 20 minutes of incubation at 4°C with Purified Rat Anti-Mouse CD16/CD32 (Mouse BD Fc BlockTM 553142), fluorescent antibodies were diluted in PBS supplemented with 2% fetal calf serum, to identify human macrophages (CD14: PE R&D FAB3832P). Cell viability was assessed with the Live/Dead Fixable Aqua Dead Cell Stain Kit (Invitrogen), following the manufacturer's instructions. After the final wash, cells were fixed in 1% paraformaldehyde and acquired with the BD FACS Canto™ II system. Post-analysis of flow cytometry data was performed using FlowJo™ software (Tree Star Inc.).

ELISA-Assay

To detect M-CSF and TIMP-1 concentration in MSC-CM, ELISA assays were performed following the manufacturer's instruction (for human, M-CSF DuoSet ELISA

DY216 and TIMP-1 DuoSet ELISA DY970; for mouse, M-CSF DuoSet ELISA DY416 and TIMP-1 DuoSet ELISA DY980).

LC-ESI MS/MS analysis

Proteins in the MSCs secretome (150 µg, as determined by the Bradford method) were precipitated with 10 % tricholoracetic acid (TCA) for 2 hours on ice. After reduction and derivatization, proteins were digested with trypsin sequence grade trypsin (Roche) for 16 hours at 37 °C using a protein:tripsin ratio of 1:50. LC-ESI-MS/MS analysis was performed on a Dionex UltiMate 3000 HPLC System with a PicoFrit ProteoPrep C18 column (200 mm, internal diameter of 75 µm) (New Objective, USA). Gradient: 1% ACN in 0.1 % formic acid for 10 min, 1-4 % ACN in 0.1% formic acid for 6 min, 4-30% ACN in 0.1% formic acid for 147 min and 30-50 % ACN in 0.1% formic for 3 min at a flow rate of 0.3 µl/min. The eluate was electrosprayed into an LTQ Orbitrap Velos (Thermo Fisher Scientific, Bremen, Germany) through a Proxeon nanoelectrospray ion source (Thermo Fisher Scientific). The LTQ-Orbitrap was operated in positive mode in data-dependent acquisition mode to automatically alternate between a full scan (m/z 350-2000) in the Orbitrap (at resolution 60000, AGC target 1000000) and subsequent CID MS/MS in the linear ion trap of the 20 most intense peaks from full scan (normalized collision energy of 35%, 10 ms activation). Isolation window: 3 Da, unassigned charge states: rejected, charge state 1: rejected, charge states 2+, 3+, 4+: not rejected; dynamic exclusion enabled (60 s, exclusion list size: 200). Five technical replicate analyses of each sample (2 different cell lines for each condition) were performed. Data acquisition was controlled by Xcalibur 2.0 and Tune 2.4 software (Thermo Fisher Scientific).

Mass spectra were analysed using MaxQuant software (version 1.3.0.5). The initial maximum allowed mass deviation was set to 6 ppm for monoisotopic precursor ions and 0.5 Da for MS/MS peaks. Enzyme specificity was set to trypsin, defined as C-terminal to arginine and lysine excluding proline, and a maximum of two missed cleavages were allowed. Carbamidomethylcysteine was set as a fixed modification, N-terminal acetylation and methionine oxidation as variable modifications. The spectra were searched by the Andromeda search engine against the mouse Uniprot sequence database (release 29.05.2013). Protein identification required at least one unique or razor peptide per

protein group. Quantification in MaxQuant was performed using the built in XIC-based label free quantification (LFQ) algorithm[107] using fast LFQ. The required false positive rate was set to 1% at the peptide and 1% at the protein level, and the minimum required peptide length was set to 6 amino acids. Statistical analyses were performed using the Perseus software (version 1.4.0.6, www.biochem.mpg.de/mann/tools/). Only proteins present and quantified in at least 3 out of 5 technical repeats were considered as positively identified in a sample and used for statistical analyses. Proteins were considered differentially expressed if they were present only in unst MSC-CM or MSC-CM or showed significant t-test difference (cut-off at 1% permutation-based False Discovery Rate) in both biological replicates. Bioinformatic analysis was carried out by DAVID software (release 6.7) (http://david.abcc.ncifcrf.gov/home.jsp) (9) in order to cluster enriched annotation groups of Biological Function within the set of identified secretome proteins. GOBF groups were filtered for significant terms (p value <0.05).

Scratch wound healing assay

In total, 10^5 cells (SVEC4 10 ATCC) were seeded on a 48 well plate in complete medium (DMEM-ATCC 30-2002 supplemented with 10% heat-inactivated FBS, 1% penicillin and streptomycin) and incubated 24 hours to reach the full confluence. The endothelial monolayer was then scratched by using a pipette tip. Cells were gently washed with PBS-/- and 200µl of medium were added (DMEM low Glucose, 1% P/S, 1% Glutamine), in the presence or absence of approximately 3µg/ml of EVs (from unst- or st- MSC-CM). When indicated, cells were treated with recombinant 50ng/ml VEGF (450-32 Peprotech), 200µM ARL 67156 (ARL67156A265 Sigma-Aldrich), 10µM Adenosine 5′-(α, β-methylene), diphosphate ADP analogue (AMP-CP M3763 Sigma-Aldrich) or 1mM N-acetyl-l-cysteine (NAC A7250 Sigma-Aldrich).

Three lines for well were drawn on the bottom of the plate. Through an inverted microscope (4× objective), pictures of the lines were taken at time 0 and after 6 hours in a humidified incubator with 10% CO_2 and 37°C. Image analysis were performed with ImageJ by calculating the Migration Rate (migration was calculated as the difference between the starting and the final distance covered by migrating endothelial cells).

Measurement of ROS by Fluorescence Microscopy

Reactive oxygen species (ROS) production was analysed with the scratch wound migration assay. Scratch experiments were performed as previously described. After 5 hours of incubation at 10% CO_2 and 37°C, ROS were detected by using CM-H2DCFDA (C6827 Thermo Scientific) following the manufacturer's instructions. Briefly, migrating endothelial cells were treated with 2.5µM CM-H2DCFDA in complete medium for 30 minutes in a humidified incubator with 10% CO2 and 37°C. Then, cells were washed with Hank's Balanced Salt Solution (HBSS, Lonza) supplemented with 2mM Ca^{2+}. Pictures were rapidly acquired with the confocal microscopy (10x objective) Leica TCS SP5 (Leica Microsystems, Wetzlar, Germany) using the software LAS-AF (Leica). Images analysis was performed by ImageJ.

Mouse retina neovascularization model

1-day-old C57BL/6N mouse pups were intraperitoneally injected with 10µg of EVs from unst- or st-MSC-CM. After 4 days, mice were sacrificed for retina collection. Both eyes were enucleated and fixed in 4% paraformaldehyde in PBS for 45 min. Retina whole mounts were dissected and marked with biotinylated isolectin B4 (Vector Laboratories), and stained with streptavidin–Alexa 488 (Invitrogen) before being flat-mounted. Pictures were rapidly acquired with the 10x objective of the confocal microscopy Leica TCS SP5 (Leica Microsystems, Wetzlar, Germany) using the software LAS-AF (Leica). Images analysis was performed by ImageJ.

Total retinal and vascular areas were measured using ImageJ. In details, we analysed the relative radial expansion and the total retinal branching point. For the retinal radial expansion, the retinal radius (from the optic nerve to the edge of the retina) and the vascular radius (from the optic nerve to the vascular front) of each petal of the retina were measured. The retinal vascular expansion was calculated as the ratio between the vascular radius and the retinal radius.

Matrigel plug assay

Anesthetized 12-week-old male C57BL/6N mice were subcutaneously injected in the dorsal back either 5µg of EV from unst- or st- MSC-CM, mixed with 400ul Matrigel Matrix (354234 Corning) supplemented with VEGF 100 ng/mL (450-32 Peprotech) and Heparin 50 units/ml. After 7 days, mice were sacrificed, and the Matrigel plugs were harvested, weighed and photographed. For the haemoglobin quantification, plugs were processed by TissueLiser in 250ul of H_2O-milliQ at the maximal frequency for 8 minutes. After centrifuging at 10000g for 10 minutes, plug haemoglobin content was measured using Drabkin's reagent kit 525 (Sigma-Aldrich) and normalized to the total protein quantity measured with the Pierce™ BCA Protein Assay Kit (Thermo Fisher Scientific), following the manufacturer's instructions.

EVs characterization

EVs were purified as previously described. An additional wash with PBS with 0.4% SDS of the filter membrane was added. Total protein of EVs was quantified by MicroBCA kit (Pierce). From 3 to 5 µg of proteins were separated by 10% SDS-PAGE under non-reductive conditions for CD39, CD63 and CD9 and reductive conditions (by adding DTT) for CD73 and TIMP1. The run was performed at 50V for 15 minutes, followed by 100V for 1.30 hours. Then, gels were transferred onto PVDF membranes, 0.45 µm (Millipore) activated with methanol (Sigma Aldrich), using Transfer Tris-Glycine buffer under 400 mA (100V) in wet by Mini TransBlot Cell system (BioRad) for 2 hrs. Then, membranes were blocked with 5% of BSA (Sigma Aldrich) in TBS 1X with 0.02% of Tween 20 for 1 hrs. Primary antibodies for western blot were used at 1:1000 dilution in TBS1X, 0.02% tween and 0.1% of BSA; anti-CD63 (MBL), anti-CD9 (eBiosciences), anti-CD39 (Biolegend), anti-CD73 (Abcam) and TIMP1 (R&D systems). Incubation with primary antibodies was performed overnight. Thus, membranes were incubated with the appropriate peroxidase-conjugated secondary antibody, ECL anti-Rabbit (GE), ECL anti-Rat (GE) and anti-Goat (BioRad). Chemiluminescence was achieved by ECL Prime Western Blot Detection reagent (GE). Images were acquired with ImageQuant LAS 4000

Mini (GE). For the EV quantification, Micro BCA™ Protein Assay Kit (Thermo Fisher Scientific) was used, following the manufacturer's instructions.

Statistical Analysis

The sample size per group was estimated from previous experience with similar experiments. There were no pre-established criteria for mice or sample exclusion: except evident technical damage. Data were analysed using Prism Software (GraphPad, La Jolla, CA, USA). Data were expressed as mean ± Standard Error (SE). Differences were assessed using *t*-test, Mann-Whitney test or One-way Anova. Statistic tests were performed between data with similar variance. Results with a *P*-value of <0.05 were considered significant.

Results

MSCs transplantation affects endothelial activation in immune reactive lymph nodes

To the purpose of understanding the physiological functions of MSCs and developing more efficient MSCs-based therapies, we exploited a mouse model of local inflammation to assess the role of transplanted MSCs in controlling the immune response. Since Zanotti el al. demonstrated that subcutaneously transplanted, either encapsulated or free, MSCs were equally efficient, we exploited for the entire study the administration of free MSCs[96].

Thus, we performed subcutaneous injections of free MSCs (not encapsulated) in the lumbar area of mice that had been previously immunized with Ovalbumin in Complete Freund Adjuvant (CFA/OVA) in the upper dorsal region. As expected, the immunization induced a robust and rapid response in the brachial draining LNs (dLNs) (Figure 1). MSCs transplantation significantly reduced this response, decreasing both the total cellularity and the volume of dLNs and affecting the recruitment of specific cell populations (Figure 1 B-E), as already described[99]. Using whole-mouse cryo-imaging analysis[102], we verified that subcutaneously injected MSCs did not migrate away from the site of injection during the experimental time (5 days), both in immunized and in untreated mice (Movie S1-S2 https: //www.nature.com/leu/journal/v30/n5/suppinfo/leu201633s1.html?url=/leu/journal/v30/n5/full/leu201633a.html). Together with our previous study[96], these data indicate that MSCs are able to dampen inflammation through the release of soluble mediators.

LN growth during immune responses is accompanied by endothelial activation and vascular expansion, two events that are required for leukocytes recruitment and orchestration of immunity. We analysed the expression of two adhesion molecules, vascular cell adhesion molecule-1 (VCAM-1) and intercellular adhesion molecule-1 (ICAM-1), that are typically up-regulated on the inflamed endothelium (Figure 2A-D). Interestingly, the dLN vessels of mice treated with MSCs had a lower expression of both VCAM-1 and ICAM-1, as demonstrated by the co-localization analysis expressed as Mander's coefficient (Figure 2B-D). Moreover, we observed that the dLNs of mice

transplanted with MSCs showed reduced density of the endothelial marker CD31 and of Lyve-1, a marker of the lymphatic endothelium, suggesting a reduced vascular expansion upon MSCs treatment (Figure 2A, C, E). Altogether, these data indicate that MSCs inhibit activation of vascular and lymphatic endothelium in the dLNs of immunized mice.

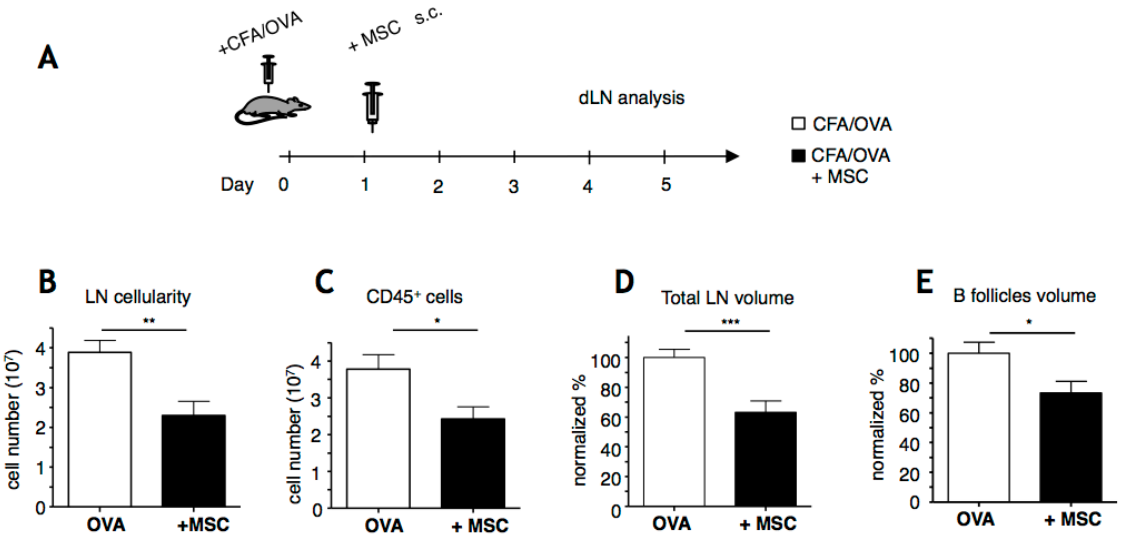

Figure 1 - MSCs affect size and cellularity of dLNs

A) Diagram of the experimental protocol designed to investigate the influence of MSCs transplantation. Mice were immunized in the dorsal back with CFA/OVA on day 0 and, on day 1, a group of animals received subcutaneous injection of 106 MSCs in the lumbar back. On day 4-5, depending on the subsequent analyses, brachial LNs were collected and processed. B-C) On day 5, dLNs were digested and analysed by flow cytometry. Data are representative of from 8 mice from 2 independent experiments; D-E) OPT data are expressed as percentage on OVA average. In B-E error bars represent SE (*$p < 0.05$; **$p < 0.01$; ***$p < 0.005$; t-test).

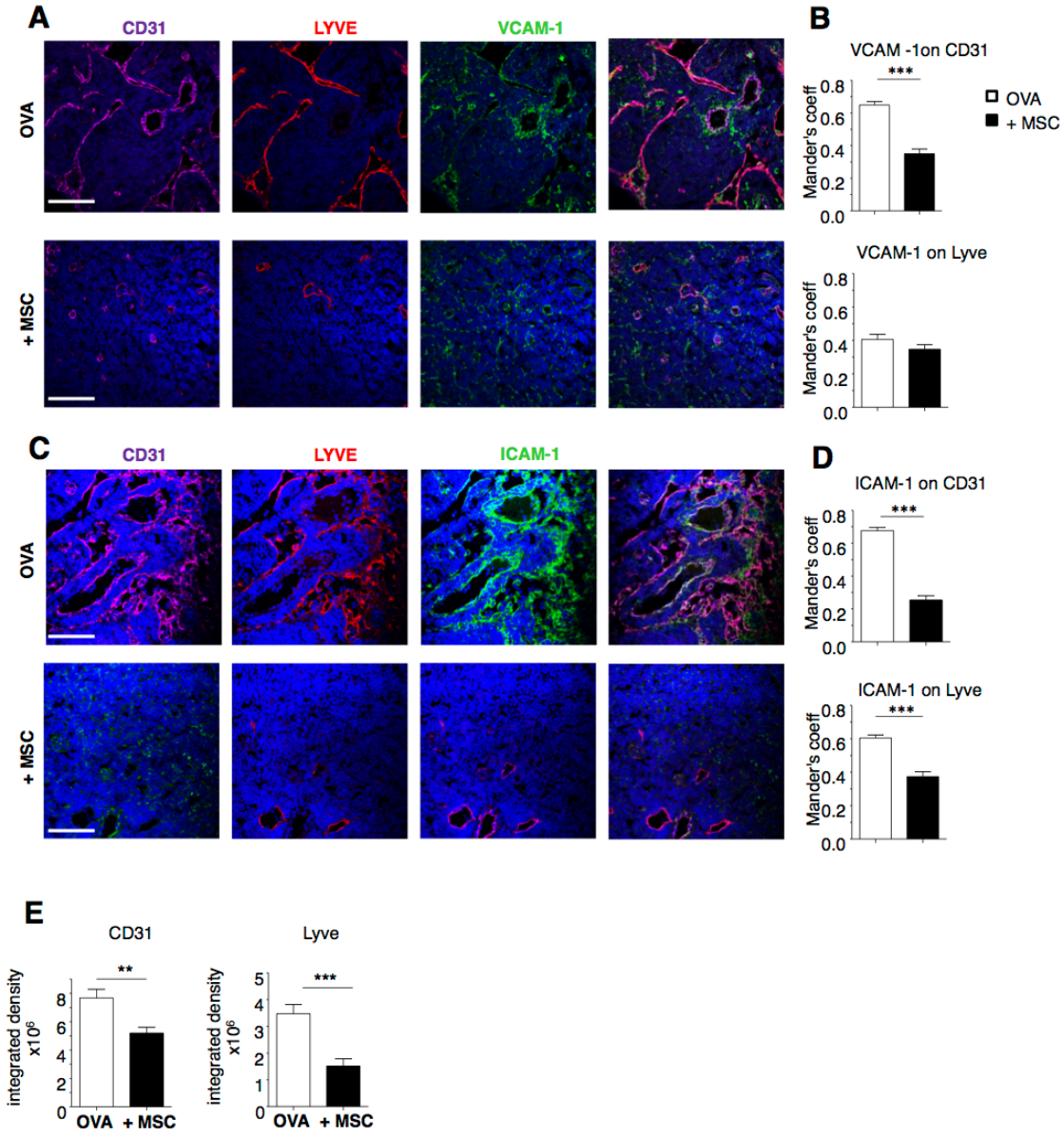

Figure 2 - MSCs inhibit endothelial activation in dLNs

Mice were treated as in Fig.1A and, on day 5, dLNs were collected, stained and analyzed by confocal microscopy. A and C) 8um frozen section were stained with anti-CD31, anti-Lyve-1 and anti-VCAM-1 or anti-ICAM-1, as indicated (10x, scale bar 200 mm). B and D) Mander's colocalization coefficient quantify the degree of overlap. E) Integrated density quantify the CD31 and Lyve-1 immunopositivity amount on cross sections of lymph node. In all graphs error bar represents SE (*p < 0.05, **p < 0.01, ***p < 0.005; t-test).

MSCs inhibit activation and elongation of HEVs and affect recruitment of T cells to dLNs

The migration of leukocytes from the bloodstream into LNs occurs via HEVs, which are postcapillary venules structurally adapted to support lymphocyte trafficking. Because of the reduced numbers of leukocytes present in the dLNs of mice treated with MSCs[96] (Figure 1), we asked if MSCs transplantation affects HEV activation, lymph node vascularisation and leukocyte migration *in vivo*.

MSCs were subcutaneously injected in the lumbar region of mice that had been previously immunized in the dorsal region with CFA/OVA, as already described (Figure 1), and HEV cells in brachial LNs were analysed. In particular, HEV cells were identified as $CD45^{-}CD31^{+}PNAd^{+}$ cells[108].The reduced number of $CD45^{-}CD31^{+}$ cells was confirmed by flow cytometry analyses (Figure 3A) and can be explained by the inhibition of endothelial cell proliferation in MSCs-treated mice, as shown by the reduced uptake of BrdU (Figure 3B). In the dLNs of mice treated with MSCs, we observed a reduction in the absolute number of HEV cells as compared to controls (Figure 3C). Moreover, HEV cells had a reduced expression of VCAM-1 (Figure 3D).

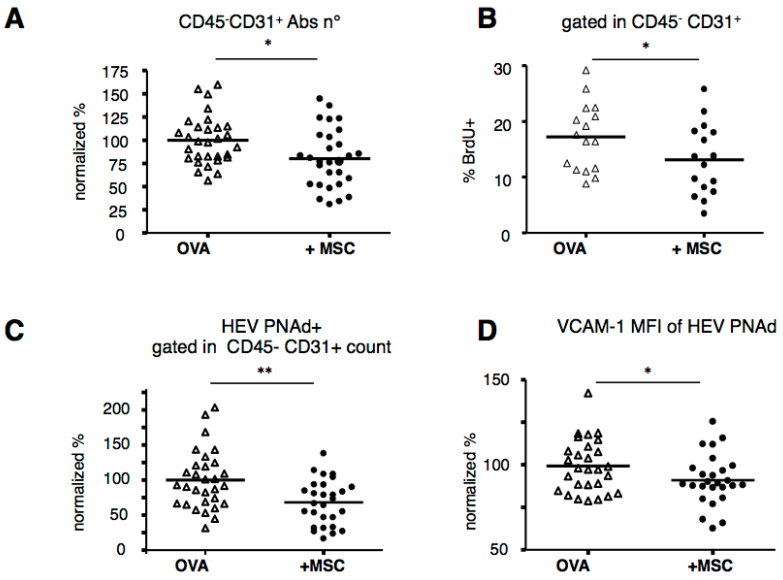

Figure 3 - MSCs inhibit HEV activation and proliferation in vivo

Mice were treated as illustrated in Figure 1A and dLNs were collected, digested and analyzed by flow cytometry. The graphs show: **A)** the absolute number of $CD45^{-}CD31^{+}$ cells per single LN expressed as normalized percentage on CFA/OVA (t-test) , **B**) BrdU incorporation cytometry after 48 h (Mann-Whitney test), **C**) HEV cell numbers and **D**) Mean Fluorescence Intensity (MFI) of VCAM-1 expression on HEV (t-test). (*p< 0.05; **p < 0.01).

Analysis of entire LNs by optical projection tomography, which allows a three-dimensional reconstruction of the HEV network, allowed us to examine the morphologic alterations that occur in HEV expansion after immunization with CFA/OVA in presence or absence of MSCs. HEVs were labelled prior to imaging by intravenous injection of fluorophore-tagged MECA-79, which recognizes the PNAd epitope on the luminal surface (Figure 4A, video S3-S4 https://www.nature.com/leu/journal/v30/n5/suppinfo/leu201633s1.html?url=/leu/journal/v30/n5/full/leu201633a.html). The HEV length was significantly impaired in mice transplanted with MSCs (Figure 4B) and the analysis of the HEV volume suggested a tendency towards vessel narrowing, although in this case the difference did not reach statistical significance (Figure 4C). In addition, the morphology of the HEV network was affected by MSCs, as shown by the significant decrease in the number of branches and segments (Figure 4D-E), indicating that MSCs limit both HEV elongation and arborisation.

The previous observation prompted us to address whether MSCs impair leukocyte homing to inflamed LNs. Fluorescently labelled naïve T cells were injected intravenously in mice previously immunized with CFA/OVA, and transplanted or not with MSCs. After 20 minutes, alexa633-conjugated MECA-79 and MEL-14 mAbs were intravenously injected to stain HEV and block L-selectin, respectively, and, after 20 additional minutes, the dLNs were harvested and prepared for two-photon microscopy acquisition[109] (Figure 4F). The analysis demonstrated that MSCs transplantation inhibited T cell homing into the inflamed LNs (Figure 4G).

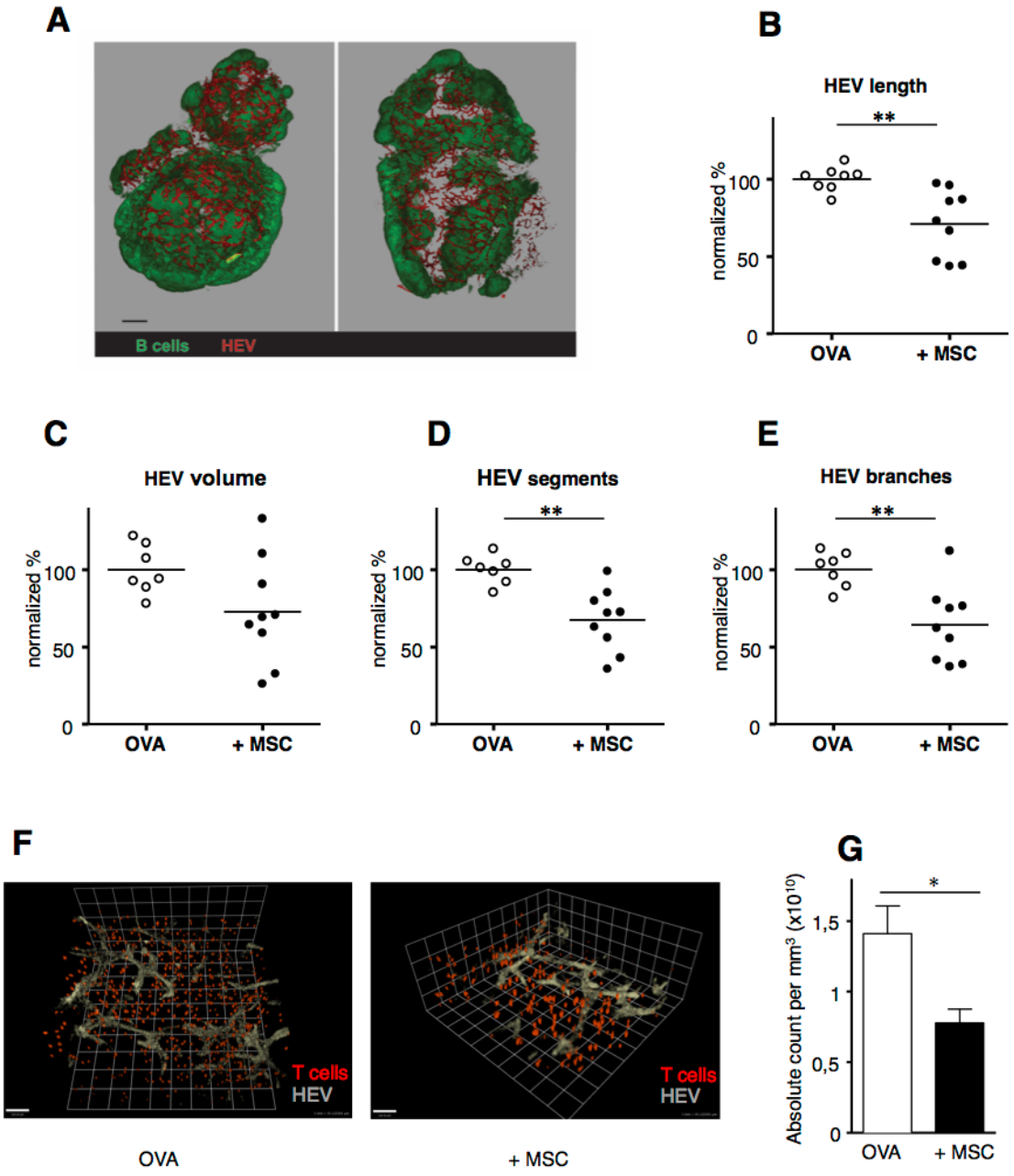

Figure 4 - MSCs suppress HEV lengthening and branching

A-E) Mice were treated as described in Fig 1A and on day 4 brachial LNs were prepared for OPT imaging (Meca-79 Alexa-594 and B220 Alexa-488). A) Representative images from OPT scanning (scale bar, 400 um). B) Total HEV length per LN. C) Total HEV volume per LN. D) Number of HEV segments per LN. E) Number of branch points per LN. F-G) 3DIF of lymphocyte homing in presence of MSCs tested at day 3 post immunization. F) Representative images. G) Absolute counts per mm3 in OVA and OVA+MSCs-treated mice, with error bars representing SE. (*p< 0.05 **p < 0.01; t-test).

Endothelial Cells are a direct target of MSCs

In order to understand whether the inhibition of endothelial cell activation and proliferation observed in immunized mice treated with MSCs was due to a direct effect of MSCs on endothelial cells, we analysed the effects of MSCs supernatants in various *in vitro* assays using a mouse vascular endothelial (1G11) and two mouse lymphatic endothelial (MELC and SVEC4-10) cell lines[98],[110]. MSCs were first expanded as an adherent monolayer until confluence, and were then stimulated for 24h in presence or absence of IL1β, IL6, and TNFα to resemble the inflammatory milieu that MSCs find *in vivo*[111],[112]. MSCs supernatant was collected as conditioned medium 18 hrs after cytokine withdrawal.

First, we analysed the effect of MSCs secretion on *in vitro* angiogenesis using the tube formation assay[113]. The soluble factors released by stimulated MSCs strongly inhibited the ability of SVEC4-10 cells to form tube networks whereas the medium collected from the unstimulated MSCs (unst MSC-CM had no effect (Figure 5A-B), indicating that in an inflammatory environment MSCs can directly inhibit angiogenesis. On the basis of these results and of the published literature[111],[112], in the following experiments we focused on the effects of the MSCs conditioned medium (MSC-CM) only.

Since the *in vivo* data indicated that MSCs transplantation affects the expression of adhesion molecules on endothelial cells (Figure 2B), we analysed the expression of VCAM-1 and ICAM-1 on MELC and 1G11 cells treated with 20 ng/ml TNFα for 24 hrs[98],[99], in the presence or in the absence of MSC-CM. In agreement with the previous data, the MSC-CM significantly reduced the expression of VCAM-1 and ICAM-1 on MELC (Figure 5C and E) and the expression of VCAM-1 on 1G11 cells (Figure 5D and F).Expression of VCAM-1 and ICAM-1 on endothelial cells is regulated by NF-kB[114] and thus we examined the nuclear localization of NF-kB complexes using immunofluorescence microscopy. As expected, in both MELC and 1G11 cells TNFα stimulation resulted in prompt translocation of p65 from the cytoplasm into the nucleus. MSCs conditioned medium inhibited NF-kB translocation in both cell lines (Figure 5G-J). Altogether, these data indicate that endothelial cell activation is directly inhibited by soluble factors released by MSCs exposed to inflammatory cytokines.

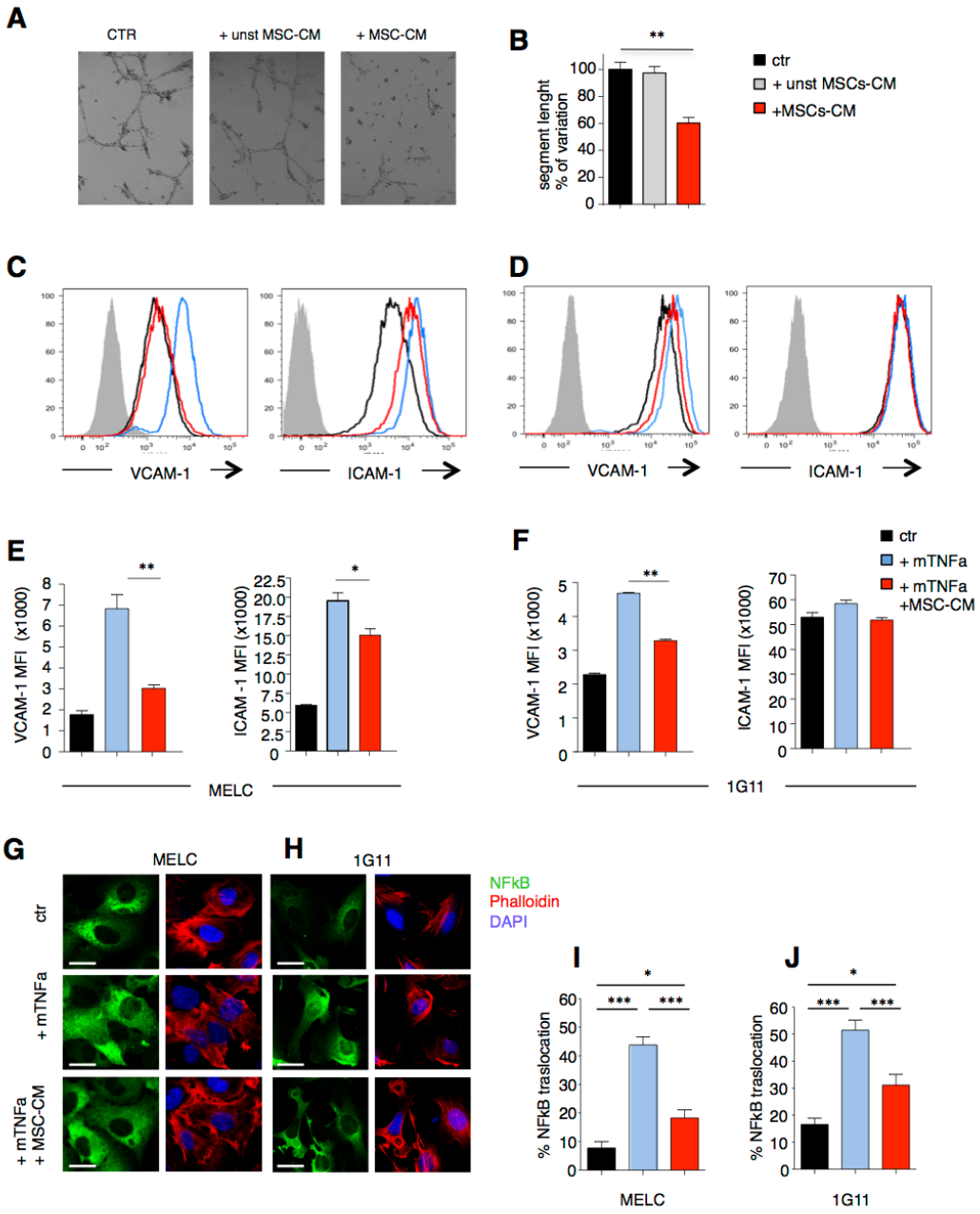

Figure 5 - Endothelial Cells are a direct target of MSCs-secreted molecules

The supernatant of MSCs stimulated with IL1b, IL6 and TNF-a (MSC-CM) or unstimulated MSCs (unst-MSCs) was collected as described in the methods section and its effect on endothelial cell lines activation was determined. A-B) SVEC4-10 network formation. Representative images at 6 hrs and segment length quantification indicated as % of variation in comparison with control condition. Data are expressed as mean ± SEM and represent the pool of 3 experiments (t-test). C-D) Expression of endothelial adhesion molecules. Representative histograms showing the Mean of Fluorescence Intensity (MFI) of VCAM-1 and ICAM-1 on MELC and 1G11 endothelial cell line. E-F) Quantitative analyses of panels C and D, respectively(t-test). G-J) TNF-a induced NF-kB translocation. Representative confocal images (40x) of MELC G) or 1G11 H) cells stained for NF-kB and phalloidin. Scale bar 10 um. I-J) Quantification of NF-kB translocation into the nucleus expressed as percentage of the total. (One representative experiment out of three; one way Anova). (*p< 0.05; **p < 0.01; ***p < 0.0001).

MSCs inhibit in vitro angiogenesis through the release of TIMP-1

In an effort to understand the molecular mechanisms responsible for the observed effects of MSCs, we performed shotgun proteomic characterization of the MSCs secretome, comparing the supernatants collected from MSCs stimulated (MSC-CM) or not (unst MSC-CM) with inflammatory cytokines. As detailed in Materials and Methods, only proteins present and quantified in at least 3 out of 5 technical repeats, in both biological replicates, were considered as positively identified; 1613 and 1630 proteins were measured in the secretome of control and stimulated MSCs, respectively.

Differential expression was considered significant if (a) a protein was present only in MSC-CM or in control or (b) its LFQ intensity resulted statistically significant as calculated by Perseus (t-test cut-off at 1% permutation-based False Discovery Rate). According to this analysis, 7.6 % or 8.3 % of the proteins detected in the secretome of control or stimulated MSCs, respectively, were differentially expressed, either up or down regulated. These proteins were clustered according to their functions using the DAVID platform[115] filtered for significant Gene Ontology Biological Process (GOBP) terms using a p value <0.05.

Concerning the 52 proteins that were significantly down-regulated or present only in the secretome of unstimulated MSCs (Table S1 http://www.nature.com/leu/journal/v30/n5/suppinfo/leu201633s1.html?url=/leu/journal/v30/n5/full/leu201633a.html), GO analysis revealed that most terms are related to metabolic processes). As for the 89 proteins that were significantly up-regulated or present only in the secretome of stimulated MSCs (Figure 6A and Table S2 http://www.nature.com/leu/journal/v30/n5/suppinfo/leu201633s1.html?url=/leu/journal/v30/n5/full/leu201633a.html), GO analysis indicated that 18% and 30% of the proteins belong to categories that are related to regulation of angiogenesis and inflammation processes, respectively (Figure 6B and Table S2 at http://www.nature.com/leu/journal/v30/n5/suppinfo/leu201633s1.html?url=/leu/journal/v30/n5/full/leu201633a.html). In particular, the presence of an "angiogenesis-related" signature among up-regulated proteins was also confirmed by analyses of human MSCs secretome, which reveals that all the 16 up-regulated proteins in stimulated-MSCs secretome common to human and mouse are modulators of angiogenesis (Table 1).

Table 1: common proteins up-regulated in stimulated vs unstimulated mouse and human MSCs secretome

Mouse Protein Id	Human Protein Id	Gene name	Protein name	Role in angiog	Refs
M0QWP1	O00468-6	AGRN	Agrin	X	(Tatrai et al., 2006)
P10605	P07858	CTSB	Cathepsin B	X	(Im et al., 2005; Mai et al., 2002)
P50228	P42830	CXCL5	C-X-C motif chemokine 5	X	(Strieter et al., 2005)
E9Q6C2	P09871	C1S	Complement C1s subcomponent		
P01027	P01024	C3	Complement C3 fragment		
Q62356	Q12841	FSTL1	Follistatin-related protein 1	X	(Ouchi et al., 2008)
E9PZ16	P98160	HSPG2	Perlecan	X	(Jiang et al., 2004; Sharma et al., 1998)
F8WH23	Q16270	IGFBP7	Insulin-like growth factor-binding protein 7	X	(van Beijnum et al., 2006)
Q07797	Q08380	LGALS3BP	Galectin-3-binding protein	X	(Piccolo et al., 2013)
P10493	P14543	NID1	Nidogen-1	X	(Semkova et al., 2014)
G5E899	P05121	SERPINE1	Plasminogen activator inhibitor 1	X	(Isogai et al., 2001), (Bruyere et al., 2010)
P12032	P01033	TIMP1	Metalloproteinase inhibitor 1	X	(Ikenaka et al., 2003), (Akahane et al., 2004)
Q80YX1	P24821	TNC	Tenascin	X	(Mai et al., 2002)
P29533	P19320	VCAM1	Vascular cell adhesion protein 1	X	(Koch et al., 1995)

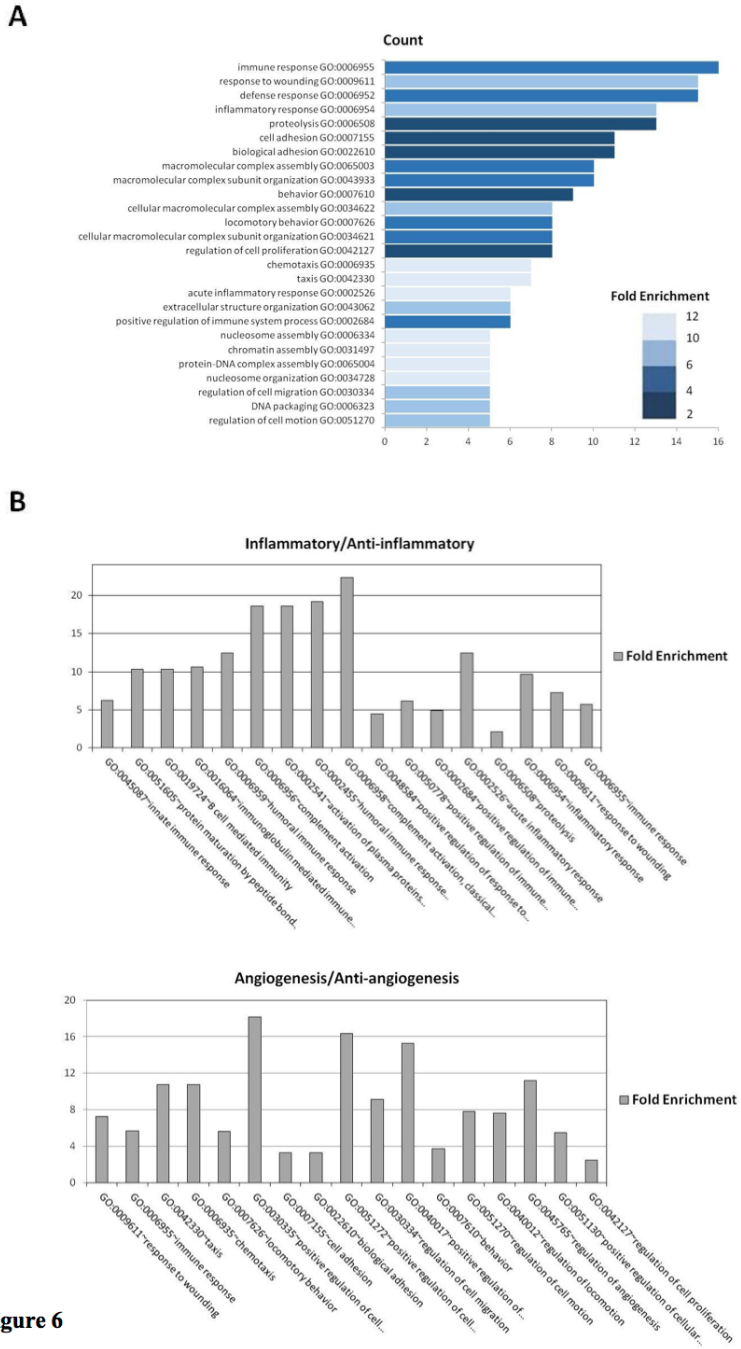

Figure 6

Figure 6 - Distribution into biological processes of the proteins up regulated in MSC-CM

The proteins that were significantly up-regulated or present only in MSC-CM were classified into different biological processes according to the GO classification system. A) The bar chart shows the count of the top 26 most enriched GO terms in MSC-CM versus unstimulated MSC-CM. Colour coding indicates the Fold Enrichment. B) Proteins categorized as modulators involved in inflammation processes and/or angiogenesis. The histograms report the GOBP groups related to angiogenesis or inflammation.

Among the several proteins up-regulated in MSCs by the inflammatory cytokines that have a direct or indirect effect on endothelial cells, we focused our attention on the tissue inhibitor of metalloproteinase-1 (TIMP-1) because of its well-known anti-angiogenic properties[116]. We thus used the tube formation assay to analyse the effect of MSCs-derived TIMP-1 on angiogenesis. While the blocking anti-TIMP-1 antibody had no effect on the ability of endothelial cells to form tubes when cultured in the supernatants of unstimulated MSCs it totally reverted the anti-angiogenic properties of the supernatant from stimulated MSCs (Figure 7A), indicating that, at least in this *in vitro* setting, TIMP1 is one of the key MSCs-secreted molecules targeting the endothelium. In an *in vivo* setting, the injection of neutralizing anti-TIMP-1 antibody[104] 1 day after MSCs transplantation reverted the MSCs-induced reduction of endothelial cell numbers and HEV in dLNs (Figure 7B-D), suggesting that TIMP-1 may be directly responsible for the anti-inflammatory effects of MSCs on LNs. To confirm this hypothesis, we used a siRNA approach to knock down TIMP-1 expression in MSCs (figure 7bis). Again, the absolute cell numbers of endothelial cells and HEV in dLN was reduced by MSC transfected with the scramble siRNA control but not by MSCs with TIMP-1 siRNA (Figure 7E-G).

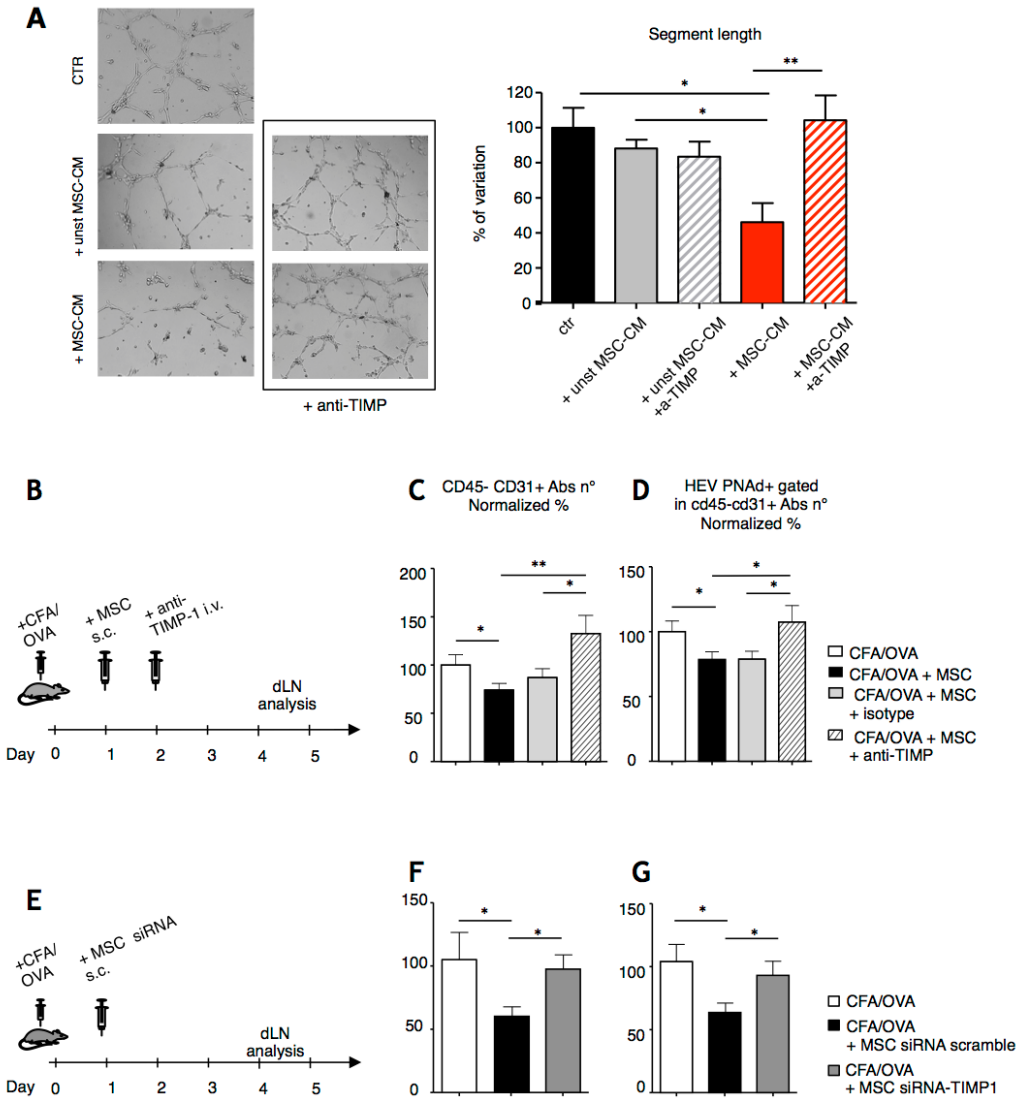

Figure 7 - TIMP-1 mediates the anti-angiogenic effect of MSC-CM in vitro and the anti-inflammatory effect of MSCs in vivo

SVEC4-10 network formation in matrigel in the presence of MSC-CM or unstMSC-CM and anti-TIMP1 blocking antibody. A) anti-mTIMP1 blocking antibody restores SVEC4-10 network formation in matrigel in the presence of MSC-CM. Representative images at 6 hrs (left) and segment length quantification as percentage of variation (right) are shown. Data are expressed as mean ± SEM (*p<0.05, **p < 0.01; One way Anova). B) Diagram of the experimental protocol designed to block the TIMP-1 activity during the anti-inflammatory effects of MSCs. Mice were immunized in the dorsal region with CFA/OVA on day 0 and, on day 1, 3 groups of animals received subcutaneous injection of 10^6 MSCs in the lumbar region. 18 hours after MSCs transplantation goat polyclonal anti-TIMP-1 IgG or isotype-matched goat IgG was i.v. administrated. On day 4 brachial LNs were collected, processed and analysed by flow cytometry; C-D) The graphs show the absolute number of $CD45^-CD31^+$ cells and HEV $PNAd^+$ cells per single LN, expressed as normalized percentage on CFA/OVA (t-test). E) Diagram of the experimental protocol designed to investigate the contribution of MSCs-derived TIMP-1 on dLN endothelium. Mice were immunized in the dorsal region with CFA/OVA on day 0. The day after, 2 groups of animals received in the lumbar region subcutaneous injection of 10^6 MSCs transfected with either scramble control siRNA or siRNA specific for TIMP1 respectively. On day 4, brachial LNs were collected, processed and analysed by flow cytometry; F-G) Graphs showing the absolute number of $CD45^-CD31^+$ cells and HEV $PNAd^+$ cells per single dLN. Data are expressed as normalized percentage on CFA/OVA (Mann-Whitney test). (*p< 0.05; **p < 0.01)

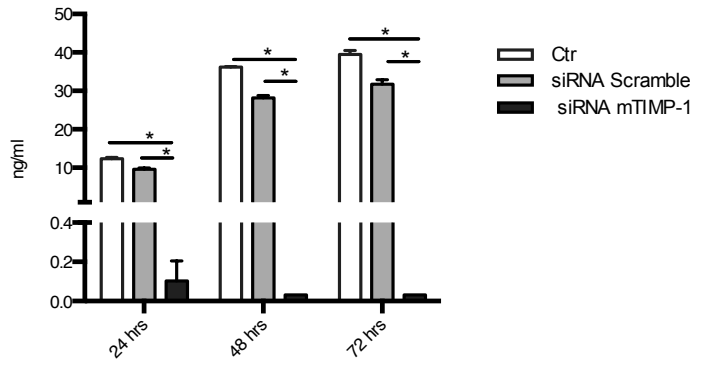

Figure 7bis - TIMP-1 siRNA Reverse Transfection

Timp-1 secretion by MSCs was analysed at 24, 48 and 72 hours after transfection by ELISA (see the method section). SiRNA scramble was used as negative control (One representative experiment out of four; *p < 0.05; **p < 0.01; ***p < 0.0001; t-test).

On the basis of these results, we speculated that the over-expression of TIMP-1 might be sufficient to mimic the effects of MSCs transplantation, in terms of inhibition of angiogenesis in the inflamed lymph nodes. TIMP-1 over-expression by AAV9-mediated gene transfer[105] in mice immunized with CFA/OVA (Figure 8A) inhibited the inflammatory reaction in the draining lymph nodes, as indicated by the reduced total cellularity (Figure 8B), which was due to a decreased number of both CD45$^+$ cells (Figure 8C) as well as of endothelial and HEV cells (Figure 8D-E).

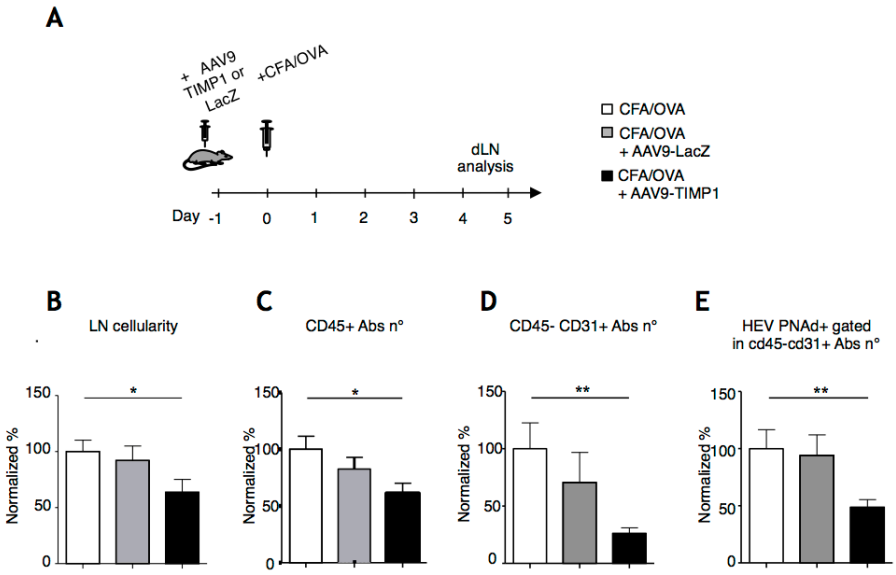

Figure 8 - TIMP-1 over-expression in vivo mimics MSCs transplantation

A) Diagram of the experimental protocol designed to over-express TIMP-1 in immunized mice. One day after AAV9-TIMP1 or AAV9-LacZ administration (day 0), mice were immunized with CFA/OVA. Brachial dLNs were collected 4 days after immunization and processed for flow cytometry. The graphs show the absolute number of total cells (B), CD45$^+$ cells (C), CD45$^-$CD31$^+$ (D) and HEV PNAd$^+$ (E) cells per single LN, expressed as normalized percentage on CFA/OVA. Error bars represent standard error, (*p < 0.05; **p < 0.01; Mann-Whitney test).

Proteomic based comparison between mouse and human MSC-CM

In our work, we took advantage of animal models to elucidate the molecular pathway involved in the effects of the mMSCs in the complex crosstalk between inflammation and angiogenesis[117]. Since it is widely accepted that significant differences exist between mouse and human MSCs[111],[118] and for the tremendous relevance of inflammation-induced angiogenesis in human diseases, we focused our attention on comparing mouse and human MSCs secretome. The proteomic results of human MSCs secretome were therefore compared with those reported for murine MSC-CM[117]. The supplemental Table1(http://www.sciencedirect.com/science/article/pii/S187439191730252X?via%Dihub#ec0005) lists the 286 proteins (out of 465, 62%) present in st hMSC-CM that have been detected also in st mMSC-CM. The number of proteins significantly up-regulated or present only in the secretome of stimulated MSCs is similar in the two species: 89 in mouse, 96 in human (Table 2). A comparative analysis of GO_BP category enrichment of overrepresented proteins in human and/or mouse (Figure 9) suggests that: a) proteins up-regulated in the secretome of stimulated MSCs from both organisms are, for the most part, involved in similar biological processes, mainly related to defence, immune and inflammatory response, chemotaxis and extracellular matrix remodelling; b) however there are clear important differences amongst human and mouse. Thus, only st mMSC-CM is enriched in proteins involved in chromatin structure assembly, cell proliferation regulation and related processes. On the contrary, complement activation, leukocyte migration, bone development and metabolic processes specifically related to collagen are amongst the statistically enriched GO functional categories in human but not in mouse. Such differences are confirmed by the observation that only 23 proteins are up-regulated or present only in stimulated MSC-CM both in mouse and human (Table 3); this again points to a fine species-related tuning of the overall effects of secretome from the two organisms; interestingly, our analysis indicates that 74% and 83% of the common up-regulated proteins are associated with angiogenesis or inflammation, respectively.

Table 2: proteins overrepresented or present only in st- hMSC-CM

Gene names	Protein names	Protein ID	H30 -Log P *t*-test	H30 *t*-Test Diff[a]	H34 -Log P *t*-test	H34 *t*-Test Diff[a]	Angiogenesis[b]	Inflammation[b]
ABI3BP	Target of Nesh-SH3	D3YTG3	Only in stimulated					
AGRN	Agrin	O00468	5.339	2.799	3.970	1.066	x	x
ALCAM	CD166 antigen	Q13740	Only in stimulated				x	x
ARHGAP1	Rho GTPase-activating protein 1	Q07960	Only in stimulated					
BMP1	Bone morphogenetic protein 1	P13497	3.745	1.175	4.642	0.751	x	x
C1R	Complement C1r subcomponent	P00736	8.619	2.624	6.801	2.132		x
C1S	Complement C1s subcomponent	P09871	6.886	1.883	6.503	1.992		x
C3	Complement C3	P01024	10.267	7.920	5.001	4.683	x	x
CA12	Carbonic anhydrase 12	O43570	Only in stimulated				x	x
CCL2	C-C motif chemokine 2	P13500	9.381	6.120	10.273	9.600	x	x
CDC37	Hsp90 co-chaperone Cdc37	Q16543	Only in stimulated					x
CFB	Complement factor B	B4E1Z4	Only in stimulated				x	x
CFH	Complement factor H	P08603	5.941	2.293	6.526	2.405		x
CHI3L1	Chitinase-3-like protein 1	P36222	6.932	1.415	6.918	1.353	x	x
CLSTN1	Calsyntenin-1	O94985	4.674	0.615	3.190	0.932		
COL16A1	Collagen alpha-1(XVI) chain	A6NDR9	5.166	1.459	4.026	1.439		x
COL3A1	Collagen alpha-1(III) chain	P02461	7.283	0.588	10.347	1.865		x
COL5A2	Collagen alpha-2(V) chain	P05997	1.555	0.170	7.749	1.353		
COL7A1	Collagen alpha-1(VII) chain	Q02388	5.682	2.193	2.828	0.961		x
CSF1	Macrophage colony-stimulating factor 1	P09603	Only in stimulated				x	x
CTHRC1	Collagen triple helix repeat-cont prot 1	Q96CG8	5.339	1.314	4.189	1.134	x	
CTSB	Cathepsin B	P07858	3.149	0.636	5.472	1.500	x	x
CXCL1	Growth-regulated alpha protein	P09341	Only in stimulated				x	x
CXCL12	Stromal cell-derived factor 1	P48061	5.665	2.429	1.652	0.470	x	x
CXCL5	C-X-C motif chemokine 5	P42830	Only in stimulated				x	x
CXCL6	C-X-C motif chemokine 6	P80162	Only in stimulated				x	x
CYR61	Protein CYR61	O00622	Only in stimulated				x	x
DCN	Decorin	P07585	5.699	0.835	5.760	1.253	x	x
EFEMP2	EGF-cont fibulin-like extrac matrix prot 2	O95967	3.013	1.193	5.790	1.640		x
EIF6	Eukaryotic translation initiation factor 6	P56537	Only in stimulated				x	x
ELN	Elastin	F8WAH6	4.693	1.332	5.715	2.206	x	x
EXT1	Exostosin-1	Q16394	3.775	1.085	2.266	0.485		
EXT2	Exostosin-2	Q93063	Only in stimulated					
FBLN1	Fibulin-1	P23142	4.242	0.867	6.450	1.323	x	
FBN1	Fibrillin-1	P35555	6.035	0.969	6.557	1.909	x	x
FKBP1A	Peptidyl-prolyl cis trans isomerase	P62942	Only in stimulated					x
FN1	Fibronectin	P02751	5.787	0.793	5.421	0.358	x	x
FNDC1	Fibronectin type III domain-cont prot 1	Q4ZHG4	5.245	2.301	7.588	1.418	x	x
FSTL1	Follistatin-related protein 1	Q12841	3.823	0.817	7.039	1.968	x	x
GALNT2	Polypeptide *N*-acetylgalactosaminyltransferase 2	Q10471	2.914	0.542	2.860	0.895	x	
GBP1	Interferon-induced guanylate-binding prot 1	P32455	Only in stimulated				x	x
GC	Vitamin D-binding protein	P02774	Only in stimulated					x
HLA-A	HLA class I histocompatibility antigen, A-24 alpha chain	P05534	5.130	1.393	3.813	1.312		x
HLA-C	HLA class I histocompatibility antigen, Cw-7 alpha chain	A2AEA2	3.071	1.381	3.304	1.231		x
HSPG2	Base membr-spec hepar sulf proteoglycan core prot	P98160	8.735	1.796	9.468	2.141	x	x
HYOU1	Hypoxia up-regulated prot 1	Q9Y4L1	Only in stimulated				x	x
ICAM1	Intercellular adhesion molecule 1	P05362	Only in stimulated				x	x
IGFBP4	Insulin-like growth factor-binding prot 4	P22692	4.346	1.526	3.986	1.009	x	x
IGFBP6	Insulin-like growth factor-binding prot 6	P24592	Only in stimulated				x	x
IGFBP7	Insulin-like growth factor-binding prot 7	Q16270	2.725	0.397	4.650	0.947	x	x
IL6	Interleukin-6	P05231	Only in stimulated				x	x
IL8	Interleukin-8	P10145	Only in stimulated				x	x
INHBA	Inhibin beta A chain	P08476	7.879	3.140	5.875	1.448	x	
ITIH2	Inter-alpha-trypsin inhibitor heavy chain H2	P19823	3.742	1.104	1.276	0.382		x
ITM2B	Integral membrane protein 2B;BRI2	Q9Y287	3.573	1.994	5.351	1.035		
KRT6B	Keratin, type II cytoskeletal 6B	P04259	Only in stimulated					
LAMA4	Laminin subunit alpha-4	Q16363	2.027	0.234	1.925	0.173	x	
LAMB2	Laminin subunit beta-2	P55268	5.174	3.708	4.936	1.006		
LEPRE1	Prolyl 3-hydroxylase 1	Q32P28	Only in stimulated				x	x
LGALS3BP	Galectin-3-binding protein	Q08380	8.011	1.487	6.749	1.314	x	x
LOXL2	Lysyl oxidase homolog 2	Q9Y4K0	6.219	1.195	5.732	1.521	x	x
LYZ	Lysozyme C	P61626	3.547	0.507	1.328	0.607		x
MAN1A1	Mannosyl-oligosaccharide 1,2-alpha-mannosidase IA	P33908	Only in stimulated				x	x
MANBA	Beta-mannosidase	O00462	Only in stimulated					
MMP1	Interstitial collagenase	P03956	Only in stimulated				x	x
MMP10	Stromelysin-2	P09238	Only in stimulated				x	x
MMP13	Collagenase 3	G5E971	Only in stimulated				x	x
MMP2	72 kDa type IV collagenase	P08253	6.555	1.090	7.061	1.043	x	x
MMP3	Stromelysin-1	P08254	Only in stimulated				x	x
NID1	Nidogen-1	P14543	3.840	0.925	3.450	0.890	x	x
NID2	Nidogen-2	Q14112	4.384	1.133	3.823	0.855		
NUCB1	Nucleobindin-1	Q02818	5.878	0.985	3.867	0.703		
PLOD1	Procollagen-lysine,2-oxoglutarate 5-dioxygenase 1	B4DR87	3.944	0.876	2.180	0.264		
PLOD2	Procollagen-lysine,2-oxoglutarate 5-dioxygenase 2	O00469	5.967	2.636	5.402	2.331	x	

Table 1 (continued)

Gene names	Protein names	Protein ID	H30 -Log P t-test	H30 t-Test Diff[a]	H34 -Log P t-test	H34 t-Test Diff[a]	Angiogenesis[b]	Inflammation[b]
PSMA5	Proteasome subunit alpha type-5	P28066	Only in stimulated					
PSME2	Proteasome activator complex subunit 2	Q9UL46	Only in stimulated					
PTX3	Pentraxin-related protein PTX3	P26022	7.000	3.580	8.516	3.256	x	x
PXDN	Peroxidasin homolog	Q92626	6.359	1.401	5.119	1.122		
QPCT	Glutaminyl-peptide cyclotransferase	Q16769	3.070	1.972	4.593	2.140		x
QSOX1	Sulfhydryl oxidase 1	O00391	5.232	1.616	9.152	2.155	x	
RNASE4	Ribonuclease 4	P34096	Only in stimulated				x	x
SDC4	Syndecan-4	P31431	1.696	0.810	3.199	1.321	x	x
SDF4	45 kDa calcium-binding prot	Q9BRK5	2.014	0.353	3.547	0.862	x	
SERPINB2	Plasminogen activator inhibitor 2	P05120	Only in stimulated					x
SERPINE1	Plasminogen activator inhibitor 1	P05121	8.172	2.596	6.111	1.557	x	x
SLC39A14	Zinc transporter ZIP14	Q15043	Only in stimulated					
SLC3A2	4F2 cell-surface antigen heavy chain	P08195	Only in stimulated					
SOD2	Superoxide dismutase [Mn]	P04179	Only in stimulated				x	x
SRGN	Serglycin	P10124	5.249	1.412	3.353	1.084	x	
SRPX2	Sushi repeat-containing prot SRPX2	O60687	7.209	2.708	3.423	2.482	x	x
SSB	Lupus La protein	P05455	Only in stimulated					
STC2	Stanniocalcin-2	O76061	Only in stimulated				x	
TIMP1	Metalloproteinase inhibitor 1	P01033	2.940	1.254	5.763	1.081	x	x
TNC	Tenascin	P24821	6.040	1.645	7.257	1.329	x	x
TNFAIP6	Tumor necrosis factor-inducible gene 6 protein	P98066	Only in stimulated					x
VCAM1	Vascular cell adhesion protein 1	P19320	5.307	3.003	5.227	2.623	x	x

[a] t-Test diff: difference of log(2) mean intensity of a protein in technical replicas of st- versus unst hMSC-CM from t-test analysis using Perseus [28] as detailed in the text.
[b] Proteins related to angiogenesis or inflammation according to criteria detailed in "Materials and methods".

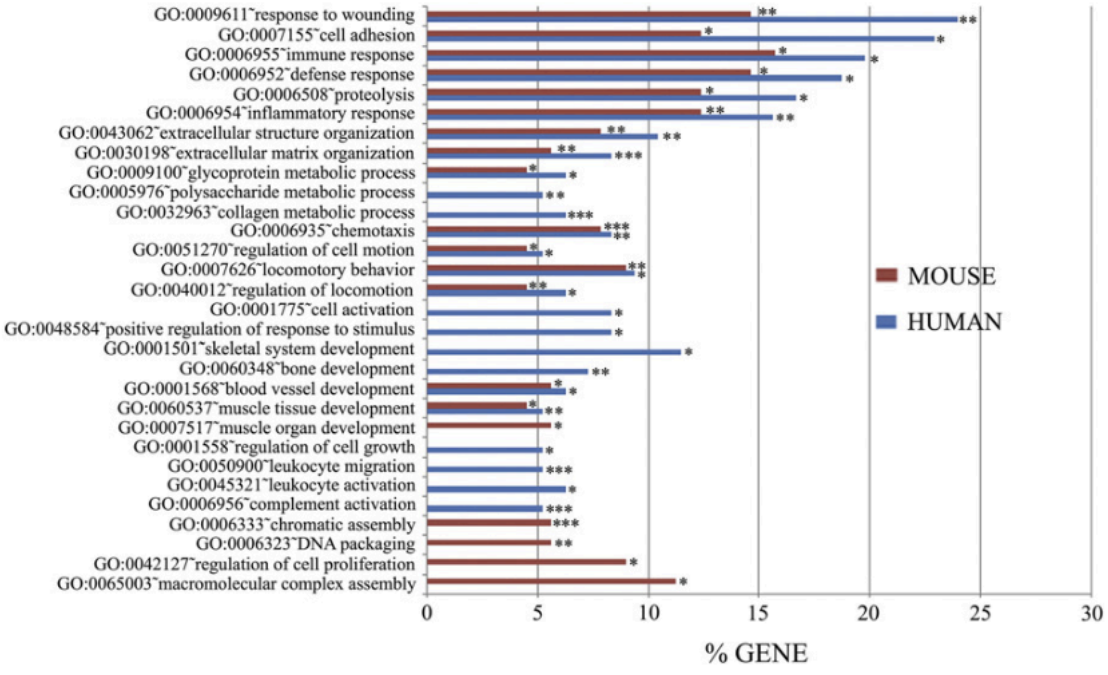

Figure 9 - Distribution into biological processes of the proteins overrepresented in stimulated hMSC-CM in human and mouse

The proteins that were significantly up-regulated or present only in stimulated MSC-CM were classified into different biological processes according to the Gene Ontology classification system (GOBP) using DAVID software; confidence level: medium; only categories showing modified Fisher exact EASE score p value b 0.05 and at least 5 counts in hMSCs are represented. The bars represent the percentage of proteins involved in a category out of the total number of overrepresented proteins in human (96) or mouse (89) secretome. Asterisks indicate fold enrichment range for each category: * 1–5, ** 6–10, *** N10.

Table 3: proteins overrepresented or present only in st- MSC-CM common to mouse and human

Gene names	Protein names	Angiogenesis[a]	Infllammation[a]
AGRN	Agrin	x	x
C1R	Complement C1r subcomponent		x
C1S	Complement C1s subcomponent		x
C3	Complement C3	x	x
CSF1	Macrophage colony-stimulating factor 1	x	x
CTSB	Cathepsin B	x	x
CXCL1	Growth-regulated alpha protein	x	x
CXCL5	C-X-C motif chemokine 5	x	x
EXT1	Exostosin-1		
EXT2	Exostosin-2		
FSTL1	Follistatin-related protein 1	x	x
HSPG2	Basem membr-spec heparan sulfate proteoglycan core prot	x	x
IGFBP7	Insulin-like growth factor-binding protein 7	x	x
IL6	Interleukin-6	x	x
LAMB2	Laminin subunit beta-2		
LGALS3BP	Galectin-3-binding protein	x	x
MMP13	Collagenase 3	x	x
NID1	Nidogen-1	x	x
PLOD2	Procollagen-lysine,2-oxoglutarate 5-dioxygenase 2	x	
SERPINE1	Plasminogen activator inhibitor 1	x	x
TIMP1	Metalloproteinase inhibitor 1	x	x
TNC	Tenascin	x	x
VCAM1	Vascular cell adhesion protein 1	x	x

Functional evidence of human and mouse MSCs secretome similarities or differences

Our proteomic results indicate that the majority of secreted proteins from both human and mouse MSCs are associated with inflammation and angiogenesis (Table 1 and [117]). To identify specific functional analogies or differences of human and mouse MSCs in the regulation of these two important processes, we focused on two proteins, M-SCF/CSF1 and TIMP1, which are present in st MSC-CM of both species and play a key role in immunity/inflammation and angiogenesis, respectively[119,43].

Macrophage colony-stimulating factor (M-CSF)

M-CSF is a growth factor secreted by a large variety of cells including macrophages, endothelial cells, fibroblast and lymphocytes. By interacting with its membrane receptor (CSF1R or M-CSF-R), it stimulates the survival, proliferation, and differentiation of monocytes and macrophages[120],[121]. Our proteomic data indicated that M-CSF (CSF1) is up-regulated in the secretome of both human and mouse MSCs upon stimulation by inflammatory cytokines (Tables 1 and 2). Thus, we investigated the ability of MSC-CM to generate monocyte-derived macrophages in vitro. Surprisingly, our data revealed an important difference between mouse and human MSC-CM (Figure 10). When compared to the positive control (recombinant mouse M-CSF), both unst mMSC-CM or st mMSC-CM were unable to induce macrophage differentiation (F4/80+, CD11b+ cells) efficiently. In this case, stimulation of mMSCs with pro-inflammatory cytokines did not change the properties of the secretome (Figure 10 A). In contrast, the culture of human monocytes in the presence of st hMSC-CM produced the same percentage of differentiated macrophages as the positive control (recombinant human M-CSF) (Figure 10 B). These data reflect the amount of mouse or human M-CSF detectable by ELISA in unst or st human and mouse MSC-CM (Fig. 10). Thus, although M-CSF is up-regulated in both human and mouse MSC-CM upon stimulation by inflammatory cytokines, the amount of M-CSF secreted by mMSCs is too low to be detected by ELISA and to induce macrophage differentiation efficiently. Notably, proteomic data on human M-CSF (CSF1) fully agree with functional assays and ELISA analysis. As reported in Table 1, M-CSF is amongst the proteins showing the highest increase in stimulated human secretome according to mass spectrometric analysis; the apparent discrepancy in the presence of CSF1 in unst hMSC-CM between ELISA (showing low levels of M-CSF in unst hMSC-CM, Fig. 10) and proteomics (listing M-CSF as absent in unst hMSC-CM in Table 1) is due to the high stringency used to filter quantitative proteomic data in the present report (detection in at least 3 out of 5 technical replicas in both patients). In fact, M-CSF was detected also in low amounts in 4 out of 5 replicas of unstimulated secretome of donor H34 but only in 2 out of 5 replicas of donor H30 and consequently listed as "non-detected" in unst hMSC-CM.

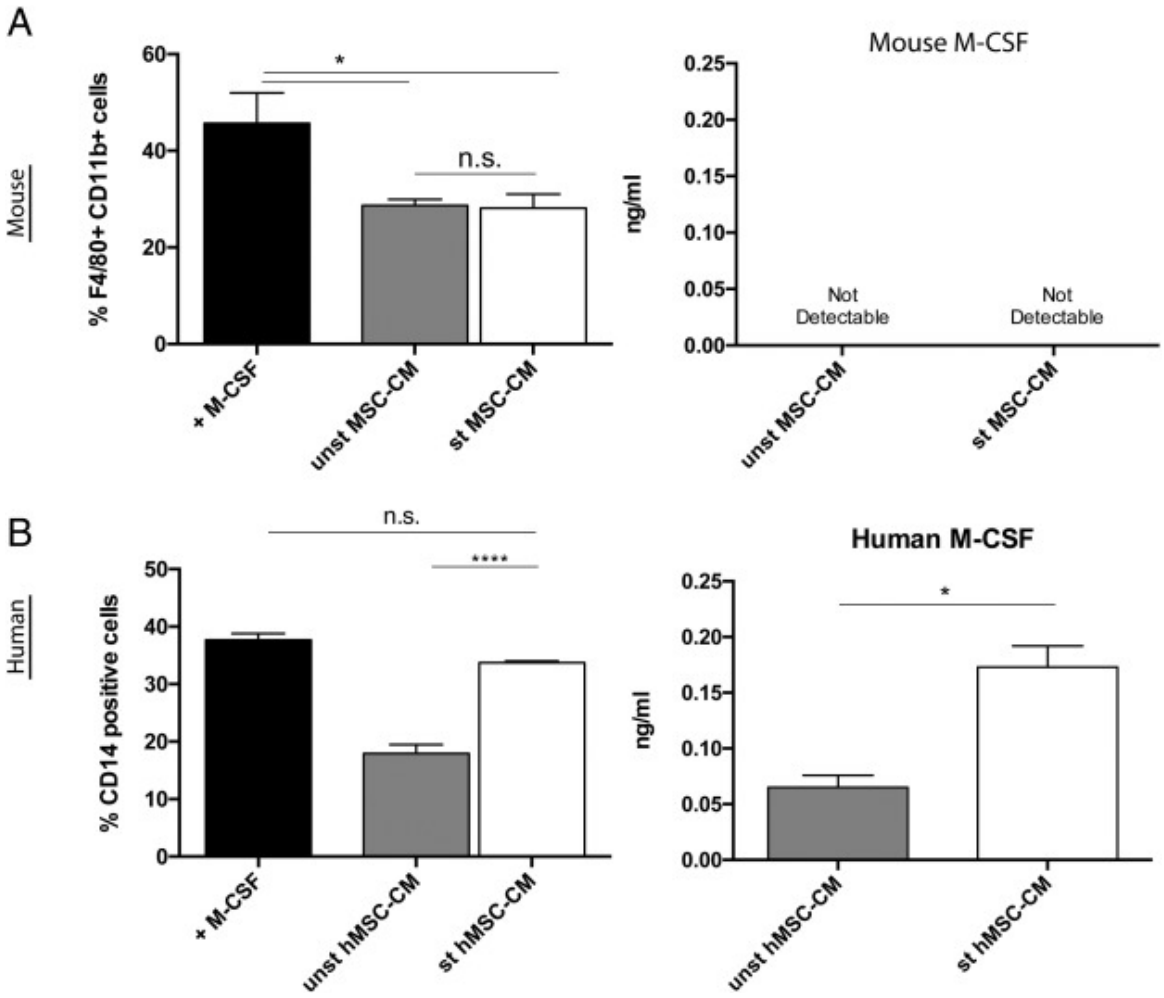

Figure 10 - Human and mouse MSCs conditioned media differentially stimulate monocytes differentiation

A) Mouse bone marrow cells were cultured with murine M-CSF (as positive control), unstimulated or stimulated mouse MSC-CM for 5 days. Differentiation to macrophages was assessed by Flow Cytometry as percentage of F4/80 + CD11b + cells. Right panel: mouse M-CSF concentration in conditioned media was analysed by ELISA. Undetectable cytokine levels were reported for both preparations. B) Human PBMCs were cultured with human M-CSF (as positive control), unstimulated or stimulated human MSC-CM for 5 days. Macrophages were analysed by Flow Cytometry as CD14 + cells. Right panel: human M-CSF quantification by ELISA assay shows higher cytokine levels in st hMSC-CM than unst hMSC-CM. A and B, left panels: 3 independent experiments, data are expressed as mean ± SEM (*$p < 0.05$, ****$p < 0.0001$, One way ANOVA). A and B, right panels: 2 independent experiments, data are expressed as mean ± SEM (*$p < 0.05$, parametric t-test).

TIMP-1

Concerning angiogenesis, we analysed the effect of mMSC-CM on in vitro angiogenesis exploiting the tube formation assay[119]. As we reported in Figure 11 A, soluble factors released by stimulated mMSCs strongly inhibited the ability of mouse endothelial cell SVEC4-10 cell line to form tube networks. In contrast, unst mMSC-CM had no effect on tube formation. In order to assess the hMSC angiogenetic role, we performed the same experiments using HUVEC cells (Human Umbilical Vein Endothelial Cells) (Figure 11 B). In agreement with the data obtained with mMSCs, soluble factors secreted by hMSCs affected the ability of HUVEC cells to form tubes. Interestingly, in the case of human cells, MSC-CM was able to inhibit tube formation even when MSCs had not been primed by cytokines. However, pre-activation with pro-inflammatory cytokines strengthened the anti-angiogenic effects of hMSC-CM, thus supporting our hypothesis that, during an inflammatory response, MSC target angiogenesis and thus dampen the inflammatory response[117]. Using both in vitro and in vivo approaches, we demonstrated that mMSCs anti-angiogenic effect is mediated by TIMP-1[117]. Because the proteomic analyses indicate that TIMP-1 is one of the proteins up-regulated in both human and mouse st MSC-CM (Table 2), we compared the results obtained by blocking TIMP-1 in SVEC4-10 cells incubated in the presence of mMSC-CM (Figure 12A) with those generated using HUVEC cells and hMSC-CM (Fig. 6B). By inhibiting TIMP-1 activity with a specific blocking antibody, we observed the complete recovery of HUVEC cell ability to form tubes even in the presence of st hMSC-CM, indicating that TIMP1 is one of the key secreted molecules targeting endothelial cells in both mouse and human MSCs. TIMP-1 concentration was measured by ELISA in st and unst, human and mouse MSC-CM (Figure 13 A for mouse and B for human). In accordance with our data of tubulogenesis showing that unst mMSC-CM has no effect on angiogenesis (Figs. 11 and 12, panel A), the concentration of TIMP-1 in mMSC-CM was about 5-times higher when cells had been primed by pro-inflammatory cytokines. Thus, in mouse MSCs, the anti-angiogenic phenotype is acquired only after licensing with pro-inflammatory cytokines, i.e. when TIMP-1 levels rise from about 3 ng/mL to 25 ng/mL. In hMSCs, however, the basal high level of secreted TIMP1 may explain the partial anti-angiogenic effect of the unst hMSC-CM (Figs. 11 and 12, panel B). In fact, in support of this hypothesis, TIMP-1 blockade restored the formation of the endothelial network in the presence of unst or st

hMSC-CM.

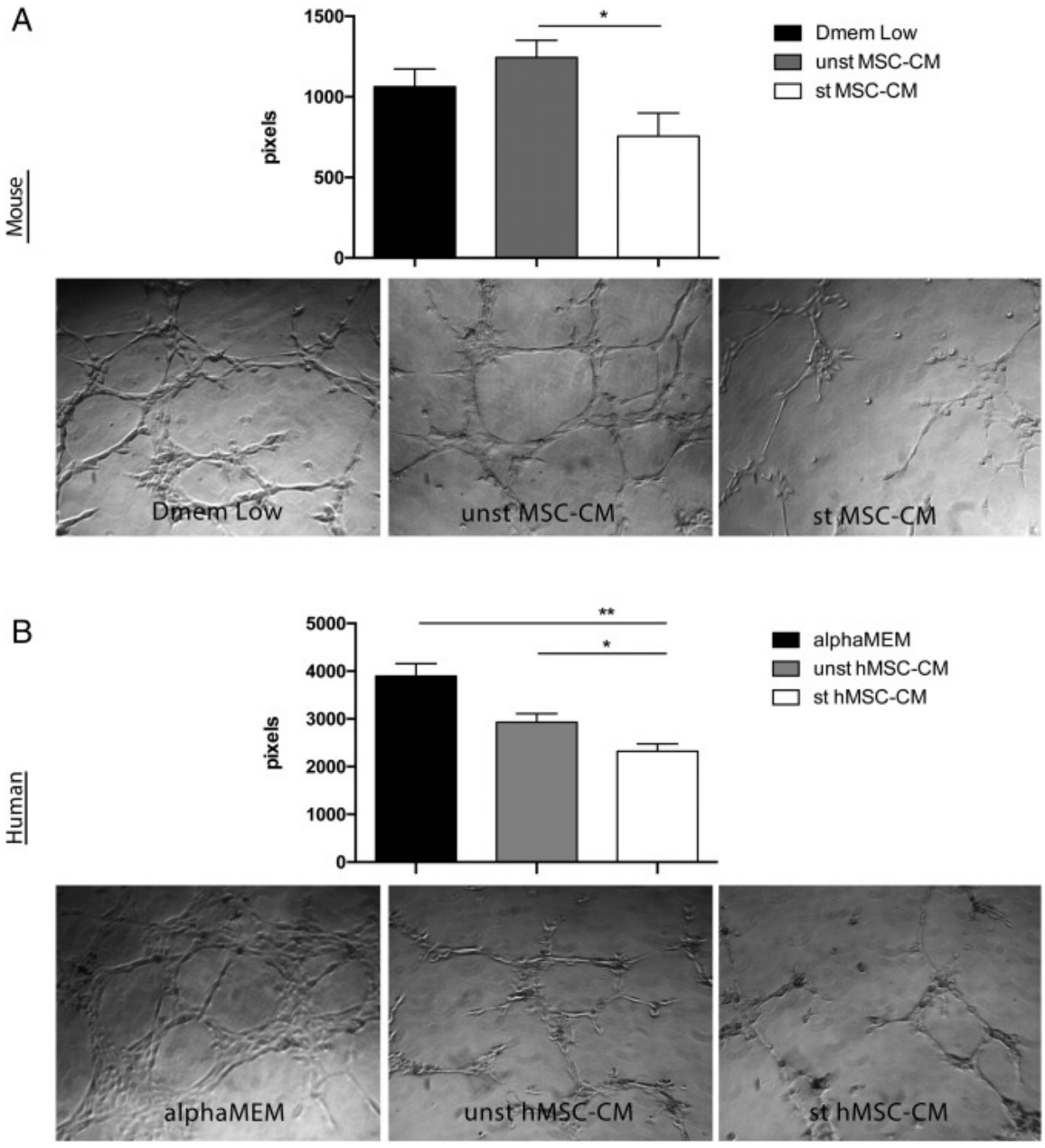

Figure 11 - Effect of human or mouse MSCs conditioned medium on tube formation assay

The effect of unstimulated or stimulated MSCs media on endothelial cells was determined by a tube formation assay. Cells were seeded on the top of a matrigel phase in the presence of unstimulated or stimulated A) mouse, B) human MSC-CM. 6 h later, images were acquired with a phase contrast inverted microscope at 4× objective magnification. Analysis was performed with ImageJ Angiogenesis Analyzer. A) SVEC4-10 network formation; quantification of the tube segment length (expressed in pixel number) and representative images at 4 h. B) Huvec network formation; quantification of the tube segment length and representative images (expressed in pixel number) at 4 h. 3 independent experiments, data are expressed as mean ± SEM (*p b 0.05, **p b 0.01, One-way ANOVA).

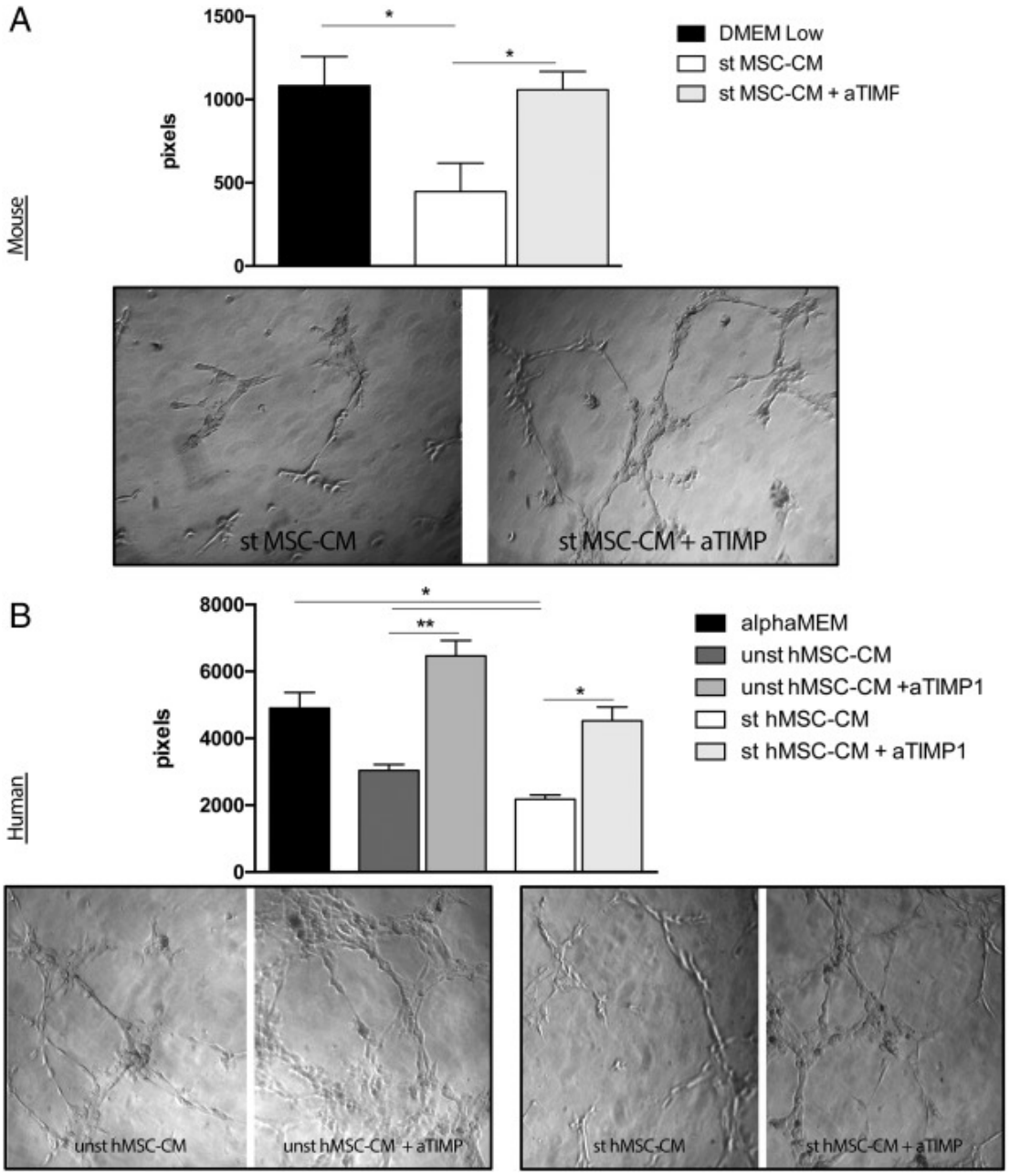

Figure 12 - Timp-1 blocking reverts the anti-angiogenic effect of mouse and human MSCs conditioned media

In order to investigate the role of MSCs-derived TIMP-1 on angiogenesis, the tube formation assay was performed in the presence of A) mouse or B) human TIMP-1 blocking antibody. Representative images of A) SVEC4-10 cell line or B) Huvec cells are taken with a phase contrast inverted microscope at 4 × objective magnifications. Graphs show the quantification of the tube segment length measured with ImageJ Angiogenesis Analyzer. Data are expressed as mean ± SEM (*p b 0.05, **p b 0.01; One way ANOVA), 3 independent experiments.

Again, proteomic data fully agree with functional assays and ELISA results for human TIMP1. As reported in Table 1, this protein is listed amongst those overrepresented in st hMSCs but showing relative lower level increase following stimulation. Additional bioinformatics analyses of proteomic data further support the observation that even relatively small changes in the level of TIMP1 can result in very significant modulation of secretome properties. First of all, its level will greatly influence the proteolytic potential of the secretome and, consequently, the overall activity of a number of secretome components, including proteins which level is not increased following stimulation and proteins not directly involved in inflammation and angiogenesis; secondly, but not less importantly, TIMP1 is functionally related to a number of overrepresented proteins in stimulated secretome besides proteases (Supplemental Table 3 at http://www.sciencedirect.com/science/article/pii/S187439191730252X?via%3Dihub#ec0005), like cytokines and structural proteins (such as IL6, IL8, CCL2 CXCL12, COL3A1). The complete list of the 54 proteins of stimulated hMSC-CM functionally correlated to TIMP1 according to String[122] is reported in Supplemental Table 3 (at http://www.sciencedirect.com/science/article/pii/S187439191730252X?via%3Dihub#ec0005).

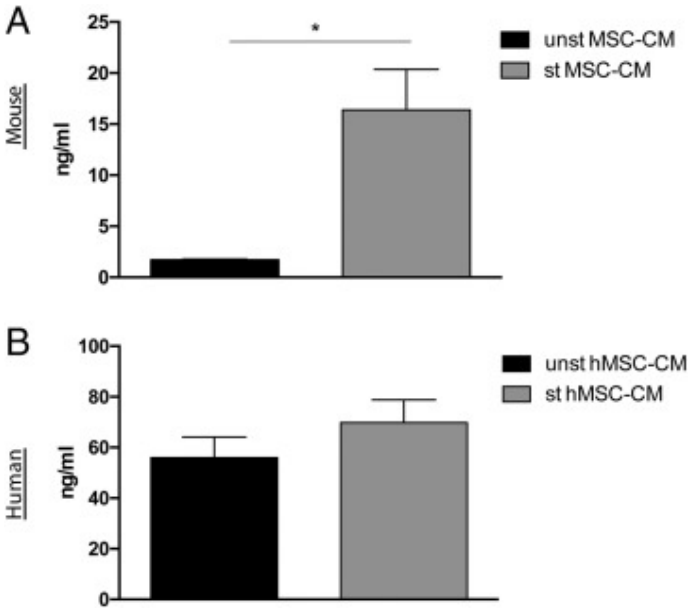

Figure 13 - Mouse and human MSCs-derived TIMP-1 quantification

MSCs-derived TIMP-1 concentration in A) mouse and B) human unstimulated or stimulated MSCs conditioned medium was measured with ELISA. Data are expressed as mean ± SEM (*p b 0.05, parametric t-test), 2 independent experiments.

Extracellular vesicles recapitulate the phenotype of MSC-CM from which they are isolated

Our findings suggest that MSCs display a strong therapeutic potential, thanks to their ability to inhibit/control pathological angiogenesis. However, the clinical application of this approach needs the development of a standardized and safe protocol for MSCs-based cell therapy, which is still missing (as discussed in chapter 5). In an effort to achieve a cost-effective and safer approach, we focused our attention on an alternative procedure, consisting in exploiting MSCs-derived products rather than MSCs themselves. Thus, we evaluated the effect of extracellular vesicles derived from MSC-CM on angiogenesis. EV employment offers several advantages, such as high stability and wide dissemination potential, supporting the fascinating possibility of an industrialized EVs-based therapy[90].

EVs were obtained from unstimulated or stimulated murine MSC-CM by ultrafiltration. Their quality and quantity were validated by Nanosight analysis (data not shown). To investigate the effect of EVs on angiogenesis, we performed the tube formation assay with SVEC4-10 cells and we compared the effects of EVs isolated from unstimulated or stimulated MSCs (EVs unst- or st- MSC-CM, respectively) with whole medium (CM). As previously demonstrated (Figure 5), stimulated MSC-CM decreases the tube length, in contrast to control and unstimulated MSC-CM. Interestingly, the same anti-angiogenic effect was exerted by EVs from st-MSC-CM, which strongly inhibit the ability of SVEC4-10 to form capillary-like, tubular structures (Figure 14 A, B).

Our previous data demonstrated the prominent role of TIMP1 as anti-angiogenic mediator of st-MSCs. Thus, we examined whether TIMP1 is involved in the anti-angiogenic effect exerted by EVs derived from st-MSC-CM. Firstly, we verified the presence of TIMP1 in our EVs by Western Blot. We found that TIMP1 is highly enriched in EVs st-MSC-CM, while the expression of the extracellular vesicles' markers CD63 and CD9 (92)was unaffected (Figure 14 C). Then, we repeated the tube formation assay using TIMP1 blocking antibody (Figure 14 D) and found that the antiangiogenic effect displayed by EVs isolated from st-MSC-CM is TIMP1-dependent (Figure 7 A).

Altogether, these results indicate that EVs show the same inhibitory effect on angiogenesis of the conditioned media they are isolated from.

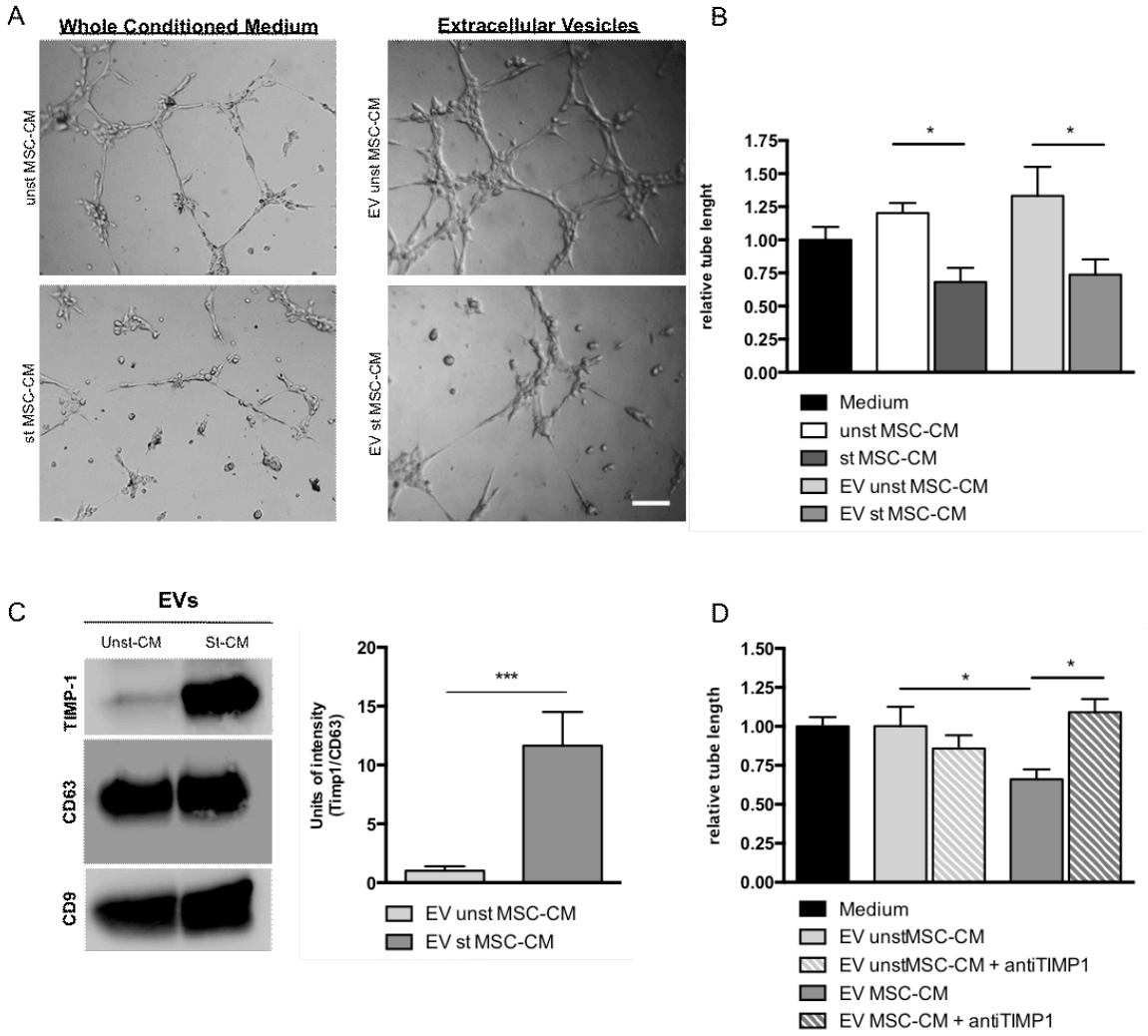

Figure 14 - EVs from MSC-CM fully mimic the whole conditioned medium

The comparative analysis of the whole medium conditioned by unst- or st- MSCs (unst MSC-CM or st MSC-CM) and their extracellular vesicles (EV unst or st MSC-CM), was assessed by performing the tube formation assay. SVEC4-10 cells were seeded on the top of a matrigel layer in the presence of appropriate stimuli. After 6 hours, images were acquired with a phase contrast inverted microscope at 4× objective magnification. **A**) Representative pictures of the experiment; scale bar corresponding to 100μm. **B**) Quantification of the relative tube length (normalized on medium), performed with ImageJ Angiogenesis Analyzer. 3 independent experiments, data are expressed as mean ± SEM (*p b 0.05, **p b 0.01, One-way ANOVA).**C**) The expression of TIMP-1 on EVs was analysed by Western Blot, using CD63 an CD9 as EVs-markers. 3 independent experiments; data are expressed as mean ± SEM (*p b 0.05, **p b 0.01, T-test. **D**) To investigate the role of TIMP-1 in the angiogenesis inhibition mediated by EV from st MSC-CM, the tube formation assay was performed adding a TIMP-1 blocking antibody. Quantification of the relative tube length (normalized on medium), performed with ImageJ Angiogenesis Analyzer. 3 independent experiments, data are expressed as mean ± SEM (*p b 0.05, **p b 0.01, One-way ANOVA).

The scratch wound healing assay reveals a second anti-angiogenic mechanism of EVs st- MSC-CM

Angiogenic and antiangiogenic activities can be assessed by using several in vitro assays, which are typically exploited to investigate different crucial steps of the in vivo process[124]. In particular, through the tube formation assay we evaluated the matrix digestion and the endothelial morphogenesis during the development of the tubular network[125]. However, the assembly of endothelial cells into vessel tubes in vivo also requires the coordinated migration of endothelial cells. To evaluate whether EVs play a regulatory role during this process, we exploited the scratch wound healing in vitro assay, based on the ability of cells to move in a free space in response to a pro-angiogenic factor[126].

SVECA4-10 cells were seeded to form a monolayer and, by scratching, we generated a cell-free gap in the confluent layer. Stimulation with the pro angiogenic factor VEGF induced the subsequent cell migration. EVs derived from unst- or st-MSCs were added. The distance covered by migrating cells was measured after 6 hours of incubation at 37°C 10% CO2 (Figure 15 A). As expected, in response to VEGF, the migratory ability of SVEC4-10 cells is increased in comparison to unstimulated cells (vehicle without VEGF). Treatment with EVs from unst-MSC-CM did not affect the migration of endothelial cells (Figure 15 B). In contrast, EVs isolated from st-MSC-CM completely abolished the SVEC4-10 migratory ability in response to VEGF (Figure 15 B).

This intriguingly suggests that EVs isolated from st-MSC-CM negatively control not only the matrix digestion and endothelial morphogenesis during angiogenesis (Figure 14), but also the migratory ability of endothelial cells in response to VEGF.

To evaluate the implication of TIMP1 in this process, we performed the scratch wound healing assay in presence of the TIMP1-blocking antibody (Figure 15 C). Interestingly, in contrast to what we observed in the tube formation assay, the TIMP-1 blocking treatment did not rescue the migratory ability inhibited by EVs from st- MSC-CM (Figure 15 C), suggesting the existence of a TIMP1-indipendent mechanism through which EVs derived from st-MSCs exert their anti-angiogenic effect.

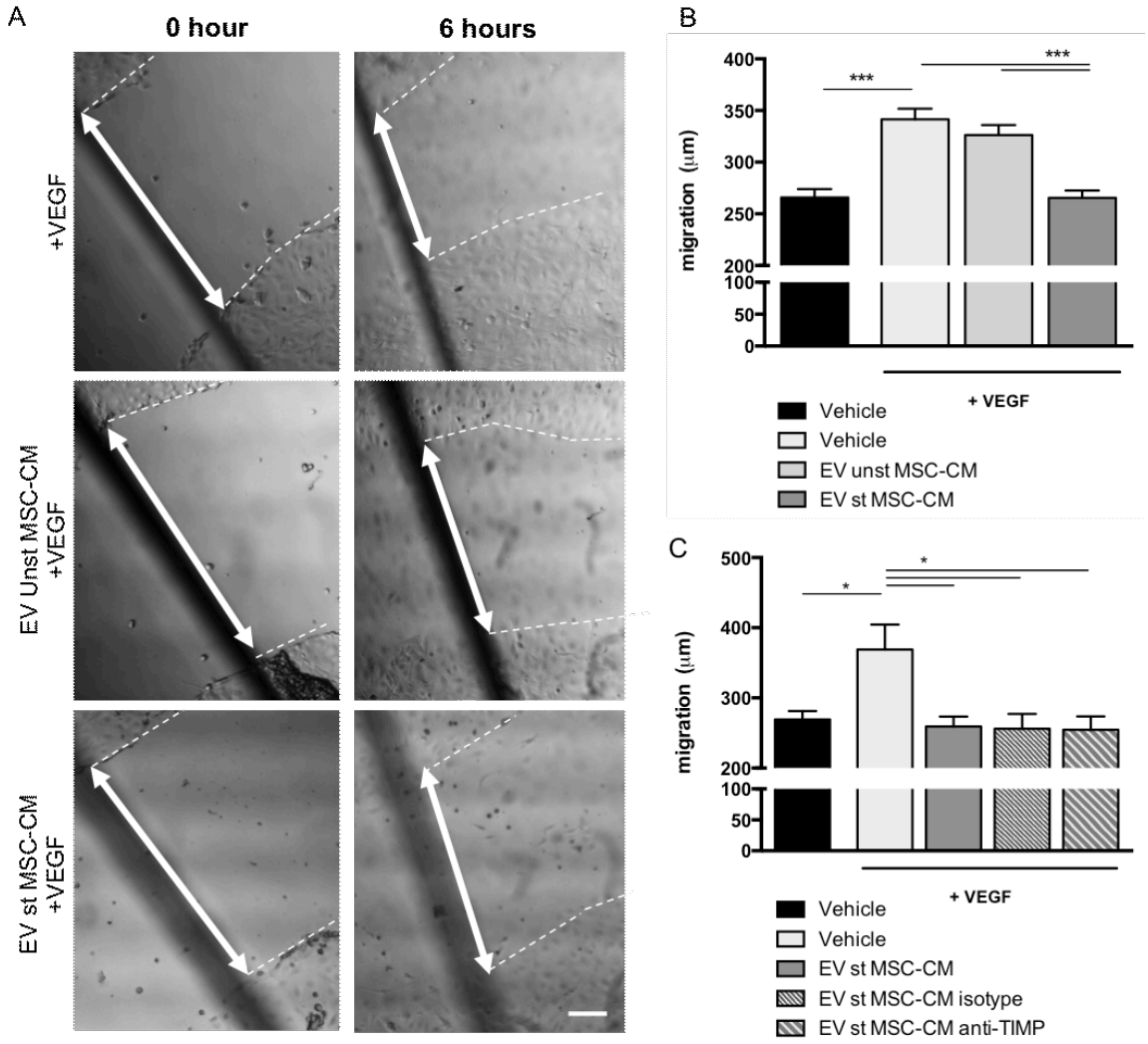

Figure 15 - EVs from st- MSC-CM inhibit the migration of endothelial cells stimulated with VEGF

The evaluation of endothelial cell migration was assessed by the scratch assay. Wound was made by scratching a line across the bottom of the dish on a confluent SVEC4-10 monolayer. Cells were treated with extracellular vesicles isolated from unst- or st- MSC-CM (EV unst or st MSC-CM). 6 hours later, cells were imaged with a phase contrast inverted microscope at 4× objective magnifications. **A**) Representative pictures; scale bar corresponding to 100μm. **B**) quantification of the migration; analysis was performed with ImageJ by measuring the initial (time 0) and the final (time 6 hours) length of the scratch. Data are expressed as means ± S.E.M. (n = 3). *P < 0.05, One-way ANOVA. **C**) To investigate the effect of TIMP-1 in the anti-angiogenic action of EVs from st- MSC-CM, the same experiment was performed with a TIMP-1 blocking antibody. Here, the quantification of the migration expressed in μm, is reported. Data are expressed as means ± S.E.M. (n = 3). *P < 0.05, One-way ANOVA.

CD39 and CD73 confer anti-angiogenic activity to EVs st-MSC-CM

In an effort to characterise the TIMP1-indipendent mechanism of EV-mediated anti-angiogenic effects, we started to investigate the possible involvement of adenosine, which has been reported to suppress the migration of several cell types[123-124]. Adenosine is a purine nucleoside that can be generated by the hydrolysis of extracellular ATP. This reaction is exerted by two enzymes confined on the cellular plasma membrane, the ectonucleotidases CD39 and CD73, catalysing, respectively, the hydrolysis of ATP to AMP, and of AMP to adenosine[125].

To investigate whether EVs from st-MSC-CM induce the accumulation of this purine, we firstly analysed the expression of CD39 and CD73 on the surface of our EVs by Western Blot (Figure 16 A). Our results show an increased level of both these proteins in EVs st-MSC-CM. in comparison with vesicles isolated from unstimulated MSCs. Additionally, we observed a CD39-specific band of higher molecular mass only in EVs derived from st-MSC-CM.

To explore whether adenosine could be responsible for the anti-angiogenic effect exerted by EVs isolated from st- MSC-CM, we performed the scratch wound healing assay as previously described (Figure 15 A) in the presence of the CD39 or CD73 inhibitors, trisodium salt hydrate (ARL 67156) and adenosine 5′ (α, β-methylene) diphosphate (AMP-CP), respectively (Figure 16 B, C). Notably, the inhibition of each enzyme fully recovers the distance covered by SVEC4-10 cells treated with EV st-MSC-CM in the presence of VEGF.

Thus, these data demonstrate that ATP metabolites, generated by CD39 and CD73 expressed by EVs isolated from st- MSC-CM, inhibit the migration of endothelial cells in response to VEGF, with a mechanism completely independent from TIMP1 activity.

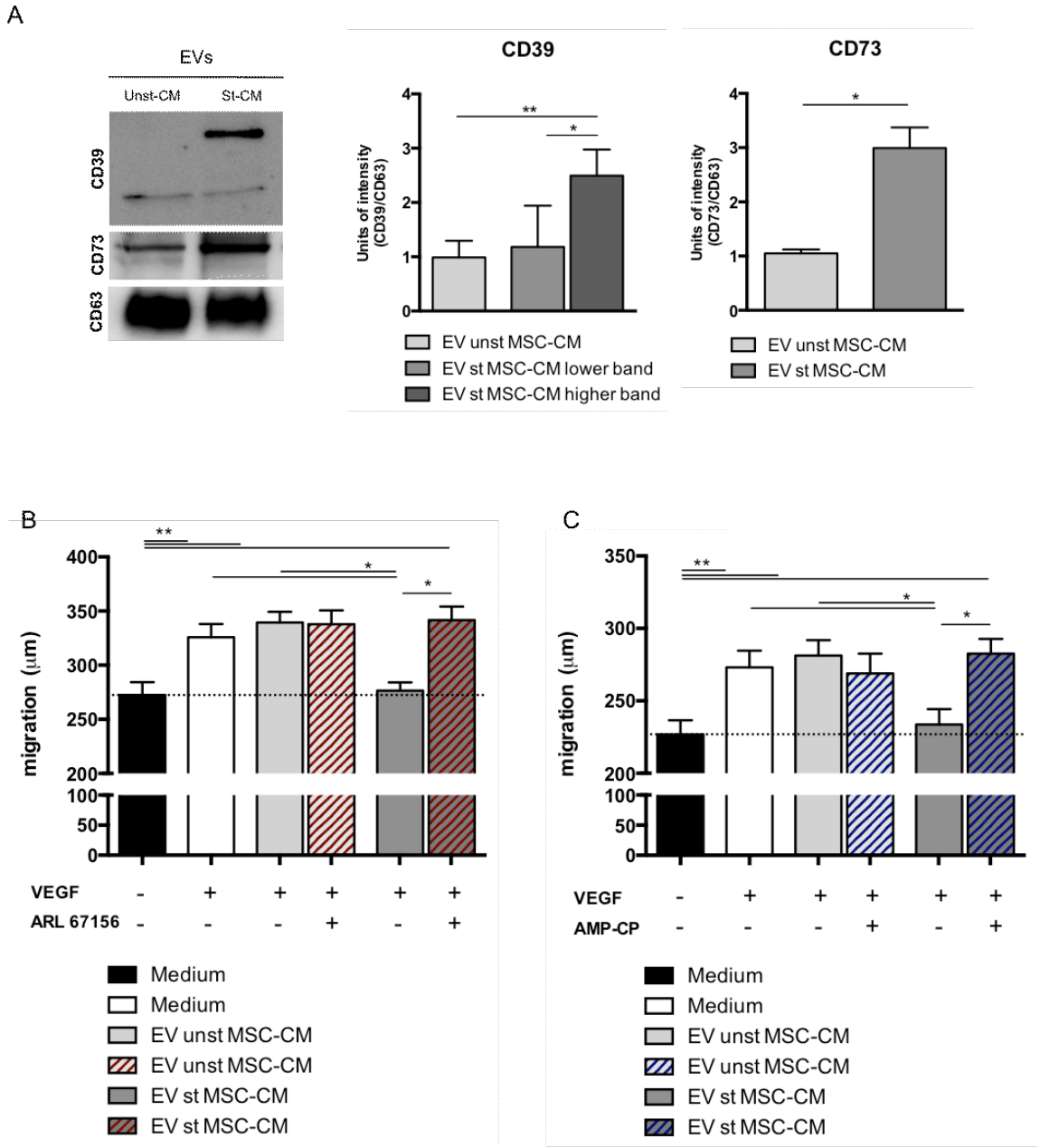

Figure 16 – Adenosine mediates the second anti-angiogenic effect of the EVs derived from st- MSC-CM

A) The expression of ectonucleotidases CD39 and CD73 on the EVs surface, responsible for the ATP hydrolysis, was investigated through the Western Blot assay, using CD63 an CD9 as EVs-markers. 3 independent experiments; data are expressed as mean ± SEM (*p b 0.05, **p b 0.01, One-Way ANOVA). The scratch assays were performed by inhibiting the activity of these enzymes, with ARL 67156 for CD39 **B**), and AMP-CP for CD73 **C**) to investigate the implication of the ATP metabolites, respectively AMP and adenosine, in the suppression of endothelial cell migration mediated by EVs derived from st- MSC-CM. Data are expressed as means ± S.E.M. (n = 3). *P < 0.05, One-way ANOVA.

EVs st-MSC-CM induce reactive oxygen species (ROS) in migrating endothelial cells

Recently, it has been extensively reported the involvement of adenosine in the regulation of the reactive oxygen species (ROS) production[126,127]. Extracellular adenosine interacts with four subtypes of G protein-coupled cell surface receptors (A1R, A2AR, A2BR, and A3R)[128]. Although the mechanism linking the adenosine receptors with ROS production is far from being fully elucidated, it has been suggested that NADPH (nicotinamide adenine dinucleotide phosphate) oxidase (NOX) plays a crucial role. Indeed, NOX activity, which generates ROS transferring electrons from NADPH to molecular oxygen, has been correlated with the activation of adenosine receptors[129,130].

Oxidative stress is recognized as a potent inducer of senescence in endothelial cells[141,132] and of dysfunctional cytoskeletal rearrangements[133,134], two mechanisms potentially responsible for altered migratory response. Thus, we hypothesised that the anti-angiogenic EVs (EVs st-MSC-CM) hydrolase extracellular ATP and cause adenosine accumulation on the endothelial cell surface, which in turn induces oxidative stress in endothelial cells, leading to the inhibition of cell migration. To validate this hypothesis, we detected ROS levels in migrating endothelial SVEC4-10 cells (Figure 17). In particular, we performed a scratch wound healing assay and assessed ROS levels by using CM-H2DCFDA, a general oxidative stress indicator. Antymycin A (AA), a chemical compound that, by interacting with the mitochondrial complex III, inhibits the electron transport causing the mitochondrial collapse and the subsequent accumulation of ROS, was used as positive control[135] (Figure 17 A).

ROS accumulation was not significantly increased in migrating SVEC4-10 cells treated with VEGF alone, or in combination with EVs from unst-MSC-CM (Figure 17 A). On the contrary, EVs derived from st- MSC-CM strongly induced ROS production at the migration front of endothelial cells. These results support our hypothesis of an implication of ROS in the inhibition of endothelial cell migration exerted by EVs st-MSC-CM. Additionally, the block of the adenosine accumulation, through the treatment with the AMP-CP (inhibitor of CD73), not only rescued the migration of endothelial cells (Figure 16 C), but also reduced ROS levels in migrating endothelial cells treated with EVs derived from st-MSC-CM (Figure 17 B). Thus, these data prove that the local production

of adenosine, due to the presence of ectonucleotidases on EVs released by st- MSCs, induces ROS production in endothelial cells, thus affecting their motility.

To finally validate this mechanism, we reduced the oxidative stress with a generic antioxidant N-Acetyl-L-cysteine (NAC). Notably, the suppression of oxidative stress induced by EVs st- MSC-CM perfectly restores the migratory ability of SVEC4-10 cells (Figure 17 C).

These results highlighted the crucial inhibitory role of EVs st- MSC-CM on migrating endothelial cells, with a mechanism dependent on ROS accumulation induced by the local production of adenosine.

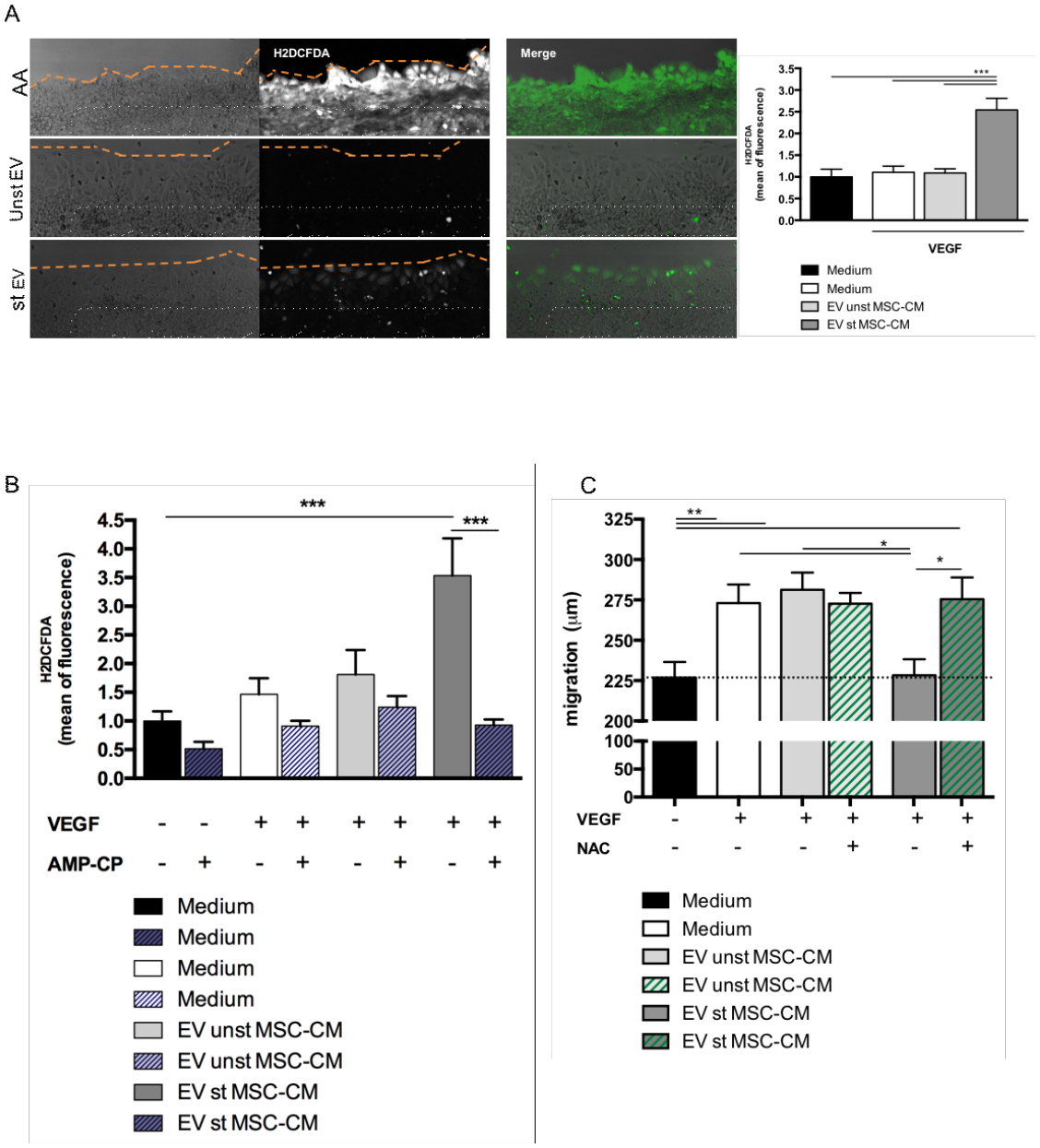

Figure 17 – Adenosine affects migrating endothelial cells, with a mechanism dependent on ROS accumulation

A) The ability of EVs from st- MSC-CM to induce an increment in the ROS levels was investigated by using CM-H2DCFDA, a general oxidative stress indicator, during scratch migration assays. Here are reported representative images. The mean of fluorescence was calculated through ImageJ and normalized on the medium. Data are expressed as means ± S.E.M. (n = 3). *P < 0.05, One-way ANOVA. **B**) In an effort to evaluate the role of adenosine in this process, experiments were repeated by blocking the CD73 activity, the final player in the ATP hydrolysis. Data are expressed as means ± S.E.M. (n = 2). *P < 0.05, One-way ANOVA. **C**) The suppression of oxidative stress induced by EVs st- MSC-CM during the scratch assay, was assess trough the treatment with a generic antioxidant N-Acetyl-L-cysteine (NAC), to confirm the inhibitory effect of ROS. Data are expressed as means ± S.E.M. (n = 2). *P < 0.05, One-way ANOVA.

Inhibition of angiogenesis *in vivo* through the treatment with EVs derived from st- MSC-CM

In an effort to develop a new therapeutic approach for pathological angiogenesis, we decided to validate the effect of EVs derived from st- MSC-CM *in vivo*. Thus, we exploited the retinal mouse model, an extensively used approach to study both physiologic and pathologic angiogenesis[136]. Indeed, in contrast to humans, mouse pups have an immature retinal vasculature at the birth; the development completes in some weeks, proceeding in a tightly regulated and organized manner, reliable for detection of any defect[136].

Thus, pups were intra-peritoneal injected with unstimulated or stimulated MSCs-derived EVs, and sacrificed 5 days later to collect retinas. Samples were dissected and stained with isolectin-B4 to measure the vasculature formation of developing retina by confocal microscopy (Figure 18 A). Remarkably, we observed a decrease in the retina vascular arborisation of pups treated with st- MSCs-derived EVs, but no effect with the unstimulated counterpart (Figure 18 B). In accordance with our *in vitro* results, EVs isolated from st-MSC-CM inhibit the angiogenic process also *in vivo*.

This anti-angiogenic effect exerted by EVs isolated from st- MSC-CM was further consolidated with another *in vivo* approach, the matrigel plug assay. It consists in the analysis of the vascularization of a matrigel plug, that was previously supplemented with EVs and then implanted in the dorsal back of C57BL/6-N mouse (Figure 18 C). The quantification of the plugs' haemoglobin content reveals a decreased vasculature in mice treated exclusively with EVs from st- MSC-CM, thus confirming the antiangiogenic proprieties of these products.

Together, all these data provide enthusiastic evidence of the therapeutic potential of extracellular vesicles derived from MSCs for the control of pathological angiogenesis.

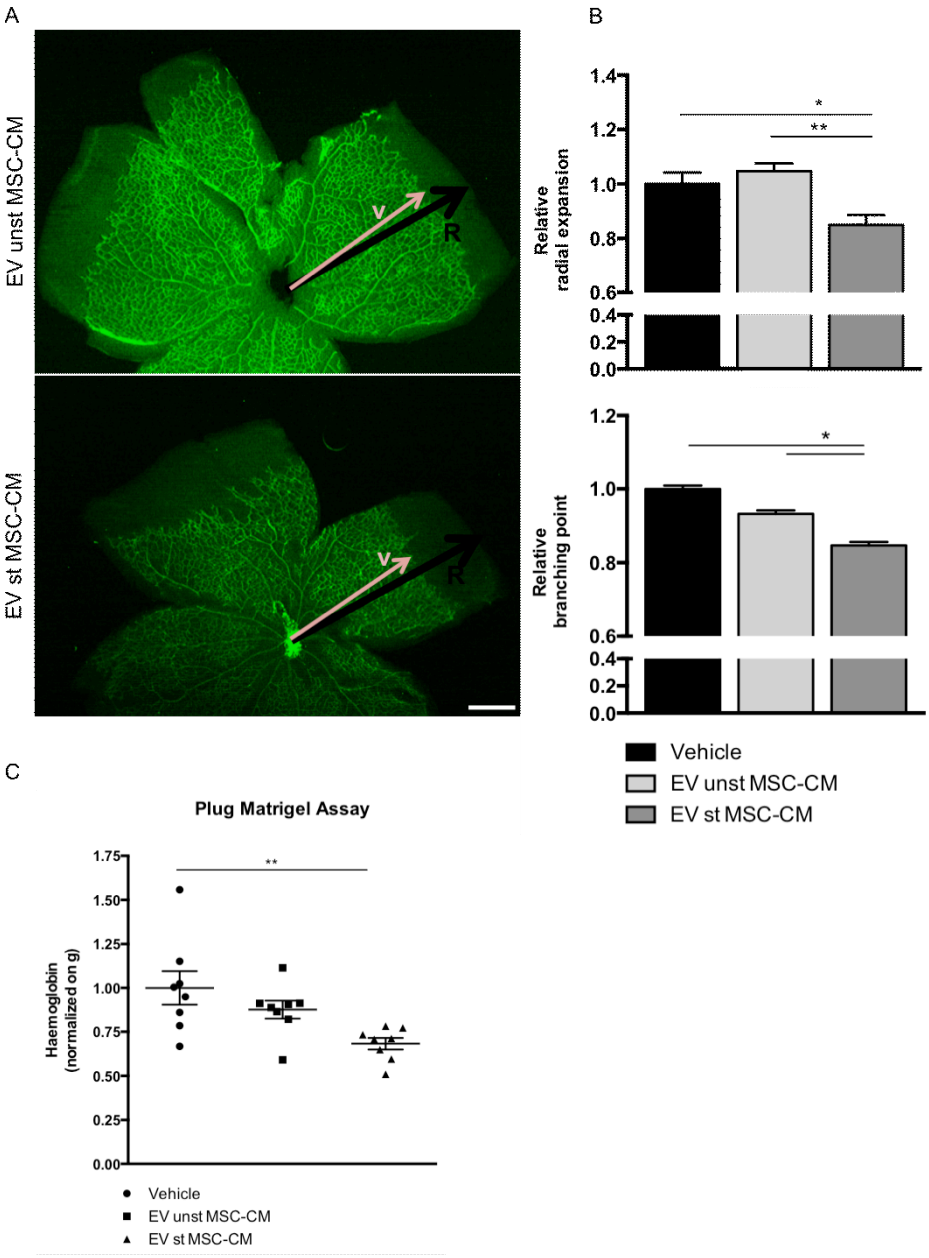

Figure 18 – In vivo therapeutic potential of EVs derived from MSCs for the control of angiogenesis

A) To assess the role of EVs isolated from MSC-CM in the angiogenesis process of developing mouse retina, 1-day-old C57BL/6N mouse pups were intraperitoneally injected with 50ul EVs from unst or st MSC-CM. After 4 days, mice were sacrificed for retina collection. Retina whole mounts were dissected and stained with isolectin B4 (Green, on the left). Digital images were captured using inverted fluorescence confocal microscope (on the right). **B**) Total retinal and vascular areas were measured using ImageJ software to calculate the relative radial expansion and the relative branching points (both normalized on pups treated with the vehicle). Data are expressed as means ± S.E.M. (n =10 pups/group in 3 different experiments). *P < 0.05, One-way ANOVA. **C**)Anesthetized 12-week-old male C57BL/6N mice were subcutaneously injected in the dorsal back with EVs from unst- or st- MSC-CM, mixed with Matrigel plus VEGF. Bare Matrigel was injected as negative control. After 7 days, mice were sacrificed, and the Matrigel plugs were harvested, for the haemoglobin quantification. Plug haemoglobin content was measured using Drabkin's reagent kit 525 (Sigma-Aldrich) and normalized to the total protein quantity measured by BCA. Data are expressed as means ± SEM (n = 8 mice/group). *P < 0.05, T test.

Discussion

MSCs have several features making them attractive for clinical implications. In particular, they are able to differentiate into multiple lineages and to secrete immune-modulatory factors, controlling the inflammatory response. Thus, multiple clinical trials are exploiting MSCs to suppress pathological inflammation. Nevertheless, when studied *in vivo,* many discrepant results have been reported, for example in the case of GVHD, sepsis, acute renal failure, autoimmune encephalomyelitis and multiple sclerosis[137]. Indeed, nowadays, positive results collected from pre-clinical trials do not yet convincingly translated into clinical efficacy. Among the reasons for these unsatisfactory results, there are gaps in the knowledge of MSC biology, of their functional roles in both physiological and pathological conditions, as well as of their mechanism of action when transplanted *in vivo*. It is interesting that very recently a Lancet Commission on regenerative medicine published a document asking for better science, better funding models, better governance, and better public and patient enrollment[95].

One of the problems related to the MSC-based therapy of immune-mediated diseases is the inflammatory milieu of the host. Indeed, to acquire an immunosuppressive phenotype, MSCs need to be properly licensed by pro-inflammatory cytokines. This means, for example, that the identification of the correct time of MSC injection is essential to appropriately activate them and, consequently, to obtain the desired therapeutic effect. For instance, MSC treatment of GVHD mouse model prolongs the survival of injured animals only when performed in a range of 1-7 days after the bone marrow transfer responsible for the induction of the disease[96,138]. Preventive MSC treatment does not show positive results in the same preclinical model[138]. In line with these results, others studies demonstrated that MSC-transplantation efficacy, in term of GVHD treatment, increases when MSCs are repeatedly administered at weekly intervals (days 0, +7, +14 from the bone marrow transfer). It has been suggested that this time of MSC administration probably overlaps with an interval characterized by a concentration of inflammatory cytokines sufficiently high to allow the *in vivo* licensing of MSCs, but still not excessive, which would irredeemably damage the tissue[137]. Notably, similar results have been collected in GVHD patients[137]. The critical significance of the timing of MSC-

administration timing is further highlighted in other disease models. For instance, in the experimental autoimmune encephalomyelitis model, MSCs are effective only when transplanted at the beginning of the disease (days +3 and +8), but they lose their immunosuppressive action when administered after disease stabilization (days +10 and +15)[137].

These data, together with others, clearly indicate that the *in vivo* accumulation of pro-inflammatory cytokines is required for MSC licensing, leading to the acquisition of their immunosuppressive phenotype. Our study further corroborates this concept. We demonstrated that only MSCs stimulated with a cocktail of pro-inflammatory cytokines suppress the inflammatory response. Intriguingly, we found that the pro-inflammatory micro-environment induces a remarkable change in the whole MSC secretome, leading to the release of proteins mainly involved in the regulation of angiogenesis. Indeed, hemodynamic changes, encountering vasodilatation and increased permeability, are the first observable events in the inflammation. When a robust immune response develops, infiltrating and dividing lymphocytes markedly increase LN cellularity, leading to organ expansion. During this swelling, there is massive endothelial cell proliferation, and vascular expansion occurs[106]. Thus, both acute and chronic inflammatory processes are associated with a pronounced vascular remodelling.

In this study, we identified a novel and specific effect of MSC administration, during an acute immune response, firstly on endothelial cell activation, then on HEV development and elongation and, consequently, on T-cell trafficking in the draining LN. All these processes do not require MSC homing to the inflamed tissue and, notably, they are mediated uniquely by soluble factors released by MSCs licensed by pro-inflammatory cytokines. Indeed, through a proteomic analysis of the MSC secretome, we identified that, upon the activation with inflammatory cytokines, MSCs upregulate the expression of several proteins affecting angiogenesis and inflammation through multiple pathways.

Angiogenesis requires degradation of the vascular basement membrane and remodelling of the extracellular matrix to allow endothelial cell migration and invasion into the surrounding tissue. This process depends on the action of MMPs that, degrading both matrix and non-matrix proteins, have a central role during the morphogenesis, wound healing, tissue repair, and in the progression of chronic diseases[44]. The balance between MMPs and their natural inhibitors, TIMPs, is critical for extracellular matrix remodelling

and angiogenesis. The TIMP family comprises four protease inhibitors (TIMP-1, TIMP-2, TIMP-3 and TIMP-4) able, with the exception of TIMP-4[139],to inhibit angiogenesis *in vivo*[116], through several mechanisms. By mass spectrometry, *in vitro* and *in vivo* functional assays, we identified the metalloproteinase inhibitor TIMP-1 as one of the key molecules responsible for the anti-angiogenic effects of MSCs. TIMP-1 is known to inhibit endothelial cell migration by MMP-dependent and MMP-independent mechanisms[140,141,142].The latter involves the regulation of various biological processes such as cell growth, apoptosis and differentiation through the CD63 receptor[143].In addition, TIMP-1 was shown to induce secretion of soluble VEGFR-1 by human endothelial cells, leading to a decrease of bioavailable VEGF and of blood vessel growth[144]. Interestingly, the comparative analysis of the secretomes of human and mouse MSCs stimulated by pro-inflammatory cytokines reveals 16 common proteins, and, notably, 11 of them modulate angiogenesis directly or indirectly. To note, the anti-angiogenic role of TIMP-1 already observed in the mouse model was confirmed also using human MSC conditioned medium (MSC-CM). Thus, TIMP1 is one of the key secreted molecules targeting endothelial cells in both mouse and human MSCs.

Although our data put TIMP-1 at the top of the list of MSC-derived effector molecules, we speculated that other soluble factors contribute to MSC-mediated regulation of inflammatory-associated angiogenesis. MSCs are also known to produce prostaglandin E2 and thus inhibit the activation of macrophages[79],which are a source of multiple growth factors that enhance endothelial cell proliferation and survival[145].Another interesting mediator found in the MSCs secretome is the soluble form of VCAM-1 (sVCAM-1). High levels of sVCAM-1 have been detected in the synovial fluid of patients with rheumatoid arthritis[146]and in the blood of patients with different types of cancers[147],but its origin is not entirely clear and our data suggest that MSCs may represent an important source of this molecule. Although sVCAM-1 is described as a promoter of angiogenesis[148],by altering leukocyte trafficking[149] or inhibiting T-cell activation[150], it may contribute to the MSC-induced suppression of T-cell recruitment that we observed in this study.

The results presented here clearly position endothelial cells as a key target of MSCs during the suppression of the inflammatory response. Thus, they pave the way for developing novel MSCs-based strategies that could exploit the inhibition of angiogenesis for the treatment of immune-related pathologies. Indeed, angiogenesis is involved in a

wide number of physiological and pathological conditions, such as wound healing, tumor growth, rheumatoid arthritis, inflammatory bowel disease and asthma[151]. Thus, the identification of therapies that specifically inhibit angiogenesis may represent a weapon to reduce inflammation and prevent disease progression[17].

In addition to that, these data support the concept that the physiological role of MSCs is to act as sensors of the microenvironment in which they are embedded, responding to it by the release of soluble mediators able to control the vascular remodelling. It is known, for example, that MSCs acquire pro-angiogenic properties in response to, for instance, hypoxia[152,153,154,] nitric oxide (NO) stimulation[155] or the iron chelator deferoxamine (DFX)[156], and our findings, revealing for the first time the anti-angiogenic potential of MSCs, indicate that these cells have a crucial role in connecting the endothelial cells with their microenvironment.

As stated above, several critical issues still limit the development of MSC-based therapies. First of all, the best source of MSCs for *in vivo* immunomodulation is still debated as well as the precise number of MSCs that have to be injected in order to have a beneficial effect. The complete optimization of the commercial *in vitro* expansion and long-term storage protocols is not yet ensured. Furthermore, the absence of a well-defined mechanism of action for each specific therapeutic condition makes the identification of biomarkers very difficult. Another important problem, very specific of this therapeutic approach, is the need for the complete characterization of the patient's microenvironment, in term of types and concentrations of the inflammatory cytokines required for the correct licensing of the MSCs. On the same line, it's almost unreasonable to imagine that we will be able to identify a specific interval in every patient, of countless different diseases, in which we can detect the specific cytokines' profile, essential for the efficient transfer of MSCs. In addition to all these issues, accumulating evidence of the paracrine action of MSCs, responsible for their immunosuppressive effect, suggested the idea of developing a cell-free, MSC-based therapeutic approach.

Extracellular vesicles (EVs) released by MSCs are able to suppress inflammation similarly to their cells of origins, thus making real the opportunity of MSC administration replacement with a MSC-derived product[157]. Among the many advantages of a EV-based

therapy, there are limited risk of carcinogenesis, higher stability, improved bio-distribution and, most importantly, the use of a final, non-living product whose efficacy does not depend on the host cytokine milieu[93]

Our data demonstrate that, through the definite licensing of MSCs, it is possible to obtain EVs with specific therapeutic effects. EVs released by MSCs primed by pro-inflammatory cytokines exert the same anti-angiogenic effects of their cells of origin, both *in vitro* and *in vivo*. Notably, the anti-angiogenic properties of MSC-derived EVs depend on the specific conditions for licensing that we used; indeed, EVs derived from resting MSCs do not inhibit angiogenesis, whereas those obtained from MSCs cultured in hypoxic conditions have strong pro-angiogenic properties (RA, data not shown). These results strongly support the concept of MSCs as sensor of the surrounding environment: we can hypothesize that in hypoxic conditions, when the generation of new vessels is required, MSCs secrete EVs promoting angiogenesis; on the opposite way, in a strongly inflammatory microenvironment, MSCs release EVs that, by blocking the formation of new vessels, limit and control inflammation.

Our data suggest that, in addition to the therapies of immune-mediated disorders, MSC-derived EVs may represent a novel approach for the treatment of pathological angiogenesis. We identified TIMP-1 as a crucial effector molecule in this process: EVs released by st-MSCs are strongly enriched in TIMP-1, and TIMP-1 activity is required to inhibit the endothelial cell ability to form capillary-like structures. However, the results presented here identify another - and novel - mechanism by which EVs derived from st-MSCs inhibit angiogenesis. This latter process involves the ability of st-MSC-derived EVs to hydrolyse the extracellular ATP, producing adenosine.

Extracellular ATP accumulates in the local microenvironment of several physiological and pathological conditions. For instance, hypoxia and stress damage are accompanied by elevated concentrations of extracellular ATP that seem to be involved in the progression of several vascular diseases[158]. Once in the extracellular space, ATP may be hydrolysed by two ectonucleotidases (CD39 and CD73), firstly in AMP and then into adenosine. This latter is an endogenous molecule able to control tissue homeostasis, by activating G-protein-coupled adenosine receptors (A1, A2A, A2B and A3 receptors)[159]. Interestingly, , it has been largely reported that adenosine is involved in the suppression of the immune response, acting on both immune and endothelial cells[159]. Substantial

evidence has been collected on the role of adenosine to limit the secretion, by activated macrophages, of the pro-inflammatory TNF-α and, conversely, to prompt the release of the immunosuppressive IL-10. Additionally, other studies indicate that, during an immune response, adenosine triggers the dendritic cells to acquire an anti-inflammatory phenotype[159] and inhibits their IL-12 production[160]. In this line, in the presence of adenosine, dendritic cell-ability to induce the pro-inflammatory T helper 1 (TH1) from naïve T cells strongly decreases. Furthermore, it seems that adenosine directly interacts with T cells, shifting the T helper polarization towards the anti-inflammatory phenotype TH2, principally by blocking the NF-kB activation[159]. Finally, during an inflammatory response, adenosine also regulates endothelial cell-activation. Indeed, it has been highlighted that the accumulation of extracellular adenosine reduces the expression of adhesion molecules, likewise the vascular cell adhesion molecule-1 (VCAM-1), thus preventing the leukocytes recruitment into the injured tissue[160].

Intriguingly, we found that the MSC-treatment of mice with a local inflammation largely decreases the VCAM-1 expression on the endothelium of draining lymph nodes. Notably, we revealed that EVs released by st-MSCs express functionally active CD39 and CD73 that generate adenosine. The expression of CD39 and CD73 allows st-MSC-derived EVs not only to remove the pro-angiogenic ATP from the extracellular space, but also to generate the anti-inflammatory adenosine.

Indeed, our data suggest that the main mechanism by which CD39/CD73-expressing EVs regulate the inflammatory response may be due to the negative control of the immune-related angiogenesis. Intriguingly, we demonstrated that EVs from st-MSCs, expressing CD39 and CD73, inhibit the angiogenic process through the induction of oxidative stress in endothelial cells.

It is largely described that reactive oxygen species (ROS), such as such as superoxide ($O_2^{\cdot-}$) and hydrogen peroxide (H_2O_2), act as a double-edged sword during the vascular remodelling. Indeed, low levels of ROS are required to support cell growth, migration, differentiation and gene expression. In particular, in response to hypoxia, ischemia and growth factors, low levels of extracellular ROS trigger endothelial cell proliferation and migration, cytoskeleton reorganizations and tubular morphogenesis[161]. Conversely, highly concentrated ROS are damaging for most cells, being cytotoxic and mutagenic. In

particular, oxidative stress triggers cell death, apoptosis and senescence in the endothelium during the angiogenic response, thus stopping the process[161,131].

We found that only EVs isolated from st-MSC-CM, carrying CD39 and CD73, potentially accumulate adenosine on the endothelial cell surface and this, in turn, results in the detrimental induction of oxidative stress in endothelial cells, leading to their migration inhibition.

Preliminary data recently generated in our laboratory indicate that the extracellular adenosine binds the A2BR, a subtype of G protein-coupled cell surface receptor, thus interacting with endothelial cells and activating the signalling pathway (data not shown). Moreover, we are now trying to identify the ROS source, responsible for the oxidative stress induced by EVs. With this aim, we are focusing on NADPH (nicotinamide adenine dinucleotide phosphate) oxidase (NOX), according to several studies reporting its association with adenosine receptors (A1R, A2AR, A2BR, and A3R)[126,127].

In an effort to provide useful pre-clinical data, we would like to investigate the therapeutic potential of EVs in a mouse model of pathological angiogenesis, such as the retinopathy of prematurity (ROP). The ROP is a rare retinal vasoproliferative disorder affecting preterm infants. It is characterized initially by a delay in the physiologic retinal vascular development, and subsequently by aberrant angiogenesis in the form of intravitreal neovascularization[136]. With the increase in the survival of preterm babies, ROP has become the leading cause of childhood blindness throughout the world. Thus, the identification of an anti-angiogenic therapy represents, nowadays, a real challenge to save the sight of many children[136]. Current therapies encounter the cryosurgery and the laser therapy to eliminate the avascular area in the peripheral retina, thus reducing the injured hypoxic part of the tissue. Unfortunately, only infants with advanced ROP (from stage III) can receive these treatments, because they are still far to be largely efficient and safe. Indeed, generally, these ablation therapies are expensive and able to prevent the blindness only in a few percentage of treated patients[162]. In addition, both approaches involve invasive surgeries and are associated with several side effects. For instance, laser photocoagulation may cause infectious ulcerative keratitis and it is often associated with higher risks of strabismus, astigmatism, nystagmus, myopia, and lowered visual acuity[162]. . To overcome these issues, the identification of a more efficient and safer therapeutic approach is urgently needed. Recently, anti-VEGF molecules have been exploited for the

intravitreal treatment of ROP-patients to suppress the pathological angiogenesis. The main advantage of this therapy consists in the drug administration into the vitreous body, which is not an invasive procedure. However, once the anti-VEGF treatment is concluded, a late re-activation of the disease is generally observed. In addition, adverse reactions associated with the systemic effect of this therapeutic approach still have to be elucidated.

Thus, we decided to analyse the therapeutic potential of the EVs in the ROP mouse model to beneficially remodel the retinal vasculature. This approach may represent a better cost-effective procedure, since we could exploit i) the EVs-double anti-angiogenic mechanism to prevent the treatment evasion, thus potentially increasing the treatment efficiency and ii) their ability to target selectively the migrating endothelial cells, thus limiting the systemic side effects generally associated with anti-VEGF drugs.

To summarize, this study provides results that allow to sharpen up the physiological role of MSCs and to clarify their mechanism of action during *in vivo* therapy. In particular, for the first time, we identified the endothelium as specific target of MSC-based therapy. Additionally, we developed a protocol to obtain anti-angiogenic EVs that can be exploited for novel therapeutic approaches against pathological angiogenesis.

Bibliography

1. Medzhitov, R. Inflammation 2010: new adventures of an old flame. *Cell* **140,** 771–776 (2010).

2. Jounai, N., Kobiyama, K., Takeshita, F. & Ishii, K. J. Recognition of damage-associated molecular patterns related to nucleic acids during inflammation and vaccination. *Front. Cell. Infect. Microbiol.* **2,** (2013).

3. Medzhitov, R. Origin and physiological roles of inflammation. *Nature* **454,** 428–435 (2008).

4. Alon, R. & Feigelson, S. W. Chemokine-triggered leukocyte arrest: force-regulated bi-directional integrin activation in quantal adhesive contacts. *Curr. Opin. Cell Biol.* **24,** 670–676 (2012).

5. Vestweber, D. How leukocytes cross the vascular endothelium. *Nat. Rev. Immunol.* **15,** 692–704 (2015).

6. Tedder, T. F., Steeber, D. A., Chen, A. & Engel, P. The selectins: vascular adhesion molecules. *FASEB J. Off. Publ. Fed. Am. Soc. Exp. Biol.* **9,** 866–873 (1995).

7. Vestweber, D. & Blanks, J. E. Mechanisms That Regulate the Function of the Selectins and Their Ligands. *Physiol. Rev.* **79,** 181–213 (1999).

8. Kolaczkowska, E. & Kubes, P. Neutrophil recruitment and function in health and inflammation. *Nat. Rev. Immunol.* **13,** 159–175 (2013).

9. Muller, W. A. The role of PECAM-1 (CD31) in leukocyte emigration: studies in vitro and in vivo. *J. Leukoc. Biol.* **57,** 523–528 (1995).

10. Nourshargh, S., Krombach, F. & Dejana, E. The role of JAM-A and PECAM-1 in modulating leukocyte infiltration in inflamed and ischemic tissues. *J. Leukoc. Biol.* **80,** 714–718 (2006).

11. Wegmann, F. *et al.* ESAM supports neutrophil extravasation, activation of Rho, and VEGF-induced vascular permeability. *J. Exp. Med.* **203,** 1671–1677 (2006).

12. Schenkel, A. R., Mamdouh, Z., Chen, X., Liebman, R. M. & Muller, W. A. CD99

plays a major role in the migration of monocytes through endothelial junctions. *Nat. Immunol.* **3,** 143–150 (2002).

13. Turley, S. J., Fletcher, A. L. & Elpek, K. G. The stromal and haematopoietic antigen-presenting cells that reside in secondary lymphoid organs. *Nat. Rev. Immunol.* **10,** 813–825 (2010).

14. Pennock, N. D. *et al.* T cell responses: naïve to memory and everything in between. *Adv. Physiol. Educ.* **37,** 273–283 (2013).

15. Ayala, A., Chung, C.-S., Grutkoski, P. S. & Song, G. Y. Mechanisms of immune resolution. *Crit. Care Med.* **31,** S558–S571 (2003).

16. Ortega-Gómez, A., Perretti, M. & Soehnlein, O. Resolution of inflammation: an integrated view. *EMBO Mol. Med.* **5,** 661–674 (2013).

17. Pober, J. S. & Sessa, W. C. Evolving functions of endothelial cells in inflammation. *Nat. Rev. Immunol.* **7,** 803–815 (2007).

18. Potente, M. & Mäkinen, T. Vascular heterogeneity and specialization in development and disease. *Nat. Rev. Mol. Cell Biol.* **18,** 477–494 (2017).

19. Busse, R. & Fleming, I. Vascular endothelium and blood flow. *Handb. Exp. Pharmacol.* 43–78 (2006).

20. Bonfanti, R., Furie, B. C., Furie, B. & Wagner, D. D. PADGEM (GMP140) is a component of Weibel-Palade bodies of human endothelial cells. *Blood* **73,** 1109–1112 (1989).

21. Reglero-Real, N., Colom, B., Bodkin, J. V. & Nourshargh, S. Endothelial Cell Junctional Adhesion Molecules. *Arterioscler. Thromb. Vasc. Biol.* **36,** 2048–2057 (2016).

22. Stevens, T., Garcia, J. G., Shasby, D. M., Bhattacharya, J. & Malik, A. B. Mechanisms regulating endothelial cell barrier function. *Am. J. Physiol. Lung Cell. Mol. Physiol.* **279,** L419-422 (2000).

23. Ley, K., Laudanna, C., Cybulsky, M. I. & Nourshargh, S. Getting to the site of inflammation: the leukocyte adhesion cascade updated. *Nat. Rev. Immunol.* **7,** 678–689 (2007).

24. Martin, M. U. & Wesche, H. Summary and comparison of the signaling

mechanisms of the Toll/interleukin-1 receptor family. *Biochim. Biophys. Acta* **1592,** 265–280 (2002).

25. Winsauer, G. & de Martin, R. Resolution of inflammation: intracellular feedback loops in the endothelium. *Thromb. Haemost.* **97,** 364–369 (2007).

26. Carmeliet, P. Angiogenesis in health and disease. *Nat. Med.* **9,** 653–660 (2003).

27. Monaco, C., Andreakos, E., Kiriakidis, S., Feldmann, M. & Paleolog, E. T-cell-mediated signalling in immune, inflammatory and angiogenic processes: the cascade of events leading to inflammatory diseases. *Curr. Drug Targets Inflamm. Allergy* **3,** 35–42 (2004).

28. Shibuya, M. & Claesson-Welsh, L. Signal transduction by VEGF receptors in regulation of angiogenesis and lymphangiogenesis. *Exp. Cell Res.* **312,** 549–560 (2006).

29. Carmeliet, P. Mechanisms of angiogenesis and arteriogenesis. *Nat. Med.* **6,** 389–395 (2000).

30. Carmeliet, P. & Jain, R. K. Molecular mechanisms and clinical applications of angiogenesis. *Nature* **473,** 298–307 (2011).

31. Smet, F. D., Segura, I., Bock, K. D., Hohensinner, P. J. & Carmeliet, P. Mechanisms of Vessel Branching. *Arterioscler. Thromb. Vasc. Biol.* **29,** 639–649 (2009).

32. Adams, R. H. & Alitalo, K. Molecular regulation of angiogenesis and lymphangiogenesis. *Nat. Rev. Mol. Cell Biol.* **8,** 464–478 (2007).

33. Hellström, M. *et al.* Dll4 signalling through Notch1 regulates formation of tip cells during angiogenesis. *Nature* **445,** 776–780 (2007).

34. Defilippi, P. *et al.* Actin cytoskeleton organization in response to integrin-mediated adhesion. *Microsc. Res. Tech.* **47,** 67–78 (1999).

35. Coordinating cell behaviour during blood vessel formation | Development. Available at: http://dev.biologists.org/content/138/21/4569. (Accessed: 8th September 2017)

36. Lu, X. *et al.* The netrin receptor UNC5B mediates guidance events controlling morphogenesis of the vascular system. *Nature* **432,** 179–186 (2004).

37. Gerhardt, H. *et al.* VEGF guides angiogenic sprouting utilizing endothelial tip cell filopodia. *J. Cell Biol.* **161,** 1163–1177 (2003).

38. Strasser, G. A., Kaminker, J. S. & Tessier-Lavigne, M. Microarray analysis of retinal endothelial tip cells identifies CXCR4 as a mediator of tip cell morphology and branching. *Blood* **115,** 5102–5110 (2010).

39. Mazzone, M. *et al.* Heterozygous deficiency of PHD2 restores tumor oxygenation and inhibits metastasis via endothelial normalization. *Cell* **136,** 839–851 (2009).

40. Gerhardt, H. & Betsholtz, C. Endothelial-pericyte interactions in angiogenesis. *Cell Tissue Res.* **314,** 15–23 (2003).

41. Brew, K. & Nagase, H. The tissue inhibitors of metalloproteinases (TIMPs): An ancient family with structural and functional diversity. *Biochim. Biophys. Acta* **1803,** 55–71 (2010).

42. Sorokin, L. The impact of the extracellular matrix on inflammation. *Nat. Rev. Immunol.* **10,** 712–723 (2010).

43. Sang, Q. X. A. Complex role of matrix metalloproteinases in angiogenesis. *Cell Res.* **8,** 171–177 (1998).

44. Nagase, H., Visse, R. & Murphy, G. Structure and function of matrix metalloproteinases and TIMPs. *Cardiovasc. Res.* **69,** 562–573 (2006).

45. Murphy, G. Tissue inhibitors of metalloproteinases. *Genome Biol.* **12,** 233 (2011).

46. Yana, I. *et al.* Crosstalk between neovessels and mural cells directs the site-specific expression of MT1-MMP to endothelial tip cells. *J. Cell Sci.* **120,** 1607–1614 (2007).

47. Taraboletti, G. *et al.* Shedding of the matrix metalloproteinases MMP-2, MMP-9, and MT1-MMP as membrane vesicle-associated components by endothelial cells. *Am. J. Pathol.* **160,** 673–680 (2002).

48. Jeong, J. W., Cha, H. J., Yu, D. Y., Seiki, M. & Kim, K. W. Induction of membrane-type matrix metalloproteinase-1 stimulates angiogenic activities of bovine aortic endothelial cells. *Angiogenesis* **3,** 167–174 (1999).

49. Herren, B., Levkau, B., Raines, E. W. & Ross, R. Cleavage of beta-catenin and

plakoglobin and shedding of VE-cadherin during endothelial apoptosis: evidence for a role for caspases and metalloproteinases. *Mol. Biol. Cell* **9,** 1589–1601 (1998).

50. Lehti, K. *et al.* An MT1-MMP-PDGF receptor-beta axis regulates mural cell investment of the microvasculature. *Genes Dev.* **19,** 979–991 (2005).

51. Hellström, M. *et al.* Lack of pericytes leads to endothelial hyperplasia and abnormal vascular morphogenesis. *J. Cell Biol.* **153,** 543–553 (2001).

52. Davis, G. E., Bayless, K. J., Davis, M. J. & Meininger, G. A. Regulation of tissue injury responses by the exposure of matricryptic sites within extracellular matrix molecules. *Am. J. Pathol.* **156,** 1489–1498 (2000).

53. Ramjaun, A. R. & Hodivala-Dilke, K. The role of cell adhesion pathways in angiogenesis. *Int. J. Biochem. Cell Biol.* **41,** 521–530 (2009).

54. Marom, B. *et al.* Native and fragmented fibronectin oppositely modulate monocyte secretion of MMP-9. *J. Leukoc. Biol.* **81,** 1466–1476 (2007).

55. Arroyo, A. G. & Iruela-Arispe, M. L. Extracellular matrix, inflammation, and the angiogenic response. *Cardiovasc. Res.* **86,** 226–235 (2010).

56. Friedenstein, A. J., Piatetzky-Shapiro, I. I. & Petrakova, K. V. Osteogenesis in transplants of bone marrow cells. *J. Embryol. Exp. Morphol.* **16,** 381–390 (1966).

57. Uccelli, A., Moretta, L. & Pistoia, V. Mesenchymal stem cells in health and disease. *Nat. Rev. Immunol.* **8,** 726–736 (2008).

58. Caplan, A. I. Mesenchymal stem cells. *J. Orthop. Res. Off. Publ. Orthop. Res. Soc.* **9,** 641–650 (1991).

59. Nombela-Arrieta, C., Ritz, J. & Silberstein, L. E. The elusive nature and function of mesenchymal stem cells. *Nat. Rev. Mol. Cell Biol.* **12,** 126–131 (2011).

60. Pittenger, M. F. *et al.* Multilineage potential of adult human mesenchymal stem cells. *Science* **284,** 143–147 (1999).

61. Haynesworth, S. E., Goshima, J., Goldberg, V. M. & Caplan, A. I. Characterization of cells with osteogenic potential from human marrow. *Bone* **13,** 81–88 (1992).

62. Ashton, B. A. *et al.* Formation of bone and cartilage by marrow stromal cells in diffusion chambers in vivo. *Clin. Orthop.* 294–307 (1980).

63. Sacchetti, B. *et al.* Self-Renewing Osteoprogenitors in Bone Marrow Sinusoids Can Organize a Hematopoietic Microenvironment. *Cell* **131,** 324–336 (2007).

64. Morikawa, S. *et al.* Prospective identification, isolation, and systemic transplantation of multipotent mesenchymal stem cells in murine bone marrow. *J. Exp. Med.* **206,** 2483–2496 (2009).

65. da Silva Meirelles, L., Caplan, A. I. & Nardi, N. B. In Search of the In Vivo Identity of Mesenchymal Stem Cells. *STEM CELLS* **26,** 2287–2299 (2008).

66. Kolf, C. M., Cho, E. & Tuan, R. S. Mesenchymal stromal cells. Biology of adult mesenchymal stem cells: regulation of niche, self-renewal and differentiation. *Arthritis Res. Ther.* **9,** 204 (2007).

67. Meirelles, L. da S., Chagastelles, P. C. & Nardi, N. B. Mesenchymal stem cells reside in virtually all post-natal organs and tissues. *J. Cell Sci.* **119,** 2204–2213 (2006).

68. Nauta, A. J. *et al.* Donor-derived mesenchymal stem cells are immunogenic in an allogeneic host and stimulate donor graft rejection in a nonmyeloablative setting. *Blood* **108,** 2114–2120 (2006).

69. Ehninger, A. & Trumpp, A. The bone marrow stem cell niche grows up: mesenchymal stem cells and macrophages move in. *J. Exp. Med.* **208,** 421–428 (2011).

70. Klein, D. Vascular Wall-Resident Multipotent Stem Cells of Mesenchymal Nature within the Process of Vascular Remodeling: Cellular Basis, Clinical Relevance, and Implications for Stem Cell Therapy. *Stem Cells Int.* **2016,** (2016).

71. Klein, D. *et al.* Nestin(+) Tissue-Resident Multipotent Stem Cells Contribute to Tumor Progression by Differentiating into Pericytes and Smooth Muscle Cells Resulting in Blood Vessel Remodeling. *Front. Oncol.* **4,** (2014).

72. Wang, Y., Chen, X., Cao, W. & Shi, Y. Plasticity of mesenchymal stem cells in immunomodulation: pathological and therapeutic implications. *Nat. Immunol.* **15,** 1009–1016 (2014).

73. Han, F. *et al.* Contribution of murine bone marrow mesenchymal stem cells to

pancreas regeneration after partial pancreatectomy in mice. *Cell Biol. Int.* **36,** 823–831 (2012).

74. Rose, R. A. *et al.* Bone marrow-derived mesenchymal stromal cells express cardiac-specific markers, retain the stromal phenotype, and do not become functional cardiomyocytes in vitro. *Stem Cells Dayt. Ohio* **26,** 2884–2892 (2008).

75. Prockop, D. J., Kota, D. J., Bazhanov, N. & Reger, R. L. Evolving paradigms for repair of tissues by adult stem/progenitor cells (MSCs). *J. Cell. Mol. Med.* **14,** 2190–2199 (2010).

76. von Bahr, L. *et al.* Analysis of tissues following mesenchymal stromal cell therapy in humans indicates limited long-term engraftment and no ectopic tissue formation. *Stem Cells Dayt. Ohio* **30,** 1575–1578 (2012).

77. Di Nicola, M. *et al.* Human bone marrow stromal cells suppress T-lymphocyte proliferation induced by cellular or nonspecific mitogenic stimuli. *Blood* **99,** 3838–3843 (2002).

78. Bartholomew, A. *et al.* Mesenchymal stem cells suppress lymphocyte proliferation in vitro and prolong skin graft survival in vivo. *Exp. Hematol.* **30,** 42–48 (2002).

79. Németh, K. *et al.* Bone marrow stromal cells attenuate sepsis via prostaglandin E(2)-dependent reprogramming of host macrophages to increase their interleukin-10 production. *Nat. Med.* **15,** 42–49 (2009).

80. Abumaree, M. H. *et al.* Human placental mesenchymal stem cells (pMSCs) play a role as immune suppressive cells by shifting macrophage differentiation from inflammatory M1 to anti-inflammatory M2 macrophages. *Stem Cell Rev.* **9,** 620–641 (2013).

81. Ma, S. *et al.* Immunobiology of mesenchymal stem cells. *Cell Death Differ.* **21,** 216–225 (2014).

82. Sudres, M. *et al.* Bone marrow mesenchymal stem cells suppress lymphocyte proliferation in vitro but fail to prevent graft-versus-host disease in mice. *J. Immunol. Baltim. Md 1950* **176,** 7761–7767 (2006).

83. Ren, G. *et al.* Mesenchymal stem cell-mediated immunosuppression occurs via concerted action of chemokines and nitric oxide. *Cell Stem Cell* **2,** 141–150 (2008).

84. Lee, R. H. *et al.* Multipotent stromal cells from human marrow home to and promote repair of pancreatic islets and renal glomeruli in diabetic NOD/scid mice. *Proc. Natl. Acad. Sci. U. S. A.* **103,** 17438–17443 (2006).

85. Tögel, F. *et al.* Administered mesenchymal stem cells protect against ischemic acute renal failure through differentiation-independent mechanisms. *Am. J. Physiol. Renal Physiol.* **289,** F31-42 (2005).

86. Ortiz, L. A. *et al.* Interleukin 1 receptor antagonist mediates the antiinflammatory and antifibrotic effect of mesenchymal stem cells during lung injury. *Proc. Natl. Acad. Sci. U. S. A.* **104,** 11002–11007 (2007).

87. Le Blanc, K. *et al.* Treatment of severe acute graft-versus-host disease with third party haploidentical mesenchymal stem cells. *The Lancet* **363,** 1439–1441 (2004).

88. Ankrum, J. A., Ong, J. F. & Karp, J. M. Mesenchymal stem cells: immune evasive, not immune privileged. *Nat. Biotechnol.* **32,** 252–260 (2014).

89. Sarukhan, A., Zanotti, L. & Viola, A. Mesenchymal stem cells: myths and reality. *Swiss Med. Wkly.* **145,** w14229 (2015).

90. Sharma, J. *et al.* Therapeutic Development of Mesenchymal Stem Cells or Their Extracellular Vesicles to Inhibit Autoimmune-Mediated Inflammatory Processes in Systemic Lupus Erythematosus. *Front. Immunol.* **8,** (2017).

91. Riazifar, M., Pone, E. J., Lötvall, J. & Zhao, W. Stem Cell Extracellular Vesicles: Extended Messages of Regeneration. *Annu. Rev. Pharmacol. Toxicol.* **57,** 125–154 (2017).

92. De Luca, L. *et al.* Mesenchymal Stem Cell Derived Extracellular Vesicles: A Role in Hematopoietic Transplantation? *Int. J. Mol. Sci.* **18,** (2017).

93. Rani, S., Ryan, A. E., Griffin, M. D. & Ritter, T. Mesenchymal Stem Cell-derived Extracellular Vesicles: Toward Cell-free Therapeutic Applications. *Mol. Ther.* **23,** 812–823 (2015).

94. Kordelas, L. *et al.* MSC-derived exosomes: a novel tool to treat therapy-refractory

graft-versus-host disease. *Leukemia* **28,** 970–973 (2014).

95. Cossu, G. *et al.* Lancet Commission: Stem cells and regenerative medicine. *The Lancet* **0,** (2017).

96. Zanotti, L. *et al.* Encapsulated mesenchymal stem cells for in vivo immunomodulation. *Leukemia* **27,** 500–503 (2013).

97. McAuley, D. F. *et al.* Clinical grade allogeneic human mesenchymal stem cells restore alveolar fluid clearance in human lungs rejected for transplantation. *Am. J. Physiol. - Lung Cell. Mol. Physiol.* **306,** L809–L815 (2014).

98. Sironi, M. *et al.* Generation and characterization of a mouse lymphatic endothelial cell line. *Cell Tissue Res.* **325,** 91–100 (2006).

99. Dong, Q. G. *et al.* A general strategy for isolation of endothelial cells from murine tissues. Characterization of two endothelial cell lines from the murine lung and subcutaneous sponge implants. *Arterioscler. Thromb. Vasc. Biol.* **17,** 1599–1604 (1997).

100. Roy, D., Steyer, G. J., Gargesha, M., Stone, M. E. & Wilson, D. L. 3D cryo-imaging: a very high-resolution view of the whole mouse. *Anat. Rec. Hoboken NJ 2007* **292,** 342–351 (2009).

101. Roy, D. *et al.* Multi-Scale Characterization of the PEPCK-Cmus Mouse through 3D Cryo-Imaging. *Int. J. Biomed. Imaging* **2010,** (2010).

102. Gargesha, M. *et al.* Visualization of color anatomy and molecular fluorescence in whole-mouse cryo-imaging. *Comput. Med. Imaging Graph.* **35,** 195–205 (2011).

103. Kumar, V. *et al.* Global lymphoid tissue remodeling during a viral infection is orchestrated by a B cell-lymphotoxin-dependent pathway. *Blood* **115,** 4725–4733 (2010).

104. Crocker, S. J. *et al.* Amelioration of Coxsackievirus B3-Mediated Myocarditis by Inhibition of Tissue Inhibitors of Matrix Metalloproteinase-1. *Am. J. Pathol.* **171,** 1762–1773 (2007).

105. Zacchigna, S. *et al.* Bone marrow cells recruited through the neuropilin-1 receptor promote arterial formation at the sites of adult neoangiogenesis in mice. *J. Clin. Invest.* **118,** 2062–2075 (2008).

106. Webster, B. *et al.* Regulation of lymph node vascular growth by dendritic cells. *J.*

Exp. Med. **203,** 1903–1913 (2006).

107. Cox, J. & Mann, M. MaxQuant enables high peptide identification rates, individualized p.p.b.-range mass accuracies and proteome-wide protein quantification. *Nat. Biotechnol.* **26,** 1367–1372 (2008).

108. Kumar, V., Chyou, S., Stein, J. V. & Lu, T. T. Optical projection tomography reveals dynamics of HEV growth after immunization with protein plus CFA and features shared with HEVs in acute autoinflammatory lymphadenopathy. *Front. Immunol.* **3,** 282 (2012).

109. Boscacci, R. T. *et al.* Comprehensive analysis of lymph node stroma-expressed Ig superfamily members reveals redundant and nonredundant roles for ICAM-1, ICAM-2, and VCAM-1 in lymphocyte homing. *Blood* **116,** 915–925 (2010).

110. O'Connell, K. A. & Edidin, M. A mouse lymphoid endothelial cell line immortalized by simian virus 40 binds lymphocytes and retains functional characteristics of normal endothelial cells. *J. Immunol. Baltim. Md 1950* **144,** 521–525 (1990).

111. Bernardo, M. E. & Fibbe, W. E. Mesenchymal stromal cells: sensors and switchers of inflammation. *Cell Stem Cell* **13,** 392–402 (2013).

112. Groh, M. E., Maitra, B., Szekely, E. & Koç, O. N. Human mesenchymal stem cells require monocyte-mediated activation to suppress alloreactive T cells. *Exp. Hematol.* **33,** 928–934 (2005).

113. Arnaoutova, I. & Kleinman, H. K. In vitro angiogenesis: endothelial cell tube formation on gelled basement membrane extract. *Nat. Protoc.* **5,** 628–635 (2010).

114. Zhou, Z., Connell, M. C. & MacEwan, D. J. TNFR1-induced NF-kappaB, but not ERK, p38MAPK or JNK activation, mediates TNF-induced ICAM-1 and VCAM-1 expression on endothelial cells. *Cell. Signal.* **19,** 1238–1248 (2007).

115. Huang, D. W., Sherman, B. T. & Lempicki, R. A. Systematic and integrative analysis of large gene lists using DAVID bioinformatics resources. *Nat. Protoc.* **4,** 44–57 (2009).

116. Lambert, E., Dassé, E., Haye, B. & Petitfrère, E. TIMPs as multifacial proteins. *Crit. Rev. Oncol. Hematol.* **49,** 187–198 (2004).

117. Zanotti, L. *et al.* Mouse mesenchymal stem cells inhibit high endothelial cell activation and lymphocyte homing to lymph nodes by releasing TIMP-1. *Leukemia* **30,** 1143–1154 (2016).

118. Romieu-Mourez, R., Coutu, D. L. & Galipeau, J. The immune plasticity of mesenchymal stromal cells from mice and men: concordances and discrepancies. *Front. Biosci. Elite Ed.* **4,** 824–837 (2012).

119. Hamilton, J. A. Colony-stimulating factors in inflammation and autoimmunity. *Nat. Rev. Immunol.* **8,** 533–544 (2008).

120. Tojo, N., Asakura, E., Koyama, M., Tanabe, T. & Nakamura, N. Effects of macrophage colony-stimulating factor (M-CSF) on protease production from monocyte, macrophage and foam cell in vitro: a possible mechanism for anti-atherosclerotic effect of M-CSF. *Biochim. Biophys. Acta BBA - Mol. Cell Res.* **1452,** 275–284 (1999).

121. Fixe, P. & Praloran, V. Macrophage colony-stimulating-factor (M-CSF or CSF-1) and its receptor: structure-function relationships. *Eur. Cytokine Netw.* **8,** 125–136 (1997).

122. Szklarczyk, D. *et al.* STRING v10: protein-protein interaction networks, integrated over the tree of life. *Nucleic Acids Res.* **43,** D447-452 (2015).

123. Säve, S., Mohlin, C., Vumma, R. & Persson, K. Activation of Adenosine A2A Receptors Inhibits Neutrophil Transuroepithelial Migration ▽. *Infect. Immun.* **79,** 3431–3437 (2011).

124. Lenoir, B. *et al.* Adenosine inhibits the proliferation of lymphatic endothelial cells. *Eur. Heart J.* **34,** (2013).

125. Umansky, V., Shevchenko, I., Bazhin, A. V. & Utikal, J. Extracellular adenosine metabolism in immune cells in melanoma. *Cancer Immunol. Immunother.* **63,** 1073–1080 (2014).

126. Thakur, S., Du, J., Hourani, S., Ledent, C. & Li, J.-M. Inactivation of Adenosine A2A Receptor Attenuates Basal and Angiotensin II-induced ROS Production by Nox2 in Endothelial Cells. *J. Biol. Chem.* **285,** 40104–40113 (2010).

127. Gebremedhin, D., Weinberger, B., Lourim, D. & Harder, D. R. Adenosine can mediate its actions through generation of reactive oxygen species. *J. Cereb. Blood Flow*

Metab. **30,** 1777–1790 (2010).

128. Sheth, S., Brito, R., Mukherjea, D., Rybak, L. P. & Ramkumar, V. Adenosine Receptors: Expression, Function and Regulation. *Int. J. Mol. Sci.* **15,** 2024–2052 (2014).

129. Zhou, Z. *et al.* Involvement of NADPH oxidase in A2A adenosine receptor-mediated increase in coronary flow in isolated mouse hearts. *Purinergic Signal.* **11,** 263–273 (2015).

130. Ribé, D. *et al.* Adenosine A2A receptor signaling regulation of cardiac NADPH oxidase activity. *Free Radic. Biol. Med.* **44,** 1433–1442 (2008).

131. Liu, R., Liu, H., Ha, Y., Tilton, R. G. & Zhang, W. Oxidative Stress Induces Endothelial Cell Senescence via Downregulation of Sirt6. *BioMed Research International* (2014). doi:10.1155/2014/902842

132. Bhayadia, R., Schmidt, B. M. W., Melk, A. & Hömme, M. Senescence-Induced Oxidative Stress Causes Endothelial Dysfunction. *J. Gerontol. Ser. A* **71,** 161–169 (2016).

133. Zhou, L., Li, Y. & Yue, B. Y. Oxidative stress affects cytoskeletal structure and cell-matrix interactions in cells from an ocular tissue: the trabecular meshwork. *J. Cell. Physiol.* **180,** 182–189 (1999).

134. Wilson, C. & González-Billault, C. Regulation of cytoskeletal dynamics by redox signaling and oxidative stress: implications for neuronal development and trafficking. *Front. Cell. Neurosci.* **9,** (2015).

135. Ma, X. *et al.* Mitochondrial Electron Transport Chain Complex III Is Required for Antimycin A to Inhibit Autophagy. *Chem. Biol.* **18,** 1474–1481 (2011).

136. Stahl, A. *et al.* The Mouse Retina as an Angiogenesis Model. *Invest. Ophthalmol. Vis. Sci.* **51,** 2813–2826 (2010).

137. Krampera, M. Mesenchymal stromal cell 'licensing': a multistep process. *Leukemia* **25,** 1408–1414 (2011).

138. Wei, X. *et al.* Mesenchymal stem cells: a new trend for cell therapy. *Acta Pharmacol. Sin.* **34,** 747–754 (2013).

139. Fernández, C. A. & Moses, M. A. Modulation of angiogenesis by tissue inhibitor

of metalloproteinase-4. *Biochem. Biophys. Res. Commun.* **345,** 523–529 (2006).

140. Reed, M. J., Koike, T., Sadoun, E., Sage, E. H. & Puolakkainen, P. Inhibition of TIMP1 enhances angiogenesis in vivo and cell migration in vitro. *Microvasc. Res.* **65,** 9–17 (2003).

141. Ikenaka, Y. *et al.* Tissue inhibitor of metalloproteinases-1 (TIMP-1) inhibits tumor growth and angiogenesis in the TIMP-1 transgenic mouse model. *Int. J. Cancer* **105,** 340–346 (2003).

142. Akahane, T., Akahane, M., Shah, A., Connor, C. M. & Thorgeirsson, U. P. TIMP-1 inhibits microvascular endothelial cell migration by MMP-dependent and MMP-independent mechanisms. *Exp. Cell Res.* **301,** 158–167 (2004).

143. Jung, K.-K., Liu, X.-W., Chirco, R., Fridman, R. & Kim, H.-R. C. Identification of CD63 as a tissue inhibitor of metalloproteinase-1 interacting cell surface protein. *EMBO J.* **25,** 3934–3942 (2006).

144. Bruegmann, E., Gruemmer, R., Neulen, J. & Motejlek, K. Regulation of soluble vascular endothelial growth factor receptor 1 secretion from human endothelial cells by tissue inhibitor of metalloproteinase 1. *Mol. Hum. Reprod.* **15,** 749–756 (2009).

145. Baer, C., Squadrito, M. L., Iruela-Arispe, M. L. & De Palma, M. Reciprocal interactions between endothelial cells and macrophages in angiogenic vascular niches. *Exp. Cell Res.* **319,** 1626–1634 (2013).

146. Wellicome, S. M. *et al.* Detection of a circulating form of vascular cell adhesion molecule-1: raised levels in rheumatoid arthritis and systemic lupus erythematosus. *Clin. Exp. Immunol.* **92,** 412–418 (1993).

147. Dymicka-Piekarska, V., Guzinska-Ustymowicz, K., Kuklinski, A. & Kemona, H. Prognostic significance of adhesion molecules (sICAM-1, sVCAM-1) and VEGF in colorectal cancer patients. *Thromb. Res.* **129,** e47-50 (2012).

148. Koch, A. E., Halloran, M. M., Haskell, C. J., Shah, M. R. & Polverini, P. J. Angiogenesis mediated by soluble forms of E-selectin and vascular cell adhesion molecule-1. *Nature* **376,** 517–519 (1995).

149. Kitani, A. *et al.* Soluble VCAM-1 induces chemotaxis of Jurkat and synovial fluid

T cells bearing high affinity very late antigen-4. *J. Immunol. Baltim. Md 1950* **161,** 4931–4938 (1998).

150. Kitani, A. *et al.* T cells bound by vascular cell adhesion molecule-1/CD106 in synovial fluid in rheumatoid arthritis: inhibitory role of soluble vascular cell adhesion molecule-1 in T cell activation. *J. Immunol. Baltim. Md 1950* **156,** 2300–2308 (1996).

151. Zgraggen, S., Ochsenbein, A. M. & Detmar, M. An Important Role of Blood and Lymphatic Vessels in Inflammation and Allergy. *Journal of Allergy* (2013). doi:10.1155/2013/672381

152. Liu, J. *et al.* Hypoxia Pretreatment of Bone Marrow Mesenchymal Stem Cells Facilitates Angiogenesis by Improving the Function of Endothelial Cells in Diabetic Rats with Lower Ischemia. *PLoS ONE* **10,** (2015).

153. Krock, B. L., Skuli, N. & Simon, M. C. Hypoxia-Induced Angiogenesis. *Genes Cancer* **2,** 1117–1133 (2011).

154. Madrigal, M., Rao, K. S. & Riordan, N. H. A review of therapeutic effects of mesenchymal stem cell secretions and induction of secretory modification by different culture methods. *J. Transl. Med.* **12,** (2014).

155. Du, W. *et al.* Enhanced proangiogenic potential of mesenchymal stem cell-derived exosomes stimulated by a nitric oxide releasing polymer. *Biomaterials* **133,** 70–81 (2017).

156. Oses, C. *et al.* Preconditioning of adipose tissue-derived mesenchymal stem cells with deferoxamine increases the production of pro-angiogenic, neuroprotective and anti-inflammatory factors: Potential application in the treatment of diabetic neuropathy. *PLOS ONE* **12,** e0178011 (2017).

157. Baglio, S. R., Pegtel, D. M. & Baldini, N. Mesenchymal stem cell secreted vesicles provide novel opportunities in (stem) cell-free therapy. *Front. Physiol.* **3,** (2012).

158. Gerasimovskaya, E. V., Woodward, H. N., Tucker, D. A. & Stenmark, K. R. Extracellular ATP is a pro-angiogenic factor for pulmonary artery vasa vasorum endothelial cells. *Angiogenesis* **11,** 169–182 (2008).

159. Haskó, G., Linden, J., Cronstein, B. & Pacher, P. Adenosine receptors: therapeutic

aspects for inflammatory and immune diseases. *Nat. Rev. Drug Discov.* **7,** 759–770 (2008).

160. Stagg, J. & Smyth, M. J. Extracellular adenosine triphosphate and adenosine in cancer. *Oncogene* **29,** 5346–5358 (2010).

161. Ushio-Fukai, M. & Nakamura, Y. Reactive Oxygen Species and Angiogenesis: NADPH Oxidase as Target for Cancer Therapy. *Cancer Lett.* **266,** 37–52 (2008).

162. Trinh, T. L. P., Li Calzi, S., Shaw, L. C., Yoder, M. C. & Grant, M. B. Promoting vascular repair in the retina: can stem/progenitor cells help? *Eye Brain* **8,** 113–122 (2016).

Publications

1. Proteomic analysis of the secretome of human bone marrow-derived mesenchymal stem cells primed by pro-inflammatory cytokines.

   Maffioli E, Nonnis S, **Angioni R**, Santagata F, Calì B, Zanotti L, Negri A, Viola A, Tedeschi G.

   Journal of Proteomics 2017 Aug 23;166:115-126. doi: 10.1016/j.jprot.2017.07.012. Epub 2017 Jul 21.

2. Mouse mesenchymal stem cells inhibit high endothelial cell activation and lymphocyte homing to lymph nodes by releasing TIMP-1.
   Zanotti L*, **Angioni R***, Calì B, Soldani C, Ploia C, Moalli F, Gargesha M, D'Amico G, Elliman S, Tedeschi G, Maffioli E, Negri A, Zacchigna S, Sarukhan A, Stein JV, Viola A.
   Leukemia. 2016 May;30(5):1143-54. doi: 10.1038/leu.2016.33. Epub 2016 Feb 22. *authors contributed equally

3. Identification of a novel agrin-dependent pathway in cell signaling and adhesion within the erythroid niche.
   Anselmo A, Lauranzano E, Soldani C, Ploia C, **Angioni R**, D'amico G, Sarukhan A, Mazzon C, Viola A.
   Cell Death Differ. 2016 Aug;23(8):1322-30. doi: 10.1038/cdd.2016.10. Epub 2016 Mar 18.

4. Tailored chemokine receptor modification improves homing of adoptive therapy T cells in a spontaneous tumor model.
   Garetto S, Sardi C, Martini E, Roselli G, Morone D, **Angioni R**, Cianciotti BC, Trovato AE, Franchina DG, Castino GF, Vignali D, Erreni M, Marchesi F, Rumio C, Kallikourdis M.
   Oncotarget. 2016 May 10. doi: 10.18632/oncotarget.9280. [Epubahead of print]

OPEN

Leukemia (2016) **30,** 1143–1154

www.nature.com/leu

ORIGINAL ARTICLE

Mouse mesenchymal stem cells inhibit high endothelial cell activation and lymphocyte homing to lymph nodes by releasing TIMP-1

L Zanotti[1,12,13], R Angioni[2,3,13], B Calì[2,3], C Soldani[1], C Ploia[1], F Moalli[4], M Gargesha[5], G D'Amico[6], S Elliman[7], G Tedeschi[8,9], E Maffioli[9], A Negri[8,9], S Zacchigna[10], A Sarukhan[11], JV Stein[4] and A Viola[2,3]

Mesenchymal stem cells (MSC) represent a promising therapeutic approach in many diseases in view of their potent immunomodulatory properties, which are only partially understood. Here, we show that the endothelium is a specific and key target of MSC during immunity and inflammation. In mice, MSC inhibit activation and proliferation of endothelial cells in remote inflamed lymph nodes (LNs), affect elongation and arborization of high endothelial venules (HEVs) and inhibit T-cell homing. The proteomic analysis of the MSC secretome identified the tissue inhibitor of metalloproteinase-1 (TIMP-1) as a potential effector molecule responsible for the anti-angiogenic properties of MSC. Both *in vitro* and *in vivo*, TIMP-1 activity is responsible for the anti-angiogenic effects of MSC, and increasing TIMP-1 concentrations delivered by an Adeno Associated Virus (AAV) vector recapitulates the effects of MSC transplantation on draining LNs. Thus, this study discovers a new and highly efficient general mechanism through which MSC tune down immunity and inflammation, identifies TIMP-1 as a novel biomarker of MSC-based therapy and opens the gate to new therapeutic approaches of inflammatory diseases.

Leukemia (2016) **30,** 1143–1154; doi:10.1038/leu.2016.33

INTRODUCTION

Mesenchymal stem cells (MSC) are multipotent progenitor cells with self-renewable capacity and the potential to differentiate into various mesodermal lineages.[1] MSC are present in the stromal fraction of many tissues, where they reside close to blood vessels,[2] a trait that is shared with pericytes. Indeed, when analyzed *in vitro*, MSC and pericytes display similar morphological and functional features, although the two cell types are likely to have different functions *in vivo*.[3] Although pericytes regulate capillary homeostasis and architecture,[4] the *in vivo* functional role of MSC is less clear and it is likely to be tissue-specific. For example, in the bone marrow, MSC contribute to the formation of the 'niche' for the hematopoietic stem cells (HSC), thus providing an appropriate microenvironment for hematopoiesis.[5] In other tissues, MSC may be involved in homeostatic control and tissue repair.[6]

A well-established feature of MSC is their ability to inhibit inflammation and immunity, both *in vitro* and *in vivo*. In mouse models of human diseases, MSC have been shown to be highly immunosuppressive being effective, for example, in the treatment of experimental autoimmune encephalomyelitis,[7] collagen-induced arthritis[8] or graft-versus-host disease.[9] On the basis of these experimental results, MSC are now used in several clinical trials (see www.clinical trials.gov) and represent a new frontier in cellular therapy. The anti-inflammatory effect of MSC can be largely explained by their ability to secrete a vast array of soluble mediators with immunomodulatory properties, such as interleukin-10 (IL-10), prostaglandin E2, transforming growth factor, nitric oxide (for mouse MSC) and indoleamine-2,3-dioxygenase (for human MSC), and tumor necrosis factor-α (TNF-α)-stimulated protein 6 (ref. 9–11) that may act in a paracrine or endocrine manner. However, a unifying mechanism of action is still missing, and it is likely that other specific mediators and targets explaining the *in vivo* immunosuppressive effects of MSC remain to be identified.

Both inflammatory and immune responses depend on migration of leukocytes. Recruitment of neutrophils and monocytes into inflamed tissues is directed by chemokines induced by inflammatory stimuli, including bacterial lipopolysaccharide, IL-1 and TNF-α.[12,13] On the other hand, adaptive immunity starts in secondary lymphoid organs, where naive antigen-specific T cells encounter dendritic cells loaded with cognate antigen. For this to occur, T cells must enter lymph nodes (LNs) via specialized post-capillary venules that are made up of endothelial cells with cuboidal morphology and therefore called high endothelial venules (HEVs).[14,15] Endothelial cells have a major role in these processes, changing their phenotypes to support various phases of the inflammatory responses. The capacity of leukocytes to interact with the endothelium is determined by the activation of

[1]Humanitas Clinical and Research Institute, IRCCS, Rozzano, Milan, Italy; [2]Department of Biomedical Sciences, Venetian Institute of Molecular Medicine (VIMM), Padua, Italy; [3]University of Padua, Italy, Switzerland; [4]Theodor Kocher Institute, University of Bern, Bern, Switzerland; [5]BioInVision Inc., Cleveland, OH, USA; [6]Centro Ricerca 'M. Tettamanti,' Clinica Pediatrica Università degli Studi di Milano Bicocca, Monza, Italy; [7]Orbsen Therapeutics Ltd, National University of Ireland, Galway, Ireland; [8]Department of Veterinary Science and Public Health, University of Milano, Milano, Italy; [9]Filarete Foundation, Milano, Italy; [10]International Centre for Genetic Engineering and Biotechnology (ICGEB), Padriciano, Trieste, Italy and [11]INSERM, Paris, France. Correspondence: Dr L Zanotti, Division of Regenerative Medicine, Stem Cells and Gene Therapy, San Raffaele Hospital, via Olgettina 48, Milan 20100, Italy.
E-mail: zanotti.lucia@hsr.it
[12]Current address: Division of Regenerative Medicine, Stem Cells and Gene Therapy, San Raffaele Hospital, Milan, Italy.
[13]These authors contributed equally to this work.
Received 31 July 2015; revised 2 December 2015; accepted 1 February 2016; accepted article preview online 22 February 2016; advance online publication, 8 March 2016

endothelial cells that in turn leads to the expression of a variety of chemoattractants and surface adhesion molecules including intercellular adhesion molecule-1 (ICAM-1) and vascular cell adhesion molecule-1 (VCAM-1).[16] In addition, if the inflammatory stimulus persists, then angiogenesis is initiated by the migration of endothelial cells lining the venules into the tissue.[16,17] The generation of new blood vessels is required for the survival of inflammatory cells within the tissue, and thus inhibition of factors that promote angiogenesis may reduce inflammation and prevent its pathological consequences such as inflammatory tissue damage, autoimmunity, fibrosis or tumor growth.[16,18]

In this study, we have identified the endothelium as a specific and novel target of MSC-based therapy.

MATERIALS AND METHODS

Mice

C57BL/6J mice were purchased from Charles River Laboratories (Calco, Italy). All mice used as primary cell donors or recipients were between 8 and 12 weeks of age. Procedures involving animals and their care conformed to institutional guidelines in compliance with national (4D.L. N.116, G.U., suppl. 40, 18-2-1992) and international (EEC Council Directive 2010/63/UE; National Institutes of Health Guide for the Care and Use of Laboratory Animals) law and policies. The protocol was approved by the Italian Ministry of Health on 18 June 2007 and modified by Protocol 162/2011-B. All efforts were made to minimize the number of animals used and their suffering. In all the experiment, the mice were sex and age matched, no further randomization was applied.

Isolation of murine MSC

Detailed protocols are available in the Supplementary Materials and Methods.

Collection of conditioned medium

Detailed protocols are available in the Supplementary Materials and Methods.

Endothelial cell lines

Detailed protocols are available in the Supplementary Materials and Methods.

In vitro endothelial cell activation

Detailed protocols are available in the Supplementary Materials and Methods.

Tube formation assay

Detailed protocols are available in the Supplementary Materials and Methods.

Immunization with Complete Freund Adjuvant/Ovalbumin

In all, 1 mg/ml Ovalbumin (OVA) (Sigma-Aldrich, Steinheim, Germany) was emulsified in Complete Freund Adjuvant (CFA) (Sigma-Aldrich), and 100 µl of emulsion was injected subcutaneously (s.c.) in three sites in the back. After 24 h, 1×10^6 MSC were injected s.c. in the lumbar region. Immunized mice were killed 4 days later, and the brachial draining LNs (dLNs) were collected and frozen in OCT for immunofluorescence or digested for FACS analysis.

In vivo tissue inhibitor of metalloproteinase-1 immunoneutralization

Goat polyclonal anti-TIMP-1 IgG[19] (catalog no. AF980; R&D Systems, Minneapolis, MN, USA) was intravenously (i.v.) administered (0.5 mg/kg) in immunized mice 18 h after MSC transplantation. As a control, additional mice were given equivalent doses of an isotype-matched goat IgG (catalog no. AB-108-C, R&D Systems). Immunized mice were killed 2 days later, and the brachial dLNs were collected and digested for endothelial cell analysis by FACS. Data are representative of 36 LNs/group analyzed from four independent experiments.

Tissue inhibitor of metalloproteinase-1 siRNA reverse transfection

Timp-1 Silencer Select Pre-designed siRNAs (Ambion, Waltham, MA, USA) were exploited for mMSC transfection, and Silencer Select Negative Control No. 1 siRNA (Ambion) was adopted as scramble. siRNAs were diluted in Opti-MEM I reduced Serum Medium (Gibco, Waltham, MA, USA) at the final concentration of 50 nM. Diluted siRNAs were placed 100 µl/well in a 24-well tissue culture plate in the presence of 1 µl of Lipofectamine-2000 (Invitrogen, Carlsbad, CA, USA), according to the manufacturer's instructions. Murine MSC were seeded at a density of 6×10^4 cells/well and cultured in antibiotic-free medium. Medium was replaced 24 h post transfection with fresh DMEM low Glucose, 2 mM L-glutamine and 10% FCS Biosera. mMSC tissue inhibitor of metalloproteinase-1 (TIMP-1) secretion was analyzed at 24, 48 and 72 h after transfection by ELISA (R&D Systems). *In vivo* data with siRNA MSC are representative of 20 dLNs from 2 independent experiments.

AAV-mediated TIMP-1 overexpression

All the AAV vectors used in this study were generated by the AAV Vector Unit (AVU) at ICGEB Trieste (http://www.icgeb.org/avu-core-facility.html) as described previously.[20] Briefly, AAV vectors of serotype 9 were produced in HEK293T cells, using a triple plasmid co-transfection method. Viral stocks were collected after $CsCl_2$ gradient centrifugation. The total number of viral genome was determined by real-time PCR; the viral preparations had titers between 1×10^{13} and 3×10^{13} viral genome (vg) particles per ml. AAV9-TIMP-1 was intraperitoneally injected at a dose of 2×10^{11} vg in 100 µl PBS −/−. Equal amount of AAV9-LacZ was used as a control. One day after AAV9 administration, mice were immunized with CFA/OVA as discussed above (6 mice/group). Brachial dLNs were collected 4 days after immunization and digested for FACS analysis. Data are representative of one experiment out of two.

Immunofluorescence

Detailed protocols are available in the Supplementary Materials and Methods.

Flow-cytometry analyses

Detailed protocols are available in the Supplementary Materials and Methods.

LC-ESI MS/MS analysis

Detailed protocols are available in the Supplementary Materials and Methods.

Optical projection tomography

In all, 5 µg of Alexa-594 MECA-79 antibody (conjugated according to the manufacturer's instructions using the Alexa-594 conjugation kit; Invitrogen) was injected i.v. 15 min before organ harvest. Brachial LNs were excised, cleaned of surrounding fat and then incubated with AlexaFluor 488-conjugated anti-B220 (0.67 µg/ml) as previously described.[21] Further details are described in the Supplementary methods.

3D immunofluorescence

Mice were immunized and transplanted as described above. On day 3 after immunization, single-cell suspensions were obtained from LNs of C57/Bl6 wt mice. $CD4^+$ T cells were isolated using the mouse $CD4^+$ T cell isolation kit (Stem Cell Technologies, Vancouver, BC, Canada), according to the manufacturer's protocol. The lymphocytes were fluorescently labelled, injected i.v. into CFA/OVA immunized recipient mice and allowed to home for 20 min before blocking further homing with anti-L-selectin mAb. After 20 min, dLNs were isolated, treated and analyzed as previously described.[22] Data are representative of eight (CFA/OVA) and nine (+MSC) mice from three independent experiments.

Cryo imaging

MSC labelled with qTracker 655 (Life Technologies, Oslo, Norway) were s.c. injected into a control mouse or a mouse previously immunized with CFA/

OVA. Mice were killed 4 days later, frozen and cryo-imaged using the CryoViz cryo-imaging system (BioInVision, Inc., Cleveland, OH, USA) as described in Roy *et al*.[23,24] Cryo-images were acquired using the ProSCI software as described in Roy *et al*.[24] Further details are described in the Supplementary methods.

Statistical analysis

The sample size per group was estimated from previous experience with similar experiments. There were no pre-established criteria for mice or sample exclusion: except evident technical damage. Data were collected and analysis was done without the investigator knowing group allocation. Data were analyzed using the Prism Software (GraphPad, La Jolla, CA, USA). Data were expressed as mean ± s.e. Differences were assessed using *t*-test, Mann–Whitney test or one-way ANOVA. Statistic tests were performed between data with similar variance. Results with a P-value of < 0.05 were considered as significant.

RESULTS

MSC transplantation affects endothelial activation in immune reactive LNs

We have previously shown that encapsulated MSC injected s.c. are able to control systemic and local inflammation through the release of soluble factors.[9] Moreover, we have demonstrated that subcutaneous administration of MSC is more efficient than the intravenous route, probably because most of the MSC injected i.v. are trapped in the lungs and cleared after a few days.[9,25–27] On the basis of our previous data indicating that encapsulation was not required to improve the efficacy of s.c. injected MSC,[9] in this study we performed subcutaneous injections of free MSC (not encapsulated) in the lumbar area of mice that had been previously immunized with OVA in CFA (CFA/OVA) in the upper dorsal region. As expected, the immunization induced a robust and rapid response in the brachial dLNs (Figure 1). MSC transplantation significantly reduced this response, decreasing both the total cellularity and the volume of dLNs and affecting the recruitment of specific cell populations (Figures 1b–e), as already described.[9] Using whole-mouse cryo-imaging analysis,[28] we verified that s.c. injected MSC did not migrate away from the site of injection during the experimental time (5 days), both in immunized and in untreated mice (Supplementary Movies S1 and S2). Together with our previous study,[9] these data indicate that MSC are able to dampen inflammation through the release of soluble mediators.

LN growth during immune responses is accompanied by endothelial activation and vascular expansion, two events that are required for leukocytes recruitment and orchestration of immunity. We analyzed the expression of two adhesion molecules, VCAM-1 and ICAM-1, that are typically upregulated on the inflamed endothelium (Figures 2a–d). Interestingly, the dLN vessels of mice treated with MSC had a lower expression of both VCAM-1 and ICAM-1, as demonstrated by the colocalization analysis expressed as Mander's coefficient (Figures 2b–d). Moreover, we observed that the dLNs of mice transplanted with MSC showed reduced density of the endothelial marker CD31 and of Lyve-1, a marker of the lymphatic endothelium, suggesting a reduced vascular expansion upon MSC treatment (Figures 2a, c and e).

Altogether, these data indicate that MSC inhibit activation of vascular and lymphatic endothelium in the dLNs of immunized mice.

MSC inhibit activation and elongation of HEVs and affect recruitment of T cells to dLNs

The migration of leukocytes from the blood stream into LNs occurs via HEVs, which are post-capillary venules structurally adapted to support lymphocyte trafficking. Because of the reduced numbers of leukocytes present in the dLNs of mice treated with MSC (Figure 1),[9] we asked whether MSC transplantation affects HEV activation, lymph-node vascularization and leukocyte migration *in vivo*.

MSC were s.c. injected in the lumbar region of mice that had been previously immunized in the dorsal region with CFA/OVA, as already described (Figure 1), and HEV cells in brachial LNs were analyzed. In particular, HEV cells were identified as $CD45^{-}CD31^{+}$ $PNAd^{+}$ cells (Supplementary Figure S1). The reduced number of $CD45^{-}CD31^{+}$ cells was confirmed by flow-cytometry analyses (Figure 3a) and can be explained by the inhibition of endothelial cell proliferation in MSC-treated mice, as shown by the reduced uptake of BrdU (Figure 3b). In the dLNs of mice treated with MSC, we observed a reduction in the absolute number of HEV cells as compared with controls (Figure 3c). Moreover, HEV cells had a reduced expression of VCAM-1 (Figure 3d).

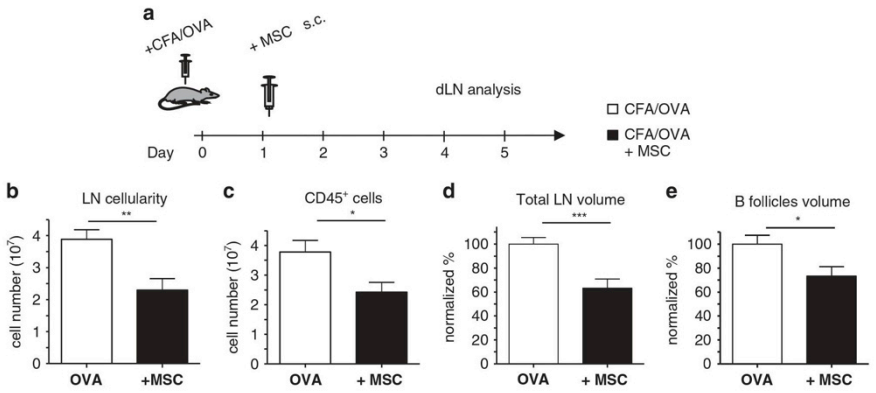

Figure 1. MSC affect size and cellularity of dLNs. (**a**) Diagram of the experimental protocol designed to investigate the influence of MSC transplantation. Mice were immunized in the dorsal back with CFA/OVA on day 0 and, on day 1, a group of animals received subcutaneous injection of 10^6 MSC in the lumbar back. On days 4–5, depending on the subsequent analyses, brachial LNs were collected and processed. (**b**, **c**) On day 5, dLNs were digested and analyzed by flow cytometry. Data are representative of eight mice from two independent experiments; (**d**, **e**) OPT data are expressed as percentage on OVA average. In (**b–e**), error bars represent s.e. (*$P < 0.05$; **$P < 0.01$; ***$P < 0.005$; *t*-test).

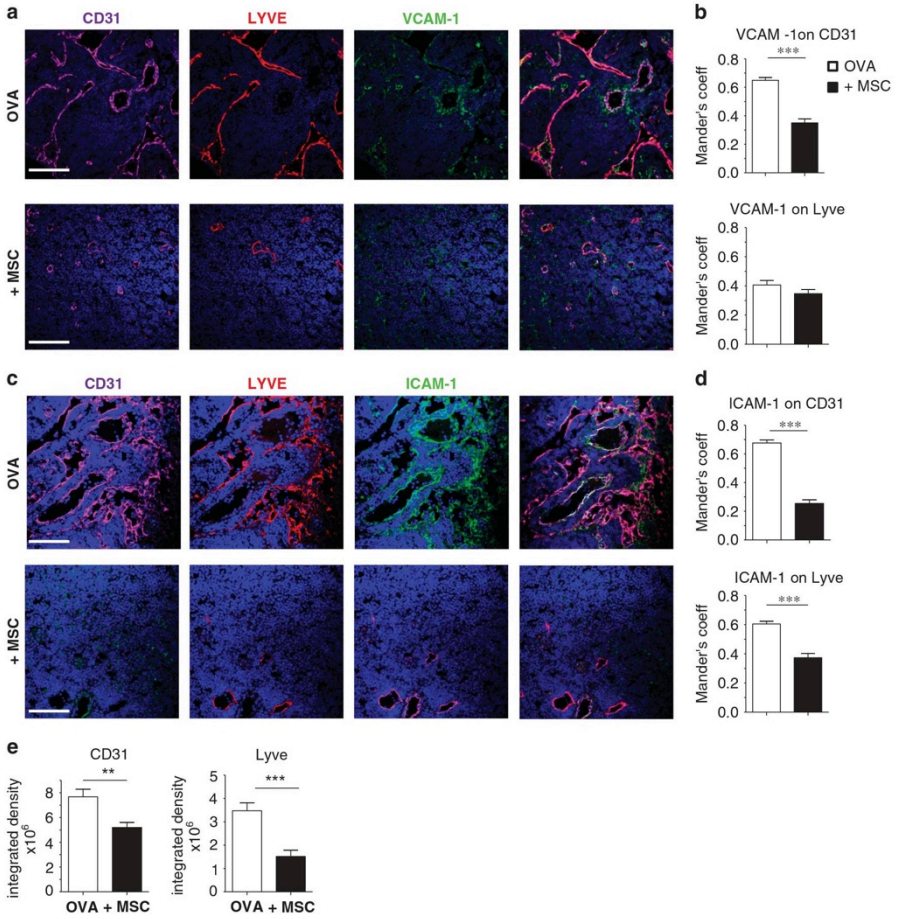

Figure 2. MSC inhibit endothelial activation in dLNs. Mice were treated as in Figure 1a and, on day 5, dLNs were collected, stained and analyzed by confocal microscopy. (**a**, **c**) 8-μm frozen section was stained with anti-CD31, anti-Lyve-1 and anti-VCAM-1 or anti-ICAM-1, as indicated (10×, scale bar 200 mm). (**b**, **d**) Mander's colocalization coefficient quantifies the degree of overlap. (**e**) Integrated density quantifies the CD31 and Lyve-1 immunopositivity amount on cross sections of lymph node. In all graphs, error bar represents s.e. (**$P < 0.01$, ***$P < 0.005$; *t*-test).

Analysis of entire LNs by optical projection tomography, which allows a three-dimensional reconstruction of the HEV network, allowed us to examine the morphologic alterations that occur in HEV expansion after immunization with CFA/OVA in the presence or absence of MSC. HEVs were labelled before imaging by intravenous injection of fluorophore-tagged MECA-79, which recognizes the PNAd epitope on the luminal surface (Figure 4a, Supplementary videos S3 and S4). The HEV length was significantly impaired in mice transplanted with MSC (Figure 4b) and the analysis of the HEV volume suggested a tendency toward vessel narrowing, although in this case the difference did not reach statistical significance (Figure 4c). In addition, the morphology of the HEV network was affected by MSC, as shown by the significant decrease in the number of branches and segments (Figures 4d and e), indicating that MSC limit both HEV elongation and arborization.

The previous observation prompted us to address whether MSC impair leukocyte homing to inflamed LNs. Fluorescently labelled naive T cells were injected i.v. in mice previously immunized with CFA/OVA, and transplanted or not with MSC. After 20 min, alexa633-conjugated MECA-79 and MEL-14 mAbs were i.v. injected to stain HEV and block L-selectin, respectively, and, after 20 additional minutes, the dLNs were harvested and prepared for two-photon microscopy acquisition (Figure 4f).[22] The analysis demonstrated that MSC transplantation inhibited T-cell homing into the inflamed LNs (Figure 4g).

Endothelial cells are a direct target of MSC

To understand whether the inhibition of endothelial cell activation and proliferation observed in immunized mice treated with MSC was due to a direct effect of MSC on endothelial cells, we analyzed the effects of MSC supernatants in various *in vitro* assays using a mouse vascular endothelial (1G11) and two mouse lymphatic endothelial (MELC and SVEC4-10) cell lines.[30–32] MSC were first expanded as an adherent monolayer until confluence, and were

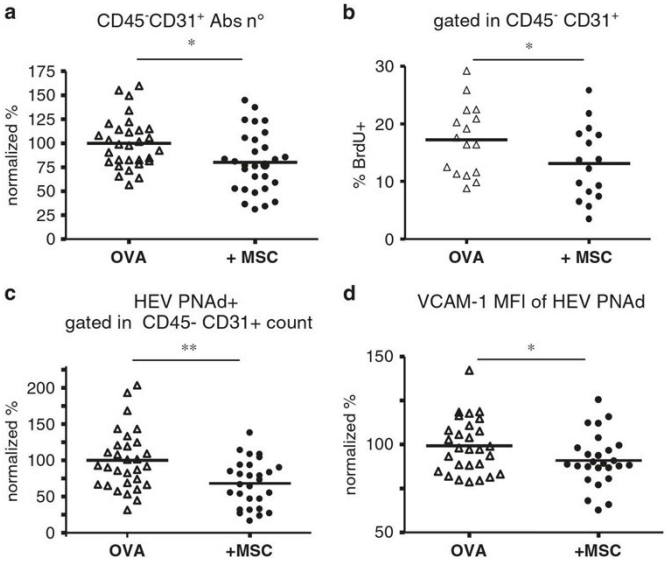

Figure 3. MSC inhibit HEV activation and proliferation in vivo. Mice were treated as illustrated in Figure 1a and dLNs were collected, digested and analyzed by flow cytometry. The graphs show (**a**) the absolute number of $CD45^-CD31^+$ cells per single LN expressed as normalized percentage on CFA/OVA (*t*-test), (**b**) BrdU incorporation cytometry after 48 h (Mann–Whitney test), (**c**) HEV cell numbers and (**d**) mean fluorescence intensity (MFI) of VCAM-1 expression on HEV (*t*-test) ($*P < 0.05$; $**P < 0.01$).

then stimulated for 24 h in the presence or absence of IL-1β, IL-6 and TNF-α to resemble the inflammatory milieu that MSC find *in vivo*.[33,34] MSC supernatant was collected as conditioned medium (CM) 18 h after cytokine withdrawal.

First, we analyzed the effect of MSC secretion on *in vitro* angiogenesis using the tube formation assay.[35] The soluble factors released by stimulated MSC strongly inhibited the ability of SVEC4-10 cells to form tube networks, whereas the medium collected from the unstimulated MSC (unst MSC-CM) had no effect (Figures 5a and b), indicating that in an inflammatory environment MSC can directly inhibit angiogenesis. This effect was also confirmed on another lymphatic endothelial cell line (MELC; Supplementary Figure S2). On the basis of these results and of the published literature,[33,34] in the following experiments we focused on the effects of the MSC-CM only.

As the *in vivo* data indicated that MSC transplantation affects the expression of adhesion molecules on endothelial cells (Figure 2b), we analyzed the expression of VCAM-1 and ICAM-1 on MELC and 1G11 cells treated with 20 ng/ml TNF-α for 24 h,[30,31] in the presence or in the absence of MSC-CM. In agreement with the previous data, the MSC-CM significantly reduced the expression of VCAM-1 and ICAM-1 on MELC (Figures 5c and e) and the expression of VCAM-1 on 1G11 cells (Figures 5d and f).

Expression of VCAM-1 and ICAM-1 on endothelial cells is regulated by NF-kB;[36] and thus, we examined the nuclear localization of NF-kB complexes using immunofluorescence microscopy. As expected, in both MELC and 1G11 cells TNF-α stimulation resulted in prompt translocation of p65 from the cytoplasm into the nucleus. MSC-CM inhibited NF-kB translocation in both cell lines (Figures 5g–j).

Altogether, these data indicate that endothelial cell activation is directly inhibited by soluble factors released by MSC exposed to inflammatory cytokines.

MSC inhibit *in vitro* angiogenesis through the release of TIMP-1

In an effort to understand the molecular mechanisms responsible for the observed effects of MSC, we performed shotgun proteomic characterization of the MSC secretome, comparing the supernatants collected from MSC stimulated (MSC-CM) or not (unst MSC-CM) with inflammatory cytokines. As detailed in Materials and methods, only proteins present and quantified in at least three out of five technical repeats, in both biological replicates, were considered as positively identified; 1613 and 1630 proteins were measured in the secretome of control and stimulated MSC, respectively.

Differential expression was considered as significant if (a) a protein was present only in MSC-CM or in control or (b) its LFQ intensity resulted statistically significant as calculated by Perseus (*t*-test cutoff at 1% permutation-based false discovery rate). According to this analysis, 7.6 or 8.3% of the proteins detected in the secretome of control or stimulated MSC, respectively, were differentially expressed, either upregulated or downregulated. These proteins were clustered according to their functions using the DAVID platform[37] filtered for significant Gene Ontology Biological Process (GOBP) terms using a P-value of < 0.05.

Concerning the 52 proteins that were significantly downregulated or present only in the secretome of unstimulated MSC (Supplementary Table S1), GO analysis revealed that most terms are related to metabolic processes (Supplementary Figure S3). As for the 89 proteins that were significantly upregulated or present only in the secretome of stimulated MSC (Supplementary Table S2 and Figure 6a), GO analysis indicated that 18 and 30% of the proteins belong to categories that are related to regulation of angiogenesis and inflammation processes, respectively (Supplementary Table S2 and Figure 6b). In particular, the presence of an 'angiogenesis-related' signature among upregulated proteins was also confirmed by preliminary analyses of

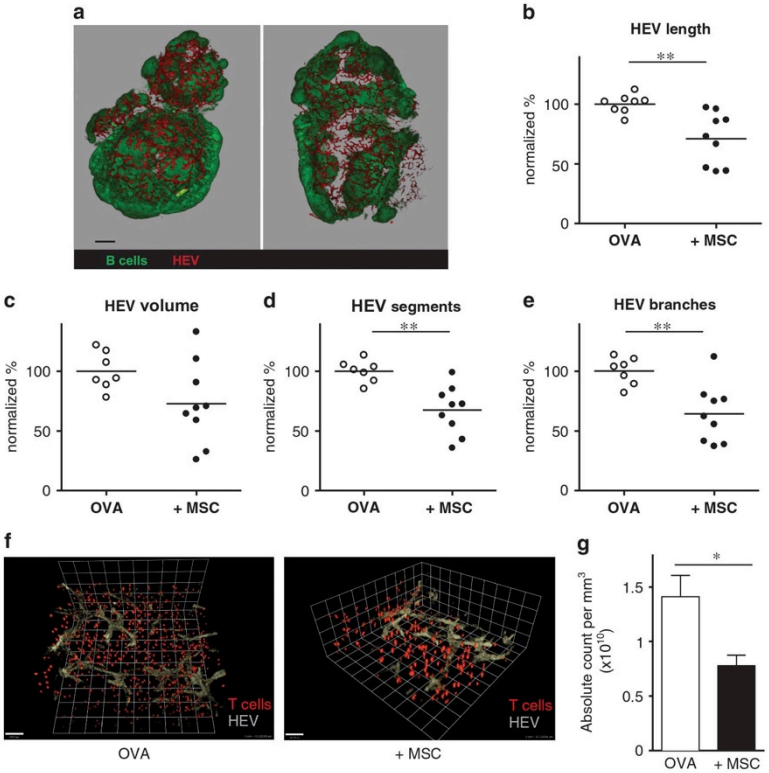

Figure 4. MSC suppress HEV lengthening and branching. (**a–e)** Mice were treated as described in Figure 1a, and on day 4 brachial LNs were prepared for OPT imaging (Meca-79 Alexa-594 and B220 Alexa-488). (**a**) Representative images from OPT scanning (scale bar, 400 μm). (**b**) Total HEV length per LN. (**c**) Total HEV volume per LN. (**d**) Number of HEV segments per LN. (**e**) Number of branch points per LN. (**f, g**) 3D immunofluorescence of lymphocyte homing in the presence of MSC tested at day 3 post immunization. (**f**) Representative images. (**g**) Absolute counts per mm^3 in OVA and OVA+MSC-treated mice, with error bars representing s.e. ($^*P < 0.05$, $^{**}P < 0.01$; *t*-test).

human MSC secretome, which reveals that all the 16 upregulated proteins in stimulated MSC secretome common to human and mouse are modulators of angiogenesis (Supplementary Table S3).

Among the several proteins upregulated in MSC by the inflammatory cytokines that have a direct or indirect effect on endothelial cells, we focused our attention on the TIMP-1 because of its well-known anti-angiogenic properties.[38] We thus used the tube formation assay to analyze the effect of MSC-derived TIMP-1 on angiogenesis. Although the blocking anti-TIMP-1 antibody had no effect on the ability of endothelial cells to form tubes when cultured in the supernatants of unstimulated MSC, it totally reverted the anti-angiogenic properties of the supernatant from stimulated MSC (Figure 7a), indicating that, al least in this *in vitro* setting, TIMP-1 is one of the key MSC-secreted molecules targeting the endothelium. In an *in vivo* setting, the injection of neutralizing anti-TIMP-1 antibody[19] 1 day after MSC transplantation reverted the MSC-induced reduction of endothelial cell numbers and HEV in dLNs (Figures 7b–d), suggesting that TIMP-1 may be directly responsible for the anti-inflammatory effects of MSC on LNs. To confirm this hypothesis, we used a siRNA approach to knock down TIMP-1 expression in MSC (Supplementary Figure S4). Again, the absolute cell numbers of endothelial cells and HEV in dLN were reduced by MSC transfected with the scramble siRNA control but not by MSC with TIMP-1 siRNA (Figures 7e–g).

On the basis of these results, we speculated that overexpression of TIMP-1 might be sufficient to mimic the effects of MSC transplantation, in terms of inhibition of angiogenesis in the inflamed lymph nodes. TIMP-1 overexpression by AAV9-mediated gene transfer[20] in mice immunized with CFA/OVA (Figure 8a) inhibited the inflammatory reaction in the draining LNs, as indicated by the reduced total cellularity (Figure 8b), which was due to a decreased number of both $CD45^+$ cells (Figure 8c) and endothelial and HEV cells (Figures 8d and e).

DISCUSSION

MSC have been studied across a range of clinical indications and represent a promising therapeutic approach in many diseases in view of their potent immunomodulatory properties. To design better therapeutic protocols and define the clinical endpoints, it is important to identify the specific targets of MSC anti-inflammatory action *in vivo*. In this study, we have demonstrated that LN endothelial cells and HEV are a direct target of MSC-based therapy.

LNs are the organs where the initiation of immune responses takes place and their structure guides and organizes the crosstalk

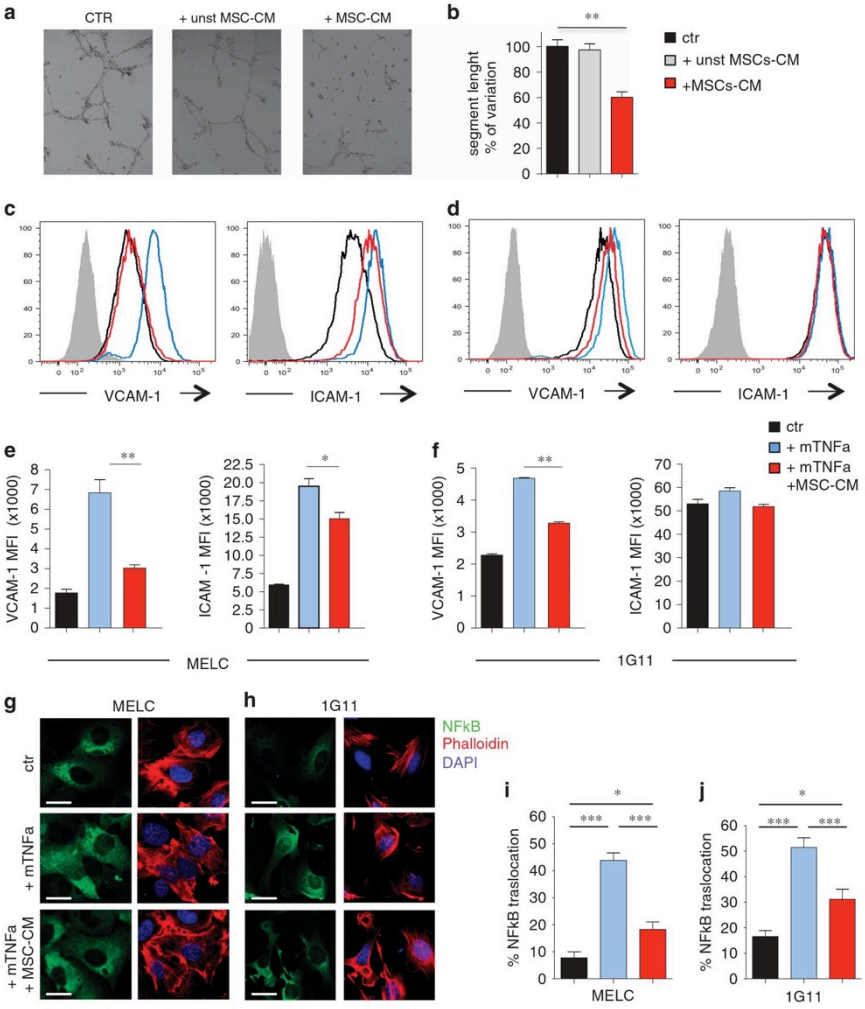

Figure 5. Endothelial cells are a direct target of MSC-secreted molecules. The supernatant of MSC stimulated with IL-1b, IL-6 and TNF-a (MSC-CM) or unstimulated MSC (unst MSC) was collected as described in Materials and methods, and its effect on endothelial cell lines activation was determined. (**a, b**) SVEC4-10 network formation. Representative images at 6 h and segment length quantification indicated as % of variation in comparison with control condition. Data are expressed as mean ± s.e.m. and represent the pool of three experiments (*t*-test). (**c**, **d**) Expression of endothelial adhesion molecules. Representative histograms showing the mean fluorescence intensity (MFI) of VCAM-1 and ICAM-1 on MELC and 1G11 endothelial cell line. (**e, f**) Quantitative analyses of (**c**) and (**d**), respectively (*t*-test). (**g–j**) TNF-a induced NF-kB translocation. Representative confocal images (×40) of MELC (**g**) or 1G11 (**h**) cells stained for NF-kB and phalloidin. Scale bar 10 um. (**I, j**) Quantification of NF-kB translocation into the nucleus expressed as percentage of the total (one representative experiment out of three; one-way ANOVA) (*$P < 0.05$; **$P < 0.01$; ***$P < 0.0001$).

between lymphocytes and antigen-presenting cells during both normal responses to pathogens and immune-mediated diseases, such as autoimmunity, allergy or graft-versus-host disease.[39] When a robust immune response develops, infiltrating and dividing lymphocytes markedly increase LNs cellularity, leading to organ expansion. During this swelling, there is massive endothelial cell proliferation and vascular expansion occurs.[40] Both acute and chronic inflammatory processes are indeed associated with pronounced vascular remodelling. Angiogenesis and lymph angiogenesis, the growth of new blood vessels and lymphatic vessels from pre-existing ones, are involved in a number of physiological and pathological conditions, such as wound healing, tumor growth, rheumatoid arthritis, inflammatory bowel disease and asthma.[41] Thus, the identification of therapies that specifically inhibit angiogenesis may represent a weapon to reduce inflammation and prevent disease progression.[16]

Recently, it was demonstrated that MSC have a potent stabilizing effect on the vascular endothelium, having the capacity of inhibiting endothelial permeability after traumatic brain injury[42] and in hemorrhagic shock.[43] Our results demonstrate that, during

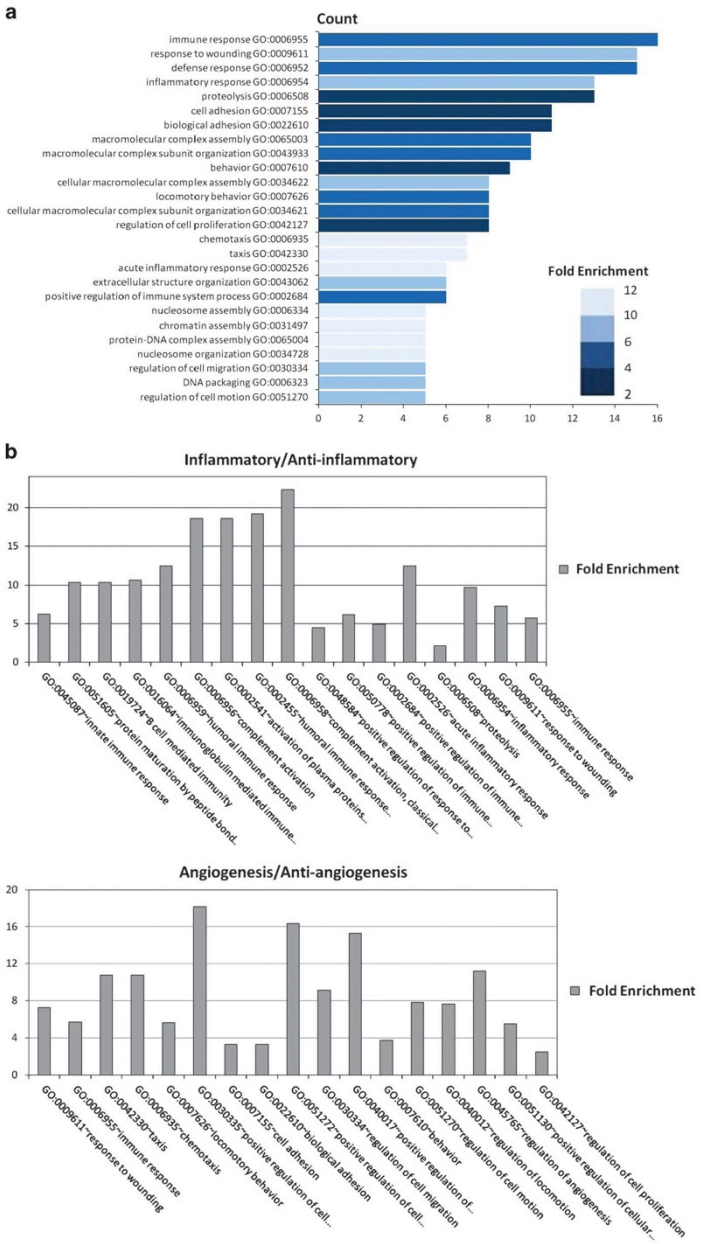

Figure 6. Distribution into biological processes of the proteins upregulated in MSC-CM. The proteins that were significantly upregulated or present only in MSC-CM were classified into different biological processes according to the GO classification system. (**a**) The bar chart shows the count of the top 26 most-enriched GO terms in MSC-CM versus unstimulated MSC-CM. Color coding indicates the fold enrichment. (**b**) Proteins categorized as modulators involved in inflammation processes and/or angiogenesis. The histograms report the GOBP groups related to angiogenesis or inflammation.

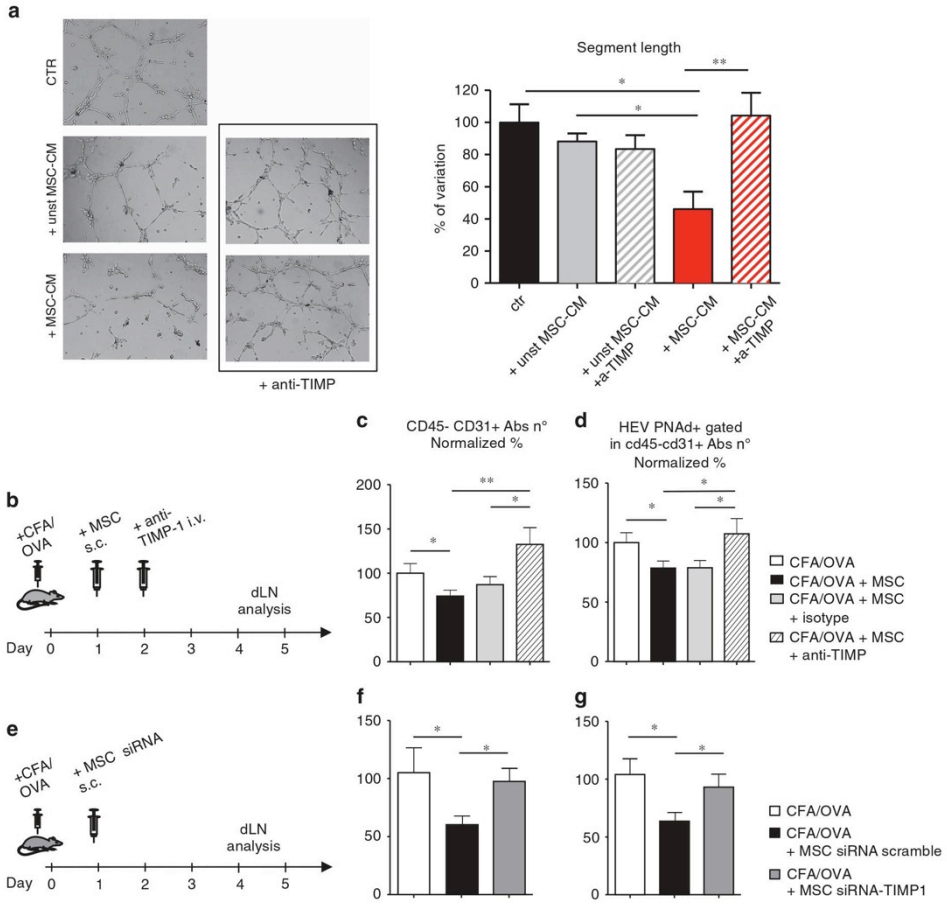

Figure 7. TIMP-1 mediates the anti-angiogenic effect of MSC-CM *in vitro* and the anti-inflammatory effect of MSC *in vivo*. SVEC4-10 network formation in matrigel in the presence of MSC-CM or unst MSC-CM and anti-TIMP-1 blocking antibody. (**a**) anti-mTIMP1 blocking antibody restores SVEC4-10 network formation in matrigel in the presence of MSC-CM. Representative images at 6 h (left) and segment length quantification as percentage of variation (right) are shown. Data are expressed as mean ± s.e.m. (*$P < 0.05$, **$P < 0.01$; one-way ANOVA). (**b**) Diagram of the experimental protocol designed to block the TIMP-1 activity during the anti-inflammatory effects of MSC. Mice were immunized in the dorsal region with CFA/OVA on day 0 and, on day 1, three groups of animals received subcutaneous injection of 10^6 MSC in the lumbar region. Eighteen hours after MSC transplantation, goat polyclonal anti-TIMP-1 IgG or isotype-matched goat IgG was i.v. administrated. On day 4,*-3 brachial LNs were collected, processed and analyzed by flow cytometry; (**c, d**) the graphs show the absolute number of $CD45^-CD31^+$ cells and HEV $PNAd^+$ cells per single LN, expressed as normalized percentage on CFA/OVA (*t*-test). (**e**) Diagram of the experimental protocol designed to investigate the contribution of MSC-derived TIMP-1 on dLN endothelium. Mice were immunized in the dorsal region with CFA/OVA on day 0. The day after, two groups of animals received in the lumbar region subcutaneous injection of 10^6 MSC transfected with either scramble control siRNA or siRNA specific for TIMP-1, respectively. On day 4, brachial LNs were collected, processed and analyzed by flow cytometry; (**f, g**) graphs showing the absolute number of $CD45^-CD31^+$ cells and HEV $PNAd^+$ cells per single dLN. Data are expressed as normalized percentage on CFA/OVA (Mann–Whitney test) (*$P < 0.05$; **$P < 0.01$).

an immune response, MSC inhibit HEV proliferation, activation and elongation in dLNs, thus reducing the recruitment of immune cells. In agreement with our data, homing of dendritic cell to dLNs was reduced in the presence of MSC in several mouse models[44,45] and *in vitro* co-cultures of MSC with endothelial cells down-regulated cytokine-induced recruitment of neutrophils and lymphocytes.[46]

In our study, the effects of MSC on endothelial cell activation, HEV elongation and T-cell trafficking do not require MSC homing to LNs and are all mediated by soluble factors released by MSC. This is in agreement with another study showing an anti-angiogenic activity for soluble factors present in media derived from MSC/glioma co-cultures.[47] The proteomic analysis of the MSC secretome indicated that, upon activation by inflammatory cytokines, MSC upregulate the expression of several proteins potentially affecting angiogenesis and inflammation through multiple pathways. Interestingly, when we compared the secretomes of human and mouse MSC, we found that only 16 proteins are upregulated in both cell types and 11 of them modulate angiogenesis directly or indirectly, thus supporting the idea that

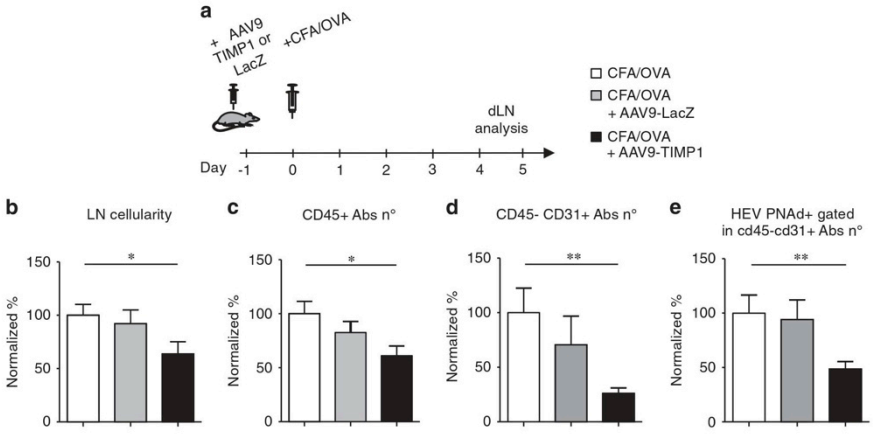

Figure 8. TIMP-1 overexpression *in vivo* mimics MSC transplantation. (**a**) Diagram of the experimental protocol designed to overexpress TIMP-1 in immunized mice. One day after AAV9-TIMP-1 or AAV9-LacZ administration (day 0), mice were immunized with CFA/OVA. Brachial dLNs were collected 4 days after immunization and processed for flow cytometry. The graphs show the absolute number of total cells (**b**), $CD45^+$ cells (**c**), $CD45^-CD31^+$ (**d**) and HEV $PNAd^+$ (**e**) cells per single LN, expressed as normalized percentage on CFA/OVA. Error bars represent standard error (*$P < 0.05$; **$P < 0.01$; Mann–Whitney test).

the endothelium is a specific target of MSC during inflammation. Notably, although many soluble factors released by cytokine-triggered MSC are positive regulators of angiogenesis, in the experimental system here described the overall *in vivo* effect of MSC is a reduced dLN vascular expansion.

Angiogenesis requires degradation of the vascular basement membrane and remodelling of the extracellular matrix to allow endothelial cells migration and invasion into the surrounding tissue. This process requires the action of matrix metalloproteinases (MMPs) that degrade both matrix and non-matrix proteins and have central roles in morphogenesis, wound healing, tissue repair and in progression of chronic diseases.[48] The balance between MMPs and their natural inhibitors, the TIMPs, is critical for extracellular matrix remodelling and angiogenesis. The TIMP family comprises four protease inhibitors: TIMP-1, TIMP-2, TIMP-3 and TIMP-4. With the exception of TIMP-4,[49] all three TIMPs inhibit angiogenesis *in vivo*,[38] although through diverse mechanisms. MSC secrete both MMPs and their inhibitors, and thus contribute to the regulation and protection of the perivascular niche.[50]

Using both *in vitro* and *in vivo* assays, we identified the metalloproteinase inhibitor TIMP-1 as the molecule responsible for the anti-angiogenic effects of MSC. TIMP-1 is known to inhibit endothelial cells migration by MMP-dependent and MMP-independent mechanisms.[51–53] The latter involve regulation of various biological processes such as cell growth, apoptosis and differentiation through the CD63 receptor.[54,55] In addition, TIMP-1 was shown to induce secretion of soluble VEGFR-1 by human endothelial cells, leading to a decrease of bioavailable VEGF and of blood vessel growth.[56] TIMP-3 has also been identified as a soluble factor produced by MSC with beneficial effects on endothelial cell function in a mouse model of traumatic brain injury;[57] however, we did not find evidence for TIMP-3 upregulation in the mouse or human MSC secretomes. It is likely that, *in vivo*, other soluble factors in addition to TIMP-1 contribute to MSC-mediated immune regulation: MSC are also known to produce prostaglandin E2 and thus inhibit the activation of macrophages,[58] which are a source of multiple growth factors that enhance endothelial cell proliferation and survival.[59] Indeed, we confirmed prostaglandin E2 secretion by stimulated MSC (not shown) and, in addition, we found that MSC release several other anti-inflammatory lipids, such as resolvinD1 and LipoxinA4 (not shown) that may also affect endothelial cell activation and/or proliferation. Another interesting mediator found in the MSC secretome is the soluble form of VCAM-1 (sVCAM-1). High levels of sVCAM-1 have been detected in the synovial fluid of patients with rheumatoid arthritis[60] and in the blood of patients with different types of cancers,[61] but its origin is not entirely clear and our data suggest that MSC may represent an important source of this molecule. Although sVCAM-1 is described as a promoter of angiogenesis,[62] by altering leukocyte trafficking[63] or inhibiting T-cell activation,[64] it may contribute to the MSC-induced suppression of T-cell recruitment that we observed in this study.

The results presented here clearly position endothelial cells as a key target of MSC-mediated immunomodulation during ongoing inflammatory responses and pave the way for developing strategies that exploit MSC-mediated inhibition of lymph-node angiogenesis in the treatment of inflammation-associated pathologies. Furthermore, by identifying TIMP-1 as a critical effector of the anti-inflammatory properties of MSC, this study pinpoints a potential new biomarker in clinical settings. Further studies on the role of TIMP-1 in human MSC are required to confirm its correlation with clinical outcomes or its value in selecting the best source of MSC for immunomodulation.

CONFLICT OF INTEREST

The authors declare no conflict of interest.

ACKNOWLEDGEMENTS

We thank Achille Anselmo, Marina Sironi and Erica Dander for assistance. We also thank the MERLIN group for scientific discussion. This work has been supported by grants from Associazione Italiana Ricerca sul Cancro (AIRC, 'Lombardia Molecular Imaging') and Ministero della Salute (Bando cellule staminali, Bando Giovani Ricercatori). This project has received funding from the European Union's Seventh Framework Programme for research, technological development and demonstration under grant agreement no 602363. LZ is supported by Fondazione Veronesi per la Ricerca. MELC and 1G11 were kindly provided by A Vecchi and M Sironi.

AUTHOR CONTRIBUTIONS

LZ designed and performed most of the experiments and wrote the manuscript; RA participated in designing and performed part of the experiments and participated in writing the manuscript; CS performed confocal microscopy experiments; CP and BC provided technical assistance throughout the project; FM and JVS performed and supervised the OPT experiments; MG performed Cryo imaging experiments; GDA and SE provided mouse and human MSC, respectively; SZ provided AAV9-TIMP-1 and AAV9-LacZ; GT, EM and AN performed the proteomic analyses; AS designed experiments and wrote the manuscript; AV coordinated the study, wrote the manuscript and provided funds.

REFERENCES

1 Caplan AI. Mesenchymal stem cells. *J Orthop Res* 1991; **9**: 641–650.
2 Crisan M, Yap S, Casteilla L, Chen CW, Corselli M, Park TS *et al.* A perivascular origin for mesenchymal stem cells in multiple human organs. *Cell Stem Cell* 2008; **3**: 301–313.
3 Covas DT, Panepucci RA, Fontes AM, Silva Jr WA, Orellana MD, Freitas MC *et al.* Multipotent mesenchymal stromal cells obtained from diverse human tissues share functional properties and gene-expression profile with CD146+ perivascular cells and fibroblasts. *Exp Hematol* 2008; **36**: 642–654.
4 Hellstrom M, Gerhardt H, Kalen M, Li X, Eriksson U, Wolburg H *et al.* Lack of pericytes leads to endothelial hyperplasia and abnormal vascular morphogenesis. *J Cell Biol* 2001; **153**: 543–553.
5 Frenette PS, Pinho S, Lucas D, Scheiermann C. Mesenchymal stem cell: keystone of the hematopoietic stem cell niche and a stepping-stone for regenerative medicine. *Annu Rev Immunol* 2013; **31**: 285–316.
6 Sensebe L, Krampera M, Schrezenmeier H, Bourin P, Giordano R. Mesenchymal stem cells for clinical application. *Vox Sang* 2010; **98**: 93–107.
7 Zappia E, Casazza S, Pedemonte E, Benvenuto F, Bonanni I, Gerdoni E *et al.* Mesenchymal stem cells ameliorate experimental autoimmune encephalomyelitis inducing T-cell anergy. *Blood* 2005; **106**: 1755–1761.
8 Djouad F, Fritz V, Apparailly F, Louis-Plence P, Bony C, Sany J *et al.* Reversal of the immunosuppressive properties of mesenchymal stem cells by tumor necrosis factor alpha in collagen-induced arthritis. *Arthritis Rheum* 2005; **52**: 1595–1603.
9 Zanotti L, Sarukhan A, Dander E, Castor M, Cibella J, Soldani C *et al.* Encapsulated mesenchymal stem cells for in vivo immunomodulation. *Leukemia* 2013; **27**: 500–503.
10 Murphy MB, Moncivais K, Caplan AI. Mesenchymal stem cells: environmentally responsive therapeutics for regenerative medicine. *Exp Mol Med* 2013; **45**: e54.
11 Sala E, Genua M, Petti L, Anselmo A, Arena V, Cibella J *et al.* Mesenchymal stem cells reduce colitis in mice via release of TSG6, independently of their localization to the intestine. *Gastroenterology* 2015; **149**: 163–176 e20.
12 Strieter RM, Burdick MD, Gomperts BN, Belperio JA, Keane MP. CXC chemokines in angiogenesis. *Cytokine Growth Factor Rev* 2005; **16**: 593–609.
13 Charo IF, Ransohoff RM. The many roles of chemokines and chemokine receptors in inflammation. *N Engl J Med* 2006; **354**: 610–621.
14 De Bruyn PP, Cho Y. Structure and function of high endothelial postcapillary venules in lymphocyte circulation. *Curr Top Pathol* 1990; **84**: 85–101.
15 Forster R, Schubel A, Breitfeld D, Kremmer E, Renner-Muller I, Wolf E *et al.* CCR7 coordinates the primary immune response by establishing functional microenvironments in secondary lymphoid organs. *Cell* 1999; **99**: 23–33.
16 Pober JS, Sessa WC. Evolving functions of endothelial cells in inflammation. *Nat Rev Immunol* 2007; **7**: 803–815.
17 Phillips RJ, Mestas J, Gharaee-Kermani M, Burdick MD, Sica A, Belperio JA *et al.* Epidermal growth factor and hypoxia-induced expression of CXC chemokine receptor 4 on non-small cell lung cancer cells is regulated by the phosphatidylinositol 3-kinase/PTEN/AKT/mammalian target of rapamycin signaling pathway and activation of hypoxia inducible factor-1alpha. *J Biol Chem* 2005; **280**: 22473–22481.
18 Medzhitov R. Origin and physiological roles of inflammation. *Nature* 2008; **454**: 428–435.
19 Crocker SJ, Frausto RF, Whitmire JK, Benning N, Milner R, Whitton JL. Amelioration of coxsackievirus B3-mediated myocarditis by inhibition of tissue inhibitors of matrix metalloproteinase-1. *Am J Pathol* 2007; **171**: 1762–1773.
20 Zacchigna S, Pattarini L, Zentilin L, Moimas S, Carrer A, Sinigaglia M *et al.* Bone marrow cells recruited through the neuropilin-1 receptor promote arterial formation at the sites of adult neoangiogenesis in mice. *J Clin Invest* 2008; **118**: 2062–2075.
21 Kumar V, Scandella E, Danuser R, Onder L, Nitschke M, Fukui Y *et al.* Global lymphoid tissue remodeling during a viral infection is orchestrated by a B cell-lymphotoxin-dependent pathway. *Blood* 2010; **115**: 4725–4733.
22 Boscacci RT, Pfeiffer F, Gollmer K, Sevilla AI, Martin AM, Soriano SF *et al.* Comprehensive analysis of lymph node stroma-expressed Ig superfamily members reveals redundant and nonredundant roles for ICAM-1, ICAM-2, and VCAM-1 in lymphocyte homing. *Blood* 2010; **116**: 915–925.
23 Roy D, Steyer GJ, Gargesha M, Stone ME, Wilson DL. 3D cryo-imaging: a very high-resolution view of the whole mouse. *Anat Rec (Hoboken)* 2009; **292**: 342–351.
24 Roy D, Gargesha M, Steyer GJ, Hakimi P, Hanson RW, Wilson DL. Multi-scale characterization of the PEPCK-C mouse through 3D cryo-imaging. *Int J Biomed Imaging* 2010; **2010**: 105984.
25 Schrepfer S, Deuse T, Lange C, Katzenberg R, Reichenspurner H, Robbins RC *et al.* Simplified protocol to isolate, purify, and culture expand mesenchymal stem cells. *Stem Cells Dev* 2007; **16**: 105–107.
26 Schrepfer S, Deuse T, Reichenspurner H, Fischbein MP, Robbins RC, Pelletier MP. Stem cell transplantation: the lung barrier. *Transplant Proc* 2007; **39**: 573–576.
27 Lee RH, Pulin AA, Seo MJ, Kota DJ, Ylostalo J, Larson BL *et al.* Intravenous hMSCs improve myocardial infarction in mice because cells embolized in lung are activated to secrete the anti-inflammatory protein TSG-6. *Cell Stem Cell* 2009; **5**: 54–63.
28 Gargesha M, Qutaish MQ, Roy D, Steyer GJ, Watanabe M, Wilson DL. Visualization of color anatomy and molecular fluorescence in whole-mouse cryo-imaging. *Comput Med Imaging Graph* 2011; **35**: 195–205.
29 Kumar V, Chyou S, Stein JV, Lu TT. Optical projection tomography reveals dynamics of HEV growth after immunization with protein plus CFA and features shared with HEVs in acute autoinflammatory lymphadenopathy. *Front Immunol* 2012; **3**: 282.
30 Sironi M, Conti A, Bernasconi S, Fra AM, Pasqualini F, Nebuloni M *et al.* Generation and characterization of a mouse lymphatic endothelial cell line. *Cell Tissue Res* 2006; **325**: 91–100.
31 Dong QG, Bernasconi S, Lostaglio S, De Calmanovici RW, Martin-Padura I, Breviario F *et al.* A general strategy for isolation of endothelial cells from murine tissues. Characterization of two endothelial cell lines from the murine lung and subcutaneous sponge implants. *Arterioscler Thromb Vasc Biol* 1997; **17**: 1599–1604.
32 O'Connell KA, Edidin M. A mouse lymphoid endothelial cell line immortalized by simian virus 40 binds lymphocytes and retains functional characteristics of normal endothelial cells. *J Immunol* 1990; **144**: 521–525.
33 Bernardo ME, Fibbe WE. Mesenchymal stromal cells: sensors and switchers of inflammation. *Cell Stem Cell* 2013; **13**: 392–402.
34 Groh ME, Maitra B, Szekely E, Koc ON. Human mesenchymal stem cells require monocyte-mediated activation to suppress alloreactive T cells. *Exp Hematol* 2005; **33**: 928–934.
35 Arnaoutova I, Kleinman HK. In vitro angiogenesis: endothelial cell tube formation on gelled basement membrane extract. *Nat Protoc* 2010; **5**: 628–635.
36 Zhou Z, Connell MC, MacEwan DJ. TNFR1-induced NF-kappaB, but not ERK, p38MAPK or JNK activation, mediates TNF-induced ICAM-1 and VCAM-1 expression on endothelial cells. *Cell Signal* 2007; **19**: 1238–1248.
37 Huang, da W, Sherman BT, Lempicki RA. Systematic and integrative analysis of large gene lists using DAVID bioinformatics resources. *Nat Protoc* 2009; **4**: 44–57.
38 Lambert E, Dasse E, Haye B, Petitfrere E. TIMPs as multifacial proteins. *Crit Rev Oncol Hematol* 2004; **49**: 187–198.
39 Lin KL, Fulton LM, Berginski M, West ML, Taylor NA, Moran TP *et al.* Intravital imaging of donor allogeneic effector and regulatory T cells with host dendritic cells during GVHD. *Blood* 2014; **123**: 1604–1614.
40 Webster B, Ekland EH, Agle LM, Chyou S, Ruggieri R, Lu TT. Regulation of lymph node vascular growth by dendritic cells. *J Exp Med* 2006; **203**: 1903–1913.
41 Zgraggen S, Ochsenbein AM, Detmar M. An important role of blood and lymphatic vessels in inflammation and allergy. *J Allergy* 2013; **2013**: 672381.
42 Pati S, Khakoo AY, Zhao J, Jimenez F, Gerber MH, Harting M *et al.* Human mesenchymal stem cells inhibit vascular permeability by modulating vascular endothelial cadherin/beta-catenin signaling. *Stem Cells Dev* 2011; **20**: 89–101.
43 Pati S, Gerber MH, Menge TD, Wataha KA, Zhao Y, Baumgartner JA *et al.* Bone marrow derived mesenchymal stem cells inhibit inflammation and preserve vascular endothelial integrity in the lungs after hemorrhagic shock. *PLoS One* 2011; **6**: e25171.
44 Chiesa S, Morbelli S, Morando S, Massollo M, Marini C, Bertoni *et al.* Mesenchymal stem cells impair in vivo T-cell priming by dendritic cells. *Proc Natl Acad Sci USA* 2011; **108**: 17384–17389.
45 Lee HJ, Ko JH, Ko AY, Kim MK, Wee WR, Oh JY. Intravenous infusion of mesenchymal stem/stromal cells decreased CCR7(+) antigen presenting cells in mice with corneal allotransplantation. *Curr Eye Res* 2014; **39**: 780–789.
46 Luu NT, McGettrick HM, Buckley CD, Newsome PN, Rainger GE, Frampton J *et al.* Crosstalk between mesenchymal stem cells and endothelial cells leads to downregulation of cytokine-induced leukocyte recruitment. *Stem Cells* 2013; **31**: 2690–2702.
47 Ho IA, Toh HC, Ng WH, Teo YL, Guo CM, Hui KM *et al.* Human bone marrow-derived mesenchymal stem cells suppress human glioma growth through inhibition of angiogenesis. *Stem Cells* 2013; **31**: 146–155.

48 Nagase H, Visse R, Murphy G. Structure and function of matrix metalloproteinases and TIMPs. *Cardiovasc Res* 2006; **69**: 562–573.
49 Fernandez CA, Moses MA. Modulation of angiogenesis by tissue inhibitor of metalloproteinase-4. *Biochem Biophys Res Commun* 2006; **345**: 523–529.
50 Lozito TP, Tuan RS. Mesenchymal stem cells inhibit both endogenous and exogenous MMPs via secreted TIMPs. *J Cell Physiol* 2011; **226**: 385–396.
51 Reed MJ, Koike T, Sadoun E, Sage EH, Puolakkainen P. Inhibition of TIMP1 enhances angiogenesis in vivo and cell migration in vitro. *Microvasc Res* 2003; **65**: 9–17.
52 Ikenaka Y, Yoshiji H, Kuriyama S, Yoshii J, Noguchi R, Tsujinoue H *et al*. Tissue inhibitor of metalloproteinases-1 (TIMP-1) inhibits tumor growth and angiogenesis in the TIMP-1 transgenic mouse model. *Int J Cancer* 2003; **105**: 340–346.
53 Akahane T, Akahane M, Shah A, Connor CM, Thorgeirsson UP. TIMP-1 inhibits microvascular endothelial cell migration by MMP-dependent and MMP-independent mechanisms. *Exp Cell Res* 2004; **301**: 158–167.
54 Jung KK, Liu XW, Chirco R, Fridman R, Kim HR. Identification of CD63 as a tissue inhibitor of metalloproteinase-1 interacting cell surface protein. *EMBO J* 2006; **25**: 3934–3942.
55 Stetler-Stevenson WG. Tissue inhibitors of metalloproteinases in cell signaling: metalloproteinase-independent biological activities. *Sci Signal* 2008; **1**, re6.
56 Bruegmann E, Gruemmer R, Neulen J, Motejlek K. Regulation of soluble vascular endothelial growth factor receptor 1 secretion from human endothelial cells by tissue inhibitor of metalloproteinase 1. *Mol Hum Reprod* 2009; **15**: 749–756.
57 Menge T, Gerber M, Wataha K, Reid W, Guha S, Cox CS Jr. *et al*. Human mesenchymal stem cells inhibit endothelial proliferation and angiogenesis via cell-cell contact through modulation of the VE-Cadherin/beta-catenin signaling pathway. *Stem Cells Dev* 2013; **22**: 148–157.
58 Nemeth K, Leelahavanichkul A, Yuen PS, Mayer B, Parmelee A, Doi K *et al*. Bone marrow stromal cells attenuate sepsis via prostaglandin E(2)-dependent reprogramming of host macrophages to increase their interleukin-10 production. *Nat Med* 2009; **15**: 42–49.
59 Baer C, Squadrito ML, Iruela-Arispe ML, De Palma M. Reciprocal interactions between endothelial cells and macrophages in angiogenic vascular niches. *Exp Cell Res* 2013; **319**: 1626–1634.
60 Wellicome SM, Kapahi P, Mason JC, Lebranchu Y, Yarwood H, Haskard DO. Detection of a circulating form of vascular cell adhesion molecule-1: raised levels in rheumatoid arthritis and systemic lupus erythematosus. *Clin Exp Immunol* 1993; **92**: 412–418.
61 Dymicka-Piekarska V, Guzinska-Ustymowicz K, Kuklinski A, Kemona H. Prognostic significance of adhesion molecules (sICAM-1, sVCAM-1) and VEGF in colorectal cancer patients. *Thromb Res* 2012; **129**: e47–e50.
62 Koch AE, Halloran MM, Haskell CJ, Shah MR, Polverini PJ. Angiogenesis mediated by soluble forms of E-selectin and vascular cell adhesion molecule-1. *Nature* 1995; **376**: 517–519.
63 Kitani A, Nakashima N, Izumihara T, Inagaki M, Baoui X, Yu S *et al*. Soluble VCAM-1 induces chemotaxis of Jurkat and synovial fluid T cells bearing high affinity very late antigen-4. *J Immunol* 1998; **161**: 4931–4938.
64 Kitani A, Nakashima N, Matsuda T, Xu B, Yu S, Nakamura T *et al*. T cells bound by vascular cell adhesion molecule-1/CD106 in synovial fluid in rheumatoid arthritis: inhibitory role of soluble vascular cell adhesion molecule-1 in T cell activation. *J Immunol* 1996; **156**: 2300–2308.

Supplementary Information accompanies this paper on the Leukemia website (http://www.nature.com/leu)

Journal of Proteomics 166 (2017) 115–126

Contents lists available at ScienceDirect

Journal of Proteomics

journal homepage: www.elsevier.com/locate/jprot

Proteomic analysis of the secretome of human bone marrow-derived mesenchymal stem cells primed by pro-inflammatory cytokines

Elisa Maffioli [a,b], Simona Nonnis [a,b], Roberta Angioni [c,d], Fabiana Santagata [a,b], Bianca Calì [c,d], Lucia Zanotti [e], Armando Negri [a,b], Antonella Viola [c,d,*], Gabriella Tedeschi [a,b,**]

[a] Università degli Studi di Milano, Dipartimento di Medicina Veterinaria, via Celoria 10, 20133 Milano, Italy
[b] Fondazione Filarete, Viale Ortles 22/24, 20139 Milano, Italy
[c] Università di Padova, Dipartimento di Scienze Biomediche, Via Ugo Bassi, 58/b, 35131 Padova, Italy
[d] VIMM - Istituto Veneto di Medicina Molecolare, Via Orus, 2, 35129 Padova, Italy
[e] Division of Regenerative Medicine, Stem Cells and Gene Therapy, San Raffaele Hospital, Milano, Italy

ARTICLE INFO

Article history:
Received 27 March 2017
Received in revised form 7 June 2017
Accepted 17 July 2017
Available online 21 July 2017

Keywords:
Secretome
MSC
Stem cells
Mass spectrometry
TIMP-1

ABSTRACT

Mesenchymal stem cells (MSC) represent an impressive opportunity in term of regenerative medicine and immunosuppressive therapy. Although it is clear that upon transplantation MSC exert most of their therapeutic effects through the secretion of bioactive molecules, the effects of a pro-inflammatory recipient environment on MSC secretome have not been characterized. In this study, we used a label free mass spectrometry based quantitative proteomic approach to analyze how pro-inflammatory cytokines modulate the composition of the human MSC secretome. We found that pro-inflammatory cytokines have a strong impact on the secretome of human bone marrow-derived MSC and that the large majority of cytokine-induced proteins are involved in inflammation and/or angiogenesis. Comparative analyses with results recently obtained on mouse MSC secretome stimulated under the same conditions reveals both analogies and differences in the effect of pro-inflammatory cytokines on MSC secretome in the two organisms. In particular, functional analyses confirmed that tissue inhibitor of metalloproteinase-1 (TIMP1) is a key effector molecule responsible for the anti-angiogenic properties of both human and mouse MSC within an inflammatory microenvironment. Mass spectrometry data are available via ProteomeXchange with identifier PXD005746

Significance: The secretion of a broad range of bioactive molecules is believed to be the main mechanism by which MSC exert specific therapeutic effects. MSC are very versatile and respond to specific environments by producing and releasing a variety of effector molecules. To the best of our knowledge this is the first study aimed at describing the secretome of human MSC primed using a mixture of cytokines, to mimic pro-inflammatory conditions encountered in vivo, by a quantitative high-resolution mass spectrometry based approach. The main output of the study concerns the identification of a list of specific proteins involved in inflammation and angiogenesis which are overrepresented in stimulated MSC secretome. The data complement a previous study on the secretome of mouse MSC stimulated under the same conditions. Comparative analyses reveal analogies and differences in the biological processes affected by overrepresented proteins in the two organisms. In particular, the key role of TIMP-1 for the anti-angiogenic properties of stimulated MSC secretome already observed in mouse is confirmed in human. Overall, these studies represent key steps necessary to characterize the different biology of MSC in the two organisms and design successful pre-clinical experiments as well as clinical trials.

1. Introduction

Mesenchymal stem cells (MSC) are a heterogeneous population of adherent cells with a self-renewable capacity and with a wide distribution in an adult organism; indeed, they can be isolated from several adult tissues including bone marrow, adipose tissue, kidney and liver [1].

As multipotent progenitor cells, depending on the stimulus and the culture conditions employed, MSC are able to differentiate into various cell types, especially of the mesodermal lineage. The maintenance of stem cell subsets in adult tissues has been suggested as the physiological role of MSC, especially in the context of bone marrow. The localization of MSC in vivo indicates that they are fundamental components of the perivascular niche, controlling maintenance and trafficking of Hematopoietic Stem Cells (HSC) and immune cells [2].

* Correspondence to: A. Viola, Università di Padova, Dipartimento di Scienze Biomediche, Via Ugo Bassi, 58/b, 35131 Padova, Italy.
** Correspondence to: G. Tedeschi, Università degli Studi di Milano, Dipartimento di Medicina Veterinaria, via Celoria 10, 20133 Milano, Italy.
E-mail addresses: antonella.viola@unipd.it (A. Viola), gabriella.tedeschi@unimi.it (G. Tedeschi).

http://dx.doi.org/10.1016/j.jprot.2017.07.012
1874-3919/

Besides their physiological role, MSC represent an impressive opportunity in term of regenerative medicine and immunosuppressive therapy. Indeed, in vitro studies demonstrated the ability of MSC to inhibit proliferation and activation of a large number of immune cells such as T cells, B-cells, natural killer cells (NK) and dendritic cells (DC) [3]. The secretion of a broad range of bioactive molecules is now believed to be the main mechanism by which MSC exert specific effects [4]. Thus, it has become increasingly important to achieve a complete qualitative and quantitative characterization of MSC secretome by –omics approaches, as confirmed by the large number of recent studies aimed at characterizing the secretome of MSC primed under different conditions [5–18]. Indeed, several studies have demonstrated that MSC are very versatile and respond to the environment by producing and releasing a variety of effector molecules [19]. This is a crucial issue when considering MSC-based therapy, because the biological activity of the transplanted cells will be strongly influenced by the inflammatory status of the host [20]. In this regard, we have recently published a paper reporting the employment of a high-throughput proteomic approach to detect the specific proteins whose expression is modulated when mouse MSC (mMSC) are primed by pro-inflammatory cytokines [21]. The main result of our study was the observation that pro-inflammatory stimulation results in up-regulation in the mMSC secretome of a number of both pro- and anti-angiogenic proteins. Amongst the latter, TIMP-1 - an endogenous inhibitor of metalloproteinases - was pinpointed as a key factor for the anti-angiogenic and anti-inflammatory effects exerted by the stimulated mMSC [21].

Human MSC (hMSC) are currently being tested in a wide range of clinical settings, mainly in autoimmune diseases (multiple sclerosis, rheumatoid arthritis, Crohn's disease, etc.), graft-versus-host disease (GvHD), wound repair, ischaemia/stroke, liver diseases and HSC engraftment. Despite the large number of ongoing clinical trials, the demonstration of a beneficial effect from hMSC in large placebo-controlled trials remains elusive. In some cases, hMSC have even been reported to lead to the exacerbation of disease symptoms [22,23]. Amongst the reasons responsible for this inconsistency, there might be differences in the responses of mouse and human MSC to the inflammatory milieu. Indeed, pre-clinical experiments in mice that are based on the use of either human or mouse MSC have important limitations: when human cells are transplanted in the mouse, it is possible that some of the cross-talks between MSC and the host are impaired and that this may strongly affect the therapeutic effects of MSC transplantation; on the other hand, mMSC may have different biological properties than hMSC. Understanding the biology of human and mouse MSC is therefore necessary to design and perform successful pre-clinical experiments as well as clinical trials.

To the best of our knowledge, the present study reports for the first time a quantitative proteomic characterization of the secretome of human, bone marrow-derived MSC primed with pro-inflammatory cytokines. Proteomic analyses were conducted under exactly the same conditions used in our previous investigation on mMSC in order to avoid variations with methodology, allowing direct comparative analysis between the results obtained with the two organisms.

2. Material and methods

2.1. Isolation of mMSC

mMSC were isolated as described [21] by flushing the femurs and tibias from 8 week-old, C57Bl/6N female mice and cultured in 25 cm^2 tissue culture flasks at a concentration of 2×10^6 cells/cm^2 using complete Dulbecco modified Eagle medium low glucose (DMEM, Lonza, Braine-L'Alleud, Belgium) supplemented with 20% heat inactivated fetal bovine serum (Biosera, Ringmer, United Kingdom), 2 mM glutamine (Lonza), 100 U/mL penicillin/streptomycin (Lonza). Cells were incubated at 37 °C in 5% CO_2. After 48 h, the non-adherent cells were removed. After reaching 70–80% confluence, the adherent cells were trypsinized (0.05% trypsin at 37 °C for 3 min), harvested and expanded in larger flasks. MSC at passage 10 were screened by flow cytometry for the expression of CD106, CD45, CD117, CD73, CD105, MHC-I, SCA-1 and CD11b and used to perform experiments (BD Pharmingen, Oxford, UK).

2.2. Collection of conditioned medium (CM) of mMSC

mMSC were plated as described [21] and let grow until confluence in ventilated cap flask. Growth medium was substituted with DMEM low glucose supplemented with 10% FBS, 2 mM glutamine, 100 U/mL penicillin/streptomycin, with (st mMSC) or without (unst mMSC) 25 ng/mL mIL1b, 20 ng/mL mIL6, 25 ng/mL mTNFa for 24 h. After three washes in DMEM low glucose, the medium was changed with DMEM low glucose supplemented with 2 mM glutamine, 100 U/mL penicillin/streptomycin for the following 18 h. Conditioned medium was harvested and centrifuged at 4000 rpm for 10 min.

2.3. Isolation of hMSC

hMSC were provided by Orbsen Therapeutics Ltd. (Galway, Ireland). Ethical approvals are granted from the NUIG Research Ethics Committee and the Galway University Hospitals Clinical Research Ethics Committee (CREC). Briefly, bone marrow was harvested from volunteers, and the cell culture was set up as previously described [24]. hMSC were characterized according to international guidelines [25]. All samples were obtained with informed consent. Procurement of the sample conformed to European Parliament and Council directives (2001/20/EC; 2004/23/EC).

2.4. Collection of conditioned medium (CM) of hMSC

hMSC were plated in with MEM Alpha with Glutamax supplemented with 10% FBS, 2 mM glutamine, 100 U/mL penicillin/streptomycin and let grow until confluence in in a humidified incubator with 5% CO_2 and 37 °C. At the moment of the confluence, medium was substituted with MEM Alpha with Glutamax supplemented with 2% FBS, 2 mM glutamine, 100 U/mL penicillin/streptomycin, with (st hMSC) or without (unst hMSC) 25 ng/mL hIL1b, 20 ng/mL hIL6, 25 ng/mL hTNFa. 24 h later, after three washes in MEM Alpha with Glutamax, the medium was changed with MEM Alpha with Glutamax supplemented with 2 mM glutamine, 100 U/mL penicillin/streptomycin for the following 18 h. Conditioned medium was harvested and centrifuged at 4000 rpm for 10 min.

2.5. Endothelial cell lines

SVEC4-10 (ATCC #CRL-2181 Manassas, VA), an endothelial cell line from murine axillary lymph nodes, was cultured in a humidified incubator with 5% CO_2 and 37 °C, in DMEM (ATCC 30-2002 Manassas, VA) supplemented with 10% heat-inactivated FBS, 1% penicillin and streptomycin.

Human Umbilical Vein Endothelial Cells (HUVEC, Lonza C2519A) were cultured in a humidified incubator with 5% CO_2 and 37 °C with EBM-2 Basal Medium supplemented by EGM-2 BulletKit (CC-3156 & CC-4176). All the plastics used for HUVEC culture were pre-coated with 0.2% gelatin in H_2O (37 °C for at least 2 h). Cells were subcultured using 0.05% trypsin, 0.02% EDTA solution.

2.6. Tube formation assay SVEC4-10

Matrigel Matrix (Corning) was thawed overnight at 4 °C. Tips and 96-well plates flat bottom were pre-chilled overnight before performing the experiment. The day of the assay, 80 μL of Matrigel were seeded in the 96-well plate and left to polymerize at 37 °C, 5% CO_2 for at least 30 min. 1.5×10^4 SVEC4-10 were first suspended in 100 μL of MSC-CM, supplemented with 10% FBS, alone or with anti-TIMP-1 (AF980 R&D) at the final concentration of 5 μg/mL, and then

seeded on the solidified matrix. The formation of the tube networks develops in 4 h at 37 °C 10% CO_2. DMEM low glucose supplemented with 10% heat-inactivated FBS were used as positive control. At the end of the incubation, cell tubes were imaged with a phase contrast inverted microscope at 4× objective magnifications and analysis was performed with ImageJ Angiogenesis Analyzer.

2.7. Tube formation assay HUVEC

Matrigel Matrix (Corning) was thawed overnight at 4 °C. The day of the assay, 100 μL of Matrigel were seeded in the 96-well plate and left to polymerize at 37 °C, 5% CO_2 for at least 30 min. 2×10^4 HUVEC were first suspended in 100 μl of hMSC-CM, supplemented with 10% FBS, alone or with anti-TIMP-1 (AF970 R&D) at the final concentration of 5 μg/mL, and then seeded on the solidified matrix. The formation of the tube networks develops in 4 h at 37 °C 10% CO_2. MEMalpha supplemented with 10% heat-inactivated FBS were used as positive control. At the end of the incubation, cell tubes were imaged with a phase contrast inverted microscope at 4× objective magnifications and analysis was performed with ImageJ Angiogenesis Analyzer.

2.8. Isolation and differentiation of mouse bone marrow–derived monocytes

Bone marrow cell suspensions were obtained by flushing femurs and tibias of 8- to 12-week-old C57Bl/6N mice (Charles River; Sulzfeld, Germany) with complete DMEM low Glucose supplemented with 10% FCS, 1% Pen/Strep and 1% L-glutamine. Possible cellular aggregates were removed by pipetting and red cells were eliminated through ACK lysis buffer (10-548E, Lonza). Cells were washed twice with medium, seeded on 24-well plates (Corning Costar; Schiphol-Rijk, The Netherlands) at the concentration of 10^6 cells/mL and maintained in a humidified incubator with 5% CO_2 and 37 °C.

Cells were supplemented with 20 ng/mL mM-CSF as positive control, or cultured in mMSC-CM supplemented with 10% FBS. MSC-CM and mM-CSF were replaced three days later. Cells were harvested five days later by gentle pipetting and repeated washing with phosphate buffered saline (PBS), and 2 mM EDTA. Monocytes differentiation was analysed by flow cytometry.

2.9. Isolation and differentiation human blood-derived monocyte

Peripheral Blood Monocyte Cells (PBMCs) from healthy donors were isolated by centrifugation on Ficoll-Paque solution and placed on Percoll 46% vol/vol solution (Amersham Biosciences) in RPMI 1640–10% FCS and 4 mM. Monocytes were harvested, resuspended in medium–2% FCS, and let to adhere to plastic (1 h at 37 °C) in order to eliminate contaminating lymphocytes. For macrophage differentiation, 3×10^5 monocytes were seeded in 24-well plates with MEMalpha supplemented with 20% FBS in the presence of 100 ng/mL h-M-CSF as positive control, or they were cultured in hMSC-CM plus 20% FBS. After five days of differentiation, monocyte-derived macrophages were analysed by flow cytometry using CD14 staining.

2.10. Flow Cytometry analysis

The expression of macrophage surface markers was evaluated by Flow Cytometry analysis. Briefly, cells were washed and stained in PBS supplemented with 2% fetal calf serum. After 20 min of incubation at 4 °C with Purified Rat Anti-Mouse CD16/CD32 (Mouse BD Fc Block™ 553142), fluorescent antibodies were diluted in PBS supplemented with 2% fetal calf serum, to identify mouse macrophages (CD11b:PeCy7 BD 552850 and F4/80:Alexa Fluor® 488 BioRad MCA497F) and human macrophages (CD14: PE R&D FAB3832P). Cell viability was assessed with the Live/Dead Fixable Aqua Dead Cell Stain Kit (Invitrogen), following the manufacturer's instructions. After the final wash, cells were fixed in 1% paraformaldehyde and acquired with the BD FACSCanto™ II system. Post-analysis of flow cytometry data was performed using FlowJo™ software (Tree Star Inc.).

2.11. ELISA-assay

To detect M-CSF and TIMP-1 concentration in MSC-CM, ELISA assays were performed following the manufacturer's instruction (for human, M-CSF DuoSet ELISA DY216 and TIMP-1 DuoSet ELISA DY970; for mouse, M-CSF DuoSet ELISA DY416 and TIMP-1 DuoSet ELISA DY980).

2.12. LC-ESI MS/MS analysis

Five technical replicas, including steps for sample preparation and mass spectrometric analysis, were performed for each sample (st hMSC-CM from patient H30, unst hMSC-CM from patient H30, st hMSC-CM from patient H34, unst hMSC-CM from patient H34).

Proteomic analyses were performed as described [21]. Briefly, proteins were precipitated with 10% tricholoracetic acid for 2 h on ice, reduced, carbamydomethylated and digested with trypsin sequence grade trypsin (Roche) for 16 h at 37 °C using a protein:trypsin ratio of 50:1. Nano LC-ESI-MS/MS analysis was performed on a Dionex UltiMate 3000 HPLC System with a PicoFrit ProteoPrep C18 column (200 mm, internal diameter of 75 μm) (New Objective, USA) Gradient:1% ACN in 0.1% formic acid for 10 min, 1–4% ACN in 0.1% formic acid for 6 min, 4–30% ACN in 0.1% formic acid for 147 min and 30–50% ACN in 0.1% formic for 3 min at a flow rate of 0.3 μL/min. The eluate was electrosprayed into an LTQ Orbitrap Velos (Thermo Fisher Scientific, Bremen, Germany) through a Proxeon nanoelectrospray ion source (Thermo Fisher Scientific). The LTQ-Orbitrap was operated in positive mode in data-dependent acquisition mode to automatically alternate between a full scan (m/z 350–2000) in the Orbitrap (at resolution 60,000, AGC target 1,000,000) and subsequent CID MS/MS in the linear ion trap of the 20 most intense peaks from full scan (normalized collision energy of 35%, 10 ms activation). Isolation window: 3 Da, unassigned charge states: rejected, charge state 1: rejected, charge states 2+, 3+, 4+: not rejected; dynamic exclusion enabled (60 s, exclusion list size: 200). Data acquisition was controlled by Xcalibur 2.0 and Tune 2.4 software (Thermo Fisher Scientific).

Mass spectra were analysed using MaxQuant software (version 1.3.0.5) [26]. The initial maximum allowed mass deviation was set to 6 ppm for monoisotopic precursor ions and 0.5 Da for MS/MS peaks. Enzyme specificity was set to trypsin, defined as C-terminal to arginine and lysine excluding proline, and a maximum of two missed cleavages were allowed. Carbamidomethylcysteine was set as a fixed modification, N-terminal acetylation and methionine oxidation as variable modifications. The spectra were searched by the Andromeda search engine against the human UniProt sequence database (release 2014_01). Protein identification required at least one unique or razor peptide per protein group. Quantification in MaxQuant was performed using the built in XIC-based label free quantification (LFQ) algorithm [27] using fast LFQ. The required false positive rate was set to 1% at the peptide and 1% at the protein level, and the minimum required peptide length was set to 6 amino acids.

2.13. Statistical and bioinformatics analyses

Statistical analyses were performed using the Perseus software (version 1.4.0.6 [28]). Only proteins present and quantified in at least 3 out of 5 technical repeats were considered as positively identified in a sample (st hMSC-CM from patient H30, unst hMSC-CM from patient H30, st hMSC-CM from patient H34, unst hMSC-CM from patient H34). t-Test analysis of stimulated versus unstimulated technical replicas were conducted separately for samples from the two patients. Comparing the results obtained in the two analyses, proteins were considered differentially expressed in stimulated samples if they were present

Table 1
Proteins overrepresented or present only in st hMSC-CM.

Gene names	Protein names	Protein	H30		H34		Angiogenesis[b]	Inflammation[b]
		ID	-Log P *t*-test	*t*-Test Diff[a]	-Log P *t*-test	*t*-Test Diff[a]		
ABI3BP	Target of Nesh-SH3	D3YTG3	Only in stimulated					
AGRN	Agrin	O00468	5.339	2.799	3.970	1.066	x	x
ALCAM	CD166 antigen	Q13740	Only in stimulated				x	x
ARHGAP1	Rho GTPase-activating protein 1	Q07960	Only in stimulated					
BMP1	Bone morphogenetic protein 1	P13497	3.745	1.175	4.642	0.751	x	x
C1R	Complement C1r subcomponent	P00736	8.619	2.624	6.801	2.132		x
C1S	Complement C1s subcomponent	P09871	6.886	1.883	6.503	1.992		x
C3	Complement C3	P01024	10.267	7.920	5.001	4.683	x	x
CA12	Carbonic anhydrase 12	O43570	Only in stimulated				x	x
CCL2	C-C motif chemokine 2	P13500	9.381	6.120	10.273	9.600	x	x
CDC37	Hsp90 co-chaperone Cdc37	Q16543	Only in stimulated					x
CFB	Complement factor B	B4E1Z4	Only in stimulated				x	x
CFH	Complement factor H	P08603	5.941	2.293	6.526	2.405		x
CHI3L1	Chitinase-3-like protein 1	P36222	6.932	1.415	6.918	1.353	x	x
CLSTN1	Calsyntenin-1	O94985	4.674	0.615	3.190	0.932		
COL16A1	Collagen alpha-1(XVI) chain	A6NDR9	5.166	1.459	4.026	1.439		x
COL3A1	Collagen alpha-1(III) chain	P02461	7.283	0.588	10.347	1.865		x
COL5A2	Collagen alpha-2(V) chain	P05997	1.555	0.170	7.749	1.353		
COL7A1	Collagen alpha-1(VII) chain	Q02388	5.682	2.193	2.828	0.961		x
CSF1	Macrophage colony-stimulating factor 1	P09603	Only in stimulated				x	x
CTHRC1	Collagen triple helix repeat-cont prot 1	Q96CG8	5.339	1.314	4.189	1.134	x	
CTSB	Cathepsin B	P07858	3.149	0.636	5.472	1.500	x	x
CXCL1	Growth-regulated alpha protein	P09341	Only in stimulated				x	x
CXCL12	Stromal cell-derived factor 1	P48061	5.665	2.429	1.652	0.470	x	x
CXCL5	C-X-C motif chemokine 5	P42830	Only in stimulated				x	x
CXCL6	C-X-C motif chemokine 6	P80162	Only in stimulated				x	x
CYR61	Protein CYR61	O00622	Only in stimulated				x	x
DCN	Decorin	P07585	5.699	0.835	5.760	1.253	x	x
EFEMP2	EGF-cont fibulin-like extrac matrix prot 2	O95967	3.013	1.193	5.790	1.640		x
EIF6	Eukaryotic translation initiation factor 6	P56537	Only in stimulated				x	x
ELN	Elastin	F8WAH6	4.693	1.332	5.715	2.206	x	x
EXT1	Exostosin-1	Q16394	3.775	1.085	2.266	0.485		
EXT2	Exostosin-2	Q93063	Only in stimulated					
FBLN1	Fibulin-1	P23142	4.242	0.867	6.450	1.323	x	
FBN1	Fibrillin-1	P35555	6.035	0.969	6.557	1.909	x	x
FKBP1A	Peptidyl-prolyl cis trans isomerase	P62942	Only in stimulated					x
FN1	Fibronectin	P02751	5.787	0.793	5.421	0.358	x	x
FNDC1	Fibronectin type III domain-cont prot 1	Q4ZHG4	5.245	2.301	7.588	1.418	x	x
FSTL1	Follistatin-related protein 1	Q12841	3.823	0.817	7.039	1.968	x	x
GALNT2	Polypeptide *N*-acetylgalactosaminyltransferase 2	Q10471	2.914	0.542	2.860	0.895	x	
GBP1	Interferon-induced guanylate-binding prot 1	P32455	Only in stimulated				x	x
GC	Vitamin D-binding protein	P02774	Only in stimulated					x
HLA-A	HLA class I histocompatibility antigen, A-24 alpha chain	P05534	5.130	1.393	3.813	1.312		x
HLA-C	HLA class I histocompatibility antigen, Cw-7 alpha chain	A2AEA2	3.071	1.381	3.304	1.231		x
HSPG2	Base membr-spec hepar sulf proteoglycan core prot	P98160	8.735	1.796	9.468	2.141	x	x
HYOU1	Hypoxia up-regulated prot 1	Q9Y4L1	Only in stimulated				x	x
ICAM1	Intercellular adhesion molecule 1	P05362	Only in stimulated				x	x
IGFBP4	Insulin-like growth factor-binding prot 4	P22692	4.346	1.526	3.986	1.009	x	x
IGFBP6	Insulin-like growth factor-binding prot 6	P24592	Only in stimulated				x	x
IGFBP7	Insulin-like growth factor-binding prot 7	Q16270	2.725	0.397	4.650	0.947	x	x
IL6	Interleukin-6	P05231	Only in stimulated				x	x
IL8	Interleukin-8	P10145	Only in stimulated				x	x
INHBA	Inhibin beta A chain	P08476	7.879	3.140	5.875	1.448	x	
ITIH2	Inter-alpha-trypsin inhibitor heavy chain H2	P19823	3.742	1.104	1.276	0.382		x
ITM2B	Integral membrane protein 2B;BRI2	Q9Y287	3.573	1.994	5.351	1.035		
KRT6B	Keratin, type II cytoskeletal 6B	P04259	Only in stimulated					
LAMA4	Laminin subunit alpha-4	Q16363	2.027	0.234	1.925	0.173	x	
LAMB2	Laminin subunit beta-2	P55268	5.174	3.708	4.936	1.006		
LEPRE1	Prolyl 3-hydroxylase 1	Q32P28	Only in stimulated				x	x
LGALS3BP	Galectin-3-binding protein	Q08380	8.011	1.487	6.749	1.314	x	x
LOXL2	Lysyl oxidase homolog 2	Q9Y4K0	6.219	1.195	5.732	1.521	x	x
LYZ	Lysozyme C	P61626	3.547	0.507	1.328	0.607		x
MAN1A1	Mannosyl-oligosaccharide 1,2-alpha-mannosidase IA	P33908	Only in stimulated				x	x
MANBA	Beta-mannosidase	O00462	Only in stimulated					
MMP1	Interstitial collagenase	P03956	Only in stimulated				x	x
MMP10	Stromelysin-2	P09238	Only in stimulated				x	x
MMP13	Collagenase 3	G5E971	Only in stimulated				x	x
MMP2	72 kDa type IV collagenase	P08253	6.555	1.090	7.061	1.043	x	x
MMP3	Stromelysin-1	P08254	Only in stimulated				x	x
NID1	Nidogen-1	P14543	3.840	0.925	3.450	0.890	x	x
NID2	Nidogen-2	Q14112	4.384	1.133	3.823	0.855		
NUCB1	Nucleobindin-1	Q02818	5.878	0.985	3.867	0.703		
PLOD1	Procollagen-lysine,2-oxoglutarate 5-dioxygenase 1	B4DR87	3.944	0.876	2.180	0.264		
PLOD2	Procollagen-lysine,2-oxoglutarate 5-dioxygenase 2	O00469	5.967	2.636	5.402	2.331	x	

Table 1 (*continued*)

Gene names	Protein names	Protein	H30		H34		Angiogenesis[b]	Inflammation[b]
		ID	-Log P *t*-test	*t*-Test Diff[a]	-Log P *t*-test	*t*-Test Diff[a]		
PSMA5	Proteasome subunit alpha type-5	P28066	Only in stimulated					
PSME2	Proteasome activator complex subunit 2	Q9UL46	Only in stimulated					
PTX3	Pentraxin-related protein PTX3	P26022	7.000	3.580	8.516	3.256	x	x
PXDN	Peroxidasin homolog	Q92626	6.359	1.401	5.119	1.122		
QPCT	Glutaminyl-peptide cyclotransferase	Q16769	3.070	1.972	4.593	2.140		x
QSOX1	Sulfhydryl oxidase 1	O00391	5.232	1.616	9.152	2.155	x	
RNASE4	Ribonuclease 4	P34096	Only in stimulated				x	x
SDC4	Syndecan-4	P31431	1.696	0.810	3.199	1.321	x	x
SDF4	45 kDa calcium-binding prot	Q9BRK5	2.014	0.353	3.547	0.862	x	
SERPINB2	Plasminogen activator inhibitor 2	P05120	Only in stimulated					x
SERPINE1	Plasminogen activator inhibitor 1	P05121	8.172	2.596	6.111	1.557	x	x
SLC39A14	Zinc transporter ZIP14	Q15043	Only in stimulated					
SLC3A2	4F2 cell-surface antigen heavy chain	P08195	Only in stimulated					
SOD2	Superoxide dismutase [Mn]	P04179	Only in stimulated				x	x
SRGN	Serglycin	P10124	5.249	1.412	3.353	1.084	x	
SRPX2	Sushi repeat-containing prot SRPX2	O60687	7.209	2.708	3.423	2.482	x	x
SSB	Lupus La protein	P05455	Only in stimulated					
STC2	Stanniocalcin-2	O76061	Only in stimulated				x	
TIMP1	Metalloproteinase inhibitor 1	P01033	2.940	1.254	5.763	1.081	x	x
TNC	Tenascin	P24821	6.040	1.645	7.257	1.329	x	x
TNFAIP6	Tumor necrosis factor-inducible gene 6 protein	P98066	Only in stimulated					x
VCAM1	Vascular cell adhesion protein 1	P19320	5.307	3.003	5.227	2.623	x	x

[a] *t*-Test diff: difference of log(2) mean intensity of a protein in technical replicas of st- versus unst hMSC-CM from *t*-test analysis using Perseus [28] as detailed in the text.
[b] Proteins related to angiogenesis or inflammation according to criteria detailed in "Materials and methods".

only in st- or in unst- hMSC-CM or showed significant *t*-test p-value (cut-off at 1% permutation-based False Discovery Rate) in both patients.

Proteins listed in Tables 1 and 2 and Supplemental Table 2 were considered secreted or involved in inflammation/angiogenesis according to the following databases/datasets: Gene Ontology [29], NextProt [30], UniProt [31], Gene Cards [32], datasets [6,8] and manual literature mining. Bioinformatic analyses were carried out by DAVID software (release 6.7) [33]. GOBP and groups were filtered for significant terms (modified Fisher exact EASE score p value <0.05 and at least five counts). Networks of up-regulated proteins in st hMSC-CM involved in inflammation or angiogenesis was performed using String [34] (active interactions: text mining, experiments, databases).

The mass spectrometry proteomics data have been deposited to the ProteomeXchange Consortium via the PRIDE [35] partner repository with the dataset identifier PXD005746.

Table 2
Proteins overrepresented or present only in st MSC-CM common to mouse and human.

Gene names	Protein names	Angiogenesis[a]	Infflammation[a]
AGRN	Agrin	x	x
C1R	Complement C1r subcomponent		x
C1S	Complement C1s subcomponent		x
C3	Complement C3	x	x
CSF1	Macrophage colony-stimulating factor 1	x	x
CTSB	Cathepsin B	x	x
CXCL1	Growth-regulated alpha protein	x	x
CXCL5	C-X-C motif chemokine 5	x	x
EXT1	Exostosin-1		
EXT2	Exostosin-2		
FSTL1	Follistatin-related protein 1	x	x
HSPG2	Basem membr-spec heparan sulfate proteoglycan core prot	x	x
IGFBP7	Insulin-like growth factor-binding protein 7	x	x
IL6	Interleukin-6	x	x
LAMB2	Laminin subunit beta-2		
LGALS3BP	Galectin-3-binding protein	x	x
MMP13	Collagenase 3	x	x
NID1	Nidogen-1	x	x
PLOD2	Procollagen-lysine,2-oxoglutarate 5-dioxygenase 2	x	
SERPINE1	Plasminogen activator inhibitor 1	x	x
TIMP1	Metalloproteinase inhibitor 1	x	x
TNC	Tenascin	x	x
VCAM1	Vascular cell adhesion protein 1	x	x

[a] Proteins involved in angiogenesis or inflammation in both organisms according to criteria detailed in "Materials and methods".

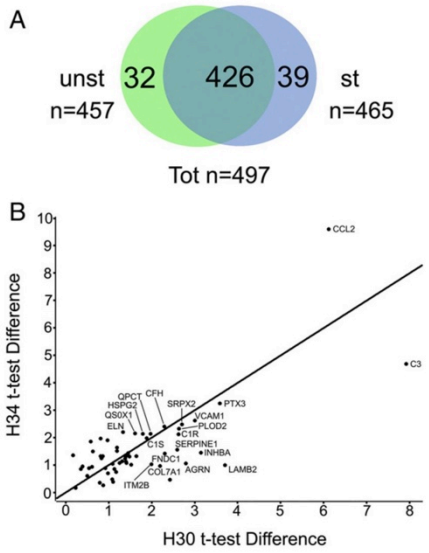

Fig. 1. Summary of the results obtained in the proteomic characterization of hMSC-CM. A. Venn diagram showing proteins detected in at least 3 out of 5 technical replicas in both patients only in stimulated hMSC-MC or unstimulated hMSC-CM or in both; B. *t*-test difference (difference of log(2) mean intensity of a protein in stimulated and unstimulated hMSC-CM replicas, [28]) observed in the two patients for the 57 proteins present in stimulated and unstimulated hMSC-MC and significantly overrepresented in stimulated hMSC-MC according to *t*-test p-value (cut-off at 1% permutation-based False Discovery Rate). Pearson correlation coefficient $R = 0.73$. Complete protein identities and detailed values are reported in Table 1.

3. Results and discussion

3.1. Proteomic characterization of hMSC secretome

Fig. 1 summarizes the results of the proteomic characterization of secretome of hMSC before and after stimulation with inflammatory cytokines; 497 proteins were present in at least 3 out of 5 technical replicas in at least one stimulation condition (stimulated or unstimulated) in both patients (donors H30 and H34). These proteins are listed in Supplemental Table 1, together with their main identification parameters. Fig. 1A highlights the number of proteins detected in stimulated human MSC conditioned medium (st hMSC-CM) and unstimulated human MSC conditioned medium (unst hMSC-CM). Amongst the 465 proteins identified in st hMSC-CM (proteins in groups 1, 2, 4 and 5 of Supplemental Table 1), 133 are listed as cytokine or chemokine or functionally related to these classes of compounds according to the NextProt database [30].

3.2. Proteins up-regulated in stimulated hMSC-CM

Since MSC enhance their therapeutic efficacy following priming by cytokines [36,37], analyses were focused on proteins overrepresented or present only in st hMSC compared to unst hMSC secretome; 39 proteins are present only in st hMSC-CM, while 426 are common to stimulated and unstimulated hMSC-CM (Fig. 1A); statistical analysis of the common proteins indicates that 57 proteins are overrepresented in st hMSC-CM (according to *t*-test p-value, cut-off at 1% permutation-based False Discovery Rate). Overall, 96 proteins are up-regulated or present only in st hMSC-CM in both patients (Table 1, which reports the *t*-test p-values and *t*-test difference for each protein in each patient). Fig. 1B, showing the *t*-test differences calculated for each patient for the 57 up-regulated proteins present in both st- and unst-hMSC-CM, allows detecting proteins showing highest increase in abundance in stimulated versus unstimulated hMSC-CM in each patient. A Pearson correlation coefficient $R = 0.73$ was calculated from data in Fig. 1B.

All proteins listed in Table 1 are predicted to be potentially secreted/extracellular/included in exosomes according to annotations in Gene Ontology [29] or NextProt [30] or UniProt [31] or Gene Cards [32]) or in datasets [6,8] or from manual literature mining.

70% and 64% of up-regulated proteins in st hMSC-CM are involved in inflammation or angiogenesis, respectively (Table 1). The extended network of interactions amongst inflammation- or angiogenesis-related proteins up-regulated in st hMSC-CM according to available experimental evidence, database and literature information is shown in Fig. 2. A number of proteases (BMP1, C1R, C1S, CFB, CTSB, MMP1, MMP2, MMP3, MMP10 MMP13, PSMA5, PSME2, QPCT) and protease inhibitors (C3, COL7A1, FBLN1, FN1INHBA, ITIH2, SERPINB2, SERPINE1, TIMP1) are up-regulated in st hMSC secretome, strengthening our suggestion that a fine but complex tuning of proteolytic activity is a key mechanism regulating MSC effects on angiogenesis and tissue remodeling [21]. In particular, MMPs are presently considered not only effectors but also regulators of a number of biological processes since they can activate, inactivate or antagonize the biological functions of growth factors, cytokines and chemokines by proteolytic processing and thus either promote or suppress inflammation and angiogenesis [38,39]. Notably several protease/protease inhibitors

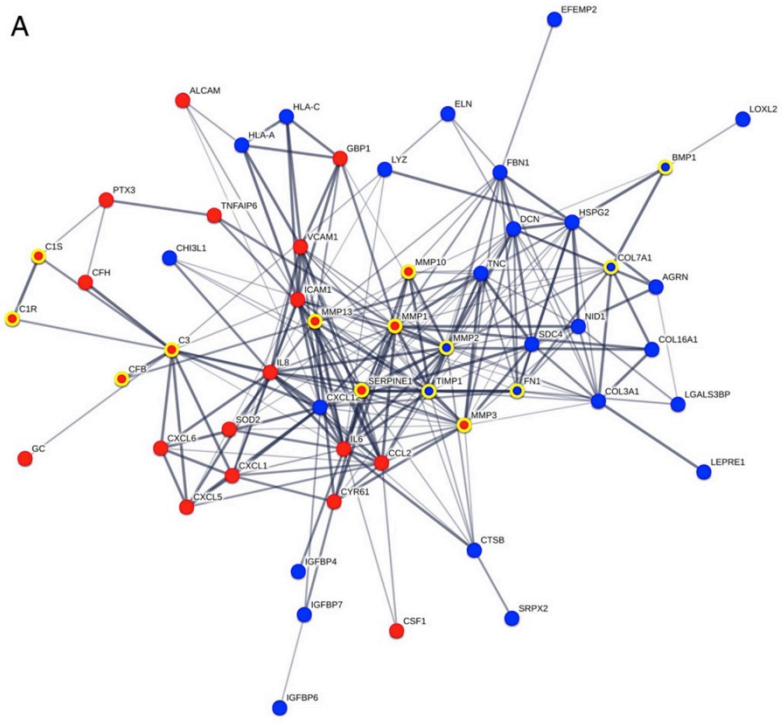

Fig. 2. Network interactions of overrepresented proteins in stimulated hMSC-CM involved in inflammation or in angiogenesis. Overrepresented proteins in stimulated hMSC-CM involved in inflammation (A) or angiogenesis (B), respectively, according to targeted accurate literature mining as reported in Table 1, have been searched for possible interactions using String [34]. Active interactions: text mining, experiments, databases; edges thickness indicates "confidence". Red symbols: proteins present only in stimulated hMSC secretome or showing high *t*-test difference according to Fig. 1B. Yellow edges indicate proteins with proteases/protease inhibitors activity.

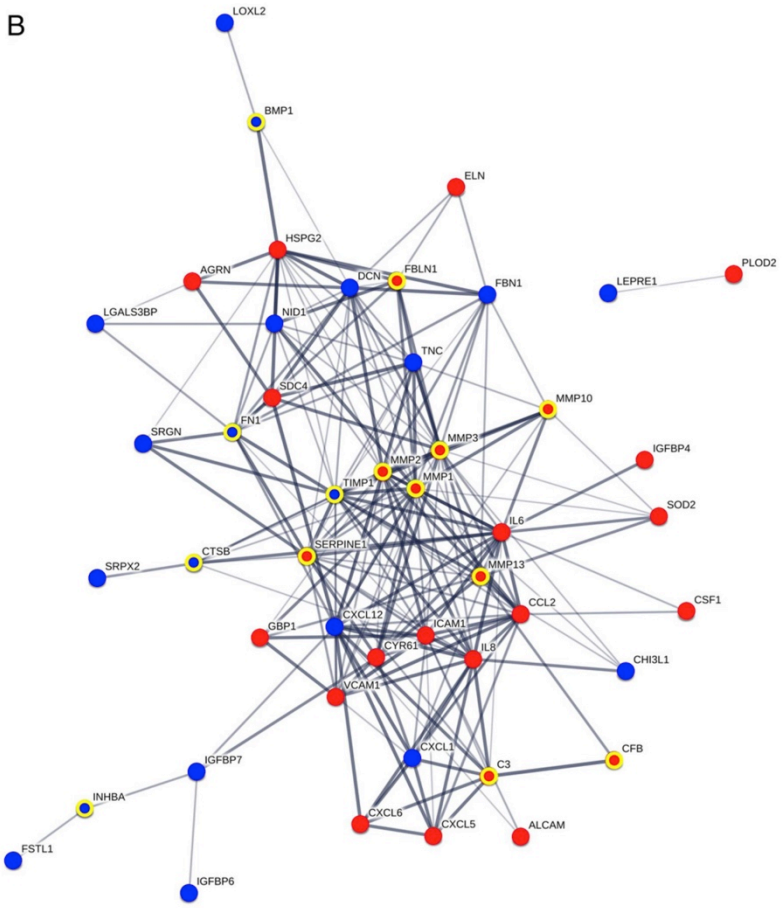

Fig. 2 (*continued*).

listed above are amongst the proteins showing large quantitative differences in stimulated vs unstimulated hMSC-CM (Table 1, Figs. 1B and 2).

Since it has been established that tissue origin, growth and stimulation conditions may influence the type and quantity of proteic components of MSC secretome [16], we compared the list of up-regulated proteins in st hMSC-CM with those reported in recent studies performed using a similar mass spectrometry based quantitative proteomic approach on human MSC. Supplemental Table 2 confirms that different stimulation conditions lead to up-regulation of largely different sets of proteins. Notably, 24 proteins (25%, highlighted in Supplemental Table 2) detected as up-regulated in our study were overrepresented also in the secretome of MSC deriving from a different adult tissue (adipose tissue) stimulated with TNF-α [11]. This finding provides new experimental evidences at the molecular level supporting the notion that the type of stimulus has a major influence on MSC secretome. As expected, considering the stimulating agent, 22 out of 24 common overrepresented proteins are related to inflammation and/or angiogenesis (Supplemental Table 2).

3.3. Proteomic based comparison between mouse and human MSC-CM

In our previous work, we took advantage of animal models to elucidate the molecular pathway involved in effects of mMSC on the complex crosstalk between inflammation and angiogenesis [21]. Because it is widely accepted that significant differences exist between mouse and human MSC [36,40], and because of the tremendous relevance of inflammation-induced angiogenesis in human diseases, we focused our attention on comparing mouse and human MSC secretome. The proteomic results of the present study were therefore compared with those reported for mMSC-CM [21]. Supplemental Table 1 lists the 286 proteins (out of 465, 62%) present in st hMSC-CM that have been detected also in st mMSC-CM. The number of proteins significantly up-regulated or present only in the secretome of stimulated MSC is similar in the two species: 89 in mouse (Table S2 of [21]), 96 in human (Table 1). A comparative analysis of GO_BP category enrichment of overrepresented proteins in human and/or mouse (Fig. 3) suggests that: a) proteins up-regulated in the secretome of stimulated MSC from both organisms are, for the most part, involved in similar biological processes, mainly related to defense, immune and inflammatory response, chemotaxis and extracellular matrix remodeling; b) however there are clear important differences amongst human and mouse. Thus, only st mMSC-CM is enriched in proteins involved in chromatin structure assembly, cell proliferation regulation and related processes. On the contrary, complement activation, leukocyte migration, bone development and metabolic processes specifically related to collagen are

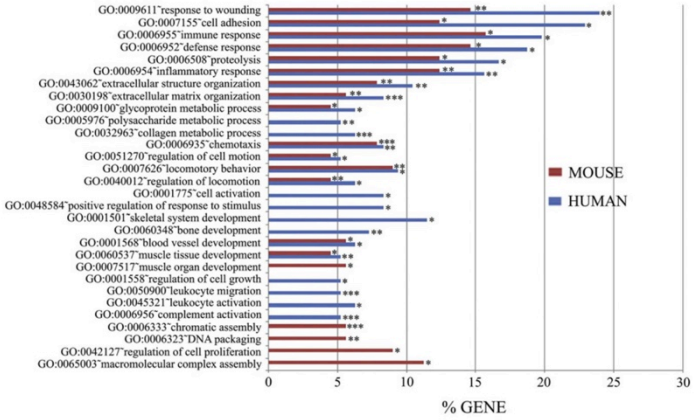

Fig. 3. Distribution into biological processes of the proteins overrepresented in stimulated hMSC-CM in human and mouse. The proteins that were significantly up-regulated or present only in stimulated MSC-CM (Table 1 and [21]) were classified into different biological processes according to the Gene Ontology classification system (GOBP) using DAVID software [33]; confidence level: medium; only categories showing modified Fisher exact EASE score p value < 0.05 and at least 5 counts in hMSC are represented. The bars represent the percentage of proteins involved in a category out of the total number of overrepresented proteins in human (96) or mouse (89) secretome. Asterisks indicate fold enrichment range for each category: * 1–5, ** 6–10, *** >10.

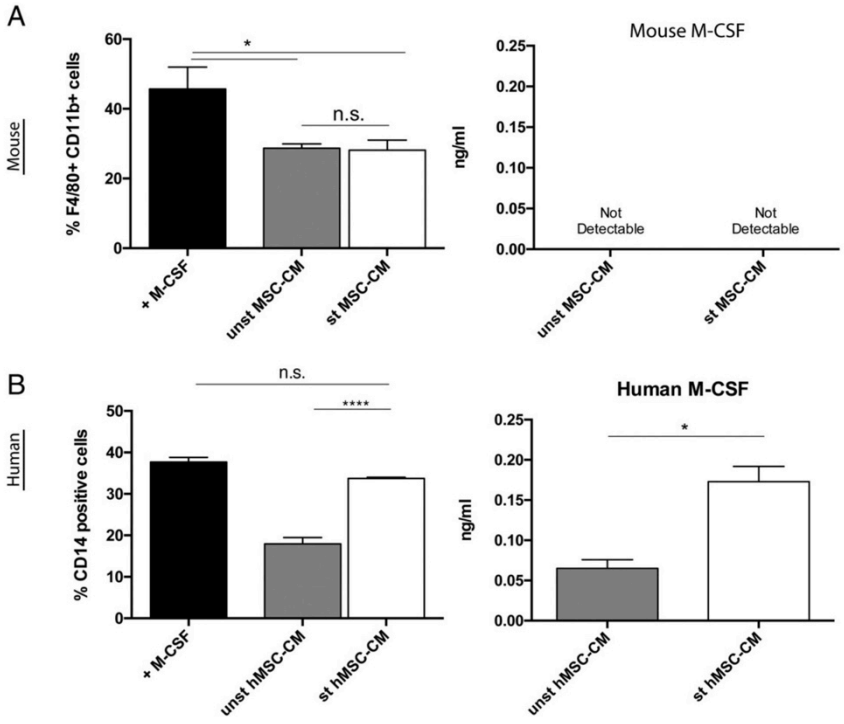

Fig. 4. Human and mouse MSC conditioned media differentially stimulate monocytes differentiation. A) Mouse bone marrow cells were cultured with murine M-CSF (as positive control), unstimulated or stimulated mouse MSC-CM for 5 days. Differentiation to macrophages was assessed by Flow Cytometry as percentage of F4/80 + CD11b + cells. Right panel: mouse M-CSF concentration in conditioned media was analysed by ELISA. Undetectable cytokine levels were reported for both preparations. B) Human PBMCs were cultured with human M-CSF (as positive control), unstimulated or stimulated human MSC-CM for 5 days. Macrophages were analysed by Flow Cytometry as CD14+ cells. Right panel: human M-CSF quantification by ELISA assay shows higher cytokine levels in st hMSC-CM than unst hMSC-CM. A and B, left panels: 3 independent experiments, data are expressed as mean ± SEM (*$p < 0.05$, ****$p < 0.0001$, One way ANOVA). A and B, right panels: 2 independent experiments, data are expressed as mean ± SEM (*$p < 0.05$, parametric *t*-test).

amongst the statistically enriched GO functional categories in human but not in mouse.

Such differences are confirmed by the observation that only 23 proteins are up-regulated or present only in stimulated MSC-CM both in mouse and human (Table 2); this again points to a fine species-related tuning of the overall effects of secretome from the two organisms; interestingly, our analysis indicates that 74% and 83% of the common up-regulated proteins are associated with angiogenesis or inflammation, respectively.

3.4. Functional evidence of human and mouse MSC secretome similarities or differences

Our proteomic results indicate that the majority of secreted proteins from both human and mouse MSC are associated with inflammation and angiogenesis (Table 1 and [21]). To identify specific functional analogies or differences of human and mouse MSC in the regulation of these two important processes, we focused on two proteins, M-SCF/CSF1 and TIMP1, which are present in st MSC-CM of both species and play a key role in immunity/inflammation and angiogenesis, respectively [41,42].

3.4.1. Macrophage colony-stimulating factor (M-CSF)

M-CSF is a growth factor secreted by a large variety of cells including macrophages, endothelial cells, fibroblast and lymphocytes. By interacting with its membrane receptor (CSF1R or M-CSF-R), it stimulates the survival, proliferation, and differentiation of monocytes and macrophages [43–45]. Our proteomic data indicated that M-CSF (CSF1) is up-regulated in the secretome of both human and mouse MSC upon stimulation by inflammatory cytokines (Tables 1 and 2 and

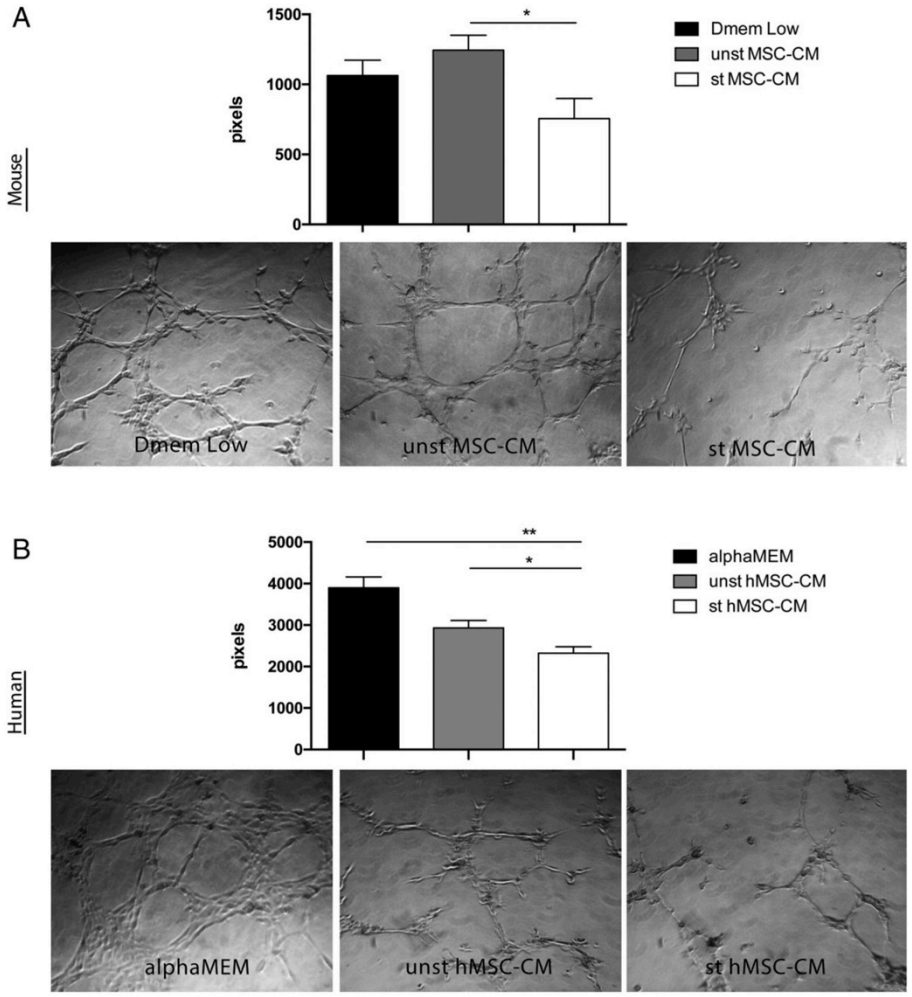

Fig. 5. Effect of human or mouse MSC conditioned medium on tube formation assay. The effect of unstimulated or stimulated MSC media on endothelial cells was determined by a tube formation assay. Cells were seeded on the top of a matrigel phase in the presence of unstimulated or stimulated A) mouse, B) human MSC-CM. 6 h later, images were acquired with a phase contrast inverted microscope at 4× objective magnification. Analysis was performed with ImageJ Angiogenesis Analyzer. A) SVEC4-10 network formation; quantification of the tube segment length (expressed in pixel number) and representative images at 4 h. B) Huvec network formation; quantification of the tube segment length and representative images (expressed in pixel number) at 4 h. 3 independent experiments, data are expressed as mean ± SEM (*$p < 0.05$, **$p < 0.01$, One way ANOVA).

Fig. 2). Thus, we investigated the ability of MSC-CM to generate monocyte-derived macrophages in vitro. Surprisingly, our data revealed an important difference between mouse and human MSC-CM (Fig. 4). When compared to the positive control (recombinant mouse M-CSF), both unst mMSC-CM or st mMSC-CM were unable to induce macrophage differentiation ($F4/80^+$, $CD11b^+$ cells) efficiently. In this case, stimulation of mMSC with pro-inflammatory cytokines did not change the properties of the secretome (Fig. 4A). In contrast, the culture of human monocytes in the presence of st hMSC-CM produced the same percentage of differentiated macrophages as the positive control (recombinant human M-CSF) (Fig. 4B). These data reflect the amount of mouse or human M-CSF detectable by ELISA in unst or st human and mouse MSC-CM (Fig. 4). Thus, although M-CSF is up-regulated in both human and mouse MSC-CM upon stimulation by inflammatory cytokines, the amount of M-CSF secreted by mMSC is too low to be detected by ELISA and to induce macrophage differentiation efficiently.

Notably, proteomic data on human M-CSF (CSF1) fully agree with functional assays and ELISA analysis. As reported in Table 1 and Fig. 2, M-CSF is amongst the proteins showing the highest increase in stimulated human secretome according to mass spectrometric analysis; the apparent discrepancy in the presence of CSF1 in unst hMSC-CM between ELISA (showing low levels of M-CSFin unst hMSC-CM, Fig. 4) and proteomics (listing M-CSF as absent in unst hMSC-CM in Table 1) is due to the high stringency used to filter quantitative proteomic data in the present report (detection in at least 3 out of 5 technical replicas in both patients). In fact, M-CSF was detected also in low amounts in 4 out of 5 replicas of unstimulated secretome of donor H34 but only in 2 out of 5 replicas of donor H30 and consequently listed as "non-detected" in unst hMSC-CM.

3.4.2. TIMP-1

Concerning angiogenesis, in our previous work [21] we analysed the effect of mMSC-CM on in vitro angiogenesis exploiting the tube

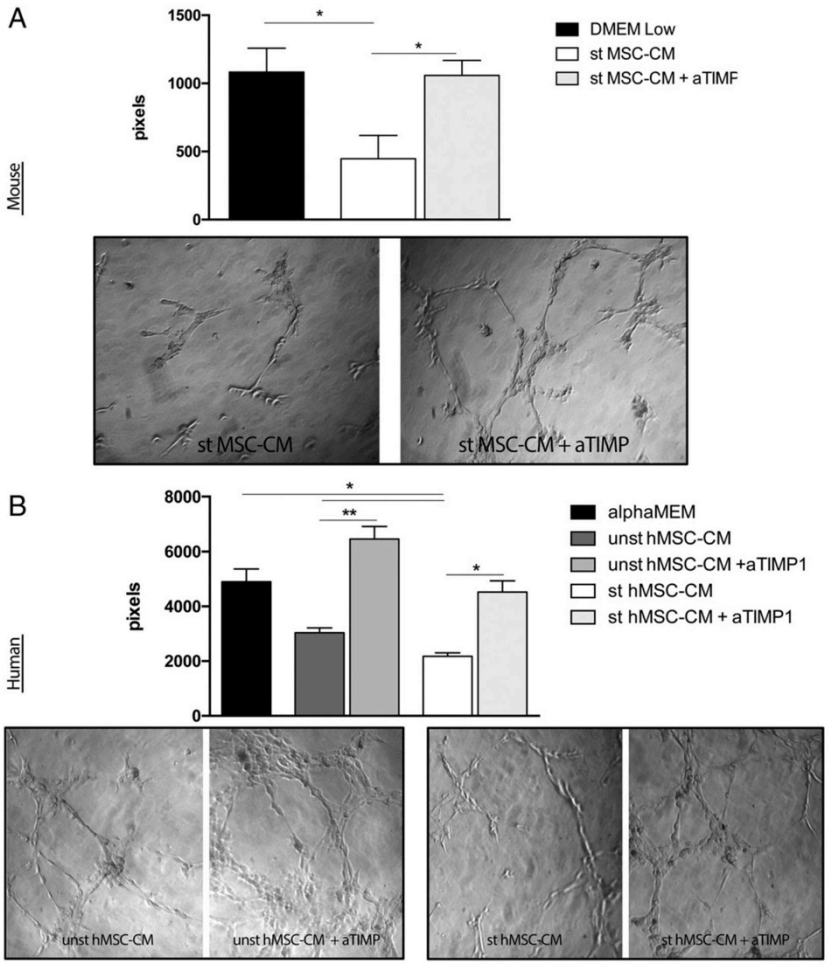

Fig. 6. Timp-1 blocking reverts the anti-angiogenic effect of mouse and human MSC conditioned media. In order to investigate the role of MSC-derived TIMP-1 on angiogenesis, the tube formation assay was performed in the presence of A) mouse or B) human TIMP-1 blocking antibody. Representative images of A) SVEC4-10 cell line or B) Huvec cells are taken with a phase contrast inverted microscope at 4× objective magnifications. Graphs show the quantification of the tube segment length measured with ImageJ Angiogenesis Analyzer. Data are expressed as mean ± SEM (*$p < 0.05$, **$p < 0.01$; One way ANOVA), 3 independent experiments.

formation assay. As we reported in Fig. 5A, soluble factors released by stimulated mMSC strongly inhibited the ability of SVEC4-10 cells, a mouse endothelial cell line, to form tube networks. In contrast, unst mMSC-CM had no effect on tube formation. In an effort to assess the angiogenetic role of hMSC, we performed the same experiments using HUVEC cells (Human Umbilical Vein Endothelial Cells) (Fig. 5B). In agreement with the data obtained with mMSC, soluble factors secreted by hMSC affected the ability of HUVEC cells to form tubes. Interestingly, in the case of human cells, MSC-CM was able to inhibit tube formation even when MSC had not been primed by cytokines. However, pre-activation with pro-inflammatory cytokines strengthened the anti-angiogenic effects of hMSC-CM, thus supporting our hypothesis that, during an inflammatory response, MSC target angiogenesis and thus dampen the inflammatory response [21].

Using both in vitro and in vivo approaches, we demonstrated that mMSC anti-angiogenic effect is mediated by TIMP-1 [21]. Because the proteomic analyses indicate that TIMP-1 is one of the proteins up-regulated in both human and mouse st MSC-CM (Table 2), we compared the results obtained by blocking TIMP-1 in SVEC4-10 cells incubated in the presence of mMSC-CM (Fig. 6A) with those generated using HUVEC cells and hMSC-CM (Fig. 6B). By inhibiting TIMP-1 activity with a specific blocking antibody, we observed the complete recovery of HUVEC cell ability to form tubes even in the presence of st hMSC-CM, indicating that TIMP1 is one of the key secreted molecules targeting endothelial cells in both mouse and human MSC.

TIMP-1 concentration was measured by ELISA in st and unst, human and mouse MSC-CM (Fig. 7A for mouse and B for human). In accordance with our data of tubulogenesis showing that unst mMSC-CM has no effect on angiogenesis (Figs. 5 and 6, panel A), the concentration of TIMP-1 in mMSC-CM was about 5-times higher when cells had been primed by pro-inflammatory cytokines. Thus, in mouse MSC, the anti-angiogenic phenotype is acquired only after licensing with pro-inflammatory cytokines, i.e. when TIMP-1 levels rise from about 3 ng/mL to 25 ng/mL. In hMSC, however, the basal high level of secreted TIMP1 may explain the partial anti-angiogenic effect of the unst hMSC-CM (Figs. 5 and 6, panel B). In fact, in support of this hypothesis, TIMP-1 blockade restored the formation of the endothelial network in the presence of unst or st hMSC-CM.

Again, proteomic data fully agree with functional assays and ELISA results for human TIMP1. As reported in Fig. 2 and Table 1, this protein is listed amongst those overrepresented in st hMSC but showing relative lower level increase following stimulation. Additional bioinformatics analyses of proteomic data further support the observation that even relatively small changes in the level of TIMP1 can result in very significant modulation of secretome properties. First of all, its level will greatly influence the proteolytic potential of the secretome and, consequently, the overall activity of a number of secretome components, including proteins which level is not increased following stimulation and proteins not directly involved in inflammation and angiogenesis; secondly, but not less importantly, TIMP1 is functionally related to a number of over-represented proteins in stimulated secretome besides proteases (Fig. 2 and Supplemental Table 3), like cytokines and structural proteins (such as IL6, IL8, CCL2 CXCL12, COL3A1). The complete list of the 54 proteins of stimulated hMSC-CM functionally correlated to TIMP1 according to String [34] is reported in Supplemental Table 3.

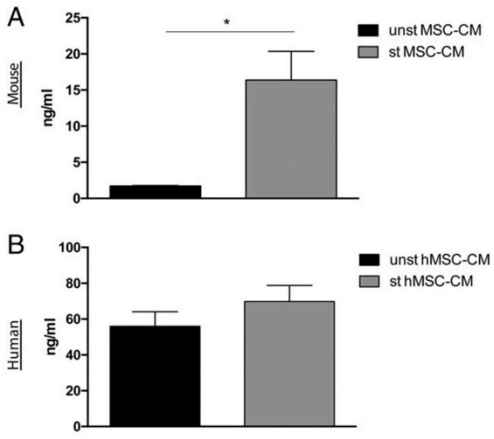

Fig. 7. Mouse and human MSC-derived TIMP-1 quantification. MSC-derived TIMP-1 concentration in A) mouse and B) human unstimulated or stimulated MSC conditioned medium was measured with ELISA. Data are expressed as mean ± SEM (*$p < 0.05$, parametric *t*-test), 2 independent experiments.

4. Conclusions

The proteomic analysis of hMSC-CM and mMSC-CM confirms that exposure to pro-inflammatory cytokines results in significantly higher secretion of a number of immunomodulatory and angiogenesis-related proteins by MSC from both species. Notably, 62% of the proteins identified in st hMSC-CM were also identified in st mMSC-CM, clearly highlighting the existence of a common signature in the secretome of human and mouse MSC. However, although human and mouse MSC show a similar proteomic signature in response to stimulation by pro-inflammatory cytokines, our data indicate that they may induce different biological responses. Thus, even if M-CSF is up-regulated in both human and mouse MSC-CM, only hMSC-CM induce macrophage differentiation efficiently because of its high concentration of M-CSF.

In both species, several up-regulated proteins are associated with angiogenesis. The extended network of interactions amongst inflammation and angiogenesis-related proteins in stimulated hMSC-CM makes it extremely difficult to assess the in vivo physiological importance of each factor. In particular, the presence of a number of protease and protease inhibitors implies the possibility of additional self-modulation of the properties of the various components of the secretome [39].

Although our data fully confirm the anti-angiogenic role of stimulated MSC for both mouse and human cells, at basal conditions MSC behavior is striking different. Indeed, while unst MSC-CM collected from mouse cells has no effect on tube formation, hMSC-CM significantly reduces angiogenesis in vitro. Finally, the anti-angiogenic role of TIMP-1 already observed in the mouse model was confirmed also using hMSC-CM: by inhibiting TIMP-1 activity with a specific blocking antibody, we observed the complete recovery of HUVEC cell ability to form tubes even in the presence of st hMSC-CM, indicating that TIMP1 is one of the key secreted molecules targeting endothelial cells in both mouse and human MSC.

Supplementary data to this article can be found online at http://dx.doi.org/10.1016/j.jprot.2017.07.012.

Transparency document

The Transparency document associated with this article can be found, in online version.

Acknowledgments

This work was supported in part by funds from the Programme: "Piano di Sostegno alla Ricerca 2015/17-Linea 2", from Università degli Studi di Milano, Italy. The authors wish to thank also the European Union Seventh Framework Programme for research, technological development, and demonstration under grant agreement no. 602363 and the ERC Advanced Grant under grant agreement no. 322823.

We thank Dr. Francesca Grassi Scalvini for table preparation and Dr. Steve Elliman from Orbsen Therapeutics Ltd., National University of Ireland, Galway, Ireland for providing human MSC.

Conflict of interest

All the Authors have declared no conflict of interest.

References

[1] C. Nombela-Arrieta, J. Ritz, L.E. Silberstein, The elusive nature and function of mesenchymal stem cells, Nat. Rev. Mol. Cell Biol. 12 (2011) 126–131.
[2] C. Shi, T. Jia, S. Mendez-Ferrer, T.M. Hohl, N.V. Serbina, L. Lipuma, I. Leiner, M.O. Li, P.S. Frenette, E.G. Pamer, Bone marrow mesenchymal stem and progenitor cells induce monocyte emigration in response to circulating toll-like receptor ligands, Immunity 34 (2011) 590–601.
[3] M.P. De Miguel, S. Fuentes-Julián, A. Blázquez-Martínez, C.Y. Pascual, M.A. Aller, J. Arias, Arnalich-Montiel, Immunosuppressive properties of mesenchymal stem cells: advances and applications, Curr. Mol. Med. 12 (2012) 574–591.
[4] D. Kyurkchiev, I. Bochev, E. Ivanova-Todorova, M. Mourdjeva, T. Oreshkova, K. Belemezova, S. Kyurkchiev, Secretion of immunoregulatory cytokines by mesenchymal stem cells, World J. Stem Cells 6 (2014) 552–570.
[5] N. Kalinina, D. Kharlampieva, M. Loguinova, I. Butenko, O. Pobeguts, A. Efimenko, L. Ageeva, G. Sharonov, D. Ischenko, D. Alekseev, O. Grigorieva, V. Sysoeva, K. Rubina, V. Lazarev, V. Govorun, Characterization of secretomes provides evidence for adipose-derived mesenchymal stromal cells subtypes, Stem Cell Res Ther 6 (2015) 221.
[6] B. Rocha, Secretome analysis of human mesenchymal stem cells undergoing chondrogenic differentiation, J. Proteome Res. 13 (2014) 1045–1054.
[7] A.J. Salgado, J.C. Sousa, B.M. Costa, A.O. Pires, A. Mateus-Pinheiro, F.G. Teixeira, L. Pinto, N. Sousa, Mesenchymal stem cells secretome as a modulator of the neurogenic niche: basic insights and therapeutic opportunities, Front. Cell. Neurosci. 9 (2015) 249.
[8] S.P. Kristensen, L. Chen, M. Overbeck Nielsen, D.W. Qanie, I. Kratchmarova, M. Kassem, J.S. Andersen, Temporal profiling and pulsed SILAC labeling identify novel secreted proteins during ex vivo osteoblast differentiation of human stromal stem cells, Mol. Cell. Proteomics (2012) 989–1007.
[9] J.M. Kim, J. Kim, Y.H. Kim, K.T. Kim, S.H. Ryu, T.G. Lee, P.G. Suh, Comparative secretome analysis of human bone marrow-derived mesenchymal stem cells during osteogenesis, J. Cell. Physiol. 228 (2013) 216–224.
[10] Y.A. Choi, J. Lim, K.M. Kim, B. Acharya, J.Y. Cho, Y.C. Bae, H.I. Shin, S.Y. Kim, E.K. Park, Secretome analysis of human BMSCs and identification of SMOC1 as an important ECM protein in osteoblast differentiation, J. Proteome Res. 9 (2010) 2946–2956.
[11] M.J. Lee, J. Kim, M.Y. Kim, Y.S. Bae, S.H. Ryu, T.G. Lee, J.H. Kim, Proteomic analysis of tumor necrosis factor-alpha-induced secretome of human adipose tissue-derived mesenchymal stem cells, J. Proteome Res. 9 (2010) 1754–1762.
[12] D.J. Kumar, C. Holmberg, S. Balabanova, L. Borysova, T. Burdyga, R. Beynon, G.J. Dockray, A. Varro, Mesenchymal stem cells exhibit regulated exocytosis in response to Chemerin and IGF, PLoS One 10 (2015), e0141331.
[13] A. De Boeck, A. Hendrix, D. Maynard, M. Van Bockstal, A. Daniëls, P. Pauwels, C. Gespach, M. Bracke, O. De Wever, Differential secretome analysis of cancer-associated fibroblasts and bone marrow-derived precursors to identify microenvironmental regulators of colon cancer progression, Proteomics 13 (2013) 379–388.
[14] S. Yu, Y. Zhao, Y. Ma, L. Ge, Profiling the secretome of human stem cells from dental apical papilla, Stem Cells Dev. 25 (2016) 499–508.
[15] P.R. Amable, M.V.T. Teixeira, R.B.V. Carias, J.M. Granjeiro, Borojevic, Protein synthesis and secretion in human mesenchymal cells derived from bone marrow, adipose tissue and Wharton's jelly, Stem Cell Res Ther 5 (2014) 53.
[16] A. Clabaut, C. Grare, T. Léger, P. Hardouin, O. Broux, Variations of secretome profiles according to conditioned medium preparation: the example of human mesenchymal stem cell-derived adipocytes, Electrophoresis 36 (2015) 2587–2593.
[17] J.J. Bara, S. Turner, S. Roberts, G. Griffiths, R. Benson, J.M. Trivedi, K.T. Wright, High content and high throughput screening to assess the angiogenic and neurogenic actions of mesenchymal stem cells in vitro, Exp. Cell Res. 333 (2015) 93–104.
[18] S. Riis, A. Stensballe, J. Emmersen, C.P. Pennisi, S. Birkelund, V. Zachar, Fink, Mass spectrometry analysis of adipose-derived stem cells reveals a significant effect of hypoxia on pathways regulating extracellular matrix, Stem Cell Res Ther 7 (2016) 52.
[19] M.B. Murphy, K. Moncivais, A.I. Caplan, Mesenchymal stem cells: environmentally responsive therapeutics for regenerative medicine, Exp. Mol. Med. 45 (2013) 54.
[20] M. Krampera, Mesenchymal stromal cell 'licensing': a multistep process, Leukemia 25 (2011) 1408–1414.
[21] L. Zanotti, R. Angioni, B. Calì, C. Soldani, C. Ploia, F. Moalli, M. Gargesha, G. D'amico, S. Elliman, G. Tedeschi, E. Maffioli, A. Negri, S. Zacchigna, A. Sarukhan, J.V. Stein, A. Viola, Mouse mesenchymal stem cells inhibit high endothelial cell activation and lymphocyte homing to lymph nodes by releasing TIMP-1, Leukemia 30 (2016) 1143–1154.
[22] J. Ankrum, J.M. Karp, Mesenchymal stem cell therapy: two steps forward, one step back, Trends Mol. Med. 16 (2010) 203–209.
[23] N.A. Kishk, N.T. Abokrysha, H. Gabr, Possible induction of acute disseminated encephalomyelitis (ADEM)-like demyelinating illness by intrathecal mesenchymal stem cell injection, J. Clin. Neurosci. 20 (2013) 310–312.
[24] D.F. McAuley, G.F. Curley, U.I. Hamid, J.G. Laffey, J. Abbott, D.H. McKenna, X. Fang, M.A. Matthay, J.W. Lee, Clinical grade allogeneic human mesenchymal stem cells restore alveolar fluid clearance in human lungs rejected for transplantation, Am. J. Phys. Lung Cell. Mol. Phys. 306 (2014) L809–15.
[25] M. Dominici, K. Le Blanc, I. Mueller, I. Slaper-Cortenbach, F. Marini, D. Krause, R. Deans, A. Keating, D.J. Prockop, E. Horwitz, Minimal criteria for defining multipotent mesenchymal stromal cells. The International Society for Cellular Therapy position statement, Cytotherapy 8 (2006) 315–317.
[26] J. Cox, M. Mann, MaxQuant enables high peptide identification rates, individualized p.p.b.-range mass accuracies and proteome-wide protein quantification, Nat. Biotechnol. 26 (2008) 1367–1372.
[27] J. Cox, M.Y. Hein, C.A. Luber, I. Paron, N. Nagaraj, M. Mann, Accurate proteome-wide label-free quantification by delayed normalization and maximal peptide ratio extraction, termed MaxLFQ, Mol. Cell. Proteomics 13 (2014) 2513–2526.
[28] S. Tyanova, T. Temu, P. Sinitcyn, A. Carlson, M.Y. Hein, T. Geiger, M. Mann, J. Cox, The Perseus computational platform for comprehensive analysis of (prote)omics data, Nat. Methods 13 (2016) 731–740.
[29] The Gene Ontology Consortium, Gene ontology consortium: going forward, Nucleic Acids Res. 43 (2015) D1049–56.
[30] P. Gaudet, P.A. Michel, M. Zahn-Zabal, I. Cusin, P.D. Duek, O. Evalet, A. Gateau, A. Gleizes, M. Pereira, D. Teixeira, Y. Zhang, L. Lane, A. Bairoch, The neXtProt knowledgebase on human proteins: current status, Nucleic Acids Res. 43 (2015) D764–70.
[31] The UniProt Consortium, UniProt: a hub for protein information, Nucleic Acids Res. 43 (2015) D204–12.
[32] G. Stelzer, R. Rosen, I. Plaschkes, S. Zimmerman, M. Twik, S. Fishilevich, T. Iny Stein, R. Nudel, I. Lieder, Y. Mazor, S. Kaplan, D. Dahary, D. Warshawsky, Y. Guan-Golan, A. Kohn, N. Rappaport, M. Safran, D. Lancet, The GeneCards suite: from gene data mining to disease genome sequence analysis, Curr. Protoc. Bioinformatics 54 (2016) 1.30.1–1.30.33.
[33] D.W. Huang, B.T. Sherman, R.A. Lempicki, Bioinformatics enrichment tools: paths toward the comprehensive functional analysis of large gene lists, Nucleic Acids Res. 37 (2009) 1–13.
[34] D. Szklarczyk, A. Franceschini, S. Wyder, K. Forslund, D. Heller, J. Huerta-Cepas, M. Simonovic, A. Roth, A. Santos, K.P. Tsafou, M. Kuhn, P. Bork, L.J. Jensen, C. von Mering, STRING v10: protein-protein interaction networks, integrated over the tree of life, Nucleic Acids Res. 43 (2015) D447–52.
[35] J.A. Vizcaíno, A. Csordas, N. del Toro, J.A. Dianes, J. Griss, I. Lavidas, G. Mayer, Y. Perez-Riverol, F. Reisinger, T. Ternent, Q.W. Xu, R. Wang, H. Hermjakob, 2016 update of the PRIDE database and related tools, Nucleic Acids Res. 44 (D1) (2016) D447–56.
[36] M.E. Bernardo, W.E. Fibbe, Mesenchymal stromal cells: sensors and switchers of inflammation, Cell Stem Cell 13 (2013) 392–402.
[37] M.E. Groh, B. Maitra, E. Szekely, O.N. Koç, Human mesenchymal stem cells require monocyte-mediated activation to suppress alloreactive T cells, Exp. Hematol. 33 (2005) 928–934.
[38] L. Nissinen, V.M. Kahari, Matrix metalloproteinases in inflammation, Biochim. Biophys. Acta (2014) 2571–2580.
[39] D. Rodríguez, C.J. Morrison, C.M. Overall, Matrix metalloproteinases: what do they not do? New substrates and biological roles identified by murine models and proteomics, Biochim. Biophys. Acta 2010 (1803) 39–54.
[40] R. Romieu-Mourez, D.L. Coutu, J. Galipeau, The immune plasticity of mesenchymal stromal cells from mice and men: concordances and discrepancies, Front. Biosci. (Elite Ed.) 4 (2012) 824–837.
[41] John A. Hamilton, Colony-stimulating factors in inflammation and autoimmunity, Nat. Rev. Immunol. 8 (7) (2008) 533–544.
[42] Qing Xiang Amy Sang, Complex role of matrix metalloproteinases in angiogenesis, Cell Res. 8 (1998) 171–177.
[43] N. Tojo, E. Asakura, M. Koyama, T. Tanabe, N. Nakamura, Effects of macrophage colony-stimulating factor (M-CSF) on protease production from monocyte, macrophage and foam cell in vitro: a possible mechanism for anti-atherosclerotic effect of M-CSF, Biochim. Biophys. Acta 1452 (1999) 275–284.
[44] M.F. Gruber, T.L. Gerrard, Production of macrophage colony-stimulating factor (M-CSF) by human monocytes is differentially regulated by GM-CSF, TNF alpha, and IFN-gamma, Cell. Immunol. 142 (1992) 361–369.
[45] P. Fixe, V. Praloran, Macrophage colony-stimulating-factor (M-CSF or CSF-1) and its receptor: structure-function relationships, Eur. Cytokine Netw. 8 (1997) 125–136.